Integrin-mediated Interactions between Cells and Biomimetic Materials

Dissertation to obtain the Degree of Doctor of Natural Sciences

(Dr. rer. nat.)

from the Faculty of Chemistry and Pharmacy

University of Regensburg

Presented by

Robert Knerr

from Hemau

November 2006

This work was carried out from July 2002 until June 2006 at the Department of Pharmaceutical Technology of the University of Regensburg.

The thesis was prepared under supervision of Prof. Dr. Achim Göpferich.

To my family

and Beate

‚Die Wissenschaft von heute ist der Irrtum von morgen.'

Jakob von Üxküll

Table of Contents

Chapter 1

Introduction

and

Goals of the Thesis

1) The Need for Biomimetic Biomaterials

According to the Global Information Incorporation, the sales volume of medical implants in the US will rise to more than 70 billion US$ in 2009 with an annual growth of more than 10 %.[1] This enormous amount confirms the increasing need for materials that can help to heal or at least attenuate tissue defects as a consequence of severe injuries or diseases. Besides the growing demand in cosmetic surgery (192.000 silicone implants / year), the annual consumption of 200 million catheters, 16 million renal dialyzers or one million cardiovascular stents for example illustrates the importance of the development of adequate materials for the replacement of parts of the human body (Table 1).[2]

This development in former times used to follow a trial-and-error-strategy. Materials developed for industrial applications that were found to be adequately suitable for producing medical devices were modified as far as necessary and further on called a *biomaterial*.[3] Not before the 1980s, the National Institute of Health in the US defined a concept of a biomaterial as "any substance, other than a drug, or combination of substances, synthetic or natural in origin, which can be used for any period of time, as a whole or as a part of a system which treats, augments or replaces any tissue, organ or function of the body".[4] Klee and Hoecker described these biomaterials as replacements of tissues that have been damaged or destroyed through pathological processes, fulfilling those functions of the replaced body parts.[5]

To be able to fulfill the aforementioned demands, biomaterials must exhibit certain characteristics. An ideal material for this purpose avoids auto-immune responses after application, interacts specifically with cells, degrades to non-toxic products on an appropriate time scale and can be replaced by healthy natural tissue.[3] This definition introduces the concept of *biocompatibility*, which means an inertness in terms of thrombogenic, allergenic, carcinogenic and toxic reactions.[6] This inertness is hard to achieve, knowing that immediately after exposure of an artificial material to biological fluids proteins readily adsorb to its surface. This non-specific reaction as a consequence can trigger severe immunological reactions, leading to an inflammation, encapsulation or the rejection of the applied device.[7]

A further step in the development of a biomaterial after reducing such undesirable side-reactions by suppressing the initial protein adsorption and, therefore, making the implant "invisible" for the human body, is the concept of rendering materials biologically active. By attaching signaling molecules, such as growth factors, adhesion molecules or enzymes, the natural environment of cells can be mimicked, not only allowing for the integration of the artificial material in the body, but additionally contributing to the healing process.[2] This can be achieved by selectively interacting with a targeted cell type, such as endothelial cells through biomolecular recognition events or by presenting growth factors, such as the mitogen PDGF. [8,9] This concept of modifying surfaces with natural compounds and copying the accustomed surroundings of cells is called *biomimetic* and since its central hypothesis seems to be very promising, extensive research has been performed in the last decade in this field.[8]

As all the aforementioned reactions predominantly occur at the interface between biomaterials and the surrounding body fluids, the focus for the design of new biomaterials especially lies on improving the surface performance of materials. In recent years, cell biology, material science as well as surface science have made significant advances,[2,10,11] now allowing for the definition of detailed requirements for the materials, whose implementation can now be controlled adequately with the improved analytical techniques. Hence, the necessary tools for the realization of improvements in the field of biomaterial design are available, but since the performance of the medical devices applied until today is still far from being ideal, many problems have to be solved in future studies in this field.

Therefore, especially two major goals have to be achieved. First, the suppression of non-specific reactions, such as protein adsorption or uncontrolled cell adhesion. Since these events entail the aforementioned difficulties in terms of immunological responses or implant rejections, a main focus has to be laid on their suppression or at least reduction. Several attempts have already been carried out to render artificial materials "invisible" for the human immune system, as for instance physical treatments.[5] Among several coatings that were also applied to exercise a degree of control over the way the human body responds to a biomaterial, by far the most attention has been given to poly(ethylene glycol) (PEG) coatings. Besides its ability to reduce the non-specific protein adsorption and, therefore, cell adhesion, it offers the possibility to achieve a second major goal in surface science, namely to render surfaces biomimetic by attaching bioactive signaling molecules via functional groups of PEG.

Although this approach seems to be very promising, the ideal biomaterial with completely satisfying properties could not be found so far. Hence, further knowledge on the interactions of biomaterials with biological environments has to be acquired. To understand in more detail, what is the actual state of the art in this scientific field, the following sections of this introduction will explain, how biomaterials interact with cells and how these interactions can be directed on the molecular level using certain cellular receptors. The focus here especially lies on so-called integrins, which mediate the adhesion of cells on surfaces. Thus, they might be of great help to achieve guided cell adhesion. Furthermore, a strategy to simplify investigations on complex biomaterial surfaces using the concept of self-assembled monolayers (SAMs) will be presented, as these have gained increasing importance in the last decade in surface sciences. Moreover, a range of suitable analytical techniques, which are especially qualified for surface analysis, will be introduced.

Taken together, these sections will point out a strategy for improving biomaterial surfaces, which may help to understand and ameliorate the performance of artificial materials and, particularly, to suggest, how biomaterial surfaces should be designed on the molecular level.

Device	Number / year	Biomaterial
Intraocular lens	2.700.000	PMMA
Contact lens	30.000.000	Silicone acrylate
Vascular graft	250.000	PTFE, PET
Hip and knee prostheses	500.000	Titanium, PE
Catheter	200.000.000	Silicone, Teflon
Heart valve	80.000	Treated pig valve
Cardiovascular stent	> 1.000.000	Stainless steel
Breast implant	192.000	Silicone
Dental implant	300.000	Titanium
Pacemaker	130.000	Polyurethane
Renal dialyzer	16.000.000	Cellulose
Left ventricular assist device	> 100.000	Polyurethane

Table 1: Medical implants used in the United States (adapted from [2]).

2) The Interactions of Cells with Biomaterials

Protein Adsorption to Surfaces

Cells and artificial materials interact in most cases in an indirect way. After exposure of a material to a biological fluid, in general proteins immediately adsorb, cover the surface and therefore change the physicochemical characteristics more or less completely.[7] Of course, the type and amount of proteins adsorbing is strongly dependent on the properties of the applied biomaterial, nevertheless, a direct interaction of cells and materials seems to be of minor significance. Wilson called this phenomenon a "translation of structure and composition of the surface into a biological language" by the adsorbed proteins.[12]

Without considering these first steps of interactions, a reasonable design of biomaterials is not possible. Since this event is rather non-specific, the subsequent adhesion, spreading and proliferation of cells also will be hard to control.[13] On the other hand, if the driving forces of protein adsorption can be understood, it should be possible to counter steer or in the best case exploit this phenomenon as far as possible.[8]

However, to a certain aspect, it is also described that cells interact directly with biomaterials via so-called weak chemical bonding, such as hydrogen bondings, electrostatic, polar or ionic interactions between various molecules on the cell membrane and functional chemical groups of the applied biomaterials, which means without the presence of proteins or their functional parts. [32] But it was described by different groups that these cells undergo rapid apoptosis, if they are not able in a relatively short period of time to synthesize and deposit proteins on the surface.[32]

In general, adsorption phenomena are driven by a number of enthalpic and entropic forces.[12] In an aqueous system, a protein bears a hydration shell due to dipole – dipole interactions of the water molecules with polar groups of the protein. Also surfaces interact with water molecules and as for proteins, the intensity of the interactions strongly depends on their hydrophilicity, or hydrophobicity, respectively. If a protein approaches to a surface, this wettability of protein and surface will determine the energy barrier of stripping off the water shell.[14-19] On hydrophobic surfaces, this barrier will be rather low, as the water's entropy will strongly decrease. On hydrophilic surfaces, in contrast, strong dipole – dipole interactions of protein and surface will lead to a high barrier. This explains, why rather hydrophilic surfaces with strong interactions with water do not adsorb proteins

as readily as it was found for hydrophobic surfaces. In contrast, the hydrophobic interactions of surfaces with non-polar regions of proteins allow for dehydration due to the entropic and enthalpic changes.[20,21,22]

For these hydrophobic interactions strong disadvantages have to be considered. In water, as described above, proteins are highly hydrated, exposing their polar regions to the outside, shielding the non-polar regions in the inside. This thermodynamically driven self-assembly leads to the so-called secondary, tertiary and quaternary structures of proteins.[23] When proteins interfere with the non-polar regions of a material surface, the three dimensional structure of proteins can be changed, since hydrophobic parts are presented on the outer regions.[24,25,26] This process of structural changes also was shown to be one of the major reasons for the adsorption still taking place on hydrophilic surfaces.[27,28] Such effects can lead to a complete loss of biological activity, as it was described by Horbett, especially on hydrophobic surfaces.[24]
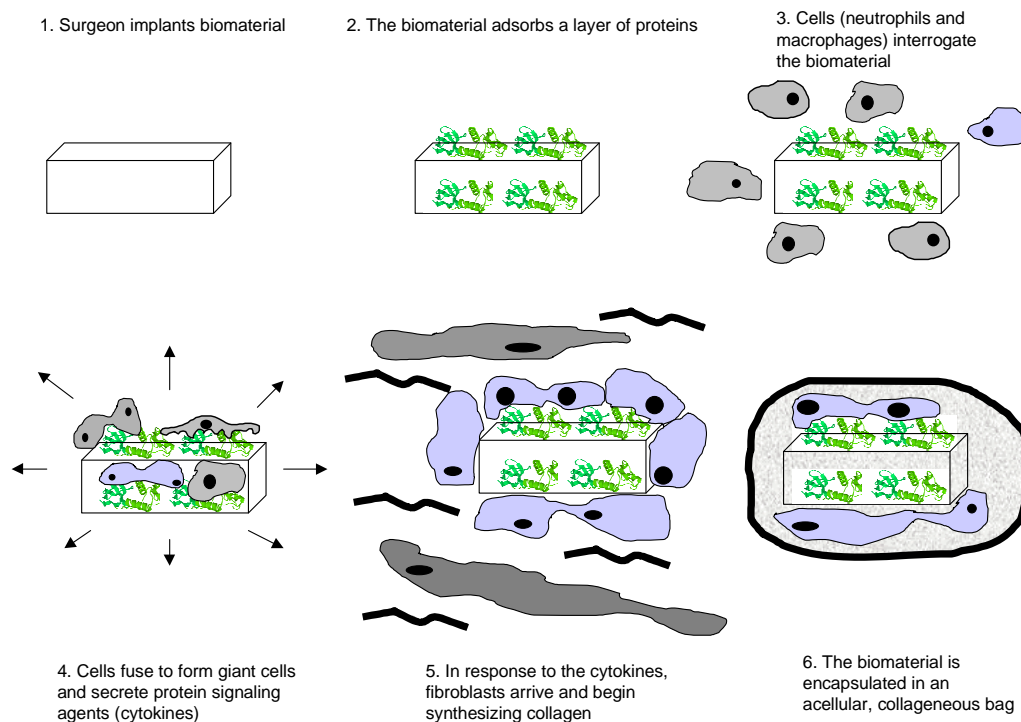
An additional contribution for the attraction of proteins to surfaces can be charges.[14,29] Of course, opposite charges can lead to attractive forces, but in aqueous systems these are frequently shielded by hydrating water, reducing their influence to a certain extent,[30] but on the other hand making it more difficult to predict their effects on protein adsorption. Moreover, the ionic strength, the pH value and the isoelectric points of the molecules involved play an essential role, since the resulting electrochemical double layer is strongly influenced by these factors.[31] Although all these interactions may occur on the atomic scale, the global charges on proteins and the surface zeta potential appear to dominate electrostatically driven adsorption.[31] The fact that also cell surfaces are charged, this may additionally contribute to the subsequent adhesion of cells on the corresponding surfaces.

Hence, it can be concluded that protein adsorption is a very complex phenomenon, in which very different thermodynamic aspects have to be considered. But as a lot of investigations have shed light on protein – surface interactions, there might be the chance to exploit these reactions for improving the subsequent interactions of cells with biomaterials.[2,3,5,7-9,12,15-17]

Controlling protein adsorption on biomaterial surfaces

Adsorption of "good" proteins

There are two different strategies discussed at the moment how to design biomaterials.[5] The first approach is to control protein adsorption as far as possible and exploit the advantages of certain proteins to guide the behavior of cells into a desired direction.

For fibronectin for example it is well known that this protein strongly induces the adhesion of endothelial cells and in consequence reduces the adhesion of other cells.[5] Endothelial cells often are highly desirable on biomaterial surfaces after implantation, since these cells form the inner layer of blood vessels and therefore guarantee a high biocompatibility. Vascular grafts following this strategy of attaching fibronectin and therefore endothelial cells are already well established in surgery.[8] Without such a protective layer, an applied biomaterial shows the usual fate: proteins adsorb in a non-specific manner, immune cells (neutrophils and macrophages) invade. Since the "foreigner" can not be taken up, the macrophages fuse into giant cells. Subsequently, cytokines are released and call in other cells, such as fibroblast. These then synthesize collagen for a complete encapsulation of the implanted material into an acellular, avascular collagen bag (see Figure 1).[2] In consequence, the applied device can not be integrated in the surrounding tissue. Therefore, by preadsorbing fibronectin to the surface and via subsequent fibroblast attachment, implant rejections can be prevented.[8] For that reason, special techniques, such as plasma etching of surfaces in the presence of sulfur dioxide to increase fibronectin adsorption, were applied in order to guarantee a high biocompatibility due to the adsorption of a certain advantageous protein type.[5] Also for vitronectin such positive effects on biocompatibility are described. Since its attraction to surfaces is described to be even higher than the affinity of fibronectin, it is present at a far greater concentration after exposure to fetal bovine serum (FBS).[36] In general, more or less hostile surfaces can be made highly attractive for certain cell types by preadsorption of favored proteins, which additionally reduce the adsorption of other, unfavorable proteins. This approach strongly increases the biocompatibility of artificial materials and is therefore a viable tool in designing biomaterials. However, this concept should be improved, since it is still quite non-specific. A different strategy, which could be more promising is to prevent protein adsorption completely (see below).

1. Surgeon implants biomaterial   2. The biomaterial adsorbs a layer of proteins   3. Cells (neutrophils and
                                                                                                 macrophages) interrogate
                                                                                                 the biomaterial

4. Cells fuse to form giant cells   5. In response to the cytokines,   6. The biomaterial is
and secrete protein signaling   fibroblasts arrive and begin   encapsulated in an
agents (cytokines)   synthesizing collagen   acellular, collageneous bag

Figure 1: Fate of an implant with "conventional" surface properties. After implantation, proteins adsorb and entail an immunological response, in most cases leading to an encapsulation of the applied device in a collageneous bag.[2]

Strategies for preventing protein adsorption on biomaterials

A different approach for designing biomaterials instead of guiding the adsorption of proteins is to generate completely inert surfaces in terms of protein adsorption to suppress any non-desired side reactions, such as immune responses. To these materials cell adhesion motifs can be attached to induce the adhesion of the desired cell types, since fragments of proteins were described, which can selectively bind certain cells.[34]

Several strategies to reach the first goal, rendering surfaces inert, have already been shown to be promising.[44] A physical approach to reduce protein adsorption is surface treatment by plasma etching.[15,45] By applying an electrical field to a gas, electrons and ions are produced with a high kinetic energy. If surfaces are brought into contact with these accelerated charge carriers, their surface in general is roughened and acquires a more hydrophilic character.[5] As discussed earlier, these more hydrophilic surfaces adsorb less protein.[12] Nevertheless, although the wettability increases, this approach only can reduce protein adsorption, due to its quite non-specific character, this technique does not lead to protein resistant surfaces.[5]

Also the attachment of phosphorylcholine molecules to a certain extent reduced protein adsorption.[46,47] These molecules self-assemble in phospholipid bilayers and are quite similar to cell membranes.[48] Therefore they are described as "cytomimetic".[49] These surfaces were described to reduce albumin adsorption 80-fold.[44]

An even more promising coating of surfaces can be reached by using polysaccharides.[50,51] These coatings reduce protein adsorption strongly, in some cases extremely sensitive techniques, such as surface-MALDI mass spectrometry (matrix assisted laser desorption/ionization) had to be used to detect single protein molecules. However, even with these potent techniques, in some cases albumin adsorption for example was not detectable.[51] On the other hand some proteins, such as IgG adsorb equally effectively on different polysaccharide coatings.[51] The reason for the reduction of protein adsorption on polysaccharides is assumed to be the high hydration of the surfaces, leading to a good wettability and therefore highly unfavorable energetic reactions when proteins approach.[44]

By far the most attention in terms of protein resistance is drawn to coatings with poly(ethylene glycol) (PEG).[7] Also PEG coated surfaces exhibit repulsion forces due to the good solubility of this polymer in water, Kingshott described PEG surfaces as the most promising strategy to minimize the adhesion of biomolecules, since PEG coatings in numerous studies had the lowest protein coverage.[44]

For the immobilization of this polymer, different techniques are described. Hydrophobic surfaces can be modified by physical adsorption of PEG, but for this application, only high-molecular PEGs (MW >100.000 Da) can be used.[52,53] The drawback of this technique is that the polymer chains can easily be displaced by macromolecules with a higher affinity to the surface.[7] An increase in the adsorption of PEG to surfaces and a stronger interaction can be reached by using block copolymers with hydrophobic segments.[54,55] With an increasing hydrophobic part and decreasing PEG chain length, the attachment to the surface is additionally increasing.[7] In numerous studies, an effect of the PEG chain density on the surface was described: the more PEG on the surface, the less protein adsorb.[56,57]

The adsorbing amount of PEG derivatives on the surface is influenced by several factors, for example by solvent characteristics. According to de Gennes, PEG can adopt different conformations on the surface.[58] If the surface can interact strongly with the polymer chains and is large in relation to the amount of PEG, the polymer adopts a "pancake conformation" (Figure 2).[59] If the attraction of PEG to the surface is low and additionally the interactions with the solvent are strong ("good solvent"), also the so-called "mushroom

conformation" is possible. With increasing concentrations of polymers on the surface, for example due to a higher concentration in solution, the polymer "mushrooms" begin to interact. By further increasing the concentration, the polymer chains are allowed to interfere. Van der Waals interactions then might lead to a loss in energy, which is high enough to overcome the entropic barrier of a chain strengthening. The polymers then can change into a "brush-like conformation".

These facts are not only valid for the adsorption of PEG to surfaces, but also for covalent PEG grafting to surfaces. By applying this strategy, activated PEG derivatives with functional end groups are bound to functional groups of the surface. This implies, that the surface as well as PEG have functional groups, which is a limiting factor for several materials, such as titanium or poly(ethylene). However, for some of these surfaces the use of γ-irradiation or UV is an alternative to graft PEG.[7] An other drawback of the covalent grafting technique is the availability of functional groups. The more PEG is bound, the more difficult it becomes for further polymer chains to reach the functional groups, leading to a low grafting density. This may reduce the protein resistance dramatically.[7]
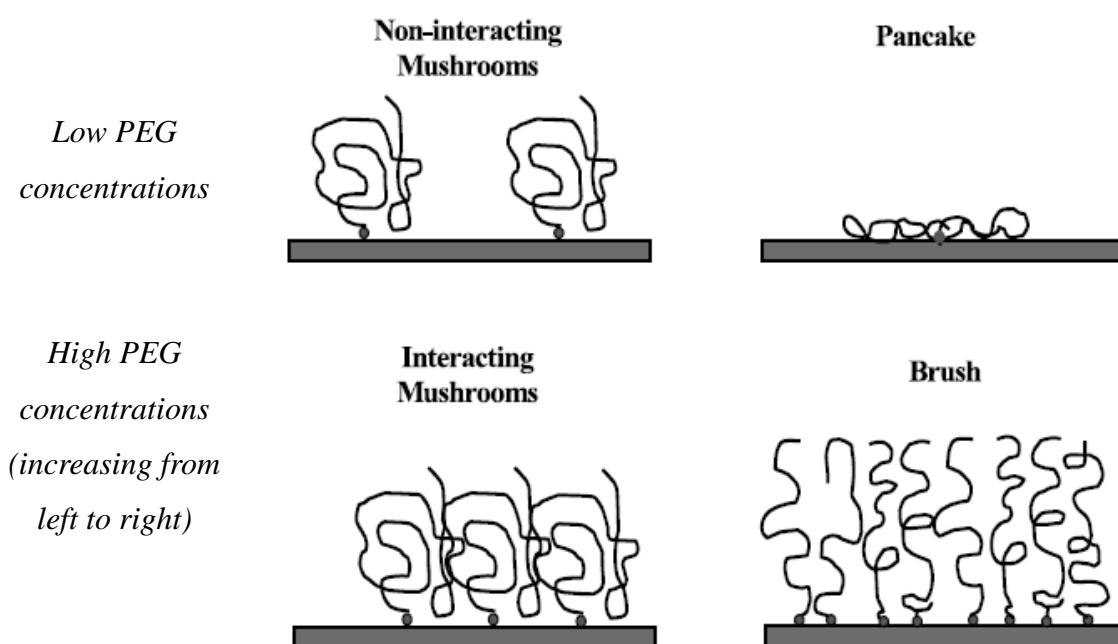

Figure 2: Different conformations of PEG on surfaces. Depending on the solvent characteristics, polymer chains adopt a mushroom ("good solvent") or a pancake (bad solvent") conformation. At higher PEG concentrations, polymer chains begin to interact. Increasing to concentration leads to an adoption of a brush-like state of PEG on the surface.

A highly promising approach on the other hand is to modify the bulk of water-insoluble polymers with PEG by copolymerization. Poly(anhydrides) in a plethora of studies were modified with PEG, resulting in block copolymers.[60,61,62] For poly(lactic acid) for example, this strategy was shown to be very promising. By varying the molecular weights of the different blocks, numerous derivatives with an extremely broad range of physicochemical properties could be synthesized.[60,63] The resulting water-insoluble polymers could be applied in different fields of pharmaceutical technology, such as the manufacture of controlled release devices or scaffolds for cell culture systems.[64] In all applications, these polymers were shown to reduce protein adsorption significantly and therefore increase their biocompatibility. [60,63,64]

If these so-called PEG-PLAs are processed under certain conditions, solid materials in almost every form can be generated by using the corresponding templates.[65] If these structures then are applied in aqueous systems, the PEG chains assemble on the surface of these devices due to the mobility of the polymer chains in the swollen bulk material.[66] This PEG corona then is highly hydrated, preventing protein adsorption as explained above. Several studies described a reduction in adsorbed amounts of more than 90%.[61]

By far the most promising approach, however, is the formation of self-assembled monolayers of PEG derivatives, since by using this strategy, the highest density of PEG chains on the surface can be reached.[56,57] The protein repellant effect of these surfaces is based on the same principles as for all other surfaces described so far, but due to the high density of PEG, for several surfaces even a complete suppression of protein adsorption was described.[67,68,69] However, these systems, which will be described in more detail in section 4 of this chapter, in most cases can not be used as classical biomaterials for direct applications in the human body due to the low biocompatibility of the materials available for this strategy. Therefore, they are more or less only used as model systems *in vitro* for drawing conclusions on how to design improved biomaterials.

Hence, summarizing, it is obvious that very different strategies are currently exploited to improve the interactions of cells with biomaterials. Significant ameliorations could be reached in recent years, although the gold standard could not be defined so far. Therefore, further studies have to be conducted to learn more about cell – surface interactions. A possible further improvement of biomaterials may be achieved by exploiting the vantages

of the biomimetic concept. This means, besides reducing non-specific events on a material surface, the attachment of bioactive compounds in order to achieve a specific cell signaling. As especially the initial steps of cell adhesion are critical in terms of the fate of an applied material, cell adhesion receptors, such as integrins may be helpful, since they could induce the adhesion of favorable cell types on material surfaces and, hence, may organize the integration of the artificial device into the human body. Therefore, in the following section the structure, mode of action, and ligands of the corresponding cell adhesion receptors (called integrins) are presented, to be able to develop a suitable strategy to design biomaterial surfaces.

3) The Structure and Functions of Integrins

As mentioned in the previous section, integrins are central regulators of cell – biomaterial interactions. Therefore, the question is how far these integrins can be exploited to modulate cellular responses to materials.

Integrins are heterodimeric transmembrane receptors, consisting of one α and one β subunit.[70] They contain a large extracellular (EC) domain with approximately 1000 amino acids for the α, and 750 amino acids for the β subunit, respectively.[70] Via a membrane-spanning region, these EC domains are linked to a short cytoplasmic tail. This tail is responsible for interactions with the cytoskeleton and therefore determines the inside-out as well as the outside-in signaling.[72]

Special structural features of the EC domains are a seven-fold homologous repeat forming the so-called β-propeller and an extra, independently folding domain of approximately 180 amino acids, which can be found in 7 α subunits, the so-called I domain (I for inserted) within the β-propeller.[35] This region together with a region contained in all β subunits is responsible for the ability of integrins to bind ligands. Hence, both subunits are involved in ligand binding, although the α subunit seems to be responsible for ligand specificity.[74,75] To be able to interact with ligands at all, divalent cations are necessary, bound near the ligand binding site in the β-propeller.[35]

So far 22 different human integrin receptors have been described, composed of different combinations of 18 α and 8 β subunits.[35] The ligand specificity of these receptors is determined by the α/β combination. In general, integrins are divided into three different groups.[71] First, integrins containing the β_1 subunit, which can combine with 12 different α subunits, form the largest group. These integrins are widely expressed in different cell types and predominantly mediate the interactions of cells with ECM proteins. Second, integrins containing the β_2 and β_7 subunits, which are found on blood cells exclusively, are responsible for cell – cell interactions via cadherins for example. The third group contains α_v subunits and also can be found in very different types of cells, such as blood cells, endothelial or epithelial cells. Actually, there are only two integrins that can not be classified in these three groups: The highly specific $\alpha_{IIb}\beta_3$ in platelets and $\alpha_6\beta_4$ integrins in keratinocytes.[71]

Cells do not only express one single integrin type, but a very complex mixture of cell adhesion receptors. Therefore, they can bind to a large variety of ligands, which are listed in Table 2.[71] Most of these ligands contain the cell recognition tripeptide sequence RGD (arginine, glycine, aspartic acid), which is mainly responsible for the binding to integrins.[34]

In contrast to growth factor receptors, integrins do not show any enzymatic activity (except for β_3), instead they transfer signals by conformational changes and by interacting with kinases.[75] In stationary cells, the affinity state of integrins is in an active form, except for circulating blood cells, where integrins are inactivated.[71] However, this state only can be adopted after receiving signals from inside the cell, for example by G-protein-coupled receptors.[76] Several other signaling cascades have been shown to regulate the integrin function, as for example via interactions with the protein talin.[77]

Also vice versa, a signaling from the outside to the cytoplasm can be triggered after ligand binding, resulting in conformational changes. Multiple binding sites of ligands, which were described for fibronectin for example, or intrinsic properties of integrins moreover can lead to a clustering of receptors in so-called focal adhesion and the recruitment of cytoplasmic protein complexes.[39]

Via complex intracellular signaling cascades, involving focal adhesion kinase (FAK), Rho, Src and others, as well as four actin binding proteins (talin, α-actinin, filamin and tensin), integrins are linked to the actin cytoskeleton.[70] Actin is the major cytoskeletal protein consisting of 43 kDa monomers, which are polymerized into long filamental chains. Via these links, integrins can modify cytoskeletal features and therefore influence cell adhesion, spreading, migration, cell cycle progression, differentiation and anchorage-dependent cell survival.[72]

After initial adhesion of cells onto surfaces and focal adhesion formation, integrin triggered cascades modulate the organization of actin networks by stimulation of Rho-GTPases, which then stimulate further specialized cascades.[35] This finally results in filopodial extensions at the cell periphery, the formation of lamellopodia protrusions and membrane ruffles, as well as stress fibers and focal adhesion assembly.[75] Also in cell migration Rho-GTPases are involved, whereas Rac and Cdc42 are responsible for protrusion and cell polarity.[78] Furthermore, integrin recycling via endosomal pathways to

the advancing lamellopodia was described, with a completion of an endo-exocytic cycle within 30 minutes.[71]

Also for cell survival integrins play an essential role. The phosphorylation of tyrosine 397 in FAK and its kinase activity seems to induce necessary signaling cascades for preventing apoptosis.[79]

	Integrin	Matrix molecule	Other ligands
	$\alpha_1\beta_1$	Col I, IV, VI; Ln	
	$\alpha_2\beta_1$	Col I,II,III,IV,VII,XI; Ln	
	$\alpha_3\beta_1$	Ln 2/4, 5, 10/11; TP	Inv
	$\alpha_4\beta_1$	Fn; CS-GAG	VCAM-1, Inv, Im
	$\alpha_5\beta_1$	Fn; Fg; dCol	Disintegrins, Im, Inv
Subfamily (i)	$\alpha_6\beta_1$	Ln	Inv, sperm fertilin
	$\alpha_7\beta_1$	Ln 1, 2/4	
	$\alpha_8\beta_1$	Fn; Vn; Tn	
	$\alpha_9\beta_1$	Col I; Ln; Tn; OP	VCAM-1
	$\alpha_{10}\beta_1$	Col II	
	$\alpha_{11}\beta_1$	Col I	
	$\alpha_D\beta_2$		ICAM-3
	$\alpha_L\beta_2$		ICAM-1, 2, 3, 4, 5
	$\alpha_M\beta_2$	Fg	ICAM-1, iC3b, FX
Subfamily (ii)	$\alpha_X\beta_2$	Fg	IC3b
	$\alpha_4\beta_7$	Fn	MAdCAM-1, VVAM-1, disintegrins
	$\alpha_E\beta_7$		E-cadherin
	$\alpha_v\beta_1$	Fn; Vn	TGFβ LAP
	$\alpha_v\beta_3$	Vn; Fg; Fn; bSp; Tn; TP; OP; MAGP-2, fibrillins, Del1, dCol	VWF, disintegrins, L1-CAM
Subfamily (iii)	$\alpha_v\beta_5$	Vn; bSp; Fn	
	$\alpha_v\beta_6$	Fn; Tn	TGFβ LAP
	$\alpha_v\beta_8$	Col I; Fn, Ln	
	$\alpha_{IIb}\beta_3$	Fg; Fn; Vn; TP; dCol; Dec	VWF, Pl, disintegrins, L1-CAM
	$\alpha_6\beta_4$	Ln	

Abbreviations: bSP – bone sialoprotein; Dec – decorsin; Del1 – developmental endothelial locus-1; (d)Col – (denatured) collagen; CS-GAG – chondroitin sulphate glycosaminoglycan; Fg – fibrinogen; Fn – Fibronectin; FX – Factor X; iC3b – inactivated fragment of complement factor C3; ICAM – intracellular adhesion molecule; Im – intimin; Inv – invasin; Ln – laminin; L1-CAM – neutral cell adhesion molecule L1; MAGP – microfibril associated glycoprotein; MAdCAM – mucosal addressin cell adhesion molecule; OP – osteopontin; Pl – plasminogen; TGFβ LAP – transforming growth factor β latency-associated peptide; Tn – tenascin-C; TP – trombospondin; VCAM – vascular cell adhesion molecule; vWF – von Willebrand factor (adapted from [71])

It can be well understood, that integrins are involved in numerous diseases.[34,80,81] But on the other hand, if the biotechnological background is known, pathological processes can be influenced or stopped by controlling integrin activities, for example by anti-integrin-antibodies or peptidomimetics.[80] Investigations in terms of reducing blood clotting with RGD containing peptidomimetics already have been shown to be promising.[81] Furthermore, also for cell – biomaterial interactions the above mentioned facts can be exploited. By attaching selective proteins or peptides to surfaces, a selective adhesion of cells or distinct cellular responses can be triggered.[34] Massia et al. for example could show, that by attaching an $\alpha_v\beta_3$ selective ligand to surfaces, smooth muscle and endothelial cell adhesion was preferred, whereas after attaching an $\alpha_5\beta_1$ selective ligand, fibroblast attachment was stronger.[82]

Hence, modifications of biomaterial surfaces with distinct bioactive compounds seem to be a very promising way to control cell – biomaterial interactions, making this field of integrin – ligand interactions very attractive for biomaterials scientists. Combining the benefits of this strategy with the advantages of protein-repellant surfaces described in section 2 should therefore allow for a very effective and innovative biomaterial design.

To elucidate the corresponding influencing factors responsible for distinct cellular responses, however, a detailed understanding and knowledge of the existing surfaces must be at hand, since a lot of different aspects may determine the response of cells to surfaces. Therefore, simplified model surfaces, such as the mentioned self-assembled monolayers, would be of great advantage. To learn more about the characteristics of such systems, the following section will describe their preparation, growth and properties, as well as their possible application in the field of surface engineering.

4) Self-assembled Monolayers (SAMs) as Model Systems

The need for model systems

Due to the complexity of cell – biomaterial interactions, investigations in this field are sometimes cumbersome. Minor changes of the system of interest can lead to strong changes of cellular responses. Degradation products of the biomaterial used for example may adsorb to the surface, changing the adsorption profile of different proteins.[63] This of course then strongly alters the interactions with cell adhesion receptors, leading to a completely different cell response. Also swelling of the underlying biomaterial could modulate protein adsorption due to a different wettability, having the same consequences.[66]

These facts already indicate that investigations in this field have to be simplified by reducing the number of factors that might affect the reaction or interaction of interest. Therefore, simplified model substrates are gaining increasing importance. The most popular approach to design surfaces with very distinct physicochemical properties is to fabricate self-assembled monolayers of alkanethiols.[83] Due to the ease of preparation and the facile tunability of their surface characteristics, in a plethora of studies self-assembled monolayers of alkanethiols were used and characterized extensively.[83-88] The enormous interest in these model systems is also founded in the wide range of possible applications. They are used for corrosion prevention,[89] changing wettability characteristics[90] or mechanical properties of surfaces, such as friction or lubrication.[91]

Also in the field of biomaterials design, self-assembled monolayers can serve as suitable model substrates. Since the interactions of cells and biomaterials particularly take place on the outer few nanometers of a biomaterial,[7,8] by mimicking the surface characteristics with simplified SAMs, detailed investigations on how to improve cell-material interactions can be performed.[83] Additionally, influences of the underlying bulk material can be excluded and therefore simplify investigations concerning a suitable design for biomaterials´ surfaces.

Schreiber defined the concept of self-assembly as "the spontaneous formation of complex hierarchical structures from pre-designed building-blocks", with the affinity of the headgroup of a surfactant to a substrate being the driving force for an adsorption process.[83] The most popular system in terms of SAMs consist of chemisorbed alkanethiols on gold, but also other systems, such as organosilicon layers on OH-

terminated surfaces were described.[92] However, these systems could not reach the highly ordered states, as they are described for alkanethiols on gold.
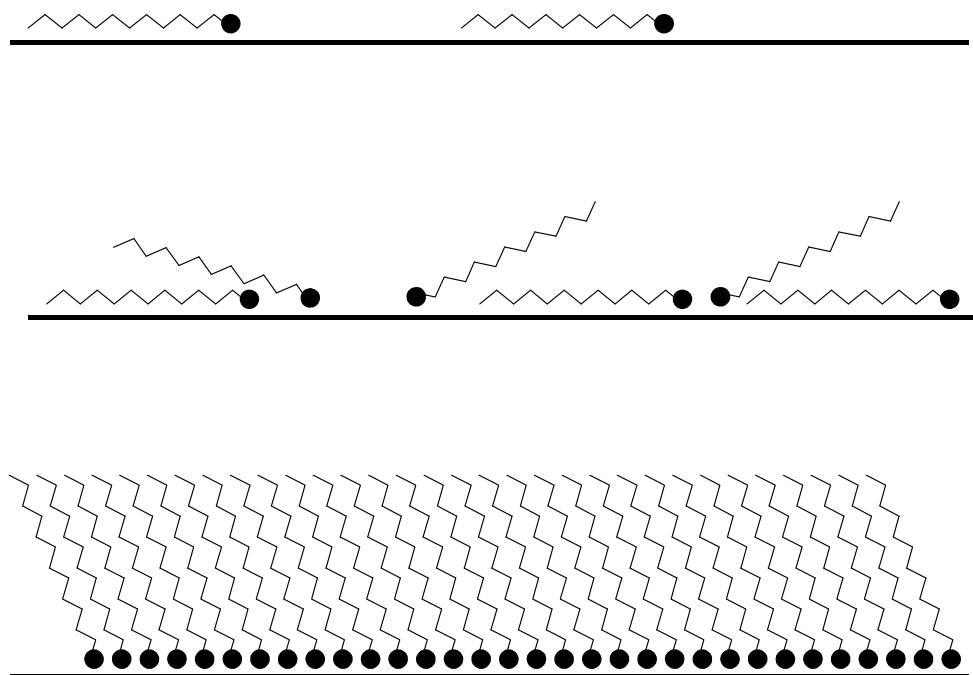
Monolayer formation of alkanethiols on gold

In the literature numerous studies dealing with self-assembled monolayers of thiolated compounds on gold can be found.[83-92] The procedure to generate such surfaces is quite similar in most cases. Besides rarely used methods, such as evaporation techniques in ultra high vacuum (UHV), most groups deposit alkanethiols on gold from solution, the solvents that are usually used for this application are ethanol or hexane.[83] The gold substrate in the majority of cases consists of freshly evaporated films. Since the cleanness of these substrates has a strong impact on the time scale of monolayer formation, a common approach is to clean the surfaces directly before use with a "piranha solution" (7:3 concentrated H_2SO_4/30% H_2O_2).

The primary driving force for the adsorption process in the case of alkanethiols on gold is chemisorption, with a free energy of 126 kJ/mol due to the high affinity of sulfur to gold.[83] Whitesides stated that the resulting bond is formed by a thiolate and a positively charged gold cation, liberating hydrogen, although they could not detect the generated hydrogen directly.[88] Moreover, his group described that SAMs formed of dialkyl disulfides were indistinguishable from alkanethiol SAMs, indicating the same bond is formed as for thiols. However, in the review by Schreiber, the fact that the distance between sulfur atoms on the surface is only 2.2Å instead of the theoretical value of 5Å, led to the assumption that sulfur atoms form pairs on the surface including gold atoms. Therefore he discussed, whether the two valency model is not valid for sulfur in this case.[83] Hence, the nature of the bond formed by alkanethiols on gold is still a matter of discussion.

Besides chemisorption, also the physisorption of alkanethiols to gold contributes to the formation of well-ordered structures. For dodecanethiol, a high free energy value of 109 kJ/mol due to physisorption was described, which is in the range of chemisorption for the same compound, indicating that van der Waals interactions contribute significantly to the monolayer formation.[83] Moreover, it was found that alkanethiols on gold are tilt about 30° with respect to the surface normal.[67] The reason therefore is the maximization of van der Waals interactions, resulting in the extraordinary high value of 109 kJ/mol.

Also during monolayer formation, physisorption is part of the process. In the initial state of the adsorption, alkanethiols were found to lay down flat on the surface due to physisorption.[93,94] This precursor state enhances the chance for the alkanethiols to take the energy barrier of 29 kJ/mol to chemisorb. With increasing concentrations of alkanethiols on the surface, the laying-down state changes to a "standing-up phase" (Figure 3).[93]

Figure 3: Different phases of monolayer formation. Initial physisorption of alkanethiols increases the chance to take the energy barrier for chemisorption. After increasing the concentration of molecules on the surface, the initial laying-down phase changes to a standing-up phase. Due to a maximization of van der Waals interactions, alkanethiols are tilt by 30° with respect to the surface normal (adapted from [83]).

The growth curve of such monolayers is assumed to follow a Langmuir growth curve according to equation 1:

$$\frac{d\Theta}{dt} = R(1-\Theta).$$
(1)

(Θ = number of free binding sites; t = time; R = rate constant; Assumptions: number of adsorption sites per surface of the adsorber is constant and only capable of binding one adsorbate molecule. The adsorption enthalpy per site is constant and not depending on the load. There is no interaction between the adsorbed molecules, and there is no surface diffusion.)

Nevertheless, in fact most chemisorption processes of alkanethiols slightly differ from this predicted growth kinetics, since the ideal conditions necessary for this process are not given. The adsorbing molecules interact and the binding sites on the surface are not completely independent. It was shown for example that alkanethiols in the initial state form islands of growth on the surface.[95] Only after the concentration of compounds on the surface is high enough, also the defect sites between these islands are covered with alkanethiols.

Also the time scale of monolayer growth is still a matter of discussion. Several groups stated that within several minutes most of the adsorption process takes place, while after that the adsorption is significantly decreased.[96,97] Others found that the formation is a process of at least 24 hours, with a more or less constant increase of sulfur atoms on the substrate.[104] Nevertheless, it is widely accepted that reorganization phenomena take place over several hours. According to Himmelhaus et al. the formation of an alkanethiol monolayer can be distinguished in three different processes with different time scales. The first and fastest step is the chemisorption, the second, which is 3 to 4 times slower, is the straightening of the hydrocarbon chain. The last step then is a reorientation of the head groups, but this step is up to 70 times slower than the straightening.[98] Impurities on the surface and in solution also might influence the adsorption kinetics, but contaminants are ultimately displaced by the growing SAM.[83,99] Furthermore, several factors are described influencing the growth kinetics of alkanethiols on gold, such as the chain length of the compounds, the concentration in solution and of course the solvent.

Applications of self-assembled monolayers

As already mentioned, SAMs of alkanethiols can be used in different technological fields due to the extremely broad range of surface characteristics. Also in the field of biomaterial design, numerous applications were described. Since the end groups of alkanethiols can be modified with almost every functional group, Facheux et al. investigated the influence of charged end groups on protein adsorption, revealing that positively charged amine-terminated SAMs adsorbed the highest amount of vitronectin, what already can be a hint, which types of cells predominantly will attach after applying such biomaterials in vivo.[13] Also larger end groups can be attached. Whitesides in a plethora of studies investigated the effect of oligo(ethylene glycol) (OEG) end groups of alkanethiols on protein adsorption.[67,88,96] By increasing the hydrophilicity of the SAMs, protein adsorption in

some cases was completely suppressed. Mrksich also attached OEG end groups and investigated the adhesion of cells. By micro-contact printing he moreover could pattern surfaces and found that cells only attached to areas, where no OEG was patterned, indicating a complete reduction of cell adhesion on OEG-terminated SAMs.[100,101,102] Herrwerth et al. even went one step beyond, attaching high-molecular weight PEGs to alkanethiols, but could show that also in this case well defined monolayers were formed.[103]

These few examples already show that SAMs can be a very helpful tool in getting information on biomaterial design. Due to the high density of functional groups on the model surface, an ideal case scenario of more complex surfaces can be generated. With suitable techniques, which are described in the following section, highly specific interactions of cells with biomaterials can be investigated to further improve the knowledge in this scientific field.

In surface sciences numerous well established techniques are already available, which allow for a detailed determination of interfacial processes. But for specific applications such as SAMs on gold, a deliberate choice has to be made to reveal meaningful results. Hence, for the specific characterization of protein adsorption and cell adhesion involving integrins, the most suitable techniques will be presented in the following section and a short justification for their application during the studies if this thesis will be given.

5) Surface Sensitive Analytical Techniques

Since interactions of biomaterials and biological environments predominantly occur on the surface of applied materials, the design and the surface properties strongly determine the fate of a biomaterial.[2] Therefore, the surface characterization is a central issue in this scientific field and has to be carried out thoroughly. In recent years, the sensitivity and accuracy of the analytical methods has made significant progress, providing the materials scientist with a large arsenal of different techniques.[9,10] Various microscopic, spectroscopic and thermodynamic methods have proven to give very detailed information on the composition and performance of biomaterials. In the following section the most important surface analysis techniques used within the studies of this thesis will be briefly presented and the basis for the decision to use these will be explained.

Atomic force microscopy (AFM)

The most common microscopic technique used in the field of polymeric biomaterials is atomic force microscopy (AFM).[104] This technology can provide information of the three dimensional surface structure with an extremely high resolution. Depending on the used equipment, features of only several nanometers can be detected.[105,106] One of its strongest benefits is the fact that surfaces can be investigated in vacuum, air and liquids without any necessary modifications before analysis.[107] Especially for biomaterials, which are more or less exclusively used in aqueous environments, this is a great benefit. Also materials that are supposed to change their appearance and properties, for example after swelling, can be characterized in their state after application.[105,106]

The principle of AFM is based on a tip attached to a cantilever, scanning a surface and measuring forces between the tip and the surface. The AFM can be operated in different modes: contact, non-contact and tapping mode. Since for our studies tapping mode seemed to be the most promising approach, only this mode will be presented in more detail here.

In tapping mode, the cantilever bearing the tip is forced to oscillate at or near its resonance frequency, reflecting a laser on the back of the tip to a split photodiode detector. The tip then lightly taps the sample surface with an amplitude in the range of few nanometers. This contact reduces the maximum amplitude of the oscillation. Therefore, in a feedback loop, the cantilever is raised by a piezoelectric device until the tip is again allowed to oscillate at

a certain amplitude. The data of these movements are transferred to a PC, calculating the three dimensional structure of the scanned surface. With this technique, images of a typical size of 500 x 500 nm^2 to 15 x 15 µm^2 are recorded.[107]

This tapping mode furthermore allows for characterizing material properties by creating so-called phase images. Using this mode, the phase difference between the oscillation of the piezoelectric crystal that drives the cantilever and the oscillation of the cantilever itself is measured. Since interactive forces between tip and surfaces are different for surfaces with different viscoelastic properties, modified surface characteristics can be visualized due to different phase shifts. This technique even was shown to have a higher spatial resolution than usual topography data of surfaces.[108,109]

In summary, the AFM may be an extremely useful tool for designing surfaces. Since it allows for the determination of topographical data and material properties simultaneously with a resolution in the nanometer scale, artificial surfaces can be characterized very detailed, what is especially important for a distinct characterization of the SAMs used as model systems within the studies of this thesis.

Surface plasmon resonance (SPR)

An optical technique which was shown to provide important information on surfaces is surface plasmon resonance (SPR). Here, the attenuated total reflectance of lasers at interfaces of materials with different optical densities is used to characterize the refractive index of approximately 300 nm above this interface. One of these materials has to be a metal, since it must exhibit free electron behavior, the other a dielectric. If the laser beam travels through the optical dense medium and reaches the medium with a lower density, the light is reflected into the dense medium. Nevertheless, a certain fraction of the laser energy is able to penetrate into the less dense medium to a distance of one wavelength, which is called the evanescent wave and propagates along the interface. If the incoming light meets a certain angle, this evanescent wave can resonantly excite the oscillating electrons of the metal, resulting in a loss of energy of the incoming light and the angle of the incoming light allowing for this interaction, the so-called SPR angle, depends on the refractive index right above the thin metal film. Hence, if this refractive index changes, for example due to the adsorption of proteins, also the SPR angle changes. Therefore, reactions on the surface can be monitored in a time resolved manner, allowing for the determination of kinetics as well as quantifications, since the indirectly measured refractive index depends on the concentration of molecules of interest near the surface.[110] In numerous studies the benefits

of SPR helped to characterize organic mono- or bilayers, polymer films and interactions of biomaterials with proteins, DNA and viruses, making it extremely interesting for our investigations in terms of biomaterials and cells. Especially for the characterization of protein adsorption, this tool was used extensively and thus can serve as a "standard technique" allowing for comparisons with literature data.

Matrix-assisted laser desorption/ionization – Time of flight (MALDI-ToF)

A surface sensitive mass spectrometry technique is matrix-assisted laser desorption ionization time-of-flight mass spectrometry (MALDI-ToF). Macromolecules on surfaces are analyzed by irradiation with pulsed UV lasers after coating with matrix molecules. These matrices in general are olefinic organic compounds of few hundred Da, such as sinapic acid, and are used to transfer the energy of the UV laser to the macromolecules on the surface.[111] The analytes subsequently are ejected to the vapor phase where their mass is analyzed due to the time they need to reach the detector. Since smaller compounds are accelerated stronger, the time they need is shorter. The great benefit of MALDI-ToF is the more or less unlimited mass detection range (except for mass regions below 500 Da), making it suitable for analyzing biomolecules and artificial polymers.[111] For PEG for example the mass distribution of this polymer could be characterized precisely in several studies.[112,113] A drawback of this technique is that it can only be applied after covering the surfaces with matrix compounds, making an in situ analysis impossible.[107] Moreover, this technique can not provide quantitative data.[114] However, especially for analyses in terms of polymer identification and characterization, this technique seems to be very promising. Since several polymers were synthesized in the studies of this thesis, MALDI-ToF was chosen as a potent identification method for these compounds.

Time of flight – secondary ion mass spectrometry (ToF-SIMS)

The second mass spectrometric method relevant for our investigations is time-of flight secondary ion mass spectrometry (ToF-SIMS), which is an extremely sensitive and effective technique to determine the composition of biomaterial surfaces.[115] In contrast to MALDI-ToF, in this case no special sample preparation is necessary. For analysis, the surfaces are treated with beams of ions or atoms of high energy (typically 5 – 25 keV).[116] The resulting fragments/ions generated by this bombardment then are accelerated in a vapor phase and as for MALDI-ToF analyzed by the time they need to reach the detector.

With this method, an extremely high mass resolution can be reached.[117] However, this technique is destructive in the area in which it is applied. On the other hand this allows penetrating into deeper regions of the biomaterial investigated, since with every laser shot the outermost atoms are removed from the surface.[116,118]

This technique moreover can not only be applied for the characterization of biomaterial composition, but also for interactions with biomolecules.[118] Since for every compound typical fragments are generated by the laser bombardment, compounds can be identified by the resulting fragment pattern.[119] By analyzing larger surface areas and looking for certain fragments, it is even possible to map the distribution of certain compound on the surface, as it was done for micropatterned surfaces for example.[120]

Hence, this technique provides the possibility to characterize protein – surface interactions with an extremely high sensitivity, allowing for the determination, whether surfaces can resist the adsorption of proteins for example.

Water contact angle measurements (WCA)

Also thermodynamic methods are used for the characterization of surfaces. Before the microscopic techniques that are used today were developed, more or less all interest was focused on macroscopic properties such as surface tension and wetting properties.[101] In fact, the great potential of investigations on wettability and on hydrophilicity or hydrophobicity, respectively, is still recognized today.[121]

The major thermodynamic methods used today are based on contact angle measurements. This straightforward technique is carried out by determining the angle of the tangent associated with a sessile drop and a biomaterial surface in air. This angle is assumed to be determined by the outermost 3 –10 Å of a surface.[115] This method can provide useful information on the wettability of a surface in relatively short time, but it is sensitive enough to follow surface modifications of polymers.[107] However, caution has to be paid in terms of wettability, if surfaces are analyzed that are allowed to swell after setting the fluid drop on the material.[61,106]

Therefore, this technique may offer the possibility to determine slight modifications of artificial surfaces, such as the conversion of different functional groups of polymeric materials, what may be of great interest in the characterization of cell – biomaterial interactions.

Quartz crystal microbalance (QCM)

In recent years, a complementing analytical technique has emerged as a very valuable tool in the characterization of interfacial reactions. Based on the piezoelectric effect, Sauerbrey in the 1950s found a linear relationship for mass deposition and the frequency responses of oscillating quartz discs, therefore he called such devices quartz crystal microbalances (QCM).[123] In the 1980s, Nomura and Okuhara found oscillator circuits that allowed for applying this technique not only in vacuum or air, but also in liquids.[124] This was more or less the starting point for the development of this valuable tool in biotechnology. The high sensitivity (in the range of nanograms) of these devices, the possibility to characterize interfacial reactions in situ and label free, and the chance to determine these reactions in a time resolved manner made this method very attractive.[125]

If an electric field is applied to a quartz disc, ions within the quartz are slightly displaced. Inversing and repeating this step by applying a DC voltage leads to the generation of a material wave in the quartz. Depending on the cut angle, different resonator types can be generated, such as thickness-shear-mode, plate and flexural resonators. Since the temperature coefficient of thickness-shear-mode resonators is almost 0 between 0 and 50°C, this is the most suitable for QCM resonators.[125]

Applying a DC voltage leads to the generation of a material wave with a certain resonance frequency propagating into the medium above the quartz disc. In liquids, the decay length of this wave is approximately 250 nm.[126] If now rigid masses adsorb tightly to the resonator and in an ideal case one assumes the material properties of quartz and adsorbed mass as equal, the wavelength of the material wave has be elongated to fulfill the resonance conditions. But then, since the velocity remains the same, the resonance frequency is decreasing. Hence if rigid masses adsorb, the resonance frequency decreases proportionally to the amount of mass, described by Sauerbrey in equation (2).[124]

$$\Delta f = -\frac{2f_o{}^2}{A\sqrt{\rho_q \mu_q}}\Delta m \qquad (2)$$

(f = frequency; f_0 = fundamental frequency; A = sensor area; ρ_q = density of the quartz; μ = displacement; m = mass)

This relation of frequency shift and mass adsorption makes the QCM a valuable tool for characterizing adsorption reactions, the covalent attachment of peptides and proteins to surfaces, the evolution of material films (including indirect thickness measurements) and the determination of the kinetics of ligand – receptor interactions.[127] Although there are also some significant drawbacks, such as non-ideal behavior in the case of viscoelastic materials, the different mass sensitivity in the center and on the edges of the resonator or the limit of detection of layers thicker than 250 nm, this technique seems to be very powerful.[125] Moreover, in recent years, several groups also could show the detectability of cell adhesion processes using the QCM, making it an ideal technique for the aim to characterize protein adsorption as well as cell adhesion.[128,129,130] With this technique, both goals could be achieved using the same technique.

6) Goals of the Thesis

The previous sections showed that interactions of cells with biomaterials are a very complex phenomenon. Consequently, further investigations have to be realized to improve the performance of artificial materials. Based on the self-assembly concept of alkanethiols on gold, it was therefore the goal of this thesis to develop a straightforward and versatile model system for PEG-rich biomaterials, which can be used to assess the interactions of cells with such materials. The developed model had to consist of a layer of PEG, which is packed with a reasonable density to reduce interactions with proteins and, therefore, with cells to a high extent, exploiting the steric repulsion effect, as it is the case for numerous biomaterials with attached PEG chains. The necessary polymers for such a system had to be synthesized and characterized intensively. Also the model system itself had to be defined exactly, to be able to draw conclusions on how different parameters influence the corresponding interactions. Especially the impact of the end group modifications of the PEG moiety on protein adsorption had to be investigated, as well as the ability to reduce or induce the adhesion of cells. In addition, the correlation of the results of the simplified model system and a biomaterial, which is frequently used (PEG-PLA), was of outstanding interest.

Biomaterials exhibiting PEG on the surface are described in numerous studies to reduce non-specific protein adsorption.[7,44] Since investigations of this phenomenon on the surface may strongly be hampered by intrinsic effects of the underlying biomaterial, such as swelling or erosion, simplified model systems, for instance self-assembled monolayers (SAMs), may be of great advantage. Hence, it was the aim to synthesize and characterize polymers that allow for producing SAMs that can suppress protein adsorption as far as possible, in the best case to exclude it completely. To be as close to the real biomaterial surface as possible, we did not only investigate oligo(ethylene glycol) surfaces, which are frequently described in literature, but aimed to characterize high molecular weight poly(ethylene glycol) derivatives. To achieve this goal, in **Chapter 2** the modification of poly(ethylene glycol) monomethyl ether with alkanethiols for the generation of SAMs on gold, using a new synthesis strategy, is described. These surfaces were analyzed extensively using different techniques, such as AFM or contact angle measurements. Also the formation of SAMs with these polymers was determined by means of the QCM

technique. Moreover, the ability to reduce the non-specific adsorption of single proteins, as well as complex protein mixtures was investigated with SPR, Tof-SIMS and contact angle measurements to reveal, whether these surfaces can be used as model systems for investigating further cell – biomaterial surface interactions.

Modern biomaterials not only have to be biocompatible, but also tend to use the biomimetic concept of specific cell signaling via attached bioactive compounds. The necessary functional groups of the polymers consequently had to be introduced to the developed SAMs. Therefore, a different PEG derivative containing an amine end group also was modified with alkanethiols in order to generate SAMs presenting these functional groups for subsequent modifications with biomolecules. We demonstrated that the developed synthesis strategy also is applicable to the amine functionalized PEG derivative. The success of the synthesis was shown by NMR, HPLC and MALDI-ToF. The impact of this end group modification on the physicochemical characteristics of the resulting SAMs, such as their wettability, and protein adsorption were evaluated using QCM, SPR and contact angle measurements. Also the attachment of peptidic cell adhesion motifs to the SAM surfaces was shown to be successful. **(Chapter 3)**.

The quartz crystal microbalance was assumed to provide us with further details of the initial steps of cellular adhesion compared to conventional cell culture techniques, since it can provide this information in real-time. Thus, we tried to qualify a QCM equipment, which so far was not applied to evaluate cell adhesion processes. With this setup, the adhesion characteristics on protein-repellant SAMs were investigated. Also the proof of principle of the biomimetic concept, which means to reduce non-specific interactions, but to allow a specific cell signaling, was aimed to be elucidated by attaching cell adhesion peptides to SAMs. Moreover, detachment processes with the enzyme trypsin and soluble cell adhesion peptides and the influence of different medium compositions were characterized to demonstrate the benefits of this QCM equipment in terms of the real-time assessment of cell adhesion processes **(Chapter 4)**.

In **Chapter 5** problems of the QCM technique in terms of the quantification of cell adhesion are described and suggestions, how to overcome these challenges, are made. To evade the drawback of the different lateral sensitivity of the sensor surface, a homogeneous distribution of cells has to be guaranteed. Therefore, the pump speed of the dynamic flow-

through setup had to be adjusted, the success of this strategy is demonstrated. Moreover, an improved QCM technique, measuring the viscoelastic properties of adhesive layers also is presented, which can avoid problems with the distribution of cells in the QCM system by determining "fingerprints" of cell adhesion processes independently of the spatial distribution. Additionally, with this so-called QCM-D technique it is possible to get information on the adhesion strength of cells on the corresponding surface, what is shown by analyzing cell adhesion under serum-free and serum-containing conditions.

Besides attaching adhesion peptides to surfaces, also tethering growth factors is a common concept in the field of biomimetic materials. Growth factors and cell adhesion receptors are described to share certain signaling pathways in cells. Since the impact of cell adhesion on growth factor signaling is well described, but on the other hand very little is known about the impact of growth factors on cell attachment, we aimed to investigate this phenomenon by adding soluble growth factors to the culture medium and by attaching this signaling molecules to the SAMs. To achieve this goal, we treated cells with growth factors for different time scales and with different concentrations. By determining the extent of cell adhesion using the QCM technique, we even could draw conclusions on the molecular mechanisms of the growth factor – cell interactions. **(Chapter 6)**.

Moreover, of course, it was a goal to assess, whether the results obtained with our developed model system are in agreement with results of the biomaterials they should mimic. Therefore, we additionally characterized the physicochemical properties of PEG-PLA film surfaces and investigated protein adsorption and cell adhesion on these biomaterials, using the same analytical techniques as for the model system. The impact of polymer end groups on the contact angle of PEG-PLA films was shown, as well as the consequences on the protein adsorption characteristics. Furthermore, influences of different molecular weight compositions on interactions with cell suspensions are presented **(Chapter 7)**.

Hence by performing these studies, we aimed to get a more detailed understanding of the complex interactions of PEG-rich biomaterials with biological environments. The acquired results may help to design new biomaterials, which allow for a more specific signaling on material surfaces to improve the overall performance of artificial materials applied to heal or at least attenuate tissue defects of the human body.

References

[1] http://www.the-infoshop.com/annual/es40660-usa-medical.html

[2] Castner D.G.; Ratner B.D.: Biomedical surface science: foundations to frontiers. Surf Sci, 500, 28-60, 2002.

[3] Dillow A.K.; Tirrell M.: Targeted cellular adhesion at biomaterial interfaces. Curr Opin Sol State. 3, 252 – 259, 1998.

[4] Clinical applications of Biomaterials. NIH Consens Statement 1982. Nov 1-3; (4)5; 1-19.

[5] Klee D.; Hoecker H.: Polymers for biomedical applications: Improvement of the interface biocompatibility. Adv Poly Sci, 149, 1-57.

[6] Klinkmann H.; Falkenhagen D.; Courtney J.M.; Gurland H.J.: Uremia therapy. Springer, Berlin Heidelberg New York, 1987.

[7] Lee J.H.; Lee H.B.; Andrade J.D.: Blood compatibility of polyethylene oxide surfaces. Prog Polym Sci, 20, 1043-1079, 1995.

[8] Tirrell M.; Kokkoli E.; Biesalski M.: The role of surface science in bioengineered materials. Surf Sci, 500, 61-83, 2002.

[9] Hubbell J.A.: Biomaterials in tissue engineering. Biotechnology, 13, 565-576,1995.

[10] Parent C.A.; Devrotes P.N.: A cell's sense of direction. Science, 284, 765-770, 1999.

[11] Ratner B.D.: Advances in the analysis of biomedical interest. Surf Interf Anal, 23, 521-528, 1995.

[12] Wilson C.J.; Clegg R.E.; Leavesley D.I.; Pearcy M.J.: Mediation of biomaterial-cell interactions by adsorbed proteins: A review. Tissue Engineering, 11, 1/2, 1-18, 2005.

[13] Facheux N.; Schweiss R.; Lützow K.; Werner C.; Groth T.: Self-assembled monolayers with different terminating groups as model substrates for cell adhesion studies. Biomaterials, 25, 2721-2730, 2004.

[14] Haynes C.A.; Norde W.: Globular proteins at solid/liquid interfaces. Colloids Surfaces B Biointerfaces, 2, 517-566, 1994.

[15] Horbett T.A.: Proteins: Structure, properties and adsorption to surfaces. In: Ratner B.D.; Hoffmann A.S.; Schoen F.J.; Lemons J.E.: Biomaterials Science, San Diego, CA: Academic Press, 133-141, 1996.

[16] Norde W.: Adsorption of proteins from solution at the solid–liquid interface. Adv Colloid Interface Sci, 25, 267-340, 1986.

[17] Norde W.: Driving forces for protein adsorption at solid surfaces. In: Malmsten M., Biopolymers at Interfaces. New York: Marcel Dekker, 27–54, 1998.

[18] Vogler E.A.: Structure and reactivity of water at biomaterial surfaces. Adv. Colloid Interface Sci. 74, 69-117, 1998.

[19] Worch H.: Special thin organic coatings. In: Helsen J.A.; Breme H.J.: Metals as Biomaterials. Chichester: John Wiley & Sons, 177–196, 1998.

[20] Jönsson U.; Ivarsson B.; Lundström I.; Berghem L.: Adsorption behavior of fibronectin on well characterized silica surfaces. J Colloid Interface Sci, 90, 148-163, 1982.

[21] Absolom D.R.; Zingg W.; Neumann A.W.: Protein adsorption to polymer particles: Role of surface properties. J Biomed Mater Res, 21, 161-171, 1987.

[22] MacDonald D.E.; Deo N.; Markovic B.; Stranick M.; Somasundaran P.: Adsorption and dissolution behavior of human plasma fibronectin on thermally and chemically modified titanium dioxide particles. Biomaterials 23, 1269-1279, 2002.

[23] Bohnert J.A.; Horbett T.A.: Changes in adsorbed fibrinogen and albumin interactions with polymers indicated by decreases in detergent elutability. J Colloid Interface Sci, 111, 363-377, 1986.

[24] Horbett T.A.: Biological activity of adsorbed proteins. In: Malmsten M.: Biopolymers at Interfaces. New York: Marcel Dekker, 393–413, 2003.

[25] Horbett T.A.: The role of adsorbed proteins in animal cell adhesion. Colloids Surfaces B Biointerfaces 2, 225-240, 1994.

[26] Horbett T.A.: The role of adsorbed adhesion proteins in cellular recognition of biomaterials. Biomaterials Science, 2nd Edition, 237-246, 2004.

[27] Norde W.; Giacomelli C.E.: Conformational changes in proteins at interfaces: From solution to the interface, and back. Macromol Symp, 145, 125-136, 1999.

[28] Giacomelli C.E.; Norde W.: The adsorption–desorption cycle: Reversibility of the BSA–silica system. J. Colloid Interface Sci. 233, 234-240, 2001.

[29] Norde W., Haynes C.A.: Reversibility and the mechanism of protein adsorption. In: Horbett T.A.; Brash J.L.: Proteins at Interfaces II: Fundamentals and Applications. Washington, D.C.: American Chemical Society, 26–40, 1995.

[30] Hanein D.; Geiger B.; Addadi L.: Fibronectin adsorption to surfaces of hydrated crystals: An analysis of the importance of bound water in protein substrate interactions. Langmuir, 9, 1058-1065, 1993.

[31] Brash J.L.; Horbett T.A.: Proteins at interfaces: An overview. In: Horbett T.A.; Brash J.L.: Proteins at Interfaces II: Fundamentals and Applications. Washington, D.C.: American Chemical Society, 1–23, 1995.

[32] Bacakova L.; Filova E.; Rypacek F.; Svorcik V.; Stary V.: Cell adhesion on artificial materials for tissue engineering. Physiol Res, 53, Suppl. 1, S35-S45, 2004.

[33] Aplin A.E.; Howe A.K.; Juliano R.L.: Cell adhesion molecules, signal transduction and cell growth. Curr Opin Cell Biol, 11, 737-744, 1999.

[34] Hersel U., Dahmen C., Kessler H.: RGD modified polymers: biomaterials for stimulated cell adhesion and beyond. Biomaterials, 24, 4385-4415, 2003.

[35] Newham P.; Humphries M.J.: Integrin adhesion receptors: structure, function and implications for biomedicine. Mol Medicine Today, July 1996, 304-313, 1996.

[36] Bale M.D.; Wohlfahrt L.A.; Mosher D.F.; Tomasini B.; Sutton R.C.: Identification of vitronectin as a major plasma protein adsorbed on polymer surfaces of different copolymer composition. Blood, 74, 2698-2706, 1989.

[37] Dalton S.L.; Marcantonio E.E.; Assoian R.K.: Cell attachment controls fibronectin and $\alpha5\beta1$ integrin levels in fibroblasts. J. Biol. Chem. 267, 8186-8191, 1992.

[38] Burridge K.; Fath K.: Focal contacts: Transmembrane links between the extracellular matrix and the cytoskeleton. Bioessays 10, 104-108, 1989.

[39] Owen G. R.; Meredith D.O.; Gwynn I; Richards R.G: Focal adhesion quantification – A new assay of material biocompatibility? : Review. Eur Cells Mater, 9, 85-96, 2005.

[40] Van Kooten T.G.; von Recum, A.F.: Cell adhesion to textured silicone surfaces: The influence of time of adhesion and texture on focal contact and fibronectin fibril formation. Tissue Eng. 5, 223-240, 1999.

[41] Webb K.; Hlady V.; Tresco P.A.: Relationships among cell attachment, spreading, cytoskeletal organization, and migration rate for anchorage-dependent cells on model surfaces. J. Biomed Mater Res 49, 362-368, 2000.

[42] Gronthos S.; Simmons P.J.; Graves S.E.; Robey P.G.: Integrin-mediated interactions between human bone marrow stromal precursor cells and the extracellular matrix. Bone, 28, 174-181, 2001.

[43] Garcia A.J.; Vega M.D.; Boettiger D.: Modulation of cell proliferation and differentiation through substrate dependent changes in fibronectin conformation. Mol Biol Cell, 10, 785-798, 1999.

[44] Kingshott P.; Griesser H.J.: Surfaces that resist bioadhesion. Curr Opin Solid St M, 4, 403-412, 1999.

[45] Baier R.E.; Dutton R.C.: Initial events in interactions of blood with a foreign surface. J Biomed Mater Res, 3, 191-206, 1969.

[46] Hsiue G.H.; Lee S.D.; Chang P.C.; Kao C.Y.: Surface characterization and biological properties study of silicone rubber membrane grafted with phospholipid as biomaterial via plasma induced graft copolymerization. J Biomed Mater Res, 42, 134-147, 1998.

[47] Van der Heiden A.P.; Willems G.M.; Lindhout T.; Pijpers A.P.; Koole L.H.: Adsorption of proteins onto poly(ether urethane) with a phosphorylcholine moiety and influence or preadsorbed phospholipid. J Biomed Mater Res, 40, 195-203, 1998.

[48] Iwasaki Y.; Sawada S.I.; Nakabayashi N.; Khang G.; Lee H.B.; Ishihara K.: The effect of the chemical structure of the phospholipid polymer on fibronectin adsorption and fibroblast adhesion on the gradient phospholipid surface. Biomaterials, 20, 2185-2191, 1999.

[49] Marra K.G.; Winger T.M.; Hanson S.R.; Chaikof E.L.: Cytomimetic biomaterials. 1. In situ polymerization of phospholipids on an alkylated surface. Macromolecules, 30, 6483-6488, 1997.

[50] Kingshott P.: Interfacial interactions of protein and lipid adsorption to contact lens surfaces, PhD thesis, University of New South Wales, Sydney, Australia, 1998.

[51] McArthur S.L.; McLean K.M:; Kingshott P.; St.John H.A.W.; Chatelier R.C.; Griesser H.J.: Effect of polysaccharide structure on protein adsorption. Colloids Surf, B, Biointerfaces, 17,1,37-48, 2000.

[52] Hiatt C.W.; Shelokow A.; Rosenthal E.J.; Galimore J.M.: Treatment of controlled pore glass with poly(ethylene oxide) to prevent adsorption of rabies virus. J Chromatogr, 56, 362, 1971.

[53] Hawk G.L.; Cameron J.A.; Dufault L.B.: Chromatography of biological materials on polyethylene glycol-treated controlled-pore glass. Prep Biochem, 2, 193-203, 1972.

[54] Lee J. H.; Kopecek J.; Andrade J. D. : Protein-resistant surfaces prepared by PEO-containing block copolymer surfactants. J Biomed Mater Res, 23(3), 351-68,1989.

[55] Jeon S.I.; Lee J.H.; Andrade J.D.; De Gennes P.G.: Protein-surface interactions in the presence of polyethylene oxide. J Colloid Interface Sci, 142, 149-158, 1991.

[56] Unsworth L.D.; Sheardown H.; Brash J.L.: Polyethylene oxide surfaces of variable chain density by chemisorption of PEO-thiol on gold: adsorption of proteins from plasma studied by radiolabelling and immunoblotting. Biomaterials, 26, 5927-5933, 2005.

[57] Unsworth L.D.; Sheardown H.; Brash J.L.: Protein resistance of surfaces prepared by sorption of end-thiolated poly(ethylene glycol) to gold: effect of surface chain density. Langmuir, 21, 1036-1041, 2005.

[58] De Gennes P.G.: Scaling theory of polymer adsorption. Le Journal de Physique, 37, 1445-1452, 1976.

[59] Vermette P.; Meagher L.: Interactions of phospholipid and poly(ethylene glycol)-modified surfaces with biological systems: Relation to physicochemical properties and mechanisms. Coll Surf, B, Biointerfaces, 28, 153-189, 2003.

[60] Tessmar J.; Mikos T.; Goepferich A.: The use of poly(ethylene glycol)-block-poly(lactic acid) derived copolymers for the rapid creation of biomimetic surfaces. Biomaterials, 24, 4475-4486, 2003.

[61] Lieb E.; Tessmar J.; Hacker M.; Fischbach C.; Rose D.; Blunk T.; Mikos A.G.; Goepferich A.; Schulz M.B.: Poly(D,L-lactic acid)-poly(ethylene glycol)-monomethyl ether diblock copolymers control adhesion and osteoblastic differentiation of marrow stromal cells. Tissue Eng, 9, 1, 71-84, 2003.

[62] Lieb E.; Hacker M.; Tessmar J.; Kunz-Schughart L.A.; Fiedler J.; Dahmen C.; Hersel U.; Kessler H.; Schulz M.B.; Goepferich A.: Mediating specific sell adhesion to low adhesive diblock copolymers by instant modification with cyclic RGD peptides. Biomaterials, 26, 2333–2341.

[63] Lucke, A., Tessmar, J., Schnell, E., Schmeer, G., Göpferich, A.: Biodegradable poly(D,L-lactic acid)-poly(ethylene glycol) monomethyl ether diblock copolymers. Structures and surface properties relevant to their use as biomaterials. Biomaterials, 21, 2361-2370, 2000.

[64] Wang S.; Cui W.; Bei J.: Bulk and surface modification of polylactide. Anal Bioanal Chem, 381, 547-556, 2005.

[65] Hacker M.; Tessmar J.; Neubauer M.; Blaimer A.; Blunk T.; Goepferich A.; Schulz M.B.: Towards biomimetic scaffolds: anhydrous scaffold fabrication from biodegradable amine-reactive diblock copolymers. Biomaterials, 24 (24), 4459-4473, 2003.

[66] v. Burkersroda F.; Gref R.; Goepferich A.: Erosion of biodegradable block copolymers made of poly(D,L-lactic acid) and poly(ethylene glycol). Biomaterials, 16, 1599-1607, 1997.

[67] Pale-Grosdemange C.; Simon E.S.; Prime K.L.; Whitesides G.M.: Formation of self-assembled monolayers by chemisorption of derivatives of oligo(ethylene glycol) of structure $HS(CH_2)_{11}(OCH_2CH_2)_mOH$ on gold. J Am Chem Soc, 113, 12-20, 1991.

[68] Mrksich M.; Whitesides G.M.: Patterning self-assembled monolayers using microcontact printing: a new technology for biosensors? Trends Biotechnol, 13, 228-235, 1995.

[69] Mrksich M.; Dike L.E.; Tien J.; Ingber D.E., Whitesides G.M.: Using microcontact printing to pattern the attachment of mammalian cells to self-assembled monolayers of alkanethiolates on transparent films of gold and silver. Exp Cell Res, 235, 305-313, 1997.

[70] Alberts B.; Bray D.; Lewis J.; Raff M.; Roberts K.; Watson J.D.: Molecular biology of the cell, 3rd edition, Garland Publishing, New York, NY, USA, 1994.

[71] Nilsson S.: Structural and functional aspects of β_1 integrin signaling. Digital Comprehensive Summaries of Uppsala Dissertations from the Faculty of Medicine 136, Acta Universitatis Upsaliensis Uppsala, 2006.

[72] Van der Flier A.; Sonnenberg A.: Function and interactions of integrins. Cell Tissue Res, 305, 285-298, 2001.

[73] Hynes R.O.; Integrins: versatility, modulation, and signaling in cell adhesion. Cell, 69, 1, 11-25, 1992.

[74] Sastry S.K.; Horwitz A.F.: Integrin cytoplasmic domains: mediators of cytoskeletal linkages and extra- and intracellular initiated transmembrane signaling. Curr Opin Cell Biol, 5, 5, 819-831, 1993.

[75] Juliano R.L.: Signal transduction by cell adhesion receptors and the cytoskeleton: Functions of integrins, cadherins, selectins and immunglobulin-superfamily members. Annu Rev Pharmacol Toxicol, 42, 283-323, 2002.

[76] Hynes R.O.: Integrins: bidirectional, allosteric signaling machines. Cell, 110, 6, 673-87, 2002.

[77] Vinogradova O.: A structural mechanism of integrin alpha(IIb)beta(3) "inside-out" activation as regulated by its cytoplasmic face. Cell, 110, 5, 587, 2002.

[78] Hall A.: Rho GTPases and the control of cell behavior. Biochem Soc Trans, 33, 5, 891-895, 2005.

[79] Frisch S.M.: Control of adhesion-dependent cell survival by focal adhesion kinase. J Cell Biol, 134,3, 793-799, 1996.

[80] Horton M.A.: Arg-Gly-Asp (RGD) peptides and peptidomimetics as therapeutics: Relevance for renal diseases. Exp Nephrol, 7, 178-184, 1999.

[81] Ojima I.; Chakravarty S.; Dong Q.: Antithrombotic agents: From RGD to peptide mimetics. Bioorganic and Medicinal Chemistry, 3, 4, 337-360, 1995.

[82] Massia S.P.; Hubbel J.A.: Covalent surface immobilization of Arg-Gly-Asp and Tyr-Ile-Gly-Ser-Arg containing peptides to obtain well defined cell-adhesive substrates. Anal Biochem, 187, 292-301, 1990.

[83] Schreiber F.: Structure and growth of self-assembling monolayers. Prog Surf Sci, 65, 151-256, 2000.

[84] Pale-Grosdemange C.; Simon E.S.; Prime K.L.; Whitesides G.M.: Formation of self-assembled monolayers by chemisorption of derivatives of oligo(ethylene glycol) of structure $HS(CH_2)_{11}(OCH_2CH_2)_mOH$ on gold. J Am Chem Soc, 113, 12-20, 1991.

[85] Tokumitsu S.; Liebich A.; Herrwerth S.; Eck W.; Himmelhaus M.; Grunze M.: Grafting of alkanethiol-terminated poly(ethylene glycol) on gold. Langmuir, 18, 8862-8870, 2002.

[86] Vanderah D.J.; Pham C.P.; Springer S.K.; Silin V.; Meuse C.W.: Characterization of a series of self-assembled monolayers of alkylated 1-thiaoligo(ethylene oxides)$_{4-8}$ on gold. Langmuir, 16, 6527-6532, 2000.

[87] Harder P.; Grunze M.; Dahint R.; Whitesides G.M.; Laibinis P.E.: Molecular conformation in oligo(ethylene glycol)-terminated self-assembled monolayers on gold and silver surfaces determines their ability to resist protein adsorption. J Phys Chem B, 102, 426-436, 1998.

[88] Biebuyck H.A.; Bain C.D.; Whitesides G.M.: Comparison of organic monolayers on polycrystalline gold spontaneously assembled from solutions containing dialkyl disulfides or alkanethiols. Langmuir, 10, 1825-1831, 1994.

[89] Scherer J.; Vogt M.R.; Magnussen O.M.; Behm R.J.: Corrosion of Alkanethiol-Covered Cu(100) Surfaces in Hydrochloric Acid Solution Studied by in-Situ Scanning Tunneling Microscopy. Langmuir, 13, 7045-7051, 1997.

[90] Facheux N.; Schweiss R.; Lützow K.; Werner C.; Groth T.: Self-assembled monolayers with different terminating groups as model substrates for cell adhesion studies. Biomaterials, 25, 2721-2730, 2004.

[91] Xiao X.; Hu J.; Charych D.H.; Salmeron M.: Chain Length Dependence of the Frictional Properties of Alkylsilane Molecules Self-Assembled on Mica Studied by Atomic Force Microscopy. Langmuir, 12, 235-237, 1996.

[92] Sagiv J.: Organized monolayers by adsorption. 1. Formation and structure of oleophobic mixed monolayers on solid surfaces. J Am Chem Soc, 102, 92-98, 1980.

[93] Camillone N.; Eisenberger P.; Leung T.Y.B.; Schwartz P.; Scoles G.; Poirier G.E.; Tarlov M.J.: New monolayer phases of n-alkane thiols self-assembled on Au(111): Preparation, surface characterization, and imaging. J Chem Phys, 101, 11031-11036, 1994.

[94] Staub R.; Toerker M.; Fritz T.; Schmitz-Huebsch T.; Sellam F.; Leo K.: Flat Lying Pin-Stripe Phase of Decanethiol Self-Assembled Monolayers on Au(111). Langmuir, 14, 6693-6698, 1998.

[95] Barrena E.; Ocal C.; Salmeron M.: Evolution of the structure and mechanical stability of self-assembled alkanethiol islands on Au(111) due to diffusion and ripening. J Chem Phys, 111, 9797-9802, 1999.

[96] Bain C.D.; Troughton E.B.; Tao Y.T.; Evall J.; Whitesides G.M.; Nuzzo R.G.: Formation of monolayer films by the spontaneous assembly of organic thiols from solution onto gold. J Am Chem Soc, 111, 321-335, 1989.

[97] Dannenberger O.; Buck M.; Grunze M.: Self-assembly of n-alkanethiols: A kinetic study by second harmonic generation. J Phys Chem B, 103, 2202-2213, 1999.

[98] Himmelhaus M.; Eisert F.; Buck M.; Grunze M.: Self-assembly of n-alkanethiol monolayers. A Study by IR-visible sum frequency spectroscopy (SFG). J Phys Chem B, 104, 576-584, 2000.

[99] Saito N.; Matsuda T.: Protein adsorption on self-assembled monolayers with water soluble non-ionic oligomers using quartz-crystal microbalance. Materials Science and Engineering C, 6, 261-266, 1998.

[100] Mrksich M.; Whitesides G.M.: Patterning self-assembled monolayers using microcontact printing: a new technology for biosensors? Trends Biotechnol, 13, 228-235, 1995

[101] Mrksich M.; Dike L.E.; Tien J.; Ingber D.E., Whitesides G.M.: Using microcontact printing to pattern the attachment of mammalian cells to self-assembled monolayers of alkanethiolates on transparent films of gold and silver. Exp Cell Res, 235, 305-313, 1997.

[102] Houseman B.T.; Mrksich M.: Efficient solid phase synthesis of peptide substituted alkanethiols for the preparation of substrates that support the adhesion of cells. J Org Chem, 63, 7552-7555, 1998.

[103] Herrwerth S.; Rosendahl C.; Feng C.; Fick J.; Eck W.; Himmelhaus R.; Dahint R.; Grunze M.: Covalent coupling of antibodies to self-assembled monolayers of carboxy-functionalized poly(ethylene glycol): Protein resistance and specific binding of biomolecules. Langmuir, 19, 1880-1887, 2003.

[104] I. Amato: Biomaterials. Reverse engineering the ceramic art of algae. Science, 276, 1982, 1997.

[105] Vansteenkiste S. O.; Davies M. C.; Roberts C. J.; Tendler S. J. B.; Williams P. M.: Progress in Surface Science, 57, 95-136, 1998.

[106] Werner C., Jacobasch H. J.: Surface characterization of polymers for medical devices. Int J Artificial Organs, 22, 160-176, 1999.

[107] Merret K.; Cornelius R.M.; McClung W.G.; Unsworth L.D.; Sheardown H.: Surface analysis methods for characterizing polymeric biomaterials. J Biomater Sci Polymer Edn, 13, 6, 593-621, 2002.

[108] Holland N. B.; Marchant R. E.: Individual plasma proteins detected on rough biomaterials by phase imaging AFM. J Biomed Mater Res, 51, 307-315, 2000.

[109] Cullander C.: Light microscopy of living tissue: the state and future of the art. J Invest Dermatol, Symp Proc, 32, 166-171, 1998.

[110] Green R.J.; Frazier R.A.; Shakesheff K.M.; Davies M.C.; Roberts C.J.; Tendler S.J.B.: Surface Plasmon Resonance analysis of dynamic biological interactions with biomaterials. Biomaterials, 21, 1823-1835, 2000.

[111] Gross M. L.: Mass Spectrometry in the Biological Sciences: A Tutorial, Series C: Mathematical and Physical Sciences, 353. Kluwer Academic Publishers, Boston, 1992.

[112] Kinumi T.; Saisu T.; Takayama M.; Haruki N.: Matrix-assisted laser desorption/ionization time-of-flight mass spectrometry using an inorganic particle matrix for small molecule analysis. J Mass Spect, 35, 417-422, 2000.

[113] Knerr R.; Weiser B.; Drotleff S.; Steinem C.; Goepferich A.: Self-assembling PEG Derivatives for Protein-repellant Biomimetic Model Surfaces on Gold. Biomaterialien, , 7 (1), 12-20, 2006.

[114] McLean K.M.; McArthur S.L.; Chatelier R.C.; Kingshott P.; Griesser H.J.: Hybrid biomaterials: Surface-MALDI mass spectrometry analysis of covalent binding versus physisorption of proteins. Coll Surf B, Biointerfaces, 17, 23-35, 2000.

[115] Johnston E.E.; Ratner B.D.: Surface characterization of plasma deposited organic thin films. J Elec Spectroscopy and Related Phenomena, 81, 303-317, 1996.

[116] Ratner B.D.; Tyler B.J.; Chilkoti A.: Analysis of biomedical polymer surfaces: polyurethanes and plasma-deposited thin films. Clinical Materials 13, 71-84, 1993.

[117] Griesser H.J.; Kingshott P.; McArthur S.L.; McLean K.; Kinsel G.R.; Timmons R.B.: Surface MALDI mass spectrometry in biomaterials research. Biomaterials, 25, 4861-4875, 2004.

[118] Leonard D.; Mathieu H. J.: Characterisation of biomaterials using ToF-SIMS. Fresenius´ J Anal Chem, 365, 3, 1999.

[119] Perez-Luna V. H.; Hooper K. A.; Kohn J.; Ratner B. D.: Surface characterization of tyrosine-derived polycarbonates. J Appl Polymer Sci, 63, 1467-1479, 1997.

[120] Belu A.M.; Graham D.J.; Castner D.G.: Time-of-flight secondary ion mass spectrometry: techniques and applications for the characterization of biomaterial surfaces. Biomaterials, 24, 3635-3653, 2003.

[121] De Queiroz A. A. A.; Barrak E. R.; de Castro S. C.: Thermodynamic analysis of the surface of biomaterials. J Mol Structure, 394, 271-279, 1997.

[123] Sauerbrey G.: The use of quartz oscillators for weighing thin layers and for microweighing. Z phys, 155, 206-222, 1959.

[124] Nomura T.; Okuhara M.: Frequency shifts of piezoelectric quartz crystals immersed. in organic solvents. Anal Chim Acta, 281-284, 1982.

[125] Janshoff A.; Galla H.J.; Steinem C.: Piezoelectric mass-sensing devices as biosensors – an alternative to optical biosensors? Angewandte Chemie, Int Ed, 39, 4004-4032, 2000.

[126] Fredriksson C.; Kihlmann S.; Kasemo B.; Steel D.M.: In vitro real-time characterization of cell attachment and spreading. J Mat Sci, 9, 785 –788, 1998.

[127] O´Sullivan C.K.; Guilbault G.G.: Commercial quartz crystal microbalances - theory and applications. Biosensors and bioelectronics, 14, 663- 670, 1999

[128] Fredriksson C.; Kihlmann S.; Kasemo B.; Steel D. M.: In vitro real-time characterization of cell attachment and spreading. J Mater Sci, 9, 785-788, 1998.

[129] Marx K.A.; Zhou T.; Montrone A.; McIntosh D.; Braunhut S.J.: Quartz crystal microbalance biosensor study of endothelial cells and their extracellular matrix following cell removal: Evidence for transient cellular stress and viscoelastic changes during detachment and the elastic behavior of the pure matrix. Anal Biochem, 343, 23-34, 2005.

[130] Wegener J.; Janshoff A.; Galla H.J.: Cell adhesion monitoring using a quartz crystal microbalance: comparative analysis of different mammalian cell lines. Eur Biophys J, 28, 26-37, 1998.

[131] Drotleff S.; Lungwitz U.; Breunig M.; Dennis A.; Blunk T.; Tessmar J.; Göpferich A.: Biomimetic polymers in pharmaceutical and biomedical sciences. Eur J Pharm Biopharm, 58, 385-407, 2004.

Chapter 2

Synthesis and Characterization of Self-assembling Thioalkylated PEG Derivatives

R. Knerr[1], S.Drotleff[1], C.J. Roberts[2], C. Steinem[3], A. Göpferich[1]

[1] Department of Pharmaceutical Technology, University of Regensburg, Universitaetsstrasse 31, 93040 Regensburg, Germany

[2] Laboratory of Biophysics and Surface Analysis, School of Pharmaceutical Sciences, University of Nottingham, University Park, Nottingham NG7 2RD, United Kingdom

[3] Institute of Analytical Chemistry, Chemo- and Biosensors, University of Regensburg, 93040 Regensburg, Germany

Abstract

Within this study we could describe a simple and effective method to synthesize high molecular weight thioalkylated PEG derivatives. Characterization experiments confirmed the success of the developed synthesis route to $(MePEG_{2000}C_{11}S)_2$. We additionally could demonstrate by means of AFM, QCM, Tof-SIMS and contact angle experiments that these high molecular weight compounds are forming homogeneous monolayers on gold substrates as thioalkylated oligo(ethylene glycol) derivatives do. We found that most of the polymers adsorb within several minutes, after two hours no further mass uptake could be seen. The protein repellant effect of these self-assembled monolayers could be shown for BSA, although a complete exclusion of BSA adsorption could not be stated. Moreover, even the adsorption of complex protein mixtures, such as FBS, could be suppressed to a high extent, the protein repellant effect was close to the detection limit of SPR. However, the adsorption of proteins could not be suppressed completely (what is in good accordance to literature data), but on the other hand the amount of adsorbed protein probably lies below a threshold decisive for biological responses. To confirm these assumptions, further studies on the biological impact of this reduced adsorption should be conducted by testing the adhesion of cells on these SAMs.

Introduction

To guide the interactions of biomaterials with biological environments, the design of the surface properties is of utmost importance, since biological reactions predominantly occur on the material surface.[1] In general, proteins immediately adsorb, if a biomaterial is brought into contact with biological fluids.[2] This first and non-specific reaction more or less makes it impossible to further guide the fate of the applied device, as the subsequent interactions with cells also will be non-specific and, therefore, hard to control.[3] Hence, in numerous studies different attempts were made to control this initial step of cell – biomaterial interactions.[4,5,6] The most prominent strategy for influencing the protein adsorption characteristics of biomaterials is to attach poly(ethylene glycol) (PEG) to their surfaces.[1,6] Due to steric repulsion, this polymer allows for a strong reduction of protein adsorption.[6] For many different materials this concept was shown to be highly effective.[1-6]

However, sometimes detailed investigations in the field of protein-surface interactions are cumbersome due to intrinsic effects of the underlying biomaterial, making it difficult to estimate the influence of distinct individual factors.[4] Degradation products of polymeric systems, such as organic acids, for example, may acylate proteins, modifying the response of cellular systems to the applied device.[7] Moreover, swelling is frequently observed for polymeric systems, that can change the physicochemical properties and, therefore, the cellular response completely.[8] To reduce these effects, in recent years simplified model substrates for complex biomaterials have gained increasing importance.[9] By far the most prominent approach here is drawn to self-assembled monolayers (SAMs) of alkanethiols on gold. These SAMs can be tailored with very distinct physicochemical properties for mimicking biomaterial surfaces of interest.[10,11,12] By attaching different groups to the alkanethiols, numerous investigations on wettability, protein adsorption characteristics or cell adhesion for example were performed.[13-16]

Especially interesting for biomaterials with attached PEG derivatives are the outstanding studies of Whitesides et al., who investigated the impact of oligo(ethylene glycol) moieties attached to alkanethiols on gold.[11,15-18] They described a strong reduction of the adsorption of different kinds of proteins to these SAMs, in some cases even a complete suppression was found. Later, numerous groups also investigated this protein repellant effect and the subsequent cellular response for a plethora of different surfaces, but only few groups investigated SAMs of high molecular weight poly(ethylene glycol) derivatives. Du

et al. for example could show that the concept of self-assembly also works for mercaptoacetic acid derivatized PEGs with a molecular weight up to 5000 Da.[19] Unsworth et al. investigated this strategy for PEGs with thiol end groups without alkanes[20,21], Rundqvist et al. for PEGs with mercaptopropionic amides[22]. All these investigations were made with compounds without a longer alkane group ($C_{11} - C_{16}$) between thiol and polymer, although these alkane moieties were described as responsible for the highly ordered state of SAMs, increasing the possibility to exactly define surface characteristics and, therefore, their protein repellant effect.[9] Only the group of Grunze investigated an alkanethiol with a PEG moiety of 2000 Da[23,24] as well as Saito et al., who characterized the protein repellant characteristics of thioalkylated PEG with molecular weights of 5000 Da.[25]

Since it is well accepted that the properties of SAMs strongly depend on the structural details of the system[26], the differences of the polymers of those few studies dealing with PEG derived SAMs makes it difficult to compare the different results in terms of their protein adsorption characteristics. It is well known for example (at least for oligo(ethylene glycol) SAMs) that the alkane chain in general and its conformation and the end group in particular have an impact on the kinetics of the self-assembling process, the density of molecules on the surface and, therefore, on the protein adsorption resistance.[20,21,27] At least, all the studies have in common that SAMs consisting of poly(ethylene glycol) derivatives can reduce non-specific adsorption of proteins. But in general, very few literature can be found on PEG-containing SAMs with alkanethiol moieties, especially in terms of the SAM formation, although these compounds seem to be most effective for the generation of well-ordered surfaces and, therefore, to achieve a high degree of protein resistance.[28,29]

Therefore, in a first step, it was the aim to synthesize a PEG derivative, which can form highly ordered SAMs in order to get a more detailed insight into the time scale of monolayer formation and the potential of these SAMs to influence protein adsorption, since this will be a prerequisite to characterize cell – biomaterial interactions. To achieve this goal, we developed a new facile route to poly(ethylene glycol) derivatives with an undecanethiol group (called "MePEG$_{2000}$C$_{11}$SH", or its oxidized form "(MePEG$_{2000}$C$_{11}$S)$_2$", respectively). Furthermore, we intended to visualize resulting monolayers and aimed to give a rough time scale for the layer formation. To find out whether these polymers can reduce protein adsorption only partially or even completely,

we applied sensitive methods, such as time of flight secondary ion mass spectrometry (ToF-SIMS). With quantitative surface plasmon resonance (SPR) experiments we additionally tried to get information on whether an eventual protein adsorption might cause subsequent cell adhesion. The results should allow for an estimation, if the developed model system can be applied for investigations on specific cell-biomaterial interactions.

Materials and Methods

Polymer synthesis

$(MePEG_{2000}C_{11}S)_2$ was synthesized as published previously[30] as well as in Chapter 3 of this thesis (Figure 1). In brief: Thioacetic acid was attached to 11-bromo-undecene in a radical chain reaction to give the anti-Markovnikov product (1). This thioester was hydrolyzed in methanolic HCl according to a method developed by Bain et al.[31] To protect the free thiol (2) for the subsequent Williamson ether synthesis, 2-chloro-trityl chloride was attached by stirring in chloroform for 24 hours. To a solution of $MePEG_{2000}$, that was dried before by applying vacuum for 48 hours, in dioxane this protected alkanethiol was added in the presence of sodium hydride. The resulting Williamson ether (4) was then deprotected by dissolving in a solution of iodine in methanol. For purification, the product was precipitated several times in diethyl ether.

Polymer Characterization

^{1}H-NMR.

^{1}H-NMR (Proton nuclear magnetic resonance spectroscopy) data were recorded on a Bruker Avance 300 spectrometer. Samples were dissolved in $CDCl_3$, using tetramethyl silane as an internal reference.

HPLC-MS.

For HPLC-MS analysis, samples were analyzed using an Agilent 1100 HPLC system with degasser, binary pump, autosampler, column oven and diode array detector, coupled with a TSQ7000 mass spectrometer with API2- source (capillary temperature: 300 °C, spray voltage: 4 kV). A linear gradient of 18–90% solvent B (acetonitrile) in solvent A (double-distilled water + 0.0056 % v/v TFA) over 30 min served as a mobile phase at a flow rate of 0.9 ml/min. About 10–20 µl of the samples were separated using an analytical column (PL-RPS 300Å, 5µm). The XCALIBURR software package was used for data acquisition and analysis.
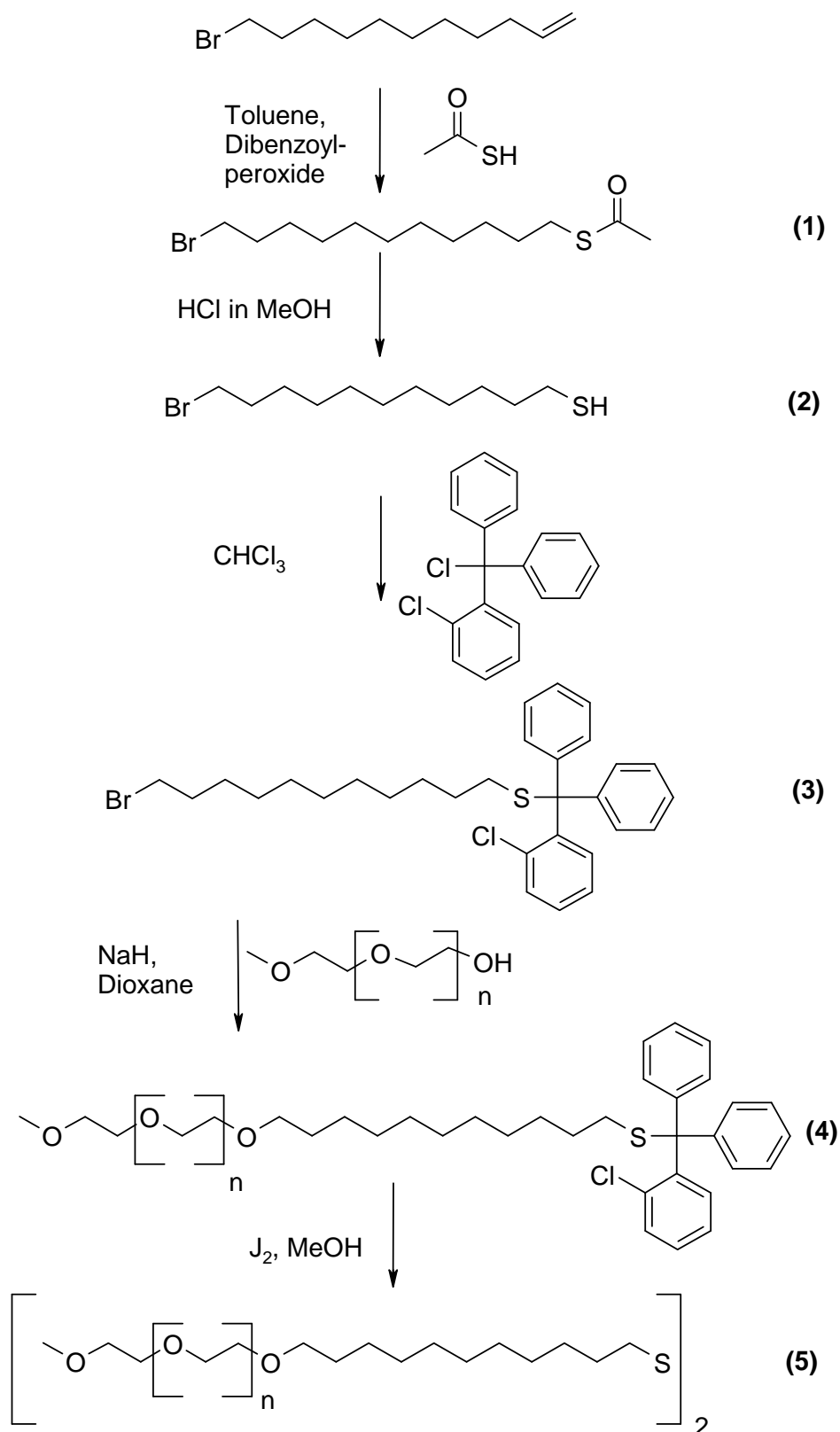
Figure 1: Synthesis scheme for (MePEG$_{2000}$C$_{11}$S)$_2$. The synthesized protected alkanethiol moiety is attached in a Williamson ether synthesis to methoxy PEG. After removing the protecting group, the oxidized dialkyl disulfide was used for further experiments.

Investigation of Monolayer Formation

Atomic Force Microscopy (AFM).

Epitaxial gold surfaces for the AFM imaging were prepared as published previously.[32] A gold ball (99,9%, Birmingham metals, UK) with a diameter of approximately 3 mm was cleaned in acetone and placed into a tungsten well, beneath a rotating shutter in a vacuum chamber. Freshly cleaved mica was placed cleaved side down onto a heating stage. After a vacuum of 10^{-5} mbar was reached, the chamber was heated up to 320°C for 6 hours to remove contaminants on the surface. Then the temperature was reduced to 310°C and the tungsten wire heated resistively for 30 seconds with the shutter over the well to outgas contaminants. After removing the shutter, the gold was allowed to evaporate onto the mica surface for half an hour. The temperature was then increased to 390°C and the gold allowed to anneal for 24 hours. The heater was then turned off and the gold film allowed to cool down to room temperature overnight. The vacuum chamber was then returned to atmospheric pressure and the gold film retrieved.

The gold covered mica was then cut into pieces of 1 cm^2 and subsequently covered with a two component epoxy glue, stuck onto microscope slides and dried for 3 hours at 100°C. Excessive glue was removed by immersing the pieces in THF for 3 minutes. After excessive rinsing with water, the mica slide was carefully removed with tweezers, the resulting epitaxial gold surface on the microscope slide was then immediately immersed in the respective polymer solution for 24 hours, subsequently rinsed with ethanol and dried in a stream of nitrogen.

Surface images were obtained with a JPK NanoWizard scanning force microscope (JPK instruments, Berlin, Germany). Measurements were performed in double distilled water, images were obtained in tapping mode by using silicon tips (NSC 12/50, Ultrasharp, Silicon-MDT Ltd., Moscow, Russia). Scan rates were set to 0.3 Hz.

Quartz crystal microbalance measurements (QCM).

A detailed description of the quartz crystal microbalance (QCM) setup is already given elsewhere.[33] In brief: AT-cut quartz plates with a 5 MHz fundamental resonance frequency were coated with gold electrodes. The setup was equipped with an inlet and outlet, which connects the fluid chamber to a peristaltic pump (pump rate: 0.46 ml/min, Ismatec Reglo Digital), allowing for the addition of polymer solutions from outside the Teflon chamber.

The frequency shift of the quartz resonator was recorded using a frequency counter (HP 53181A) connected via RS 232 to a personal computer. The oscillator circuit was supplied with a voltage of 4 V by a DC power supply (HP E3630A).

Before measuring the mass increase of polymers on the gold surfaces, gold was cleaned for 5 minutes in a hot piranha solution (sulfuric acid / aqueous hydrogen peroxide (30%), ratio 3:1) at 70°C. Afterwards, the surfaces were rinsed extensively with double-distilled water and dried in a stream of nitrogen.

For measuring the adsorption characteristics of $(MePEG_{2000}C_{11}S)_2$, 1 mM aqueous polymer solutions were prepared and added after the resonance frequency was constant.
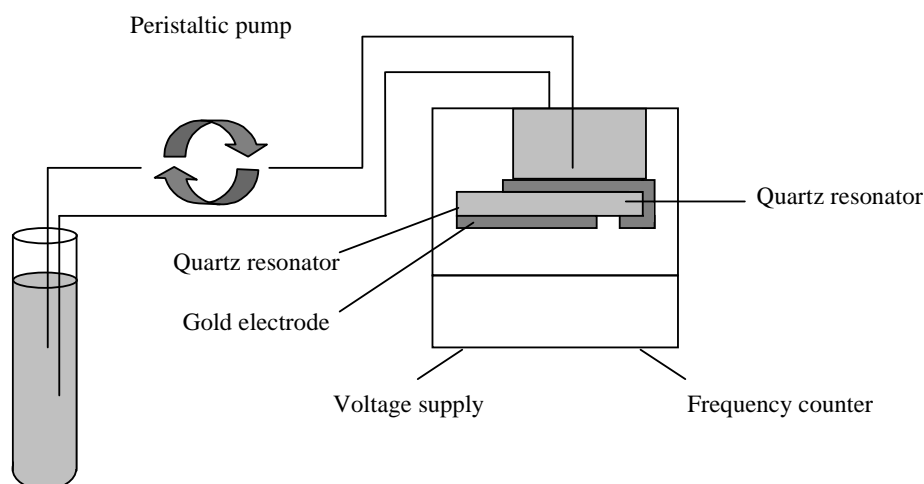
Figure 2: QCM flow through setup allowing for the addition of polymer solutions from outside the system. A decrease in resonance frequency of the oscillating quartz disc indicates a deposition of mass on the surface.

Water contact angle measurements.

The static water contact angle was determined with an OCA 15plus system (Dataphysics Instruments GmbH). Before measurements, the surfaces (similar to AFM measurements) were incubated in double-distilled water for sonication in an ultrasonic bath for several minutes. Drops of 1µl of double distilled water were set on the different surfaces for the determination of the contact angle. Measurements were collected (n = 3) and expressed as the mean ± standard deviation (SD).

SAMs were either tested after a monolayer formation of 24 hours and subsequent rinsing with ethanol and water or after a further incubation in solutions of FBS in PBS (total protein 1 mg/ml) for 1 hour, including subsequent rinsing with water.

Time-of-Flight Secondary-Ion-Mass-Spectrometry measurements (ToF-SIMS).

Time-of-flight secondary ion mass spectra were collected on a ToF-SIMS IV spectrometer (Ion-ToF GmbH Muenster, Germany) equipped with a reflectron analyzer, using 10 kV post-acceleration. A Cs^+ source was used with a beam energy of 15 keV. Both positive and negative ion spectra were collected and calibrated with a set of low-mass ions.

Gold surfaces and SAMs were prepared similar to AFM measurements and analyzed before and after incubating the surfaces for 1 hour in BSA solutions (1 mg/ml).

SPR measurements (SPR).

SPR was performed on a Biacore3000 system: $(MePEG_{2000}C_{11}S)_2$ was bound to gold sensor chips by incubating the sensor area with 1mM ethanolic polymer solutions. Similar to QCM experiments, first the surfaces were rinsed with PBS. Then the medium was changed to an FBS solution with a concentration of 1 mg/ml total protein. After 10 minutes, the surfaces were rinsed again with pure PBS. This procedure was repeated two further times and the increase of the SPR angle plotted against time.

Results and Discussion

Polymer characterization

H[1]-NMR spectroscopy revealed the following results for the intermediate steps and the final products (Figure 1 and 3):

11-bromoundecylthioacetate (1): δ 3.41 (t, 2 H), 2.87 (t, 2 H), 2.32 (s, 3 H), 1.85 (m, 2 H), 1.2-1.7 (m, 16 H). *11-bromoundecylmercaptane (2):* δ 3.41 (t, 2 H), 2.52 (m, 2 H), 1.85 (m, 2 H), 1.2-1.7 (m, 16 H). *11-bromoundecyl-(2-chloro trityl)sulfide (3):* δ 6.7-8.1 (m, 14 H), 3.41 (t, 2 H), 1.98 (t, 2 H), 1.85 (t, 2 H), 1.05-1.65 (m, 16 H). *(MePEG$_{2000}$-undecyl)-(2-chloro trityl)sulfide (4):* δ 6.7-8-1 (m, 14 H), 3.5-3.8 (m, 180 H), 3.30 (s, 3 H), 1.98 (t, 2 H), 1.05-1.65 (m, 18 H). *(MePEG$_{2000}$C$_{11}$S)$_2$ (5):* δ 3.5-3.8 (180 H), 3.30 (s, 3 H), 2.66 (t, 2 H), 1.2-1.7 (m, 18 H). A further broad peak can be observed at ~ 2.2 ppm, which stems form water.

The triplet at 2.66 obviously confirms, that the free thiol is oxidized to the corresponding disulfide. Since literature data supports, that disulfides and thiols have comparable binding characteristics on gold substrates[12], we did not perform a reduction to the thiol again to avoid having a mixture of thiol and disulfide under prolonged storage conditions.

All the other data of these NMR experiments are in good accordance with literature data, the synthesis strategy therefore seems to be successful.[19]

HPLC-MS chromatograms revealed besides several small impurity peaks two major peaks at 12 minutes and 23 minutes (Figure 4a). The mass analysis of the peak at 23 minutes shows five Gaussian distributions. These distributions arise form the distribution of chain lengths of the polymer and from to the different number of cationic adducts on account of the sample preparation. A detailed analysis of the peak between a retention time of 23.05 and 23.35 minutes is shown in Figure 4b. The single peaks of the Gaussian distribution can be identified as (MePEG$_{2000}$C$_{11}$S)$_2$ molecules with different numbers of monomers. For example a molecule of (MePEG$_{2000}$C$_{11}$S)$_2$ with all together 88 ethylene glycol units, which carries three cations (two protons and two sodium cations) due to the preparation during the analytical procedure has a theoretical mass of 4354 Da. Since the result of the ESI analysis is given as mass per charge, this value has to be divided by 4, revealing a value of

1088 Da. A peak with exactly this value can be detected. Additionally, the difference to the next peak is approximately 11 Da, exactly the fourth part of an ethylene glycol unit. This confirms that individual peaks are only due to the difference in ethylene glycol units of the polymer molecules. Also the peaks in between the major signals could be identified. They are due to $(MePEG_{2000}C_{11}S)_2$ molecules with four cation adducts, such as protons, sodium and kalium, indicating that the compound with a retention time is indeed $(MePEG_{2000}C_{11}S)_2$ with a high grade of purity.

The peak at 12 minutes could be confirmed as non-modified $MePEG_{2000}$ as we could show by analyzing the educt. Also this polymer shows a Gaussian distribution with a similar peak profile (Figure 4c).
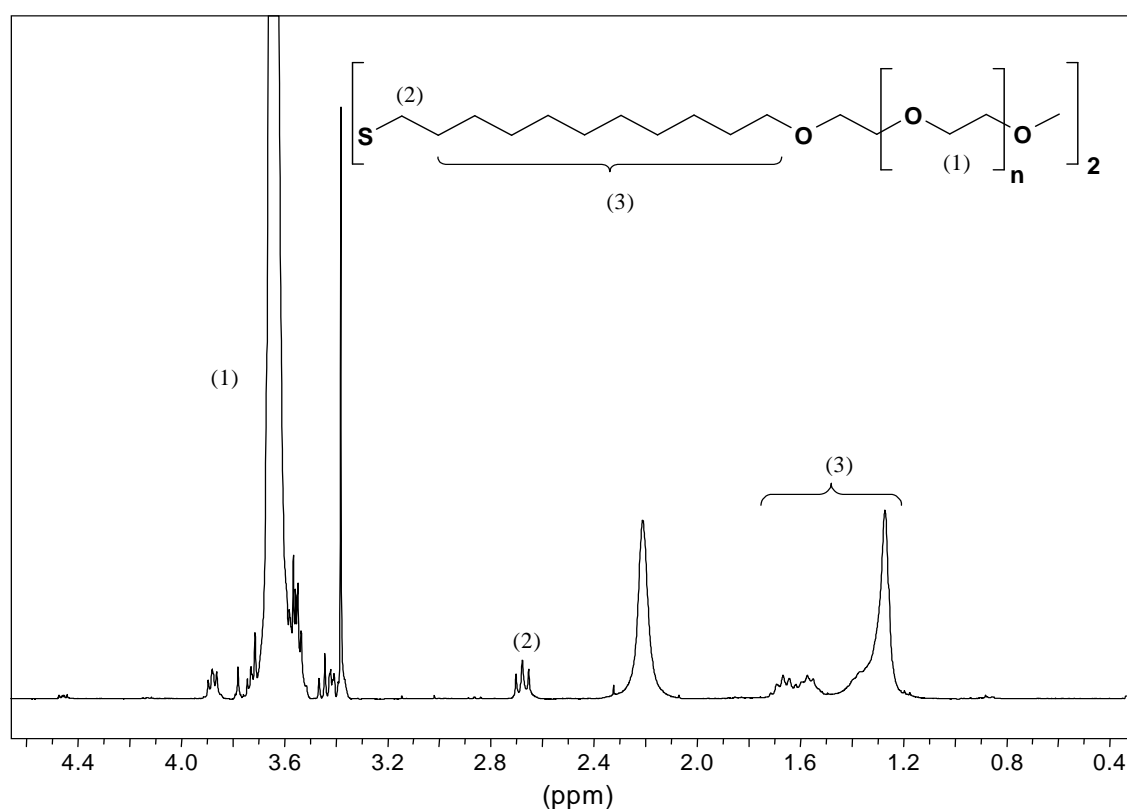
Figure 3: ^{1}H-NMR data of (MePEG$_{2000}$C$_{11}$S). The methylene groups of the alkane chain (1.20 – 1.65 ppm) and the methylene groups neighboring the disulfide obviously confirm that alkanethiol moieties are bound to PEG.
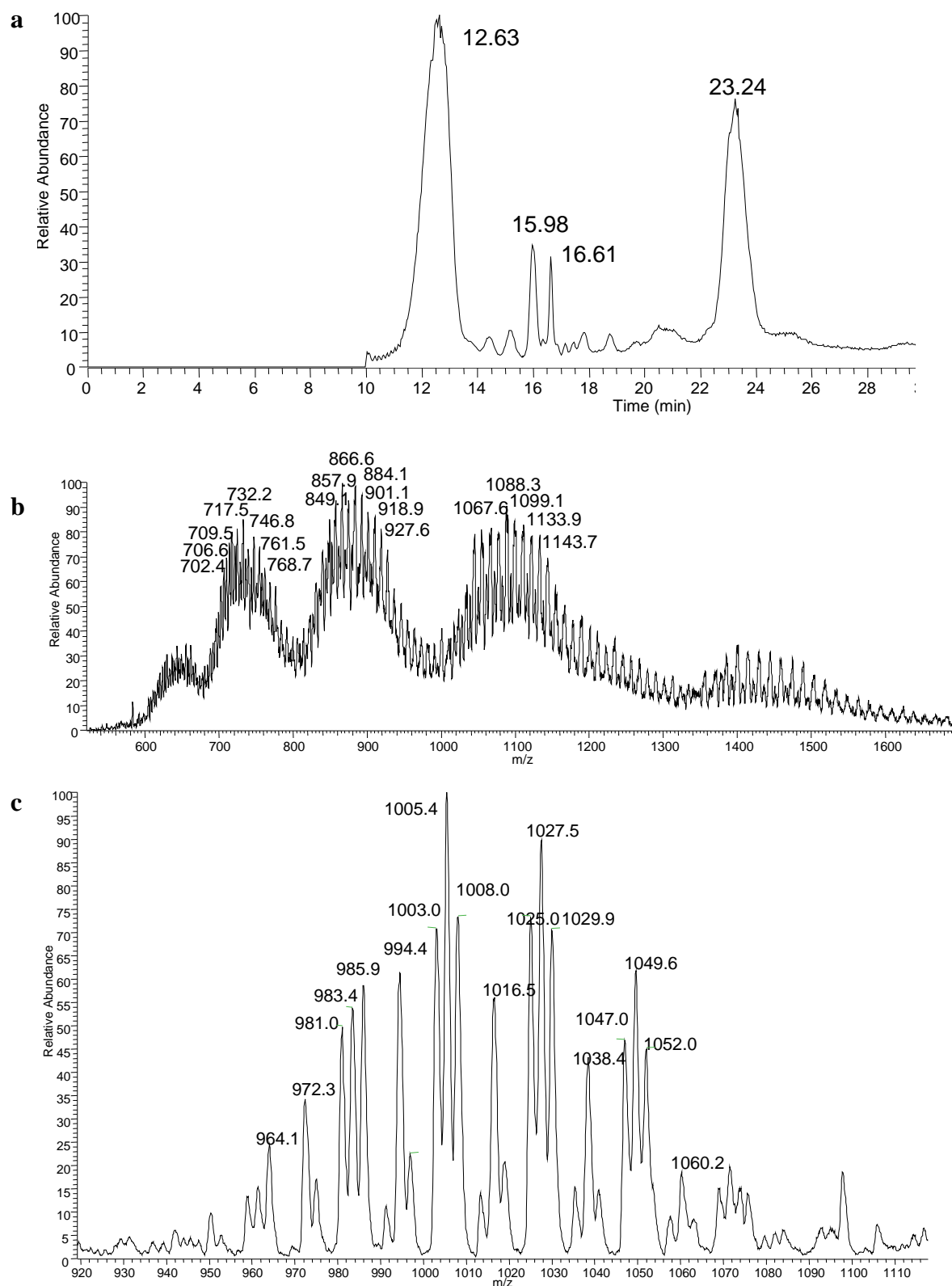
Figure 4: a: HPLC separation revealed two different main components at a retention time of 12 and 23 minutes. b: the peak at 23 minutes can be identified as (MePEG$_{2000}$C$_{11}$S)$_2$. c: The peak with a retention time of 12 minutes can be identified as MePEG$_{2000}$.

Taken together, these HPLC-MS data again confirm the identity of the desired polymers. A further chromatographic purification was not necessary for our investigations, since for the production of self-assembled monolayers on gold in literature a "autopurification" process for this type of molecules is described: after contingent physisorption of other PEG derivatives or impurities, these compounds are displaced by thiol containing compounds due to the high affinity of sulfur to gold, with a value for the adsorption energy of approximately 126 kJ/mol.[9,25]

Preparation and modification of self-assembled monolayers

Before suitable SAMs of the synthesized compounds could be prepared, in a first step epitaxial gold surfaces had to be prepared and characterized. As found to be the most suitable method for this purpose,[9] we sputtered gold onto thin slices of mica, which are flat by nature, annealed the gold at temperatures of approximately 390°C and stuck these gold surfaces onto microscope slides. Stripping off the mica slide, an epitaxial surface is can be obtained.

These surfaces were analyzed using an Atomic Force Microscope (AFM). In Figure 5a the resulting 2D topography data can be seen. The images are displayed as gold-scale representations, with the lowest points as dark pixels and highest points as bright pixels. As it is typical for gold surfaces prepared by evaporation methods, distinct terraces of gold can be detected.[34] The surface roughness is quite low with a route mean square value of only 2.6 Å, what can be extracted from the histogram plot (Figure 5c).
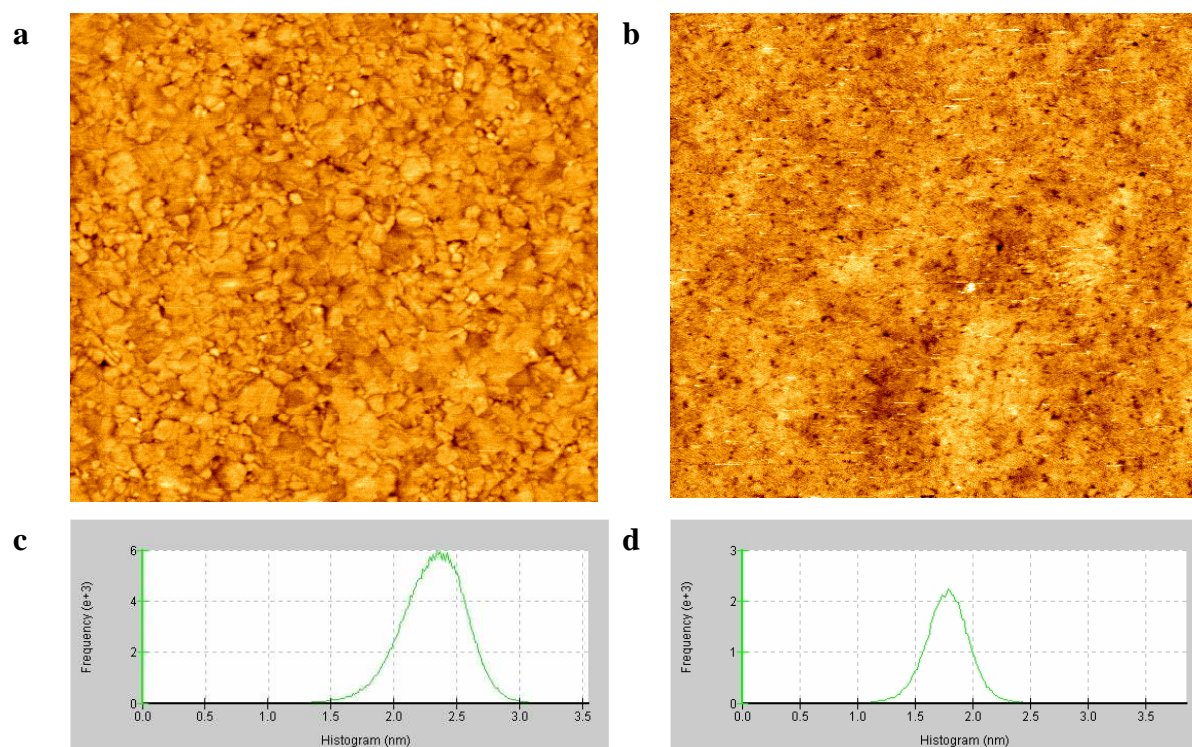
Figure 5: a: 2D topography data of non-modified gold shows the formation of typical terraces. b: 2D topography data after the incubation in polymer solutions indicate lower roughness values as for gold. Terraces can be seen any more. c: The histogram plot reveals an RMS value of 2.6 Å for gold, suggesting an extremely flat surface. d: A narrow distribution with an RMS value of 2.0 Å indicates a smoothening after the treatment with polymer solutions.

To get an impression of the time scale of monolayer formation with our system, we measured the increase of mass on the gold sensor of the QCM in a time resolved manner (Figure 6). After adding polymer solutions to the resonating quartz of the QCM, within several minutes a decrease in resonance frequency of approximately 45 Hz could be detected, with a further decrease to –60 Hz within 2 hours. After that, the resonance frequency remained constant, with typical fluctuations of several Hz over a time period of 6 hours. This suggests that more or less immediately most of the polymers were adsorbed and after approximately 2 hours the uptake of mass seemed to be finished, confirming the results of Dannenberger et al.[35] To be sure that additional mass uptake, which is below the sensitivity of the QCM, or a potential reorganization or straightening can take place, we always incubated the gold surfaces for at least 24 hours for subsequent protein adsorption experiments.
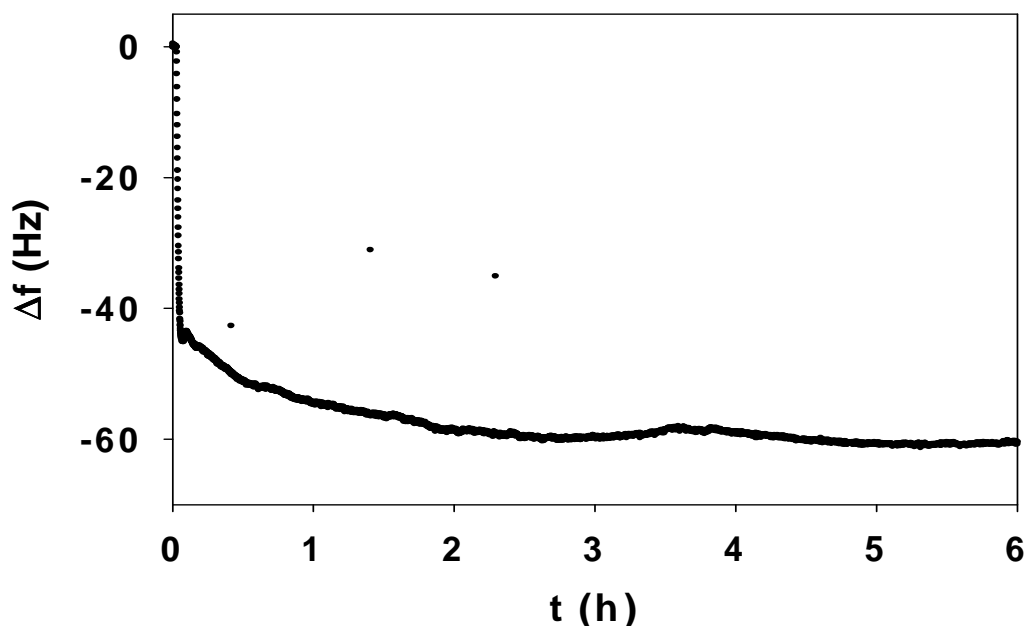
*Figure 6: QCM data indicate the kinetics of monolayer formation of (MePEG$_{2000}$C$_{11}$S)$_2$.
The resonance frequency drops by 45 Hz within several minutes and continues to decrease
for 2 hours. After that it remains constant with a total frequency shift of 60 Hz.*

To judge the homogeneity of the produced SAMs we additionally performed AFM
measurements after 24 hours of self-assembling (Figure 5b). The terraces typical for
freshly evaporated gold surfaces (Figure 5a) could not be detected any more, the surface
seems to be void of any structures and even more flat than before. In Figure 5d the
histogram plot of the topography data can be seen, the narrow Gaussian distribution
confirms the flatness of the surface with route mean square values of 2.0 Å, which
indicates an even lower surface roughness. This decrease could be explained by the
adsorption of the polydisperse polymer molecules, leveling off the ranks of the gold
terraces. Taken together, these results confirm the formation of a very homogeneous
monolayer of (MePEG$_{2000}$C$_{11}$S)$_2$ after 24 hours.

Summarizing, the data acquired in terms of monolayer formation confirm the formation of
a homogeneous monolayer of the synthesized polymers. The time scale of monolayer
formation is strongly comparable to the values of the polymers of Tokumitsu and
Herrwerth, who found that the major part of polymer adsorbs within several minutes.
Measuring the layer thickness by ellipsometry, they also stated a two step adsorption

process, which means that after 10 minutes the adsorbed globular molecules transform into a brush-like state with helical conformations of the ethylene glycol units.[17,24] Admittedly, we could not detect this transformation step, maybe due to the impreciseness of the applied method. However, in previous investigations we at least could confirm, that the generated monolayers adopt a brush-like state.[36] By impedance measurements we also found a high surface coverage of 94% for these SAMs, which was slightly less than the 97% found for octa(ethylene glycol) derivatized alkanethiols.[37] Also the ordering of the high molecular weight SAMs was assumed to be lower, probably due to the steric repulsion of the PEG moieties.[37] Thus, with the synthesized polymers we indeed can produce homogeneous and well-defined monolayers, which seem to be very suitable for mimicking PEG-rich surfaces due to the high density of PEG on these SAMs.

Protein adsorption

The intention for attaching PEG to biomaterial surfaces was to suppress any non-specific reactions on the surfaces, such as protein adsorption. Therefore it is of course of high interest, whether the SAMs we produced indeed can mimic these surfaces and reduce the adsorption of different proteins as it was described for numerous PEG-containing biomaterials.

In preliminary studies we already could show the efficacy of $(MePEG_{2000}C_{11}S)_2$ monolayers to resist the adsorption of BSA completely by means of the QCM technique.[36,37] Thus, we tried to confirm these results in this study with even more sensitive methods.

To evaluate very low levels of protein adsorption, in some cases for example antibody based techniques or radiolabelling were taken into account.[38] However, these methods sometimes are difficult to apply (e.g. lack of suitable antibodies, or regulatory restrictions for radiolabelling). Therefore, we decided to use the method of Time-of-flight Secondary-Ion-Mass-Spectrometry (ToF-SIMS), with a sensitivity in the ppm range.[38] With this technique, polymer surfaces can be characterized by analyzing the mass spectrum of generated ions after the outer 10 – 15 nm of the sample surface were fragmentized with an ion source.

First of all, we could confirm the presence of $(MePEG_{2000}C_{11}S)_2$ on the gold substrate using ToF-SIMS. The complete mass spectrum in the range of 0 – 800 m/z only revealed peaks with masses of fragments, that could be attributed to $(MePEG_{2000}C_{11}S)_2$. The most

prominent peak had a mass of 45 m/z and could be identified as a $CH_2CH_2OH^+$ fragment, which is typical for PEG derivatives (Figure 7).[38] This indicates that indeed a PEG derivative must be bound to the gold surface, substantiating the AFM, QCM and contact angle results (see below).
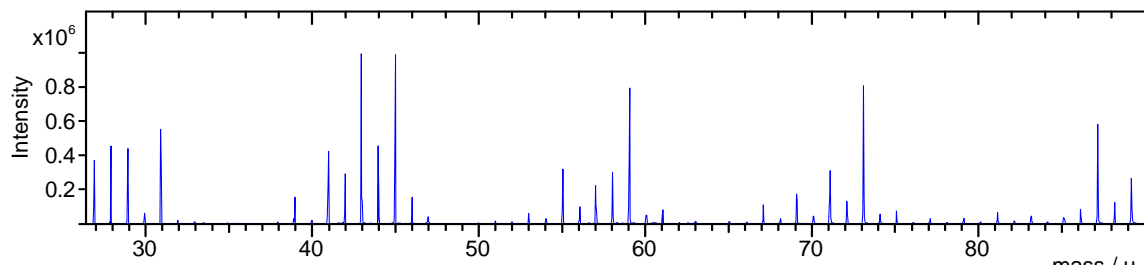

Figure 7: Pattern of fragments that could be found by means of ToF-SIMS after incubating gold substrates with polymer solutions. The most prominent peak had a mass of 45 m/z and could be identified as a $CH_2CH_2OH^+$ fragment. Other fragments consisting of C, O and H atoms confirm that $(MePEG_{2000}C_{11}S)_2$ is bound to the gold substrate.

Typical fragments of proteins, that are generated by the ion beam during ToF-SIMS mass spectrometry, are cations containing nitrogen, such as $C_4H_8N^+$ and $C_5H_{10}N^+$. Since no nitrogen can be found in $(MePEG_{2000}C_{11}S)_2$, the adsorption of proteins on these polymers can easily be identified by integrating the intensity of the respective normalized peaks with a mass of 70 ($C_4H_8N^+$) and 84 Da ($C_5H_{10}N^+$), respectively, after incubating surfaces with BSA solutions. Although there is not an exactly linear relationship of the peak intensity and the amount of adsorbed proteins in a wide range, the peak intensity at least can give a rough impression of the extent of the reduction of protein adsorption, since Tof-SIMS can be used as a semiquantitative method.[38,39]

Therefore, after immersing gold substrates in polymer solutions for 24 hours, the samples were incubated for 1 hour with solutions of BSA (1mg/ml). After rinsing with PBS we could see that for SAMs on gold ToF-SIMS analysis only revealed a small peak at 70 and 84 Da, which was extremely reduced compared to blank gold surfaces. For both peaks a reduction of approx. 95% could be seen (Figure 8). Nevertheless, compared to other methods, such as QCM for example, a certain adsorption could be detected. This in consequence means, that the concept of preventing protein adsorption by generating SAMs of $(MePEG_{2000}C_{11}S)_2$ works, but a complete exclusion of proteins from the surface can not be guaranteed, what may have consequences for further investigations on cell adhesion processes on these surfaces, since already few ng/cm^2 can have significant biological effects.[38]

Peak Intensity C4H8N+ (70 Da)

Peak Intensity C5H10N+ (84 Da)
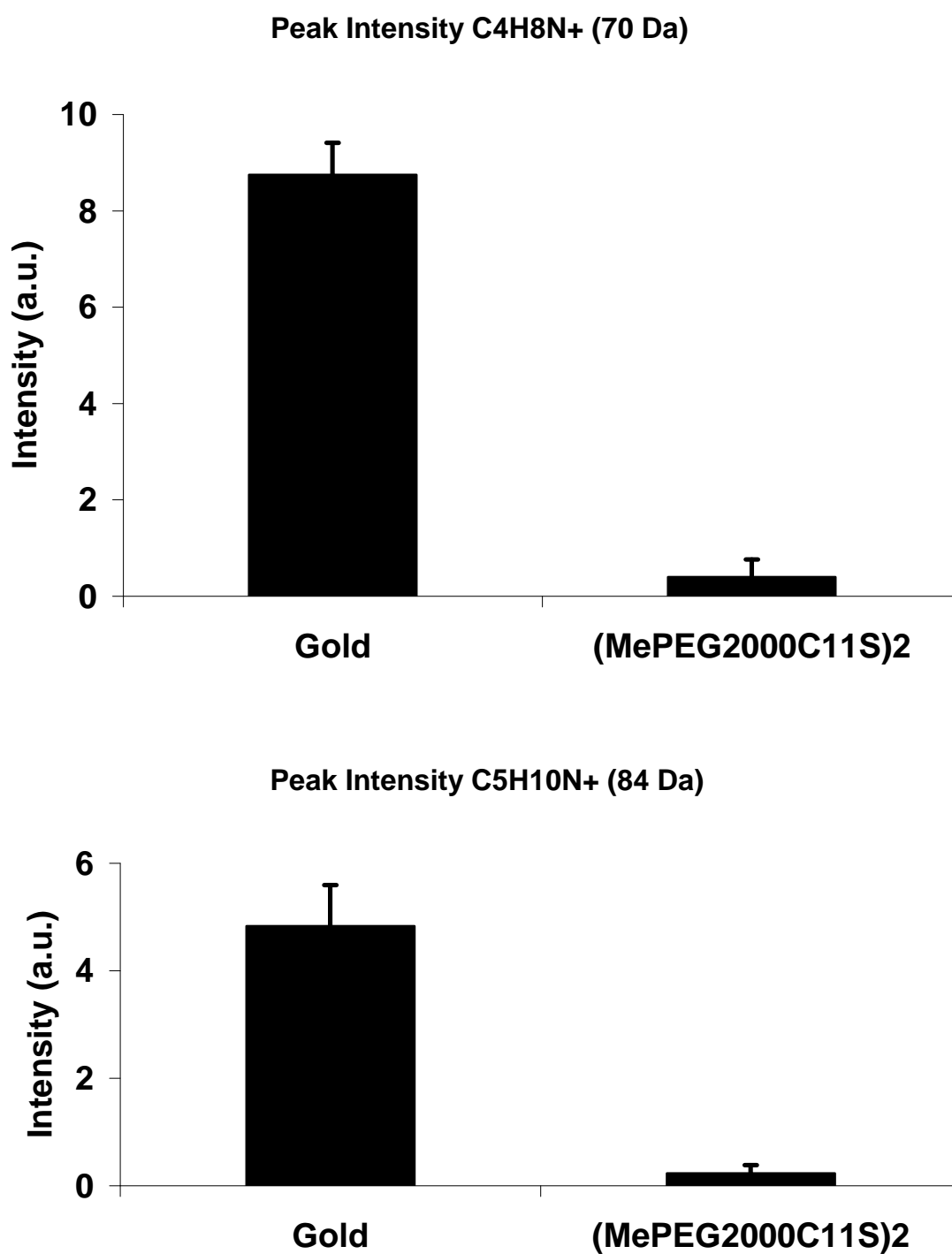
Figure 8: ToF-SIMS data show that after the incubation of gold surfaces with BSA solutions fragments typical for proteins ($C_4H_8N^+$ and $C_5H_{10}N^+$) can be detected with a mass / charge of 70 or 84 Da, respectively. On SAMs of (MePEG2000C11S)2 the signals are almost neglectable.

Thinking of biological applications for PEG rich surfaces, it is not only necessary to resist the adsorption of one single protein, but rather complex mixtures of different proteins. Therefore, we also tested the protein repellant effect by immersing the surfaces in solutions of FBS. By measuring the water contact angle, we could see that for non-modified gold surfaces, the contact angle decreases from $81\pm1°$ to $59\pm2°$. If the surfaces are incubated with non-thioalkylated $MePEG_{2000}$ solutions, the result is the same. This decrease indicates the adsorption of serum proteins, as the value is in good accordance with literature data, such as the value of 53° for a BSA layer determined by McClellan et al.[40] The water contact angles of $(MePEG_{2000}C_{11}S)_2$ also are quite similar to values of $MePEG_{2000}C_{11}SH$ SAMs on gold with 33° compared to 35° determined by Zhu et al.[28] After the treatment with FBS for one hour, the water contact angle does not change significantly to 34°. This substantiates the good protein repellant effect of the PEG SAMs.
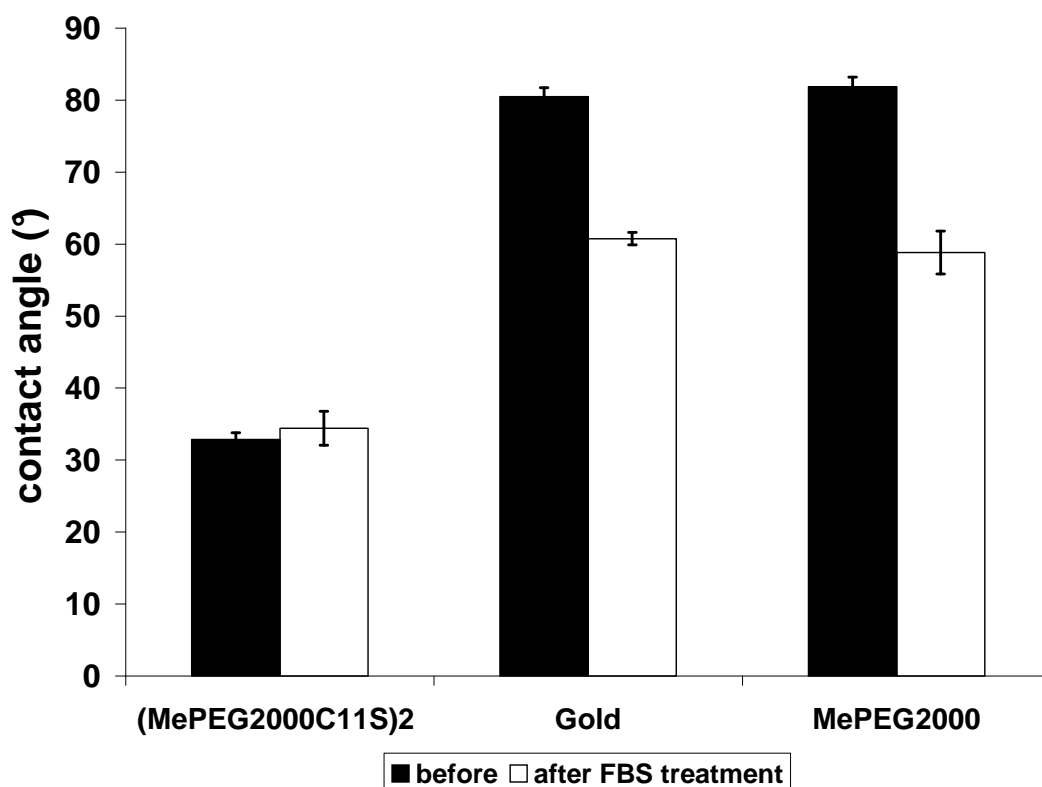
Figure 9: After incubating SAMs of (MePEG2000C11S)2 with FBS solutions, the water contact angle does not increase significantly (33 ± 1 vs. $35\pm2°$). In contrast, the contact angle decreases from $81°\pm2°$ to $59°\pm1°$ if gold surfaces (after or without preincubation in $MePEG_{2000}$ solutions) are treated with FBS solutions.

To have a more sensitive method we tried to confirm this result with SPR experiments. Again, monolayers were prepared by immersion in ethanolic polymer solutions for 24 hours and then treated the SAMs with solutions of FBS for 10 minutes. After rinsing for 500 seconds with PBS, the SPR angle dropped to the baseline level gain. Therefore we repeated this procedure two further times. Not until the third application of FBS a noticeable protein adsorption could be detected. Also these results confirm, that the SAMs can resist the adsorption of proteins to a high extent. However, as for BSA, a full resistance to any adsorption phenomena cannot be stated, although the results are quite promising thinking of suppressing the adhesion of cells on these SAMs.

In literature a value of 5 ng/cm^2 fibrinogen on surfaces is given as a threshold, below which significant platelet adhesion and activation are expected to be negligible.[20] Assuming this value to be effective also for cell adhesion phenomena in general, we calculated whether the 14 RU we determined might have any consequences. Maesawa suggested that a response of the equipment used in this study of 1 RU is equivalent to a deposition of 0.1 ng/cm^2 of protein, meaning that 1.4 ng/cm^2 of protein are present on the SAMs.[41] This very low amount would mean that probably no cellular response should take place after exposing the SAM to a cellular system.
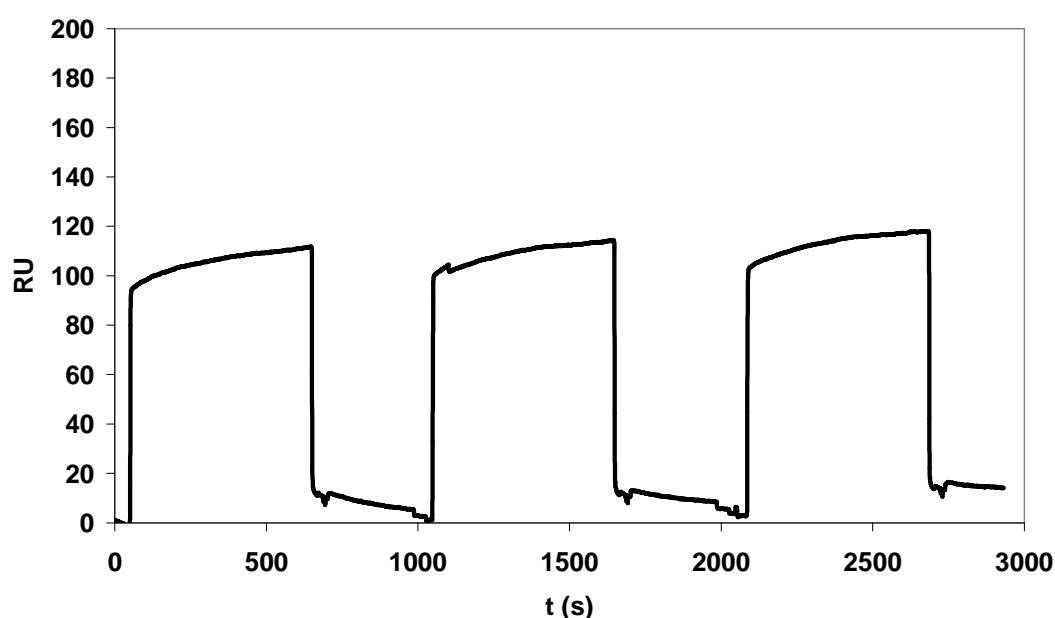
Figure 10: After the addition of FBS the SPR angle increases 100 RU, but after rinsing with PBS, the value drops to the base line again, indicating almost no proteins are adsorbing to the surface. After 3 additions of FBS, only an increase of 14 RU can be seen.

Recapitulating these results, we can confirm that the generated SAMs meet the requirements of reducing protein adsorption on model surfaces for PEG rich biomaterials below a biological significant threshold.

Conclusion

In this study we could describe a method to synthesize high molecular weight thioalkylated PEG derivatives ["(MePEG$_{2000}$C$_{11}$S)$_2$"], which are forming homogeneous monolayers on gold substrates. Due to steric repulsion of the PEG moieties, these surfaces almost exclude the adsorption of single proteins, such as BSA. Even the adsorption of complex mixtures, such as FBS, could be suppressed to a high extent. The amount of proteins that can be determined on the surface probably lies below a threshold decisive for biological responses. Hence, the suggested strategy to generate highly protein resistant model surfaces seems to be very promising.

References

[1] Castner D.G.; Ratner B.D.: Biomedical surface science: Foundations to frontiers. Surf Sci, 500, 28-60, 2002.

[2] Lee J.H.; Lee H.B.; Andrade J.D.: Blood compatibility of polyethylene oxide surfaces. Progr Polym Sci 20, 1043-1079, 1995.

[3] Drotleff S.; Lungwitz U.; Breunig M.; Dennis A.; Blunk T.; Tessmar J.; Göpferich A.: Biomimetic polymers in pharmaceutical and biomedical sciences. Eur J Pharm Biopharm, 58, 385-407, 2004.

[4] Tirrell M.; Kokkoli E.; Biesalski M.: The role of surface science in bioengineered materials. Surf Sci, 500, 61-83, 2002.

[5] Nath N.; Hyun J.; Ma H.; Chilkote A.: Surface engineering strategies for control of protein and cell interactions. Surf Sci, 570, 98-110, 2004.

[6] Jeon S.I.; Lee J.H.; Andrade J.D.; de Gennes P.G.: Protein-surface interactions in the presence of polyethylene oxide. J Colloid Interf Sci, 142, 149-166, 1991.

[7] Lucke, A., Tessmar, J., Schnell, E., Schmeer, G., Göpferich, A.: Biodegradable poly(D,L-lactic acid)-poly(ethylene glycol) monomethyl ether diblock copolymers. Structures and surface properties relevant to their use as biomaterials. Biomaterials, 21, 2361-2370, 2000.

[8] v. Burkersroda F.; Gref R.; Goepferich A.: Erosion of biodegradable block copolymers made of poly(D,L-lactic acid) and poly(ethylene glycol). Biomaterials, 16, 1599-1607, 1997.

[9] Schreiber F.: Structure and growth of self-assembling monolayers. Prog Surf Sci, 65, 151-256, 2000.

[10] Vanderah D.J.; Pham C.P.; Springer S.K.; Silin V.; Meuse C.W.: Characterization of a series of self-assembled monolayers of alkylated 1-thiaoligo(ethylene oxides)$_{4-8}$ on gold. Langmuir, 16, 6527-6532, 2000.

[11] Harder P.; Grunze M.; Dahint R.; Whitesides G.M.; Laibinis P.E.: Molecular conformation in oligo(ethylene glycol)-terminated self-assembled monolayers on gold and silver surfaces determines their ability to resist protein adsorption. J Phys Chem B, 102, 426-436, 1998.

[12] Biebuyck H.A.; Bain C.D.; Whitesides G.M.: Comparison of organic monolayers on polycrystalline gold spontaneously assembled from solutions containing dialkyl disulfides or alkanethiols. Langmuir, 10, 1825-1831, 1994.

[13] Xiao X.; Hu J.; Charych D.H.; Salmeron M.: Chain Length Dependence of the Frictional Properties of Alkylsilane Molecules Self-Assembled on Mica Studied by Atomic Force Microscopy. Langmuir, 12, 235-237, 1996.

[14] Pertsin A.J. ; Grunze M. ; Garbuzova I.A. : Low-energy configurations of methoxy triethylene glycol terminated alkanethiol self-assembled monolayers and their relevance to protein adsorption. J Phys Chem B, 102, 4918-4926, 1998.

[15] Mrksich M.; Whitesides G.M.: Patterning self-assembled monolayers using microcontact printing: a new technology for biosensors? Trends Biotechnol, 13, 228-235, 1995

[16] Mrksich M.; Dike L.E.; Tien J.; Ingber D.E., Whitesides G.M.: Using microcontact printing to pattern the attachment of mammalian cells to self-assembled monolayers of alkanethiolates on transparent films of gold and silver. Exp Cell Res, 235, 305-313, 1997.

[17] Pale-Grosdemange C.; Simon E.S.; Prime K.L.; Whitesides G.M.: Formation of self-assembled monolayers by chemisorption of derivatives of oligo(ethylene glycol) of structure $HS(CH_2)_{11}(OCH_2CH_2)_mOH$ on gold. J Am Chem Soc, 113, 12-20, 1991.

[18] Chapman R.G. ; Ostuni E. ; Yan L. ; Whitesides G.M. : Preparation of mixed self-assembled monolayers (SAMs) that resist adsorption of protein using the reaction of amines with a SAM that presents interchain carboxylic anhydride groups. Langmuir, 16, 6927-6936, 2000.

[19] Du Y.J.; Brash J.L.: Synthesis and characterization of thiol terminated poly(ethylene oxide) for chemisorption to gold surface. J Appl Polym Sci, 90, 594-607, 2003.

[20] Unsworth L.D.; Sheardown H.; Brash J.L.: Polyethylene oxide surfaces of variable chain density by chemisorption of PEO-thiol on gold: adsorption of proteins from plasma studied by radiolabelling and immunoblotting. Biomaterials, 26, 5927-5933, 2005.

[21] Unsworth L.D.; Sheardown H.; Brash J.L.: Protein resistance of surfaces prepared by sorption of end-thiolated poly(ethylene glycol) to gold: effect of surface chain density. Langmuir, 21, 1036-1041, 2005.

[22] Rundqvist J. ; Hoh J.H. ; Haviland D.B. : Poly(ethylene glycol) self-assembled monolayer island growth. Langmuir, 21, 2981-2987, 2005.

[23] Tokumitsu S.; Liebich A.; Herrwerth S.; Eck W.; Himmelhaus M.; Grunze M.: Grafting of alkanethiol-terminated poly(ethylene glycol) on gold. Langmuir, 18, 8862-8870, 2002.

[24] Herrwerth S.; Rosendahl C.; Feng C.; Fick J.; Eck W.; Himmelhaus R.; Dahint R.; Grunze M.: Covalent coupling of antibodies to self-assembled monolayers of carboxy-

functionalized poly(ethylene glycol): Protein resistance and specific binding of biomolecules. Langmuir, 19, 1880-1887, 2003.

[25] Saito N.; Matsuda T.: Protein adsorption on self-assembled monolayers with water soluble non-ionic oligomers using quartz-crystal microbalance. Materials Science and Engineering C, 6, 261-266, 1998.

[26] Himmelhaus M.; Eisert F.; Buck M.; Grunze M.: Self-assembly of n-alkanethiol monolayers. A Study by IR-visible sum frequency spectroscopy (SFG). J Phys Chem B, 104, 576-584, 2000.

[27] Herrwerth S.; Eck W.; Reinhardt S.; Grunze M.: Factors that determine the protein resistance of oligoether self-assembled monolayers – Internal hydrophilicity, terminal hydrophilicity and lateral packing density. J Am Chem Soc, 125, 9359-9366, 2003.

[28] Zhu B.; Eurell T.; Gunawan R.; Leckband D. J.: Chain-length dependence of the protein and cell resistance of oligo(ethylene glycol)-terminated self-assembled monolayers on gold. Biomed Mater Res, 56(3), 406-416, 2001.

[29] Schwendel D.; Dahint R.; Herrwerth S.; Schloerholz M.; Eck W.; Grunze M.: Temperature dependence of the protein resistance of poly-and oligo(ethylene glycol)-terminated alkanethiolate monolayers. Langmuir, 17, 5717-5720, 2001.

[30] Knerr R.; Drotleff S.; Steinem C.; Göpferich A.: Self-assembling PEG-derivatives for protein-repellant biomimetic model surfaces on gold. Biomaterialien, 7, 1, 12-20, 2006.

[31] Bain C.D.; Troughton E.B.; Tao Y.T.; Evall J.; Whitesides G.M.; Nuzzo R.G.: Formation of monolayer films by the spontaneous assembly of organic thiols from solution onto gold. J Am Chem Soc, 111, 321-335, 1989.

[32] Rossell J.P.; Allen S.; Davies M.C.; Roberts C.J.; Tendler S.J.B.; Williams P.M.: Electrostatic interactions observed when imaging proteins with the atomic force microscope. Ultramicroscopy, 96, 37-46, 2003.

[33] Kastl K.; Ross M.; Gerke V.; Steinem C.: Kinetics and thermodynamics of Annexin A1 binding to solid supported membranes: A QCM study. Biochemistry, 41,10087-10094, 2002.

[34] Gupta P.; Loos K.; Korniakov A.; Spagnoli C.; Cowman M.; Ulman A.: Facile route to ultraflat SAM-protected gold surfaces by „amphiphile splitting". Angew Chem Int Ed, 43, 520-523, 2004.

[35] Dannenberger O.; Buck M.; Grunze M.: Self-assembly of n-alkanthiols: A kinetic study by second harmonic generation. J Phys Chem B, 103, 2202-2213, 1999.

[36] Menz B.: Quarzmikrowaagestudie zur Charakterisierung der Proteinresistenz von PEG-Undecanthiol-Beschichtungen an Gold. Zulassungsarbeit, Universität Regensburg October 2005.

[37] Menz B.; Knerr R.; Göpferich A.; Steinem C.: Impedance and QCM analysis of the protein resistance of self-assembled PEGylated alkanethiol layers on gold. Biomaterials, 26, 4273-4243, 2005.

[38] Kingshott P.; McArthur S.; Thisse H.; Castner D.G.; Griesser H.J.: Ultrasensitive probing of the protein resistance of PEG surfaces by secondary ion mass spectrometry. Biomaterials, 23, 4775-4785, 2002.

[39] Griesser H.J.; Kingshott P.; McArthur S.L.; McLean K.; Kinsel G.R.; Timmons R.B.: Surface MALDI mass spectrometry in biomaterials research. Biomaterials, 25, 4861-4875, 2004.

[40] McClellan S.J.; Franses E.I.: Adsorption of bovine serum albumin at solid/aqueous interfaces. Colloids Surf A, 260, 265-275, 2005.

[41] Maesawa C.; Inaba T.; Sato H.; Iijima S.; Ishida K.; Terashima M.; Sato R.; Suzuki M.; Yashima A.; Ogasawara S.; Oikawa H.; Sato N.; Saito K.; Masud T.: A rapid biosensor chip assay for measuring of telomerase activity using surface plasmon resonance. Nucleic Acids Res, 31, No2 e4, 2003.

Chapter 3

Self-assembling PEG Derivatives for Protein-repellant Biomimetic Model Surfaces on Gold

Robert Knerr[1], Sigrid Drotleff[1], Claudia Steinem[2], Achim Göpferich[1]

[1]Department of Pharmaceutical Technology, University of Regensburg, Universitaetsstrasse 31, 93040 Regensburg, Germany

[2]Institute of Analytical Chemistry, Chemo- and Biosensors, University of Regensburg, 93040 Regensburg, Germany

Abstract

We describe a method to synthesize high molecular weight poly(ethylene glycol) derivatives (PEGs) for the preparation of protein-repellant biomimetic surfaces, which can serve as model systems for PEG rich biomaterials. The resulting polymers were characterized by a combination of nuclear magnetic resonance (NMR), matrix assisted laser desorption/ionization mass spectrometry (MALDI-MS), high pressure liquid chromatography (HPLC), HPLC-coupled MS (HPLC-MS) and water contact angle measurements (WCA). Due to their alkanethiol chain, these PEG derivatives spontaneously adsorb onto gold. Using quartz crystal microbalance (QCM) techniques and surface plasmon resonance (SPR) we could show the ability of this model system to resist the adsorption of bovine serum albumin and to reduce fetal bovine serum adsorption. Additionally, the PEG moiety allows for attaching bioactive molecules: the modification with the cell-adhesion motif GRGDS was characterized by contact angle measurements.

Introduction

In recent years, enormous efforts have been made to improve the interactions of artificial biomaterials with cells. Nevertheless, there still is a poor selectivity among these cell-surface interactions, which might lead to foreign body reactions like inflammation, encapsulation or the rejection of implanted devices for example[8]. As those biological reactions predominantly occur on the surface of such devices[2], controlling the surface chemistry is crucial for designing new and effective biomaterials. Besides enhancing the specific adhesion of cells by immobilizing bioactive molecules, preventing non-specific reactions, such as the non-specific adsorption of proteins, by "masking" the surface, is one of the most important goals in this scientific field and therefore the subject of numerous studies[10,12,13].

So far, various biomaterials have been developed and shown to be useful to create bioactive devices, such as different hydrogel materials.[3] But also water insoluble materials, such as poly(lactic acid), including its derivatives such as poly(ethylene glycol)-*block*-poly(lactic acid) derived copolymers (PEG-PLAs), have been used.[3,14,21,23] Numerous other materials contain poly(ethylene glycol) moieties as a very important part to achieve a certain degree of "protein resistance", as PEG is well known to hinder the adsorption of biomolecules.[10,12,13] Furthermore, these polymers allow for the covalent attachment of specific cell adhesion motifs to stimulate guided cell adhesion.[9,16,23]

However, the characterization and the proof of efficiency of such functionalized "biomimetic" materials sometimes is complicated, due to the intrinsic characteristics of the polymers, such as erosion and swelling as well as their response to pH changes. To exclude these influences of the bulk material, model systems with very distinct physicochemical properties would be favorably.

Self-assembled monolayers (SAMs) of alkanethiols on gold can be such a useful model. These alkanethiols or the respective dialkyldisulfides chemisorb spontaneously onto gold surfaces and pack with nearly crystalline density due to strong interactions of the alkane chains, leading to well defined surfaces.[16,17,22,28] Additionally, they are a well characterized and well established system to investigate protein adsorption[5,19,28,30] and can be employed to characterize specific ligand-receptor interactions by attaching bioactive compounds. Oligo(ethylene glycol) (OEG) terminated alkanethiols, in particular, have been shown to be a useful model for PEG-rich surfaces[6] and, therefore, also for diblock-copolymers such as PEG-PLA derivatives. Moreover, Zhu et al.[30] reported that SAMs

consisting of longer PEG chains, containing ~ 45 monomers (~ 2000 Da), were protein resistant and could even more significantly suppress cell adhesion, although recent investigations in our group showed, that SAMs of PEG chains are less ordered than OEG SAMs.[15] A further increase of the molecular weight to 5000 Da does not increase the protein repellant effect of the PEG layers, and even might decrease the protein repellant effect under certain circumstances again.[18,26] These findings suggest preferring PEG derivatives with a molecular weight of 2000 Da for biomedical applications.

As mentioned before, a further step towards biomimetic surfaces with highly specific cell-surface interactions requires the possibility to attach bioactive compounds. Consequently, functional groups have to be introduced to the polymers used for producing SAMs. In contrast to oligo(ethylene glycol) SAMs, for poly(ethylene glycol) SAMs fewer publications report on suitable synthesis strategies: Herrwerth et al. for example synthesized polymers with a molecular weight of 2000 Da with carboxylic groups, that can easily be activated for subsequent antibody coupling to the SAMs,[7] Du et al. synthesized hydroxy PEG and carboxy PEG derivatives as well.[4] However, studies with PEG derivatives of 2000 Da having an amine and an undecylthiol group could not be found.

Therefore, we intended to develop a strategy to synthesize di(amino poly(ethylene glycol)-undecyl) disulfide, $(NH_2PEG_{2000}C_{11}S)_2$. To investigate, if the introduction of an amine group and, therefore, a positive charge has an impact on protein adsorption under physiological conditions, we additionally synthesized a methoxy terminated derivative to have a direct control system that allows for comparison with literature data.[4,24,26,30] Moreover, we intended to check whether this system is suitable for attaching biomolecules to the SAMs via the functional groups of the polymers.

Materials and Methods

Synthesis

Synthesis of di(methoxy poly(ethylene glycol)-undecyl) disulfide (MePEG$_{2000}$C$_{11}$S)$_2$

To thioalkylate poly(ethylene glycol) monomethyl ether[A], the following scheme was applied (see scheme 1): 3.29ml (15mmol) of 11-bromo-undecene[A] and 5.35 ml (75 mmol) of thioacetic acid[A] were dissolved in 50 ml of toluene[B] (dried by azeotropic distillation to remove traces of water). After adding 40 mg (164µmol) of dibenzoyl peroxide[A], the reaction mixture was heated to 80°C with an oil bath for three hours. After cooling the system to room temperature, the solvent was removed by rotary evaporation under reduced pressure. The hydrolyzation of the crude product was performed in methanolic HCl according to a method developed by Bain et al.[1]

The free thiol compound (2) was then protected with 2-chlorotrityl chloride[A]: 3.5 g (13.1 mmol) of 11-bromo-undecylmercaptane (2) and 4.1 g (13.1 mmol) of the protecting group were dissolved in 50 ml of chloroform in a nitrogen atmosphere and the reaction allowed to proceed for 24 hours, before chloroform[B] was removed by rotary evaporation.

For the subsequent Williamson ether synthesis, 4 g (2 mmol) of poly(ethylene glycol) monomethyl ether were dissolved in 100 ml dioxane[B]. 240 mg (10 mmol) of sodium hydride[B] were added to the dry solution and stirred for one hour. Then the protected alkanethiol (3) was added (5,7 g; 10 mmol) and stirred for 24 hours at room temperature. After adding one ml of methanol[B] at room temperature, the crude reaction mixture was filtrated, the solvent rotary evaporated and the product (4) purified by repeated precipitation in 100 ml of diethyl ether[B].

For the deprotection, the alkylated PEG (3.1 g; 1.3 mmol) was dissolved in 20 ml of a solution of 200 mg of iodine[A] in methanol and stirred for 24 hours at room temperature. After rotary evaporating methanol, the polymer was dissolved in acetone[B] and precipitated in diethyl ether. After removing the remaining solvents by drying in a desiccator under reduced pressure, the product (5) was desalted using an ion exchanger[B] and again purified by repeated precipitation in 100 ml of diethyl ether. ^{1}H NMR (300 MHz, CDCl$_3$): δ 3.5-3.8 (180 H), 3.30 (s, 3 H), 2.66 (t, 2 H), 1.2-1.7 (m, 18 H).
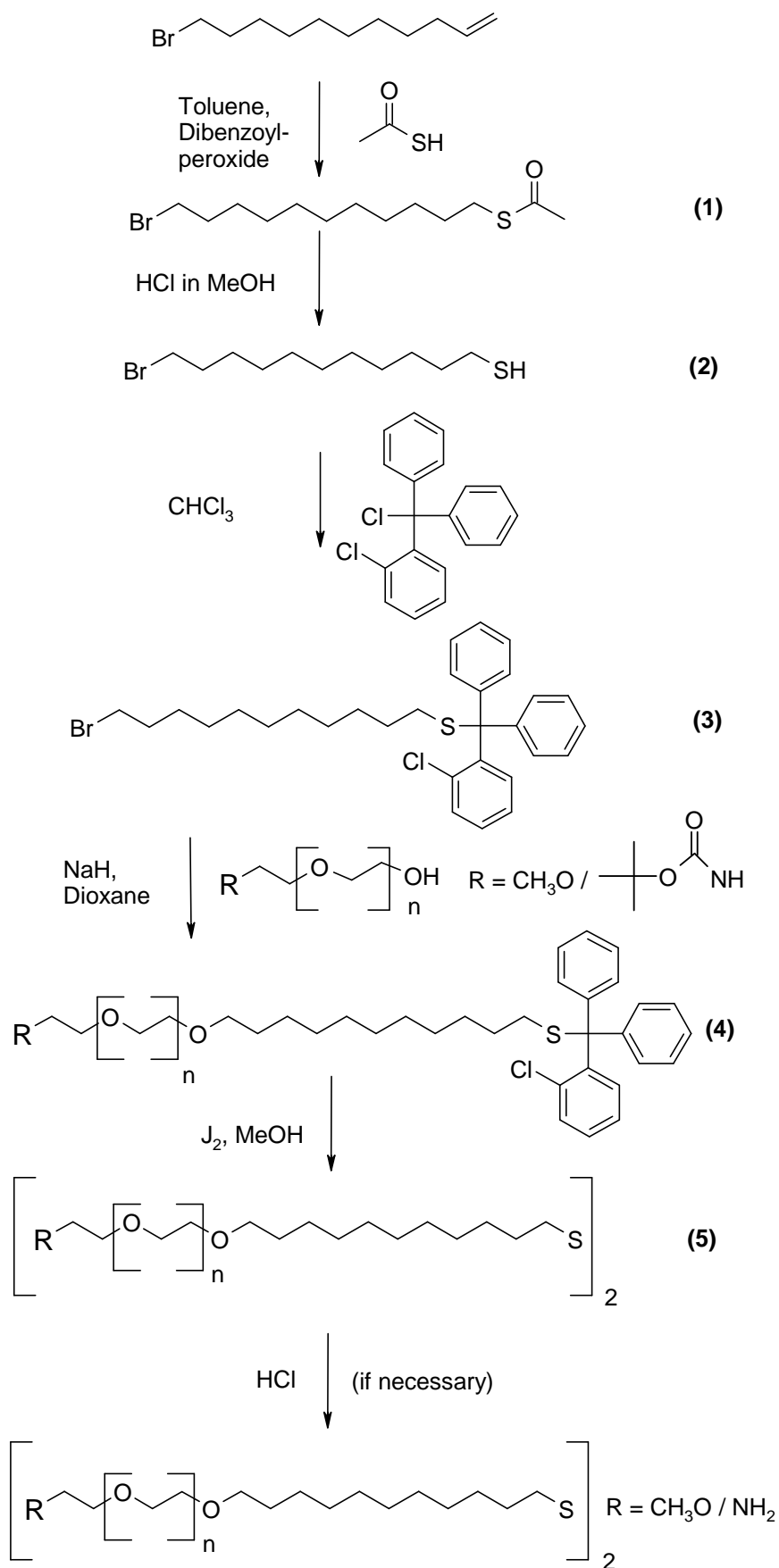
Scheme 1: *Synthesis approach for (PEG$_{2000}$C$_{11}$S)$_2$ derivatives with different end groups*

Synthesis of di(amino poly(ethylene glycol)-undecyl) disulfide ($NH_2PEG_{2000}C_{11}S)_2$

A similar procedure was applied for synthesizing the corresponding amine derivative, with several modifications: the poly(ethylene glycol)-monoamine was synthesized according to a procedure developed by Yokoyama et al.[29] To prevent alkylation of the amine group during the Williamson ether synthesis, the amine was protected with di-*t*-butyl dicarbonate[A] by stirring for 24 hours in dioxane at room temperature. To this protected polymer, the same scheme was applied as for the methoxy derivative. For the final deprotection, the polymer was stirred in 0.1M HCl[B] for 24 hours, afterwards the solution was neutralized with NaOH[B], water rotary evaporated, the product desalted again and purified by repeated precipitation in diethyl ether.^{1}H NMR (300MHz, CDCl₃): δ 3.5-3.8 (m,180 H), 2.8 (m, 2 H), 2.66 (t, 2 H), 1.2-1.7 (m, 18 H).

Polymer Characterization

^{1}H-NMR.

^{1}H-NMR (Proton nuclear magnetic resonance spectroscopy) data were recorded on a Bruker Avance 300 spectrometer[C]. Samples were dissolved in $CDCl_3$[D], using tetramethyl silane[A] as an internal reference.

MALDI-ToF MS.

Matrix assisted laser desorption/ionization mass spectrometry (MALDI-ToF MS) data were acquired on a HP G2030A spectrometer in positive ion mode. The polymer was analyzed in the range of 0-6000 m/z, data were recorded with 151 laser shots per spectrum, using sinapic acid[A] as matrix (10 mg/ml, solvent: acetonitrile). The sample was prepared on the target by depositing 1 µl of a mixture of matrix solution and polymer solution (1 mg/ml) (3:1), which was dried at room temperature by applying vacuum.

HPLC.

Samples were investigated by high pressure liquid chromatography HPLC using a setup consisting of a DGU-14A degasser, LC-10-AT pump, FCV-10AL VP gradient mixer, SIL-10 AD autosampler and SCL-10A VP controller[F]. A linear gradient of 20% to 100% solvent B (90% of acetonitrile[B] in water) in solvent A (10% acetonitrile in water) over 30 min was applied as mobile phase at a flow rate of 1.0 ml/min. 20 µl samples were separated at 40°C using a combination of a PL-RPS guard column and an analytical

column (PL-RPS 300Å, 5µm). The samples were detected with a low temperature evaporative light scattering detector.

HPLC-MS.

For HPLC-MS analysis, samples were analyzed using an Agilent 1100 HPLC system with degasser, binary pump, autosampler, column oven and diode array detector[H], coupled with a TSQ7000 mass spectrometer[I] with API2- source (capillary temperature: 300 °C, spray voltage: 4 kV). A linear gradient of 18–90% solvent B (acetonitrile) in solvent A (double-distilled water + 0.0056 % v/v TFA) over 30 min served as a mobile phase at a flow rate of 0.9 ml/min. About 10–20 µl of the samples were separated using an analytical column (PL-RPS 300Å, 5µm). The XCALIBURR software package[I] was used for data acquisition and analysis.

Water contact angle measurements (WCA).

The static water contact angle was determined with an OCA 15plus system[J]. Before measurements, the surfaces were incubated in double-distilled water for sonication in an ultrasonic bath for several minutes. Drops of 1µl of double distilled water were set on the different surfaces for the determination of the WCA. Measurements were collected (n = 6) and expressed as the mean ± standard deviation (SD). Single factor analysis of variance (ANOVA) was used in conjunction with a multiple comparison test (Tukey test) to assess the statistical significance.

Production and modification of self-assembled monolayers

To prepare polymer monolayers, AT-cut quartzes[K] with gold electrodes[L] were cleaned for 5 minutes in a piranha solution (sulfuric acid[B] / aqueous hydrogen peroxide (30%)[B], ratio 3:1) at 70°C. Afterwards, the surfaces were rinsed extensively with double-distilled water and dried in a stream of nitrogen. Then, the surfaces were incubated in 1 mM ethanolic[B] solutions of the respective polymer for at least 24 hours at room temperature. The corresponding amine can be converted into a carboxy group by incubation in a 4% solution of succinic anhydride[A] in DMF[B]. After rinsing, the acid can be activated by common DCC/NHS[A] chemistry: incubation in a 0.2M DCC / 0.05M NHS solution in DMF leads to an activated acid, which can then be modified with primary amine containing compounds. In this study, we incubated the activated surface with a solution of the pentapeptide

GRGDS[M] in PBS[N] (0.5 mg/ml) at 4°C over night, leading to a polymer monolayer bearing the bioactive compound on the surface (Scheme 2).
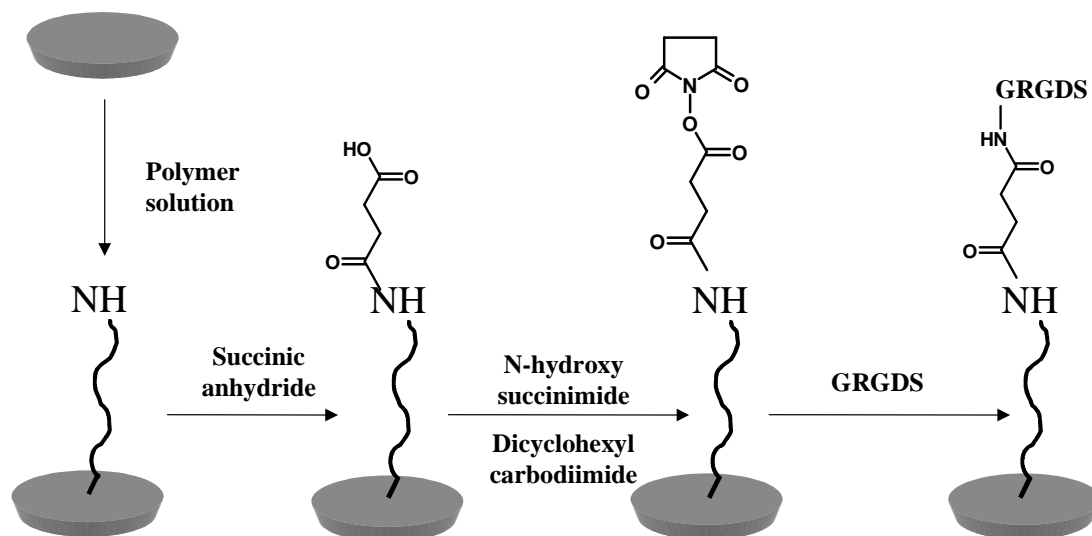
Scheme 2: Strategy for the modification of ω-amino SAMs with the pentapeptide GRGDS: Bound succinic acid can be activated with DCC/NHS and subsequently be modified with amine containing compounds.

Investigation of Protein Adsorption

QCM measurements.

A detailed description of the quartz crystal microbalance (QCM) setup is already given elsewhere[11]. In brief: AT-cut quartz plates with a 5 MHz fundamental resonance frequency were coated with gold electrodes. The setup was equipped with an inlet and outlet, which connects the fluid chamber to a peristaltic pump (pump rate: 0.46 ml/min) (Ismatec Reglo Digital[O]), allowing for the addition of protein solutions from outside the Teflon chamber. The frequency change of the quartz resonator was recorded using a frequency counter (HP 53181A,[E]) connected via RS 232 to a personal computer. The oscillator circuit was supplied with a voltage of 4 V by a DC power supply (HP E3630A[E]).

Before measuring the adsorption of proteins on the SAMs, the gold covered quartz plates were cleaned in an argon plasma, followed by an incubation in a 1 mM solution of the respective polymer in ethanol and rinsed afterwards extensively with ethanol and water and dried in a nitrogen flush.

To investigate BSA[A] adsorption, first pure PBS buffer was pumped through the flow cell until the resonance frequency was constant. Then 100 µl of a solution of 1 mg/ml BSA in

the same buffer were injected into the flow cell, resulting in a final concentration of 40 µg/ml in the system (n=3). For FBS[P] / (MePEG$_{2000}$C$_{11}$S)$_2$ experiments, 2.7 µl of FBS in 100µl of PBS (resulting in the same amount of total protein as for BSA experiments) were added to the system. Thinking of future cell culture experiments, the protein adsorption experiments with (NH$_2$PEG$_{2000}$C$_{11}$S)$_2$ were performed by adding 1 ml of FBS containing cell culture medium (Dulbecco´s modified eagle medium (DMEM[P]), total amount of protein added: 3,5 mg) (n=3).

SPR measurements.

SPR was performed on a Biacore3000 system[Q]: the corresponding polymers were bound to AU sensor chips by incubating the sensor area with 1mM ethanolic polymer solutions. Similar to QCM experiments, first the surfaces were rinsed with PBS. Then the medium was changed to an FBS solution with a concentration of 1 mg/ml total protein. After 10 minutes, the surfaces were rinsed again with pure PBS and the increase of the SPR angle plotted against time.

Results

Polymer characterization

MALDI-ToF data (Figure1) obviously confirm the identity of (MePEG$_{2000}$C$_{11}$S)$_2$. Since this polymer is a dimer of the corresponding thiols, the expected mass of one molecule should be in the range of at least 4000 Da. Indeed, we could see a Gaussian distribution in the mass per charge spectrum, with the maximum at ~ 4300 Da. This Gaussian distribution is due to the polydispersity of the polymer PEG$_{2000}$. The distance of different peaks in this distribution is 44 Da, exactly the value of one ethylene glycol unit, confirming the identity of a PEG derivative. One protonated molecule of (MePEG$_{2000}$C$_{11}$S)$_2$ with 42 ethylene glycol units per PEG moiety has a theoretical mass of 4131 Da. An exact match of measured and theoretical values can be observed.

In HPLC experiments a major peak was detected at a retention time of 26 minutes. To verify the identity of (MePEG$_{2000}$C$_{11}$S)$_2$, a reduction of the disulfide to the corresponding thiol was performed with tris(carboxyethyl)phosphine (TCEP), resulting in a decrease of the signal intensity at 26 minutes. A new peak with a retention time of 23 minutes appeared, indicating the formation of the corresponding free thiol (Fig 2). This hypothesis could be confirmed by HPLC-MS. At a retention time of 26 minutes molecules of (MePEG$_{2000}$C$_{11}$S)$_2$ could be detected. Theoretical values and mass spectrometry data again

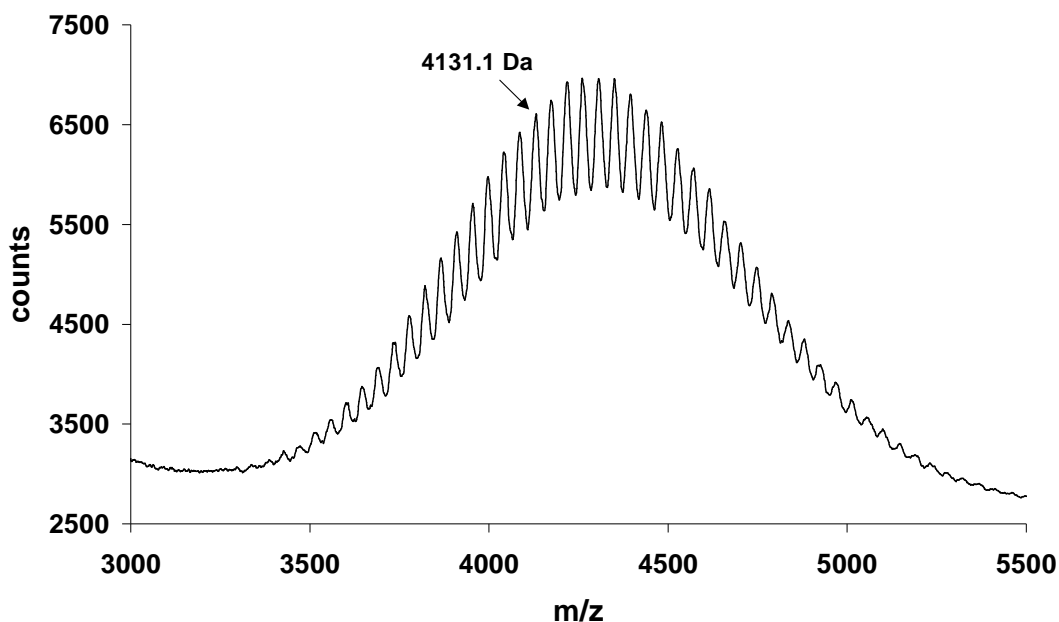matched exactly. The substance at 23 minutes was the reduced form $MePEG_{2000}C_{11}SH$. (data not shown)

Figure 1: MALDI-ToF data of $(MePEG_{2000}C_{11}S)_2$. The indicated peak shows the match of theoretical and measured values. For further details see text.
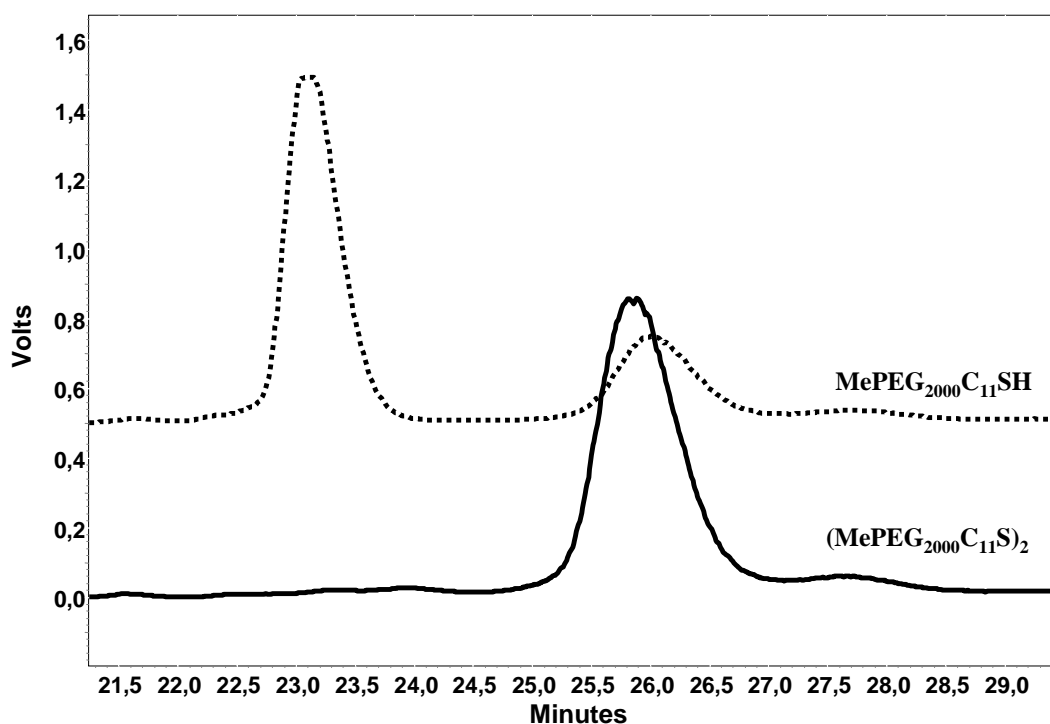

Figure 2: HPLC chromatogram of $(MePEG_{2000}C_{11}S)_2$. With the reducing agent TCEP, the peak at 26 minutes decreases, whereas a new peak arises at 23 minutes, indicating the formation of a thiol.

For $(NH_2PEG_{2000}C_{11}S)_2$, two major signals can be seen in the HPLC chromatogram for the synthesized polymer. At 21 minutes we detected the desired product, at 10 minutes non-modified PEG-monoamine (Fig 3). These findings could be confirmed by further investigations. After reducing the synthesis product with TCEP, the peak at 21 minutes shifted to 16 minutes, indicating the generation of a free thiol. HPLC-MS confirmed this hypothesis. By analyzing the different HPLC signals after electrospray ionization, all generated Gaussian distributions could be attributed to $NH_2PEG_{2000}C_{11}SH$ with different cation adducts (data not shown). Non modified PEG-monoamine was not considered as problematic, due to the high affinity of sulfur to metal surfaces, leading to a kind of "autopurification" process during the formation of PEG monolayers.

All together, these analytical data clearly verify the modified method as a successful way of synthesizing $(PEG_{2000}C_{11}S)_2$ derivatives with methoxy and amine end groups.
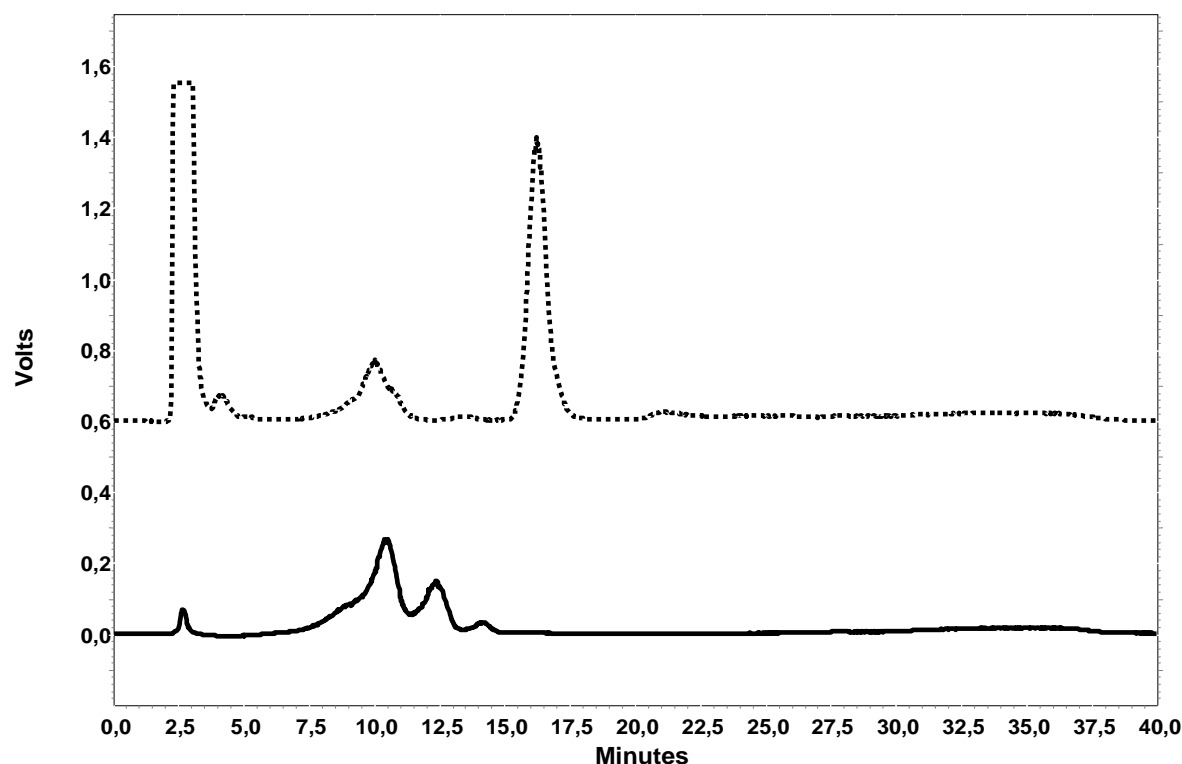
Figure 3: HPLC chromatogram of $NH_2PEG_{2000}C_{11}SH$ and NH_2PEG_{2000}. At 16 minutes, the product can be detected. Non-modified NH_2PEG_{2000} is still present in the synthesized product.

Preparation and modification of self-assembled monolayers

In literature the assembly of alkanethiols is described as a spontaneous process. Initially, the bigger part of mass adsorbes quite fast. Later on, the adsorbed mass reorganizes on the surface. Due to the high molecular weight of the PEG derivatives we incubated the gold surfaces for at least 24 hours with 1mM ethanolic polymer solutions to be sure, that the monolayer formation is completed. To verify the time scale of the self-assembly process, the adsorption of $(NH_2PEG_{2000}C_{11}S)_2$ onto gold was monitored with the QCM. We could see, that after a maximum of 3 hours the increase in mass on the surface is finished (data not shown), but we did not investigate, if a further reorganization takes place on the surfaces and therefore can not exactly define the time point, when the monolayer formation is completed.
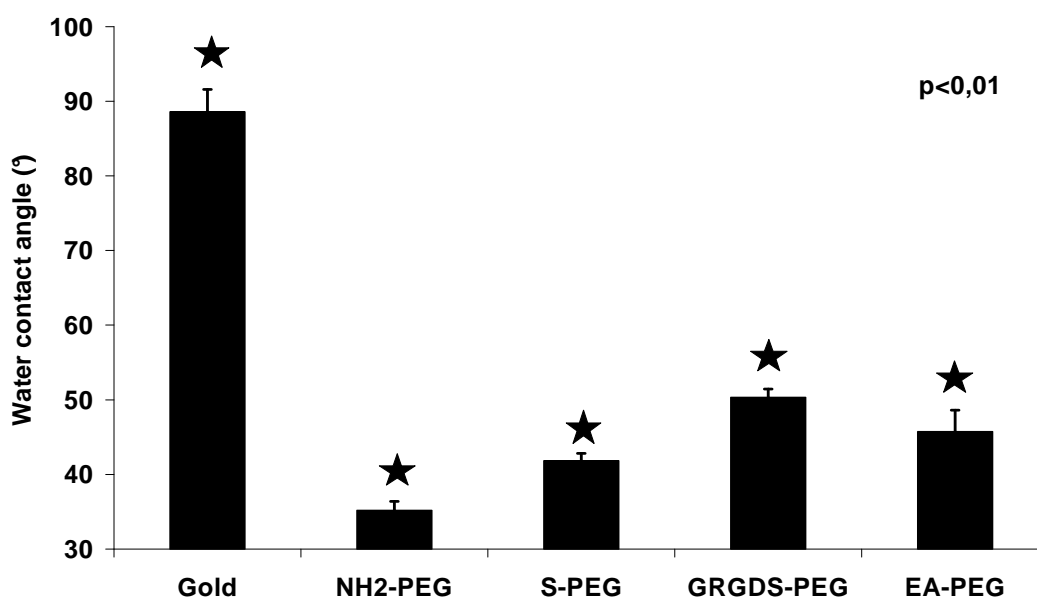
Figure 4: The water contact angle decreases significantly after incubating gold with ethanolic polymer solutions. Physisorption of non-modified PEG$_{2000}$ is neglectable. Modification of the amine group of $(NH_2PEG_{2000}C_{11}S)_2$ with succinic acid leads to an increase as well as the binding of GRGDS.

Measuring the WCA, we could see a strong decrease of the WCA. From almost 80° for gold surfaces and gold, that was incubated with non-thioalkylated PEG (PEG$_{2000}$) to approximately 35° for both synthesized compounds (Figure4). After the conversion of the free amine into a succinamide with succinic anhydride, the contact angle increased significantly to more than 40° (Figure 4). A further significant increase to more than 50°

can be seen after incubation of the succinamide with GRGDS. Although WCA measurements are an indirect method to investigate surface modifications, the binding of GRGDS seemed to be successful, as indicated by the significant changes after the different steps and subsequent cell culture experiments (data not shown).

Investigation of Protein Adsorption

The ability of the PEG monolayers to reduce the non-specific adsorption of proteins was analyzed by means of the quartz crystal microbalance technique (QCM) and surface plasmon resonance (SPR).

In Figure5, the change in resonance frequency is plotted versus time after injecting 100 µl of a solution of BSA (1 mg/ml) into the flow cell. For an unmodified gold electrode, the resonance frequency drops by ~ 40 Hz, indicating a strong adsorption of BSA, whereas the polymer coated gold surfaces hardly showed any response after an injection of 100 µl of BSA-solution.
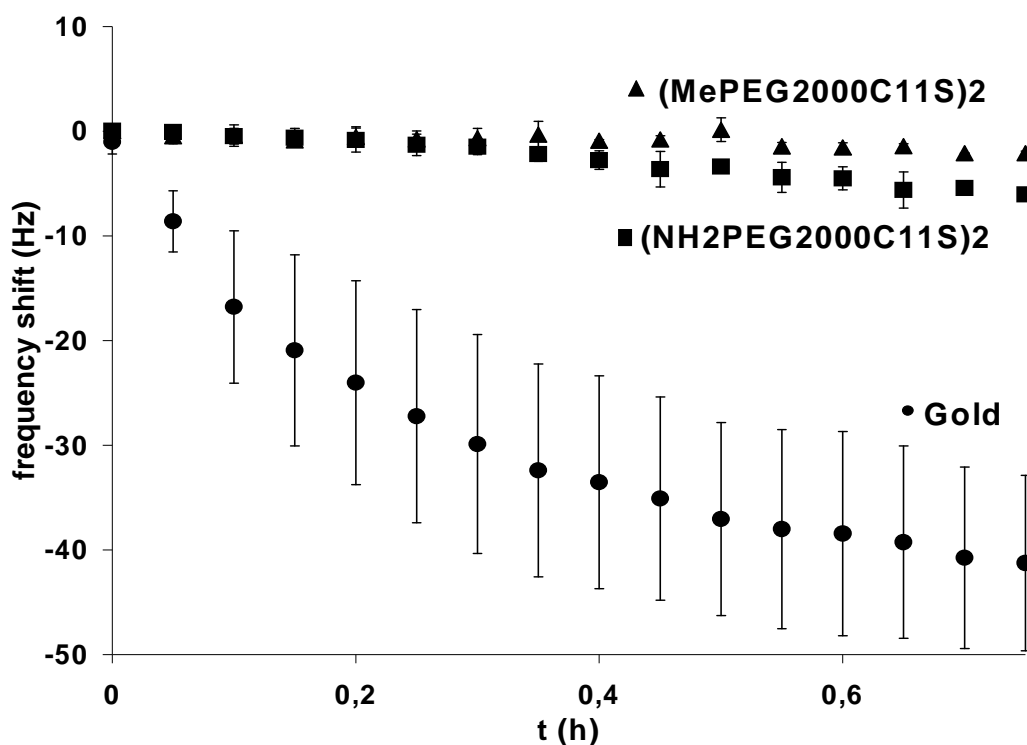
Figure 5: After adding BSA to gold surfaces, the resonance frequency decreases strongly, whereas polymer covered surfaces hardly show any response.
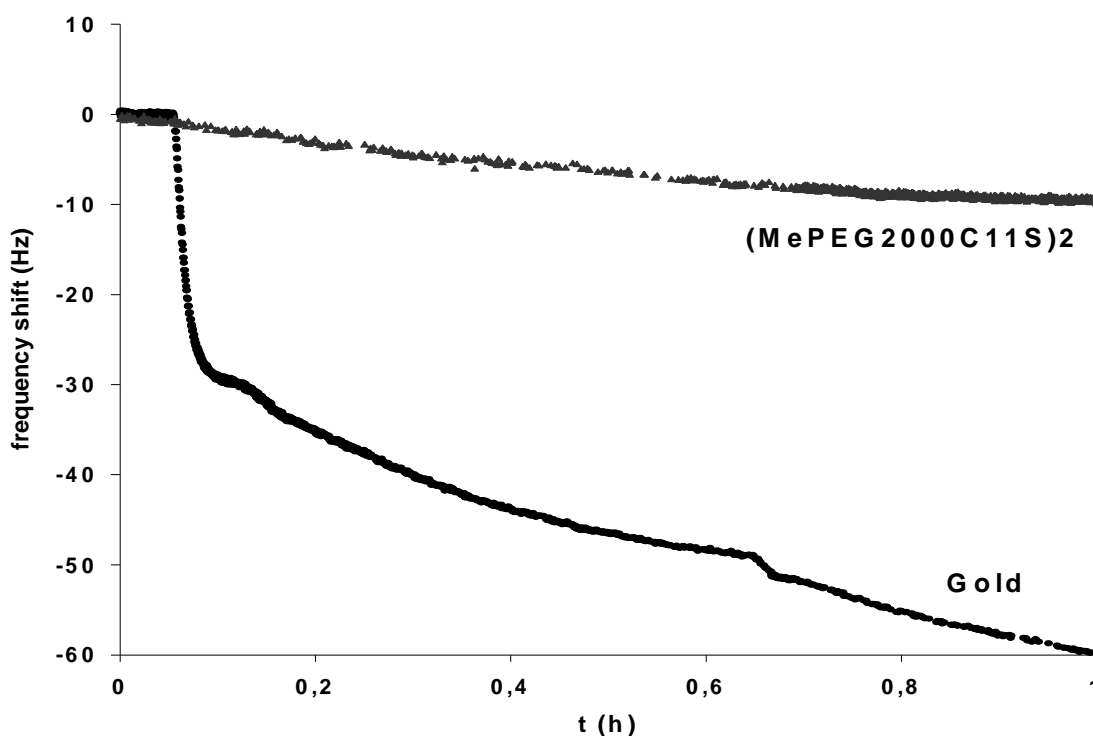
Figure 6: The QCM response is decreased significantly after the addition of FBS if the gold electrodes are modified with $(MePEG_{2000}C_{11}S)_2$. After one hour, only a minor shift of resonance frequency is detectable.

Also after the addition of 2.7 µl of fetal bovine serum in 100µl of PBS a high reduction of protein adsorption can be observed: compared to a decrease of 60 Hz after one hour for non covered gold, the frequency only dropped by 10 Hz for $(MePEG_{2000}C_{11}S)_2$ (Figure6).

For $(NH_2PEG_{2000}C_{11}S)_2$ we could also see a significant reduction of protein adsorption after adding higher amounts of protein (3.5mg total protein): after 0.2 hours the frequency decreased almost 60 Hz for non-modified gold, whereas for the polymer-covered surfaces we can only state a decrease of approximately 22 Hz. If the amine derivative is modified with the adhesion motif GRGDS, an additional slight decrease in resonance frequency of approximately 5 Hz can be seen compared to $(NH_2PEG_{2000}C_{11}S)_2$ (Figure7).
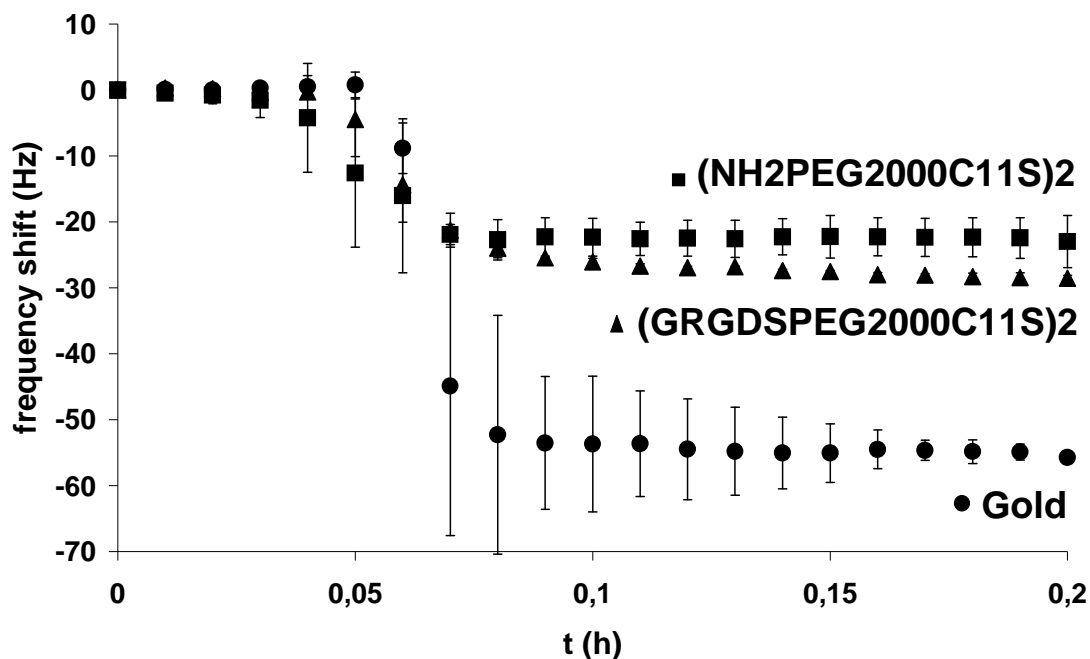
Figure 7: In contrast to (MePEG$_{2000}$C$_{11}$S)$_2$ SAMs, on obvious adsorption of FBS proteins is observed for (NH$_2$PEG$_{2000}$C$_{11}$S)$_2$.

These results were additionally confirmed by SPR: After adding the same amount of proteins for all three surfaces, an increase of 1200 RU indicates a strong protein adsorption on gold, even after flushing with pure buffer after 660 seconds (Figure8). (NH$_2$PEG$_{2000}$C$_{11}$S)$_2$ SAMs reduce the increase to 220 RU and for (MePEG$_{2000}$C$_{11}$S)$_2$ hardly any change can be detected.
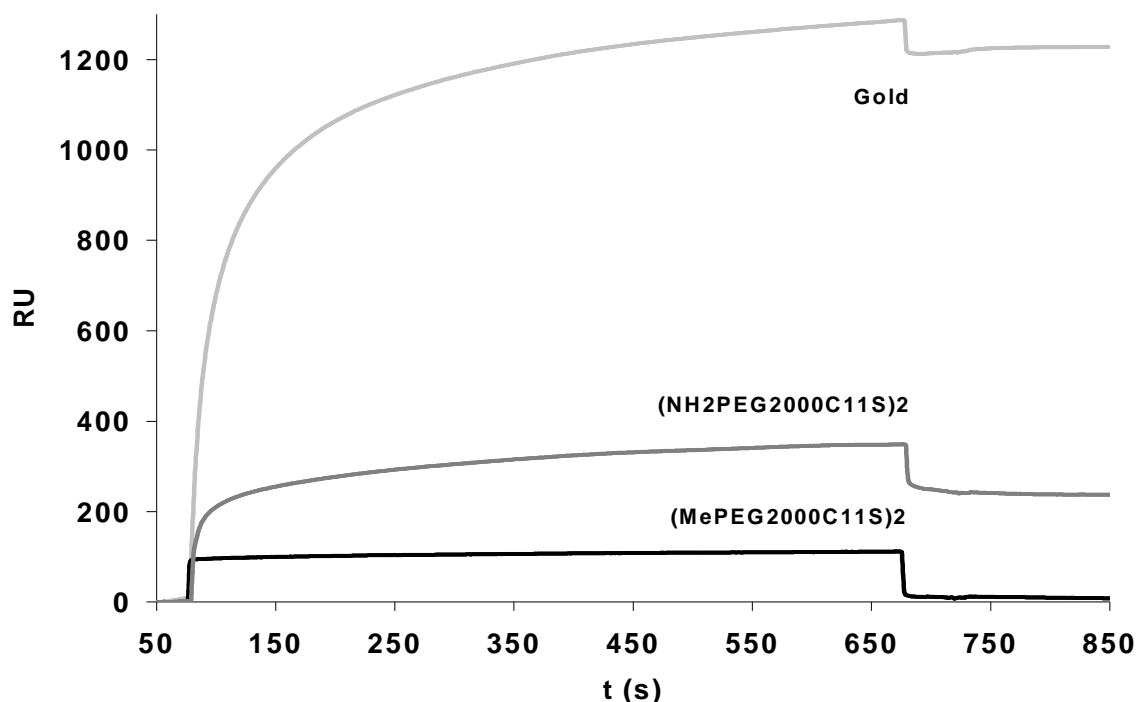
Figure 8: SPR experiments revealed similar results as the QCM: Extensive protein adsorption on gold, a reduction for $(NH_2PEG_{2000}C_{11})S_2$ and almost a resistance for $(MePEG_{2000}C_{11}S)_2$.

Discussion

Polymer synthesis and characterization

All the analytical data obviously verify that the developed strategy for synthesizing the desired PEG derivatives was successful.

The NMR data are in full accordance with theoretical values and also the chromatographic methods are unequivocal. Two further methods were applied to approve the identity of the demanded polymers: firstly, the reduction with TCEP led to a decrease of the contemplable HPLC peak. An other, more hydrophilic peak arose, clearly indicating the formation of a free thiol, as TCEP is a well known agent for the reduction of disulfides to thiols. Secondly, mass spectrometry approves the identity: For $(MePEG_{2000}C_{11}S)_2$, an exact match with theoretical values was shown with MALDI-ToF experiments. Since the developed

MALDI method did not work for $(NH_2PEG_{2000}C_{11}S)_2$, electrospray ionization was carried out for this polymer. Likewise, an exact match with theoretical values could be detected (data not shown).

Nevertheless, the synthesized polymers were not completely pure. In both chromatograms, non-modified educts were found (see Figure3), also mass spectrometry showed these impurities. But since disulfides have a high affinity to gold surfaces (similar to thiols), this fact was not considered as problematic. Because the chemisorption of the disulfides is estimated to be more specific and stronger than the physisorption of non-modified polymers, we (like others[20]) abstained from further purifications due to this "autopurification" during self-assembling.

Production and modification of self-assembled monolayers

As mentioned before, in a lot of studies the adsorption behavior of alkanethiols and dialkyldisulfides has been investigated[17,22,27]. In general, on account of the high affinity of sulfur to gold surfaces, the process of self-assembling in large parts takes place quite quickly, but until a well defined monolayer is formed, several hours are needed. In the case of alkanethiols or dialkyldisulfides, respectively, with high molecular weight polymers, such as PEG_{2000} this process might be extended. The reasons possibly are the large steric volume and the chain mobility of the polymers, constricting the molecules to order tightly.[26] Additionally, an entropy penalty for extension and ordering of the PEG chains, which probably can not be compensated by chain-chain interactions of PEG, has to be taken into account. This might lead to a lower degree of ordering.[15] For that cause, we incubated the gold surfaces at least for 24 hours, a time span, that was considered long enough to allow for the assembly of a monolayer even of high molecular weight polymers.[7] To assert these assumptions, we investigated the adsorption process on the surface by means of the QCM. Here we could detect a decrease in resonance frequency of approximately 60 Hz. This decrease indicates the chemisorption of mass to the gold surface. The major part of this decrease took place within several minutes, after that, the decrease was significantly slower. After 3 hours, no further chemisorption could be detected anymore. This substantiates the hypothesis above: the affinity of the molecules to the surface is quite high, leading to a fast chemisorption to the surface, but the process of ordering and filling the "gaps" between the bound molecules on the other hand takes a certain amount of time.

Contact angle measurements showed a significant change of surface properties, when gold was incubated with the respective ethanolic polymer solutions. Without the alkanethiol moiety, PEG_{2000} does not change the WCA, whereas the synthesized polymers led to a more hydrophilic surface, even after sonication to remove non-bound polymer. This fact also confirms, that the impurities contained in $(MePEG_{2000}C_{11}S)_2$ and $(NH_2PEG_{2000}C_{11}S)_2$ do not disturb the self-assembly notably, since chemisorption is highly favored compared to physisorption of PEG_{2000}.

Further WCA measurements demonstrated, that even minor changes to the polymer ends led to significant changes in the WCA. Introduction of succinic acid triggered a certain increase. A further increase was observed after the activation with DCC/NHS and the subsequent binding of GRGDS. Although additional charges are introduced, the hydrophobic part seems to have a greater impact on the WCA.

Investigation of Protein Adsorption

Numerous studies have been made, especially for oligo(ethylene glycol) SAMs with a high variety of OEG end groups. For PEG in contrast, mostly methoxy PEG is investigated, but some studies also deal with carboxy[7] and hydroxy PEG[25].

Since bovine serum albumin (BSA) is the most abundant protein in human plasma and, therefore, available very easily, it is very often used as a model protein for adsorption experiments. Consequently, we tested our SAMs for their ability to reduce the adsorption of BSA. QCM experiments revealed a high degree of BSA resistance: in contrast to pure gold, the polymer-covered surfaces hardly showed any decrease in resonance frequency. This indicates a high packing density of the monolayer and is in good agreement with other studies, showing the resistance of certain SAMs against non-specific adsorption of single protein solutions.[7,25,26,30]

Thinking of further cell adhesion experiments, not only the adsorption of one single protein is important, but the SAMs also should reduce the adsorption of complex protein mixtures, such as fetal bovine serum (FBS). Therefore, we tested a $(MePEG_{2000}C_{11}S)_2$ SAM by adding the same amount of total protein (100µg) of FBS. With the QCM, we could show a significant reduction of protein adsorption compared to pure gold, only a slight decrease in resonance frequency was observed (Figure6). With SPR, the amount of adsorbed protein is probably below the detection limit (Figure8). Also these results are in agreement with other studies. Zhu et al. for example reported, that FBS adsorption to OEG and a similar PEG SAM was below the detection limit of their SPR system. However, especially on the OEG

SAMs, a certain amount of protein seemed to induce non-specific cell adhesion.[30] Also Unsworth et al. could not state a complete resistance to different proteins on PEG SAMs.[26]

For $(NH_2PEG_{2000}C_{11}S)_2$, the results are different. Already with SPR, an obvious FBS adsorption can be seen, though there still is an extensive reduction compared to gold surfaces. Using higher amounts of FBS for QCM experiments, the finding is similar: the SAM can reduce FBS adsorption, but the surface is not resistant to protein adsorption in general. Possibly, there might be ionic interactions between the positively charged amino groups of the polymer and certain proteins of FBS. Also Unsworth et al. stated a "chain end chemistry effect" concerning fibrinogen adsorption.[25] For GRGDS modified SAMs, the situation is quite similar to $(NH_2PEG_{2000}C_{11}S)_2$. The amount of adsorbed protein is in the same range. Again, charges might be the reason. To verify the hypotheses concerning the differences between the two polymers, further protein adsorption experiments should be performed to investigate the impact of the polymer end groups.

Conclusion

Within this study, we could demonstrate the successful development of an ω-amino functionalized self-assembled monolayer containing a high molecular weight PEG. The synthesis strategy is also applicable to other PEG derivatives, as we could show for the corresponding methoxy PEG. The SAM formation is within the predicted time scale. Additionally, the modification with bioactive compounds was demonstrated using the cell adhesion motif GRGDS. For $(MePEG_{2000}C_{11}S)_2$, the protein adsorption characteristics are accordant to other studies. We could demonstrate, that $(NH_2PEG_{2000}C_{11}S)_2$ is resistant to certain proteins, but can not fully exclude the adsorption from complex protein mixtures.

References

[1] Bain C.D.; Troughton E.B.; Tao Y.T.; Evall J.; Whitesides G.M.; Nuzzo R.G.: Formation of monolayer films by the spontaneous assembly of organic thiols from solution onto gold. J Am Chem Soc, 111, 321-335, 1989.

[2] Castner D.G.; Ratner B.D.: Biomedical surface science: foundations to frontiers. Surf Sci, 500, 28-60, 2002.

[3] Drotleff S.; Lungwitz U.; Breunig M.; Dennis A.; Blunk T.; Tessmar J.; Göpferich A.: Biomimetic polymers in pharmaceutical and biomedical sciences. Eur J Pharm Biopharm, 58, 385-407, 2004.

[4] Du Y.J.; Brash J.L.: Synthesis and characterization of thiol terminated poly(ethylene oxide) for chemisorption to gold surface. J Appl Polym Sci, 90, 594-607, 2003.

[5] Harder P.; Grunze M.; Dahint R.; Whitesides G.M.; Laibinis P.E.: Molecular conformation in oligo(ethylene glycol)-terminated self-assembled monolayers on gold and silver surfaces determines their ability to resist protein adsorption. J Phys Chem B, 102, 426-436, 1998.

[6] Herrwerth S.; Eck W.; Reinhardt S.; Grunze M.: Factors that determine the protein resistance of oligoether self-assembled monolayers – Internal hydrophilicity, terminal hydrophilicity and lateral packing density. J Am Chem Soc, 125, 9359-9366, 2003.

[7] Herrwerth S.; Rosendahl C.; Feng C.; Fick J.; Eck W.; Himmelhaus R.; Dahint R.; Grunze M.: Covalent coupling of antibodies to self-assembled monolayers of carboxy-functionalized poly(ethylene glycol): Protein resistance and specific binding of biomolecules. Langmuir, 19, 1880-1887, 2003.

[8] Hersel U.; Dahmen C.; Kessler H.: RGD modified polymers: biomaterials for stimulated cell adhesion and beyond. Biomaterials, 24, 4385-4415, 2003.

[9] Houseman B.T.; Mrksich M.: Efficient solid phase synthesis of peptide substituted alkanethiols for the preparation of substrates that support the adhesion of cells. J Org Chem, 63, 7552-7555, 1998.

[10] Jeon S.I.; Lee J.H.; Andrade J.D.; de Gennes P.G.: Protein-surface interactions in the presence of polyethylene oxide. J Colloid Interf Sci, 142, 149-166, 1991.

[11] Kastl K.; Ross M.; Gerke V.; Steinem C.: Kinetics and thermodynamics of Annexin A1 binding to solid supported membranes: A QCM study. Biochemistry, 41, 10087-10094, 2002.

[12] Kingshott P.; Griesser H.J.: Surfaces that resist bioadhesion. Curr Opin Solid St M, 4, 403-412, 1999.

[13] Lee J.H.; Lee H.B.; Andrade J.D.: Blood compatibility of polyethylene oxide surfaces. Prog Polym Sci, 20, 1043-1079, 1995.

[14] Lieb E.; Tessmar J.; Hacker M.; Fischbach C.; Rose D.; Blunk T.; Mikos A.G.; Goepferich A.; Schulz M.B.: Poly(D,L-lactic acid)-poly(ethylene glycol)-monomethyl ether diblock copolymers control adhesion and osteoblastic differentiation of marrow stromal cells. Tissue Eng, 9, 1, 71-84, 2003.

[15] Menz B.; Knerr R.; Göpferich A.; Steinem C.: Impedance and QCM analysis of the protein resistance of self-assembled PEGylated alkanethiol layers on gold. Biomaterials, 26, 4237 – 4243, 2005.

[16] Mrksich M.; Whitesides G.M.: Patterning self-assembled monolayers using microconatct printing: a new technology for biosensors? Trends Biotechnol, 13, 228-235, 1995.

[17] Mrksich M.; Dike L.E.; Tien J.; Ingber D.E., Whitesides G.M.: Using microcontact printing to pattern the attachment of mammalian cells to self-assembled monolayers of alkanethiolates on transparent films of gold and silver. Exp Cell Res, 235, 305-313, 1997.

[18] Pasche S.; Textor, M.; Meagher, L.; Spencer N.D.; Griesser, H.J.: Relationship between Interfacial Forces Measured by Colloid-Probe Atomic Force Microscopy and Protein Resistance of Poly(ethylene glycol)-Grafted Poly(L-Lysine) Adlayers on Niobia Surfaces. Langmuir, 21, 6508 – 6520, 2005.

[19] Prime K.L.; Whitesides G.M.: Self-assembled organic monolayers - model systems for studying adsorption of proteins at surfaces. Science, 252, 1164-1167, 1991.

[20] Saito N.; Matsuda T.: Protein adsorption on self-assembled monolayers with water soluble non-ionic oligomers using quartz-crystal microbalance. Materials Science and Engineering C, 6, 261-266, 1998.

[21] Salem A.K.; Cannizzaro S.M.; Davies M.C.; Tendler S.J.B.; Roberts C.J.; Williams P.M.; Shakesheff K.M.: Synthesis and characterisation of a degradable poly(lactic acid)-poly(ethylene glycol) copolymer with biotinylated end groups. Biomacromolecules, 2, 575-580, 2001.

[22] Terrill R.H.; Tanzer T.A.; Bohn P.W.: Structural evolution of hexadecanethiol monolayers on gold during assembly: substrate and concentration dependence of monolayer structure and crystallinity. Langmuir, 14, 845-854, 1998.

[23] Tessmar J.; Mikos A.G.; Göpferich A.: The use of poly(ethylene glycol)-block-poly(lactic acid) derived copolymers for the rapid creation of biomimetic surfaces. Biomaterials, 24(24), 4475-4486, 2003.

[24] Tokumitsu S.; Liebich A.; Herrwerth S.; Eck W.; Himmelhaus M.; Grunze M.: Grafting alkanethiol-terminated poly(ethylene glycol) on gold. Langmuir, 18, 8862-8870, 2002.

[25] Unsworth L.D.; Sheardown H.; Brash J.L.: Polyethylene oxide surfaces of variable chain density by chemisorption of PEO-thiol on gold: adsorption of proteins from plasma studied by radiolabelling and immunoblotting. Biomaterials, 26, 5927-5933, 2005.

[26] Unsworth L.D.; Sheardown H.; Brash J.L.: Protein resistance of surfaces prepared by sorption of end-thiolated poly(ethylene glycol) to gold: effect of surface chain density. Langmuir, 21, 1036-1041, 2005.

[27] Vanderah D.J.; Arsenault J.; La H.; Gates R.S.; Silin V.; Meuse C.W.: Structural variations and ordering conditions for the self-assembled monolayers of $HS(CH_2CH_2O)_{3-6}CH_3$. Langmuir, 19, 3752-3756, 2003.

[28] Vanderah D.J.; Pham C.P.; Springer S.K.; Silin V.; Meuse C.W.: Characterization of a series of self-assembled monolayers of alkylated 1-thiaoligo(ethylene oxides)$_{4-8}$ on gold. Langmuir, 16, 6527-6532, 2000.

[29] Yokoyama M.; Okano T.; Sakurai Y.; Kikuchi A.; Ohsako N.; Nagasaki Y.; Kataoka K.: Synthesis of poly(ethylene glycol) with heterobifunctional reactive groups at its terminals by an anionic initiator. Bioconjug Chem, 3, 275-276, 1992.

[30] Zhu B.; Eurell T.; Gunawan R.; Leckband D. J.: Chain-length dependence of the protein and cell resistance of oligo(ethylene glycol)-terminated self-assembled monolayers on gold. Biomed Mater Res, 56(3), 406-416, 2001.

SUPPLIERS

[L] Goodfellow, 61213 Bad Nauheim, Germany.

[M] Bachem Biochemica, 69126 Heidelberg, Germany.

[N] Invitrogen GmbH, 76131 Karlsruhe, Germany.

[O] Ismatec Laboratoriumstechnik GmbH, 97877 Wertheim-Mondfeld, Germany.

[P] Biochrom AG, 12247 Berlin, Germany.

[Q] Biacore, 75450 Uppsala, Sweden.

Chapter 4

Measuring Cell Adhesion on RGD-modified Self-assembled PEG Monolayers Using the Quartz Crystal Microbalance Technique

Robert Knerr[1], Barbara Weiser[1], Sigrid Drotleff[1], Claudia Steinem[2], Achim Göpferich[1]*

[1]Department of Pharmaceutical Technology, University of Regensburg, Universitaetsstrasse 31, 93040 Regensburg, Germany

[2]Institute of Analytical Chemistry, Chemo- and Biosensors, University of Regensburg, 93040 Regensburg, Germany

Abstract

In this study, the suitability of a flow-through quartz crystal microbalance (QCM) system for the detection of the adhesion of rat marrow stromal cells (rMSCs) and 3T3-L1 fibroblasts on different surfaces is demonstrated. Frequency shifts for rMSCs of -6.7 mHz/cell and -2.0 mHz/cell for 3T3-L1 cells could be detected on non-modified gold sensors, revealing that frequency shift per cell are comparable to static setups. Modifying the sensor surface with SAMs of thioalkylated ω-amine-terminated PEG derivatives led to cell adhesion resistant surfaces, total frequency shifts of only -20±7 Hz showed that also protein adsorption was significantly reduced. Attaching 35 pm/mm^2 of the cell adhesion motif GRGDS to the SAMs induced specific cell adhesion due to RGD-integrin interactions, the resonance frequency dropped by -3.4 mHz/cell. Furthermore, the kinetics of cell detachment could be determined. The corresponding processes were completed after 10 minutes for trypsin and not before 90 minutes with GRGDS. Moreover, the detectability of cell adhesion increases after adding manganese cations was shown. The total decrease in resonance frequency was almost -80 Hz in the presence of Mn^{2+} (-6.4mHz/cell).

Introduction

Grafting poly(ethylene glycol) (PEG) chains to surfaces is a popular approach towards controlling interactions of cells with biomaterials.[1] The attractiveness of this strategy is for two reasons[2]: First of all PEG can suppress the non-specific protein adsorption to surfaces due to steric repulsion and, therefore, uncontrolled cell adhesion, since cells depend on specific proteins for anchorage.[2,3] Second, PEG moieties allow for tethering bioactive compounds to surfaces via functional end groups of PEG, leading to "biomimetic" surfaces.[4] By choosing different bioactive entities, tailor-made surfaces allowing for specific cell signaling can be created.[5,6]

Numerous analytical methods have been used in a plethora of studies investigating the adsorption characteristics of proteins to PEGylated surfaces, such as surface plasmon resonance, ellipsometry or x-ray photon electron spectroscopy.[7,8,9] Although all these methods can provide us with detailed information on certain aspects of protein adsorption, such as the amount of adsorbed mass or the kinetics, they provide us only with a narrow spectrum of information and can not be applied in situ. Moreover, these techniques fail to go one step beyond protein adsorption, which means characterizing the subsequent adhesion of cells on surfaces.

The so-called quartz crystal microbalance (QCM) in contrast can fulfill all aforementioned demands and additionally can provide this information in real-time and label-free, an obvious advantage over common photospectrometric methods.[10,11] However, compared to its use for protein adsorption experiments, only a few studies on cell adhesion using the QCM have been published.[12-28] The different cell types, that have been investigated lead to very different changes in resonance frequencies depending on the cell seeding density and of course on the different setups.[12-28] A significant drawback of all those studies is , that most of them were performed under static conditions (except for the study of Jenkins et al[18]). A static setup averts the possibility to continuously modify the composition of culture media. If the conditions have to be changed, measurements have to be interrupted or at least disturbed significantly, resulting in enormous fluctuations of the measured frequency. A dynamic flow-through setup, which is frequently used for protein adsorption experiments, would therefore be of great advantage. Medium could be changed or continuously modified without any direct intervention during measurements.

Hence in this study, we tried to explore the feasibility of such a flow through setup of a QCM to characterize the adhesion of rat marrow stromal cells (rMSCs) and 3T3-L1 cells, a well-characterized murine fibroblast cell line. rMSCs are frequently used in cell culture systems, as they can easily be differentiated into different connective tissue cell types, such as chondrocytes, osteoblasts and adipocytes.[29] Therefore, the characterization of their adhesion characteristics would be valuable for a large community. In particular, we focused on the adhesion characteristics of rMSCs on PEG monolayers, a very common model system for the aforementioned PEG rich surfaces of different biomaterials. We also intended to explore the potential of this QCM system to detect selective cell adhesion to PEG-rich surfaces with attached peptidic cell adhesion motifs. To prove the sensitivity of our system, we furthermore tried to examine the influence of enzymes, peptides and cations on the adhesion characteristics of rMSCs.

Experimental Part

Materials

Ethanol was purchased from JT Baker, Deventer, Netherlands. Dimethylformamide (DMF) and methanol were from Acros Organics (Geel, Belgium). Ascorbic acid, succinic anhydride, 11-bromo undecene, thioacetic acid, dibenzoyl peroxide, 2-chlorotrityl chloride, iodine, di-*t*-butyl dicarbonate, propidium iodine, RNAse, bovine serum albumin (BSA), dicyclohexyl carbodiimide (DCC) and N-hydroxysuccinimide (NHS) were acquired from Sigma-Aldrich Chemie GmbH (Taufkirchen, Germany). Manganese chloride, toluene, chloroform, dioxane, sodium hydride, acetone, diethyl ether, hydrochloric acid, sulfuric acid, sodium hydroxide, hydrogen peroxide solution (30%) and formaldehyde were purchased from Merck KGaA (Darmstadt, Germany), GRGDS from Bachem Biochemica (Heidelberg, Germany), Fluorescein phalloidin, Penicillin-Streptomycin solution (PenStrep) and phosphate buffered saline (PBS) from Invitrogen GmbH (Karlsruhe, Germany). Fetal bovine serum (FBS), Dulbecco´s modified eagle medium (DMEM) and trypsin were acquired from Biochrom AG (Berlin, Germany). All reagents were analytical grade and used as received without further purification, unless otherwise stated.

Polymer Synthesis

Thioalkylated ω-amine-terminated PEG derivatives have been synthesized and characterized as published previously.[7] To thioalkylate poly(ethylene glycol) monoamine with a molecular weight of 2000 Da, which was synthesized according to a method described previously[30], the following scheme was applied: 3.29ml (15mmol) of 11-bromo-undecene and 5.35 ml (75 mmol) of thioacetic acid were dissolved in 50 ml of toluene (dried by azeotropic distillation to remove traces of water). After adding 40 mg (164µmol) of dibenzoyl peroxide, the reaction mixture was heated to 80°C with an oil bath for three hours. After cooling the system to room temperature, the solvent was removed by rotary evaporation under reduced pressure. The hydrolyzation of the crude product was performed in methanolic HCl according to a method developed by Bain et al[31].

The free thiol compound was then protected with 2-chlorotrityl chloride: 3.5 g (13.1 mmol) of 11-bromo-undecylmercaptane and 4.1 g (13.1 mmol) of the protecting group were dissolved in 50 ml of chloroform in a nitrogen atmosphere and the reaction allowed to proceed for 24 hours, before chloroform was removed by rotary evaporation.

4 g (2 mmol) of poly(ethylene glycol) monoamine were protected with di-tert-butyl dicarbonate (BOC) (2 mmol) by stirring in 100 ml of dioxane over night. The protected compound was purified by repeated precipitation in diethyl ether and dried for 24 hours in vacuum. For the subsequent Williamson ether synthesis, N-BOC protected PEG was again dissolved in 100 ml dioxane. 240 mg (10 mmol) of sodium hydride were added to the dry solution and stirred for one hour. Then the protected alkanethiol (3) was added (5,7 g; 10 mmol) and stirred for 24 hours at room temperature. After adding one ml of methanol at room temperature, the crude reaction mixture was filtered, the solvent rotary evaporated and the product purified by repeated precipitation in 100 ml of diethyl ether.

For the deprotection, the alkylated PEG (3.1 g; 1.3 mmol) was dissolved in 20 ml of a solution of 200 mg of iodine in methanol and stirred for 24 hours at room temperature. After rotary evaporating methanol, the polymer was dissolved in acetone and precipitated in diethyl ether. To remove the BOC protecting group, the polymer was dissolved in 0.1 N hydrochloric acid and stirred over night. After neutralization with aqueous sodium hydroxide water was rotary evaporated, the product dissolved in chloroform and the created insoluble salts filtrated off. After removing the remaining solvents by drying in a desiccator under reduced pressure, anions were removed by using an anion exchanger before the product was again purified by repeated precipitation in 100 ml of diethyl ether. ^{1}H NMR (300 MHz, CDCl$_3$): δ 3.5-3.8 (m,180 H), 2.8 (m, 2 H), 2.66 (t, 2 H), 1.2-1.7 (m, 18 H).

*Preparation of Self-assembled Monolayers (SAMs)*

The corresponding gold surfaces were cleaned by immersing the surfaces for 5 minutes in a piranha solution (3:1 mixture of concentrated sulfuric acid and an aqueous hydrogen peroxide solution (30 vol.-%)) which was heated to 70°C. Afterwards, gold was rinsed extensively with double-distilled water, dried in a stream of nitrogen and incubated in 1 mM solutions of (NH$_2$PEG$_{2000}$C$_{11}$S)$_2$ in absolute ethanol over night. After rinsing again with absolute ethanol, the surfaces were dried again in a stream of nitrogen. The deposition of polymer on the gold surface, which was determined by impedance measurements revealing an occupancy of 95% of available binding sites, and the efficacy of the resulting monolayer to reduce the non-specific adsorption of proteins was already published elsewhere.[5,7]

If a modification with GRGDS was performed, the $(NH_2PEG_{2000}C_{11}S)_2$ SAM was incubated in a 4 wt.-% solution of succinic anhydride in dimethylformamide (DMF) over night, rinsed with DMF and dried in a stream of nitrogen. The resulting succinamide then was activated with a solution of dicyclohexyl carbodiimide (DCC, 0.2 M) and n-hydroxy succinimide (NHS, 0.05 M) for two hours, rinsed afterwards with DMF and dried with nitrogen. For binding the pentapeptide GRGDS, the activated surface was incubated in a solution of 0.5 mg GRGDS in 1 ml of phosphate buffered saline pH 7.4 (PBS) at 4°C over night allowing for the reaction of the primary amine group of GRGDS with the activated carboxylic acid and rinsed afterwards with double-distilled water. The binding of GRGDS was checked by water contact angle measurements with a method described previously.[7] For an approximate quantification SPR experiments were performed (see below).

Quartz Crystal Microbalance (QCM) Experiments

A detailed description of the QCM setup is already given elsewhere.[32] In brief: AT-cut quartz plates with a 5 MHz fundamental resonance frequency (KVG, Neckarbischofsheim, Germany) were coated with gold electrodes with a size of 0.3 cm^2 on both sides and placed in a Teflon chamber, exposing one side of the resonator to the aqueous solution. The setup was equipped with an inlet and outlet, which connects the fluid chamber to a peristaltic pump (pump rate: 100 µl/min) (Ismatec Reglo Digital, Wertheim-Mondfeld, Germany), allowing for the addition of cell suspensions from outside the Teflon chamber. Spring contacts connect the gold electrodes with the oscillator circuit (TTLSN74LS124N, Texas instruments, Dallas, TX, USA) driven by a 4 V D.C. voltage (HP E3630A, Hewlett-Packard, San Diego, CA, USA).The frequency change of the quartz resonator was recorded using a frequency counter (HP 53181A, Hewlett-Packard) connected via RS 232 to a personal computer. The Teflon chamber was thermostated at 37°C in a water-jacketed Faraday cage. Experiments were performed by adding 1ml of suspensions of 250.000 rMSCs per ml serum containing medium or per ml PBS. (For the detailed setup see Figure 1.)
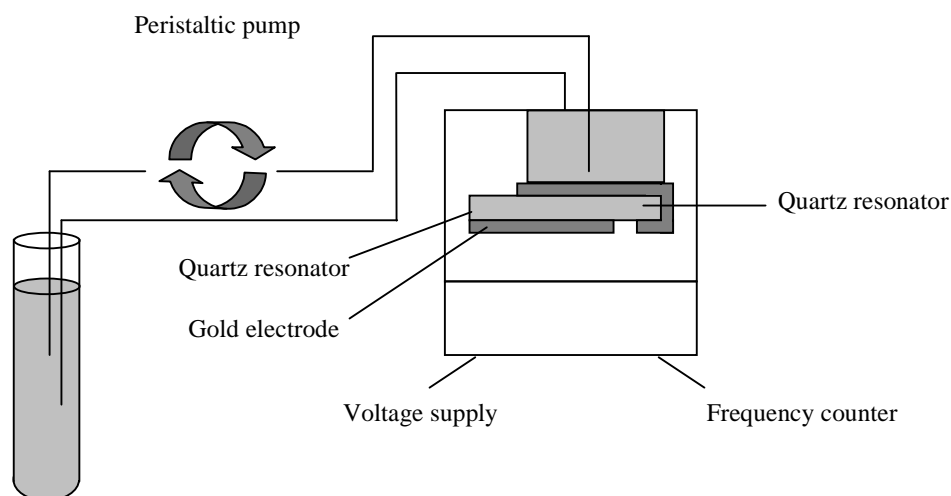
Figure 1: Flow-through setup of the QCM. With a peristaltic pump fluids can be pumped into the Teflon chamber and circulate over the gold sensor surface. Due to the piezoelectric effect and the applied DC voltage, the quartz resonator oscillates at a certain resonance frequency. If mass adsorbed to the sensor surface, the resonance frequency decreases. Modifying the sensor with SAMs stills allows for investigating interfacial processes.

Surface Plasmon Resonance (SPR)

SPR was used to estimate the density of active groups on the SAM surface. Experiments were performed on a Biacore3000 system (BIACore, Uppsala, Sweden): $(NH_2PEG_{2000}C_{11}S)_2$ was bound to gold sensor chips by incubating the sensor area with 1mM ethanolic polymer solutions for 24 hours. The resulting SAM was then modified with succinic acid similar to the SAM modifications for QCM experiments (details described above). Succinic acid afterwards was activated with EDC/NHS chemistry using the supplier's Amine Coupling Kit® and instructions resulting in amine reactive surfaces. To be able to estimate the extent of the covalent attachment of low molecular weight amine containing compounds (such as GRGDS), we quantified the covalent attachment of the high molecular weight molecule bovine serum albumin (BSA), since low molecular weight compounds (GRGDS) are below the detection limit.[33]

Similar to QCM experiments, first the corresponding surfaces were rinsed with PBS. Then the medium was changed to an aqueous 1 mg/ml BSA solution. After 10 minutes, the

surfaces were rinsed again with pure PBS. The increase in RU of activated surfaces compared to succinic acid terminated SAMs (non-activated) was used to quantify the amount of BSA on the surface according to a publication of Maesawa et al.[34]

Cell Culture

Marrow stromal cells (rMSCs), obtained from 6-week-old Sprague Dawley rats according to a procedure published by Ishaug et al[35], were cultivated under standard culture conditions (37°C, 95% relative humidity, 5% CO_2 in DMEM with 10% fetal bovine serum, 1% penicillin/streptomycin and 50 µg/ml ascorbic acid). For QCM experiments, cells were trypsinized, centrifuged at 1200 rpm for 5 minutes and the resulting cell pellet re-suspended in medium or PBS at 250.000 cells/ml. Staining of the nuclei was performed with propidium iodide. Therefore cells were fixed with ice-cold methanol for 5 minutes, washed twice with PBS and then incubated in a solution of 125µg RNAse and 1µg propidium iodide in 500 µl PBS for 30 minutes in the dark, before a final rinse with PBS. Staining of the cytoskeleton was performed with a fluorescein-labelled Phalloidin derivative (Invitrogen, Karlsruhe, Germany). Therefore, the surfaces were rinsed with PBS, cells were fixed with 3.8 vol% formaldehyde for 10 minutes at room temperature. After rinsing with PBS, the surfaces were extracted with acetone at –20°C for 5 minutes and rinsed again with PBS. Then, the cells were stained with 5µl of the methanolic dye solution in 500µl of PBS containing 1% BSA for 20 minutes. After rinsing with PBS, images were taken with a Axiovert 200M microscope coupled to scanning device LSM 510 (Zeiss, Jena, Germany) at 100-fold magnification (Ex = 469nm, EM = 516nm).

The cell density on the surface was measured with the Eclipsenet Imaging software (Nikon GmbH, Düsseldorf, Germany).

Results and Discussion

Detection of cell adhesion using non-modified sensors

In first experiments we tried to explore, whether our system (Figure 1) is feasible for the detection of cell adhesion. In Figure 2 the QCM response of our flow through system after the addition of 1 ml of a suspension of 250.000 rMSCs in medium containing 10% FBS can be seen. The decrease in resonance frequency of -65±5 Hz indicates a deposition of mass on the gold electrode due to the adsorption of serum proteins and the adhesion of cells to the surface. Staining the nuclei of the cells on the gold electrode with propidium iodide showed, that approximately 3000 cells were distributed homogeneously all over the gold electrode, whereas almost no rMSCs were found on the quartz surface (see Figure 3a).
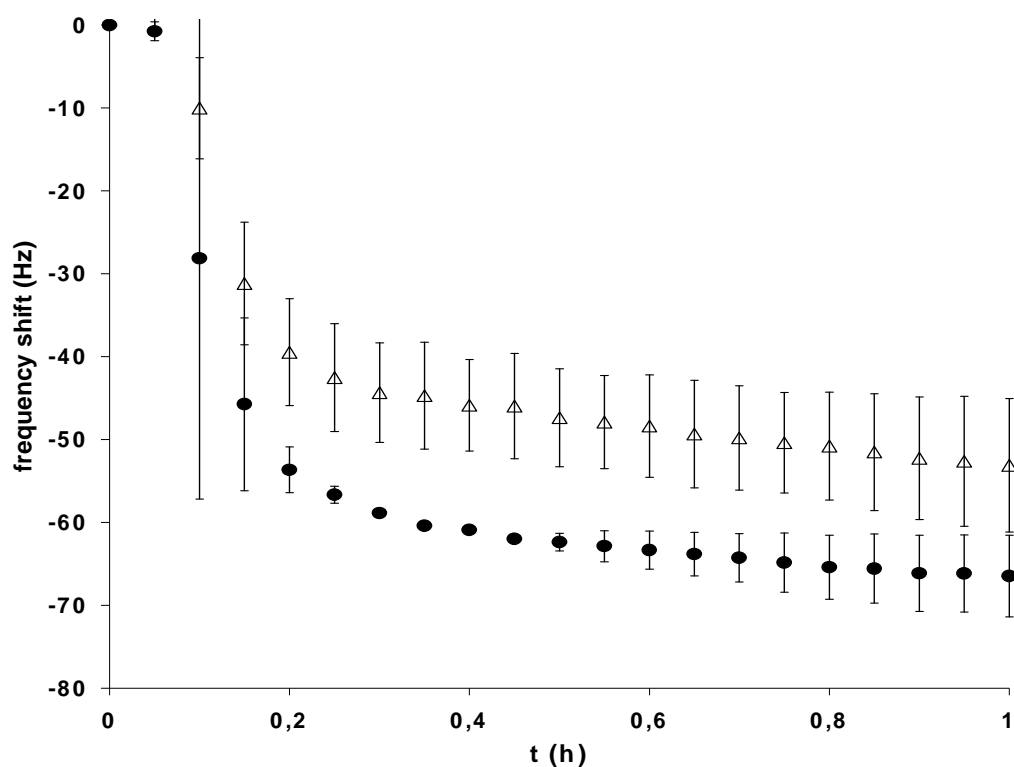
Figure 2: QCM response after the addition of 250.000 rMSCs in serum-containing medium. The decrease in resonance frequency of -65±5 Hz indicates the adsorption of proteins and the adhesion of cells (●). Similar, but slightly lower values could be determined for 3T3-L1 cells (△).

In experiments, where we added the same amount of serum containing medium without rMSCs onto gold, we could detect a frequency shift of -45 Hz (data not shown). This suggests that 3000 rMSCs cause an additional frequency shift of approximately -20 Hz. This value of course has to be handled carefully, since the composition and the viscoelasticy of the two different adsorbed "biofilms" differ to a certain extent. Compared to the investigations of Wegener et al, who detected frequency shifts of up to -530 Hz, this decrease seems to be quite small, but the frequency decrease per cell is in the same range.[14] They found approximately -2-6 mHz/cell, if we calculate 3000 cells per -20 Hz we had -6.7 mHz/cell for rMSCs.
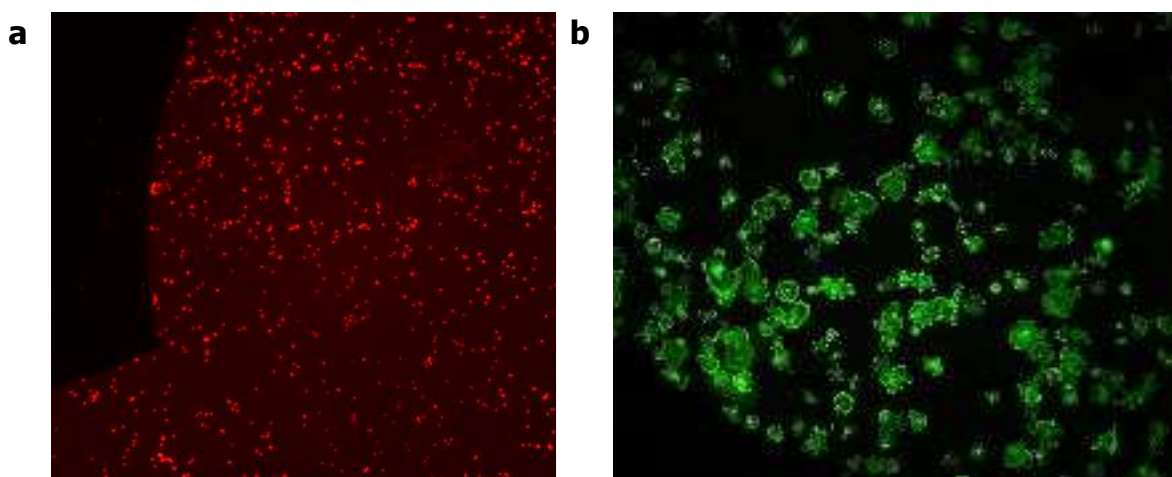
Figure 3a: Staining of the nuclei with propidium iodine shows, that rMSCs are homogeneously distributed over the sensor electrode.

Figure 3b: Staining the cytoskeleton of 3T3-L1 cells shows a surface occupancy of approximately 46%.

To assess the influence of the cell type, we performed experiments with non-differentiated 3T3-L1 cells, to be able to compare the frequency shift per cell with the results of Wegener et al, who used the same cell type. Figure 2 reveals a frequency shift of -51 Hz after the addition of 250.000 cells. Staining of the nuclei showed that again approximately 3.000 cells adhered to the surface. Phalloidin stained cells were spread and covered approximately 46% of the surface (Figure 3b). Subtracting the frequency shift of -45 Hz caused by proteins, we calculate a shift of -2.0 mHz per 3T3-L1 cell for these experiments. This result is absolutely in agreement with the frequency shift of 3T3 cells in the

experiments of Wegener et al, who found a decrease in resonance frequency of -240 Hz for a 3T3 cell monolayer consisting of 130.000 cells/cm^2, resulting in -1.85 mHz/cell for their static setup. Again it has to be mentioned that different vicoelasticies and compositions of the adsorbed biofilms were not considered and that protein adsorption and cell adhesion were assumed to be additive.

Hence, the obvious difference in total frequency shift is due to the different numbers of attached cells, since the geometries and the fundamental resonance frequency are similar. The reason for the relatively low number of attached cells in our experiments might be due to the different setup. Since we were using a flow-through system imposing a shear stress on the cells, an anchorage of the cells to the surface is of course more difficult, what might lead to that low number of attached cells which is in good agreement with numerous publications describing that shear stress can hamper cell adhesion.[36] Unfortunately, there seems to be only one publication investigating the shear stress on cells caused by a QCM under dynamic conditions,[18] making it difficult to estimate its influence on cell adhesion within this system. Experiments with higher pump speeds (and therefore higher shear stress) resulted in significantly lower cell adhesion, a fact, which supports these assumptions (data not shown) and was also described by Jenkins et al.[18]

Suppressing cell adhesion by PEGylating the surface

A completely different result was obtained when the gold electrodes were modified with $(NH_2PEG_{2000}C_{11}S)_2$. In previous investigations, we could show, that these PEG derivatives we synthesized are forming self-assembled monolayers on gold surfaces and can significantly reduce the adsorption of proteins due to the steric repulsion of PEG[5,7], an effect which has extensively been described in literature.[1-4] Figure 4 shows the effects of this PEG modification on cell adhesion. Compared to non-modified gold surfaces (Figure 2), the frequency shift decreased from -65±5 Hz to only -17±5 Hz. Since fewer proteins adsorb, what we could show in previous investigations[5,7], also the adhesion of cells is reduced, since fewer adhesion motifs are present. Figure 5 additionally shows, that indeed almost no cells can be stained on the $(NH_2PEG_{2000}C_{11}S)_2$ SAMs, only few cells can be found on a small area. This is probably due to an impurity, because in several additional experiments we could not stain any cells on $(NH_2PEG_{2000}C_{11}S)_2$ SAMs at all. In consequence, these results indicate, that the modification of the surfaces with PEG derivatives indeed leads to cell adhesion resistant surfaces under these dynamic conditions.

The frequency shift that still can be measured is similar to experiments, where only proteins are added to the system.[7] Since no cells could be stained on PEG surfaces, we conclude that the PEG modification allows for suppressing non-specific reactions and therefore offers the chance to investigate highly specific interactions of bioactive surfaces with cells.
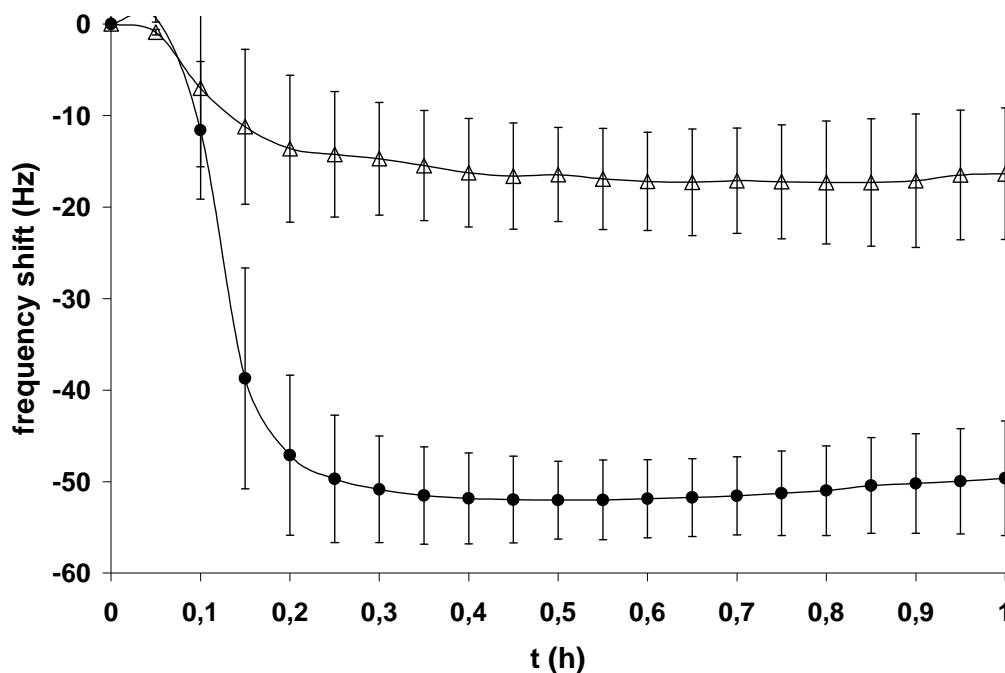

Figure 4: Covering the sensor electrode with a monolayer of amine PEG derivatives leads to a strong reduction of protein adsorption and cell adhesion compared to non-modified electrodes (△). Binding the cell adhesion molecule GRGDS to the PEG moieties leads to a decrease of -50±5 Hz, indicating a selective adhesion of cells (●).
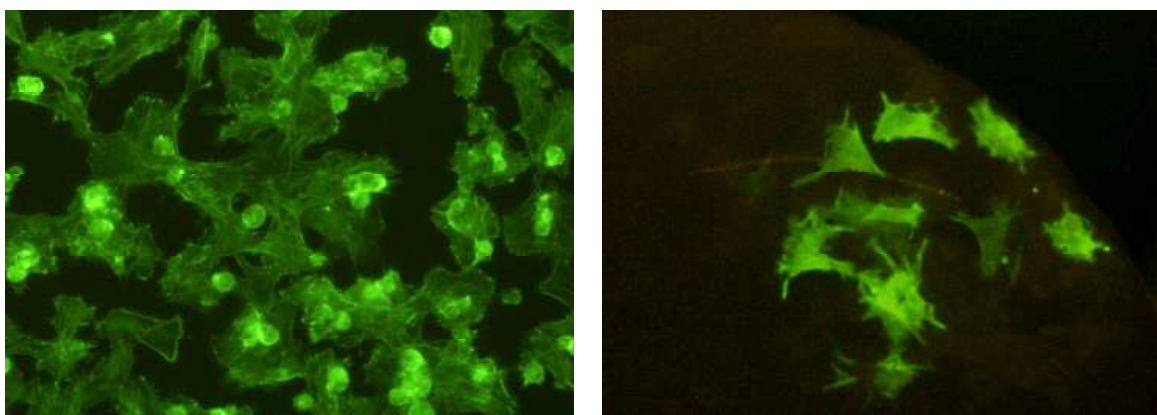
Figure 5: Staining the cytoskeleton of the rMSCs shows, that the GRGDS-modified surfaces are almost covered completely with well-spread cells(left), whereas only several cells can be found on amine PEG SAMs (right).

Inducing specific cell adhesion tethering RGD peptides to the surface

To obtain adhesive surfaces, we modified the $(NH_2PEG_{2000}C_{11}S)_2$ SAM with the cell adhesion motif GRGDS. This peptide binds to different integrins and, induces a selective adhesion of cells bearing the integrins $\alpha_v\beta_3$, $\alpha_5\beta_1$ and $\alpha_{IIb}\beta_3$.[37] In Figure 6 the modification scheme for the GRGDS-PEG is shown. After forming an amide bond with succinic anhydride, the resulting free carboxyl group can be activated with common NHS/DCC chemistry, leading to amine-reactive surfaces. Since the pentapeptide GRGDS contains a primary amine, incubating the activated surfaces with a buffered aqueous solution (pH 7.4) of GRGDS leads to a covalent attachment of this cell adhesion molecule to the SAM. To estimate the density of amine reactive groups on the surface, we quantified the covalent attachment using surface plasmon resonance (SPR). Since the detection of low molecular weight compounds, such as GRGDS, especially in the expected nanomolar range, is not possible,[38] we were using the high molecular weight protein bovine serum albumin (BSA) for quantification.
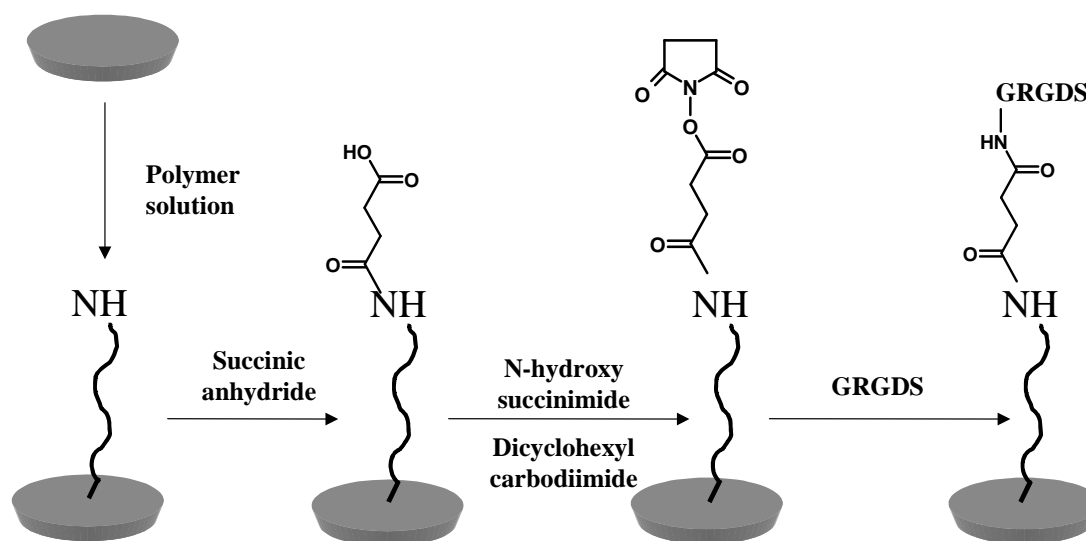

Figure 6: Modification scheme for GRGDS-modified surfaces. Gold surfaces are incubated in ethanolic solutions of PEG derivatives, resulting in amine terminated SAMs. To these, succinic acid is bound, which can be activated with DCC/NHS chemistry. Incubating these activated SAMs with GRGDS solutions leads to bioactive surfaces.

Compared to non-activated succinic acid terminated SAMs, we could see an increase of 230 RU of the SPR system after treating amine reactive surfaces for 10 minutes with BSA (Figure 7). According to the publication of Maesawa et al. this corresponds to an amount of

23 ng/cm^2 protein on the surface.[34] Assuming a molecular weight of 66 kDa for BSA, a concentration of 35 pmol/mm^2 can therefore be determined. For smaller molecules, such as GRGDS with a molecular weight of 491 Da, the surface concentration might even be higher.
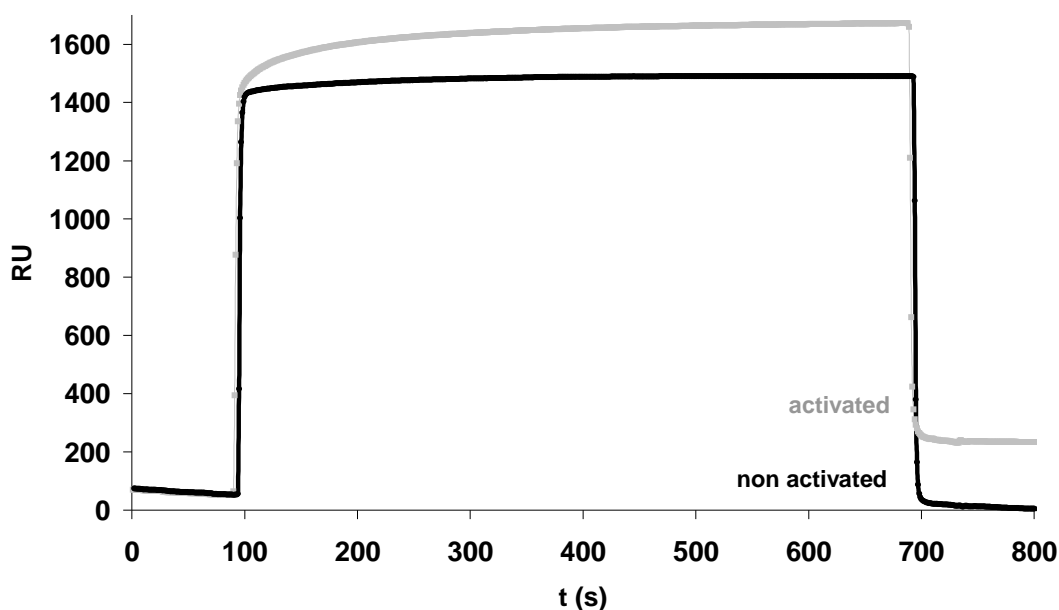

Figure 7: Binding of BSA to amine reactive surfaces results in an increase of 230 RU of the SPR system. This increase can be attributed to a covalent attachment of 23 ng/cm^2, corresponding to 35 pm/mm^2 of active groups on the surface.

Concerning the adsorption of proteins, this GRGDS modification only leads to minor changes in the amount of adsorbed proteins (data not shown)[7]. But on the other hand, in terms of cell adhesion, the effect is significant: After adding an rMSC suspension, the frequency decreases by -50±5 Hz, indicating the adhesion of cells due to interactions of GRGDS with cell adhesion receptors of the rMSCs (Figure 4). Staining the cells´ cytoskeleton with a fluorescent phalloidin derivative obviously confirms a high occupancy of the surface with well spread rMSCs. Cell counts revealed that approximately 65% of the surface was covered by cells. Ishaug et al. could determine 50.000 cells/cm^2 for confluent rMSC monolayers.[35] Calculating with an coverage of 65% on 0.3 cm^2 and a frequency

shift of -33 Hz (without the 17 Hz caused by adsorbed proteins), this reveals a value of -3.4 mHz/cell.

To investigate, if this cell adhesion on the GRGDS surfaces is due to the RGD motif or due to adsorbed proteins, we repeated the experiments under serum-free conditions in PBS buffer. Again, the difference between surfaces with attached RGD peptides and those without adhesion motifs is significant (Figure 8): For the NH_2-terminated PEG, the change in resonance frequency is less than -10 Hz, whereas for the GRGDS modified surface a drop of -50 Hz can be observed. These results insinuate, that the adsorbed proteins, which still can be found on the different SAMs, do not have a significant impact on the amount of cell adhesion.
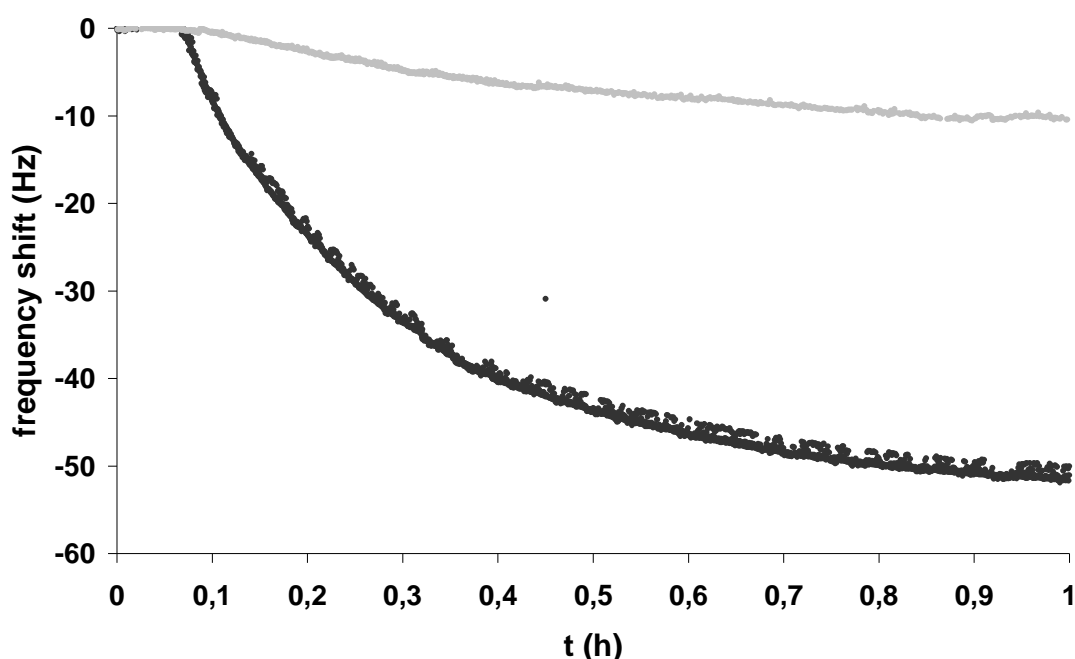

Figure 8: Cell adhesion experiments under serum-free conditions show, that by attaching GRGDS molecules to the SAMs a selective adhesion can be induced: The decrease in resonance frequency is significantly higher for GRGDS surfaces (black curve) than for amine surfaces (gray curve).

In further control experiments we confirmed the RGD-dependence of the cell-SAM interactions. Therefore, we incubated rMSCs after harvesting for 30 minutes with 1mM of soluble GRGDS in 1 ml of serum-containing medium and washed the cells afterwards with PBS before resuspending them in serum containing medium. After that treatment, the cell suspension was added onto GRGDS modified SAMs in the QCM system. As a result, we

could see that the resonance frequency only decreased by -20 Hz (Figure 9). This shift is similar to surfaces that resist cell adhesion, as was shown in Figure 4. The remaining frequency shift is due to protein adsorption.[7] This indicates that the incubation with soluble GRGDS blocks the integrin receptors of the cells, preventing the interaction of integrins with surface bound GRGDS and therefore prevents the adhesion of cells, as it could be shown in several other studies.[21] This result obviously approves the integrin dependence of the cell-surface interactions.

Another control experiment supports this assumption. When rMSCs were seeded on surfaces to which RGD motifs had been attached, the frequency dropped by approximately -60 Hz. When 1 mg of soluble GRGDS was added, the resonance frequency increased again to –10 Hz (Figure 10). This shows, that an excess of a soluble integrin ligand can displace the covalently surface-bound GRGDS from the receptor. These results are in full accordance with the studies of Li et al, who also could detach cells from RGD containing surfaces after adding soluble RGD peptides.[19]
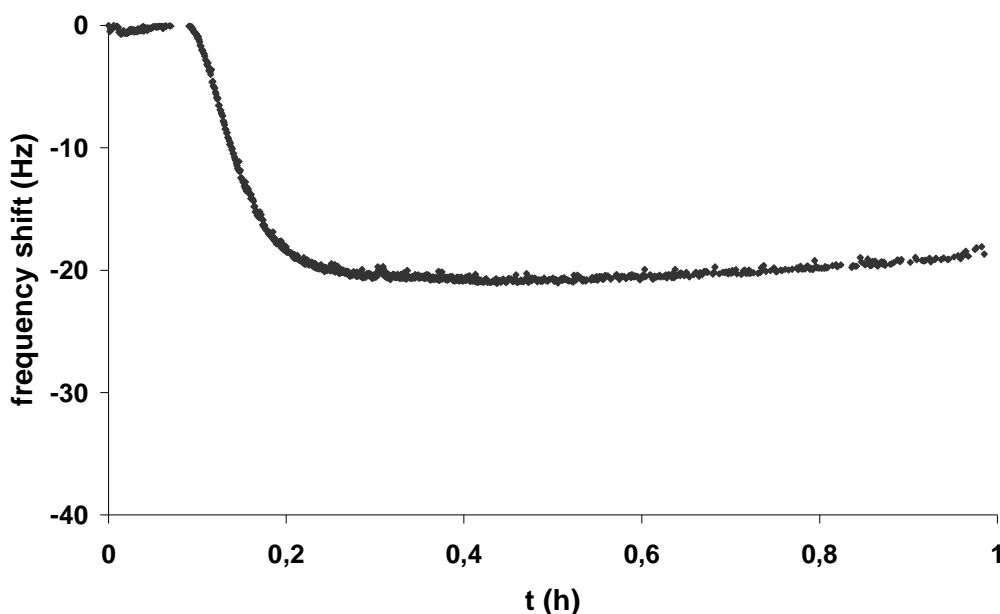
Figure 9: Incubation of the cells in 2.5 mM GRGDS-containing medium before the addition to the QCM leads to a reduction of cell adhesion, the decrease in resonance frequency is in the range of experiments, where only proteins are added to the system.

Following cell detachment form surfaces

To show that medium changes can be performed without interrupting the measurement, which normally causes strong temporary frequency shifts[23], we performed a cell detachment experiment using trypsin. This enzyme is frequently used in cell culture systems to harvest cells, because it cleaves peptide bonds after arginine residues and, therefore, cleaves the anchorages of cells to surfaces, which are predominantly mediated via proteins. In Figure 11 the effect of the addition of trypsin to rMSCs, which were attached to GRGDS-rich SAMs, can be seen. Within several minutes after the addition of the enzyme the resonance frequency increases from –70 Hz to –20 Hz. Rinsing with buffer then leads to a frequency value near the starting point. This more or less complete reversibility of frequency changes is not only due to the detachment of cells from the surface, but also due to the dissection of the adsorbed proteins on the surface, which can be removed by rinsing with PBS buffer, leading to a resonance frequency close to the starting point. This complete reversibility indicates on the one hand that the surface can be cleared from cells and proteins by trypsin and shows on the other hand that the kinetics of this process can be monitored in real-time and label free without disturbing the system.
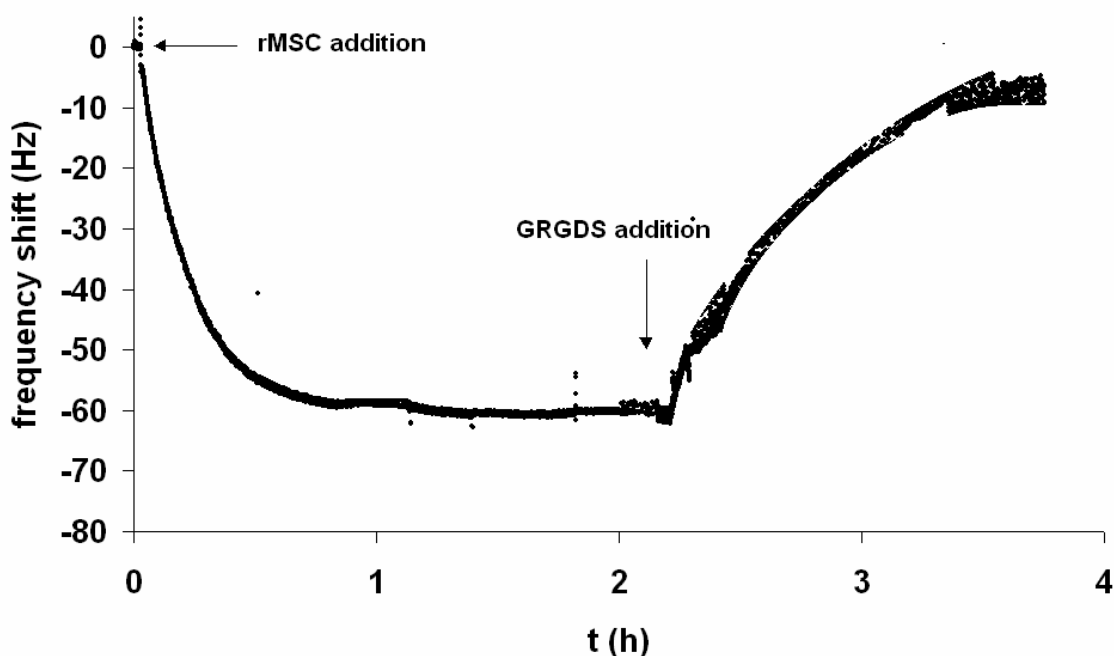

Figure 10: Adding cell suspensions to GRGDS surfaces leads to a decrease in resonance frequency, subsequent addition of soluble GRGDS triggers an increase again.

An obvious difference compared to the detachment of cells using GRGDS is the kinetics of cell detachment. With trypsin, cell detachment is complete within 10 minutes, whereas for the competitive ligand exchange at the receptor, the detachment is significantly slower (90 minutes). The detectability of these different time scales of cell detachment obviously shows that the QCM can provide extremely useful data on kinetic processes in cell culture systems, which otherwise are usually very hard to acquire by time- and material-consuming methods[10].
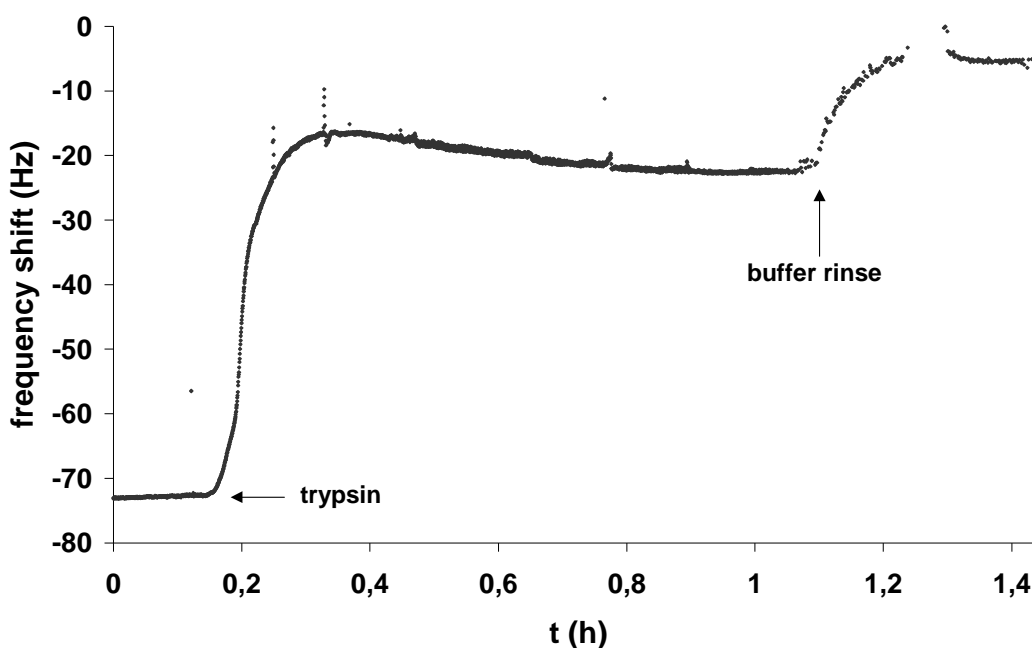

Figure 11: After the addition of the enzyme trypsin to cells attached to GRGDS surfaces, the resonance frequency increases, indicating the cleavage of the cells´ anchorage to the surface. Rinsing with buffer leads to a further increase close to the starting frequency, suggesting that also proteins are abscised from the surface.

Detection of medium changes

To further investigate, if minor modifications within this system can be detected, we tried to modify the activation state of the integrins on the cell surface. For these receptors, it is well known that they can adopt different states of affinity, depending on the presence of different divalent cations.[39,40] Without any divalent cations in the system, the integrins are completely inactive, the highest potency to increase ligand affinity of the integrins is described for manganese cations. Figure 12 shows the result of cell adhesion experiments with and without 50 µM/l Mn^{2+}. Since the decrease in resonance frequency is almost

doubled for experiments, where Mn^{2+} is present, an increase in cell adhesion is obvious (with the understanding that approximately 20 Hz are due to protein adsorption). Calculating with the same cell diameter as for manganese free experiments, this reveals of value of -6.5 mHz/cell. This fact is in full accordance with conventional cell culture studies.[41] In reverse, this means the affinity of the integrins to GRGDS peptides is increased, leading to this increase in cell adhesion. Since this effect can be detected, this experiment once more shows, that the QCM is a very sensitive tool for the characterization of cell-surface interactions and can easily give very detailed information on the effects of minor medium changes in real-time also under dynamic conditions. Therefore, the QCM is a very powerful equipment for studies on interfacial reactions on polymer surfaces. The system concomitantly offers the chance to obtain important information on how to improve cell-surface interactions.
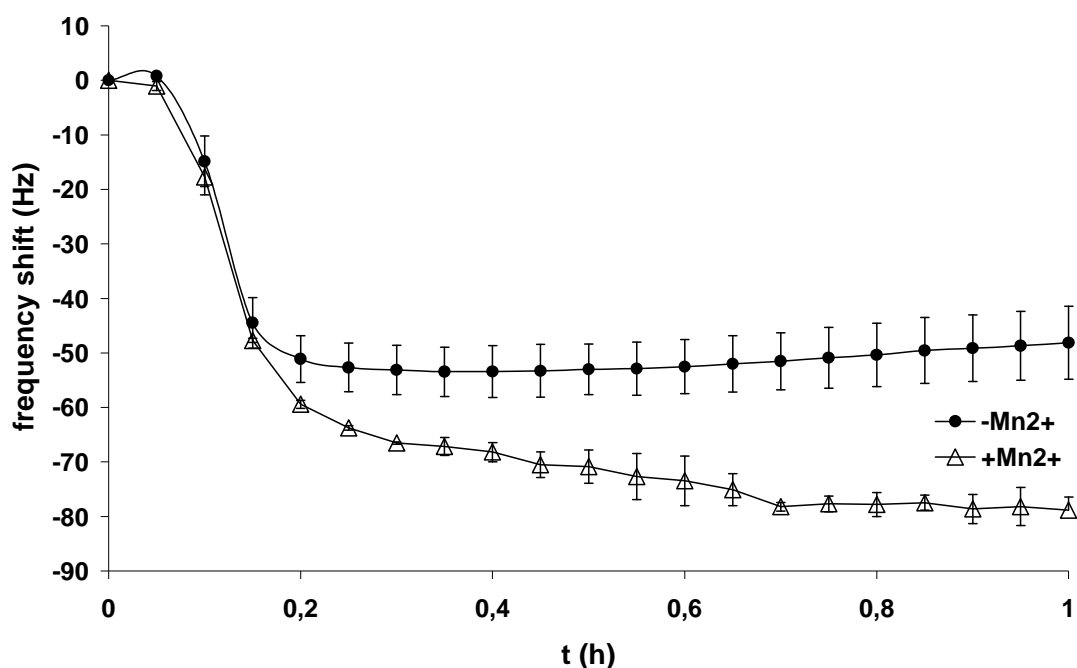

Figure 12: Time resolved QCM response after adding a cell suspension to GRGDS modified SAMs in the absence (●) or presence (△) of Mn^{2+}. The decrease in resonance frequency is significantly higher with Mn^{2+}).

Conclusion

In this study we could show that the detection of cell adhesion processes is not limited to static QCM instrumentations, but that also dynamic flow-through arrangements are possible and have significant advantages. The adhesion of rat marrow stromal cells and the murine fibroblast cell line 3T3-L1 was quantified, revealing frequency shifts of -6.7 mHz/cell, or -2.0 mHz/cell, respectively. These frequency shifts are in good agreement with previous studies, in which a static setup was used. Moreover, we could demonstrate that a modification of the sensor surface with PEG leads to cell adhesion resistant surfaces under these dynamic conditions. This allows for the characterization of specific interactions of cells with PEG surfaces, as we could show by inducing cell adhesion after attaching the cell adhesion motif GRGDS. In contrast to a static system our dynamic setup allowed to follow the kinetics of cell detachment after adding the enzyme trypsin and soluble GRGDS very easily. Moreover, slight modifications in the medium composition could be sensed, since the addition of manganese cations led to a significant increase in the QCM response, indicating the sensitivity of the applied method.

Acknowledgements

References

[1] Kingshott P.; Griesser H.J.: Surfaces that resist bioadhesion. Curr Opin Solid St M, 4, 403-412, 1999.

[2] Nath N.; Hyun J.; Ma H.; Chilkote A.: Surface engineering strategies for control of protein and cell interactions. Surf Sci, 570, 98-110, 2004.

[3] Lee J.H.; Lee H.B.; Andrade J.D.: Blood compatibility of polyethylene oxide surfaces. Prog Polym Sci, 20, 1043-1079, 1995.

[4] Drotleff S.; Lungwitz U.; Breunig M.; Dennis A.; Blunk T.; Tessmar J.; Göpferich A.: Biomimetic polymers in pharmaceutical and biomedical sciences. Eur J Pharm Biopharm, 58, 385-407, 2004.

[5] Menz B.; Knerr R.; Goepferich A.; Steinem C.: Impedance and QCM analysis of the protein resistance of self-assembled PEGylated alkanethiol layers on gold. Biomaterials, 26, 4237-4243, 2005.

[6] Tessmar J.; Mikos T.; Goepferich A.: The use of poly(ethylene glycol)-block-poly(lactic acid) derived copolymers for the rapid creation of biomimetic surfaces. Biomaterials, 24, 4475-4486, 2003.

[7] Knerr R.; Weiser B.; Drotleff S.; Steinem C.; Goepferich A.: Self-assembling PEG Derivatives for Protein-repellant Biomimetic Model Surfaces on Gold. Biomaterialien, , 7 (1), 12-20, 2006.

[8] Mrksich M.; Dike L.E.; Tien J.; Ingber D.E., Whitesides G.M.: Using microcontact printing to pattern the attachment of mammalian cells to self-assembled monolayers of alkanethiolates on transparent films of gold and silver. Exp Cell Res, 235, 305-313, 1997.

[9] Lucke, A., Tessmar, J., Schnell, E., Schmeer, G., Göpferich, A.: Biodegradable poly(D,L-lactic acid)-poly(ethylene glycol) monomethyl ether diblock copolymers. Structures and surface properties relevant to their use as biomaterials. Biomaterials, 21, 2361-2370, 2000.

[10] Marx K.A: Quartz Crystal Microbalance: A Useful Tool for Studying Thin Polymer Films and Complex Biomolecular Systems at the Solution-Surface Interface. Biomacromolecules, 4, 5, 1099-1120, 2003.

[11] Janshoff A.; Galla H.J.; Steinem C.: Piezoelectric mass-sensing devices as biosensors – an alternative to optical biosensors? Angewandte Chemie, Int Ed, 39, 4004-4032, 2000.

[12] Fredriksson C.; Kihlmann S.; Kasemo B.; Steel D.M.: In vitro real-time characterization of cell attachment and spreading. J Mat Sci, 9, 785 –788, 1998.

[13] Marx K.A.; Zhou T.; Montrone A.; McIntosh D.; Braunhut S.J.: Quartz crystal microbalance biosensor study of endothelial cells and their extracellular matrix following cell removal: Evidence for transient cellular stress and viscoelastic changes during detachment and the elastic behavior of the pure matrix. Anal Biochem, 343, 23-34, 2005.

[14] Wegener J.; Janshoff A.; Galla H.J.: Cell adhesion monitoring using a quartz crystal microbalance: comparative analysis of different mammalian cell lines. Eur Biophys J, 28, 26-37, 1998.

[15] Marx K.A.; Zhou T.; Montrone A.; Schulze H.; Braunhut S.J.: A quartz crystal microbalance cell biosensor: detection of microtubule alterations in living cells at nM nocodazole concentrations. Biosens Bioelectron, 16, 773-782, 2001.

[16] Marx K.A.; Zhou T.; Warren M.; Braunhut S.J.: Quartz Crystal Microbalance Study of Endothelial Cell Number Dependent Differences in Initial Adhesion and Steady-State Behavior: Evidence for Cell-Cell Cooperativity in Initial Adhesion and Spreading. Biotechnol Progr, 19, 987-999, 2003.

[17] Fredriksson C.; Kihlmann S.; Rodahl M.; Kasemo B.: The Piezoelectric Quartz Crystal Mass and Dissipation Sensor: A Means of Studying Cell Adhesion. Langmuir, 14, 248-251, 1998.

[18] Jenkins M.S.; Wong K.C.Y.; Chhit O.; Bertram J.F.; Young R.J.; Subaschandar N.: Quartz crystal microbalance – based measurements of shear – induced senescence in human embryonic kidney cells. Biotechnol Bioeng, 88, 3, 392 – 398, 2004.

[19] Li J.; Thielemann C.; Reuning U.; Johannsmann.: Monitoring of integrin-mediated adhesion of human ovarian cancer cells to model protein surfaces by quartz crystal resonators: evaluation in the impedance analysis mode. Biosens Bioelectron 20, 1333–1340, 2005.

 [20] Reiss B.; Janshoff A.; Steinem C.; Seebach J.; Wegener J.; Adhesion kinetics of functionalized vesicles and mammalian cells: a comparative study. Langmuir, 19, 1816 – 1823, 2003.

[21] Wegener J.; Seebach J.; Janshoff A.; Galla H.J.: Analysis of the composite response of shear wave resonators to the attachment of mammalian cells. Biophys J, 78, 2821-2833, 2000.

[22] Zhou T.; Marx K.A.; Warren M.; Schulze H.; Braunhut S.J.: The Quartz Crystal Microbalance as a Continuous Monitoring Tool for the Study of Endothelial Cell Surface Attachment and Growth. Biotechnol Progr, 16, 268-277, 2000.

[23] Marxer C.G.; Coen M.C.; Greber T.; Greber U.F.; Schlapbach L.: Cell spreading on quartz crystal microbalance elicits positive frequency shifts indicative for viscosity changes. Anal Bioanal Chem, 377, 578-586, 2003.

[24] Gryte D.M.; Ward M.D.; Hu W.S.: Real-time measurement of anchorage- dependent cell-adhesion using a quartz crystal microbalance. Biotechnol Progr, 9, 105–108, 1993.

[25] Assero G.; Satriano C.; Lupo G.; Anfuso C.D.; Marletta G.; Alberghina M.: Pericyte adhesion and growth onto Polyhydroxymethylsiloxane Surfaces Nanostructured by Plasma Treatment and Ion Irradiation. Microvascular Res, 68, 209-220, 2004.

[26] Marx K. A.; Zhou T.; Montrone A.; McIntosh D.; Braunhut S. J.: Quartz crystal microbalance biosensor study of endothelial cells and their extracellular matrix following cell removal: Evidence for transient cellular stress and viscoelastic changes during detachment and the elastic behavior of the pure matrix. Anal Biochem, 343, 23-34, 2005.

[27] Le Guillou-Buffello, D., Helary, G., Gindre, M., Pavon-Djavid, G., Laugier, P., Migonney, V.: Monitoring cell adhesion processes on bioactive polymers with the quartz crystal resonator technique. Biomaterials, , 26, 4197- 4205, 2005.

[28] Rodahl M.; Hoeoek F.; Fredriksson C.; Keller C.A.; Krozer A.; Brzezinski P.; Voinoca M.; Kasemo B.: Simultaneous frequency and dissipation factor QCM measurements of biomolecular adsorption and cell adhesion. Faraday Discuss, 107, 229 – 246, 1997.

[29] Neubauer M.; Fischbach C.; Bauer-Kreisel P.; Lieb E.; Hacker M.; Tessmar J.; Schulz M.B.; Goepferich A.; Blunk T.: Basic fibroblast growth factor enhances PPARγ ligand-induced adipogenesis of mesenchymal stem cells. FEBS Letters, 577, 277-283, 2004.

[30] Kastl K.; Ross M.; Gerke V.; Steinem C.: Kinetics and thermodynamics of Annexin A1 binding to solid supported membranes: A QCM study. Biochemistry, 41, 10087-10094, 2002.

[31] Ishaug S.L.; Crane G.M.; Miller M.J.; Yasko A.W.; Yaszemski M.J.; Mikos A.G.: Bone formation by three-dimensional stromal osteoblast culture in biodegradable polymer scaffolds. J Biomed Mater Res, 36, 17, 1997.

[32] Hersel U., Dahmen C., Kessler H.: RGD modified polymers: biomaterials for stimulated cell adhesion and beyond. Biomaterials, 24, 4385-4415, 2003.

[33] Leitinger B.; McDowall A.; Stanley P.; Hogg N.: The regulation of integrin function by Ca^{2+}. Biochim Biophys Acta, 1498, 91- 98, 2000.

[34] Sanchez-Mateos P.; Cabanas C.; Sanchez-Madrid F.: Regulation of integrin function. Semin Cancer Biol, 7, 99-109, 1996.

Chapter 5

Characterization of Cell Adhesion Processes using the QCM-D Technique

R. Knerr[1], B. Weiser[1], C. Steinem[2], A. Göpferich[1]

[1] Department of Pharmaceutical Technology, University of Regensburg, Universitaetsstrasse 31, 93040 Regensburg, Germany

[2] Institute of Analytical Chemistry, Chemo- and Biosensors, University of Regensburg, 93040 Regensburg, Germany

Abstract

The quartz crystal microbalance meanwhile has emerged as a viable tool in characterizing cell adhesion processes. However, quantification processes still are significantly hampered by an inhomogeneous distribution of adherent cells on the respective sensor surface and viscoelastic losses of the oscillating quartz due to the adherent mass.

We therefore investigated the impact of shear stress on cells in a stagnation flow point QCM setup to be able to guarantee a homogeneous cell distribution. Cell staining experiments revealed a homogeneous cell layer for pump speeds of 0.1 ml/min for this specific setup, whereas at a value of 0.46 ml/min cells only were allowed to adhere on the outer regions of the quartz, where the shear stress is assumed to be lower.

By determining the dissipation factor D, cell adhesion processes can be characterized independently of the spatial distribution on the sensor surface, avoiding the aforementioned problem completely. Moreover, plots of D versus frequency shifts can serve as "fingerprints" of cell adhesion. Hence, we assessed the dissipation factors of rat marrow stromal cell adhesion processes in the absence and presence of serum proteins. These experiments showed that under serum-free conditions cells attached on RGD-modified surfaces, but were poorly spread, indicated by a strong increase in D (9 ppm). In the presence of proteins cells were bound more firmly and formed focal adhesion complexes, substantiated by a shift in D of only 5 ppm. Moreover, in D/F pots we could determine an impact of 18 Hz for protein adsorption phenomena of an overall frequency shift of 57Hz after the addition of a serum containing cell suspension to the sensor surface.

Introduction

Since there is a certain lack of suitable tools for the characterization of cell adhesion processes in real time, the so-called quartz crystal microbalance (QCM) has gained increasing importance in recent years.[1] As conventional methods for the analysis of cellular adhesion, such as optical microscopy, often require staining or fixation procedures, the possibility for an in situ determination of cell adhesion is completely impossible for these methods.[1,2] But since the QCM, which was originally designed to measure interfacial reactions on solid-air interfaces,[3] was improved for applications on air-liquid interfaces, several groups could show the excellent suitability of the QCM for the real-time characterization of cell adhesion processes.[4-6]

According to the Sauerbrey equation, the QCM indicates the deposition of mass on surfaces.[7] Therefore, the decrease in resonance frequency of a quartz disc, which is excited to oscillate at its resonance frequency by an applied DC voltage, is measured. Unfortunately, two major drawbacks complicate the quantification of cell adhesion processes.[8,9] First, the lateral sensitivity on a QCM sensor surface varies. In the center, the sensitivity is the highest, decreasing to the outer regions according to a Gaussian distribution. Hence, cells adhering on the outside of the sensor surface contribute less to a signal than cells in the center. Second, viscoelastic effects of the adsorbed mass lead to the fact that the Sauerbrey equation becomes invalid, since it was developed for rigid masses.

To overcome these limitations and make it possible to compare frequency shifts caused by cell adhesion in different setups, a homogeneous distribution of cells on the sensor surface has to be guaranteed. This should be no major issue for static instrumentations, which are used in all studies found in literature (except the study of Jenkins et al.[12]). However, in recent studies we tested the feasibility of a dynamic setup, since such a dynamic stagnation flow point set up allows for changing medium compositions continuously without interrupting ongoing measurements.[11] Such an equipment so far only was used for other investigations, such as protein adsorption experiments or antigen – antibody reactions.[12]

This stagnation flow point set up, however, may influence the spatial distribution of cells on the sensor surface due to the generation of shear stress. In numerous studies the influence of shear stress on cell adhesion was investigated,[13] but so far no investigations concerning the consequences of shear stress in a QCM system were performed, except the study of Jenkins et al. They described the impact of shear stress on cell growth, but did not comment on the impact on the initial adhesion characteristics of cells.[12] As the influence

of shear stress may even be more important in the initial stages of cell adhesion, as a first goal of this study, we therefore focused on the impact of the intensity of the generated shear stress in a dynamic QCM setup on the distribution of cells on the sensor surface, since this might strongly influence the response of the QCM system.

The second reason for quantification problems are energy losses due to viscolelastic properties of the adsorbed mass.[1,10] In several studies, Fredriksson and Rohdal et al. tried to overcome these problems by introducing a further parameter and a different method of analysis of the generated data.[1,4,10,14] First of all, they introduced the so-called dissipation factor D, which measures the dampening of the crystal's oscillation caused by the adsorbed mass. This factor D describes the sum of the various energy dissipating subsystem in the oscillator and therefore can reveal the dissipative properties of viscoelastic layers.[10] In general, this dissipation factor increases, when biofilms form on surfaces. Fredriksson and Rodahl could show that a plot of D versus the measured frequency shift can reflect the dynamic behaviors of the adhesion and therefore can serve as a "fingerprint" of interactions of surfaces with biofilms.[10] Moreover, these so-called D/f-plots allow for the characterization of cell adhesion independent of the position on the electrode and also independent of the number of attached cells, a fact which avoids the aforementioned problem of inhomogeneous cell distributions on the surface completely.[15]

Unfortunately very few publications can be found discussing these D/f plots, as usually frequency shifts and changes of the dissipation factor are discussed separately for cell adhesion processes. It was therefore the second goal of this study to determine the dissipation factor of cell adhesion experiments and to evaluate, whether this factor and the D/f plots in particular allow for the determination of a "fingerprint" of the adhesion of rat marrow stromal cells (rMSCs). These cells are frequently used in cell culture systems, as they can be differentiated into different connective tissue cell types, such as chondrocytes, osteoblasts and adipocytes.[22] Therefore, such a detailed fingerprint would be valuable for a large scientific community.

To evaluate, whether these cell-specific characteristics are sensitive to changes in the cells´ environment, we investigated the adhesion of rMSCs on recently developed simplified model systems for PEG rich surfaces[16] in the absence and presence of serum as a kind of model experiment The mentioned model surfaces consist of self-assembled monolayers (SAMs) of protein-repellant thioalkylated poly(ethylene glycol) derivatives, to which cell adhesion inducing GRGDS pentapeptides are attached. These surfaces were already

characterized intensively by means of the QCM in terms of frequency shifts after protein and cell additions[16] and allow for suppressing non-specific reactions on the surfaces to a high extent. Hence, with these well defined surfaces, we tried to get detailed information on the influence of the composition of the cell-culture medium on cell adhesion using the benefits of the QCM-D technique.

Thus, with both major goals of this study we aimed to improve the accuracy of the analytical method and to get a maximum of information on cell adhesion processes of rMSCs.

Materials and Methods

Materials

Ethanol was purchased from JT Baker, Deventer, Netherlands. Dimethylformamide (DMF) and methanol were from Acros Organics (Geel, Belgium). Ascorbic acid, succinic anhydride, dicyclohexyl carbodiimide (DCC), and N-hydroxysuccinimide (NHS) were acquired from Sigma-Aldrich Chemie GmbH (Taufkirchen, Germany). Formaldehyde and Triton X-100 were purchased from Merck KGaA (Darmstadt, Germany), GRGDS from Bachem Biochemica (Heidelberg, Germany), fluorescein phalloidin, penicillin/streptomycin solution (PenStrep), and phosphate buffered saline (PBS) from Invitrogen GmbH (Karlsruhe, Germany). Fetal bovine serum (FBS), Dulbecco´s modified eagle medium (DMEM) and trypsin were acquired from Biochrom AG (Berlin, Germany). All reagents were of analytical grade and used as received without further purification.

Polymer Synthesis

Polymers have been synthesized and characterized as published previously.[11,16] In brief, thioacetic acid was bound to 11-bromo-undecene via a radical chain reaction with benzoyl peroxide as the initiator. The resulting thioester was hydrolyzed to the free thiol, which was then protected with 2-chlorotrityl chloride. To this compound, N-BOC protected poly(ethylene glycol)-monoamine was attached in a Williamson ether synthesis. Afterwards, both protecting groups were removed resulting in the PEGylated dialkyldisulfide di(amino poly(ethylene glycol)-undecyl) disulfide, $(NH_2PEG_{2000}C_{11}S)_2$.
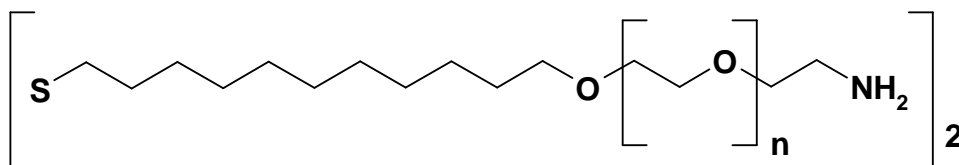

Figure 1: Chemical structure of di(amino poly(ethylene glycol)-undecyl) disulfide.

Preparation of Self-assembled Monolayers (SAMs)

Gold sensor surfaces were cleaned by immersing the surfaces for 5 minutes in a piranha solution (3:1 mixture of concentrated sulfuric acid and aqueous hydrogen peroxide (30 vol.-%), which was heated to 70°C. Afterwards, the gold was rinsed extensively with

double-distilled water, dried in a stream of nitrogen and incubated overnight in a 1 mM solution of $(NH_2PEG_{2000}C_{11}S)_2$ in absolute ethanol. After rinsing again with absolute ethanol, the surfaces were dried in a stream of nitrogen.

Subsequently, the $(NH_2PEG_{2000}C_{11}S)_2$ SAM was incubated in a 4 % (w/v) solution of succinic anhydride in dimethylformamide (DMF) overnight, rinsed with DMF, and dried in a stream of nitrogen. The resulting succinamide was then activated with 0.2 M DCC and 0.05 M NHS in DMF for two hours. For binding the pentapeptide GRGDS, the activated surface was subsequently incubated in a solution containing 0.5 mg GRGDS in 1 ml of PBS pH 7.4 at 4°C overnight, allowing for the reaction of the primary amine group of GRGDS with the activated carboxylic acid, and rinsed afterwards with double-distilled water (Figure 2). The binding of GRGDS was ascertained by water contact angle measurements with a method described previously and SPR experiments revealing a surface concentration of GRGDS of 0.3 pm/cm^2.[16]
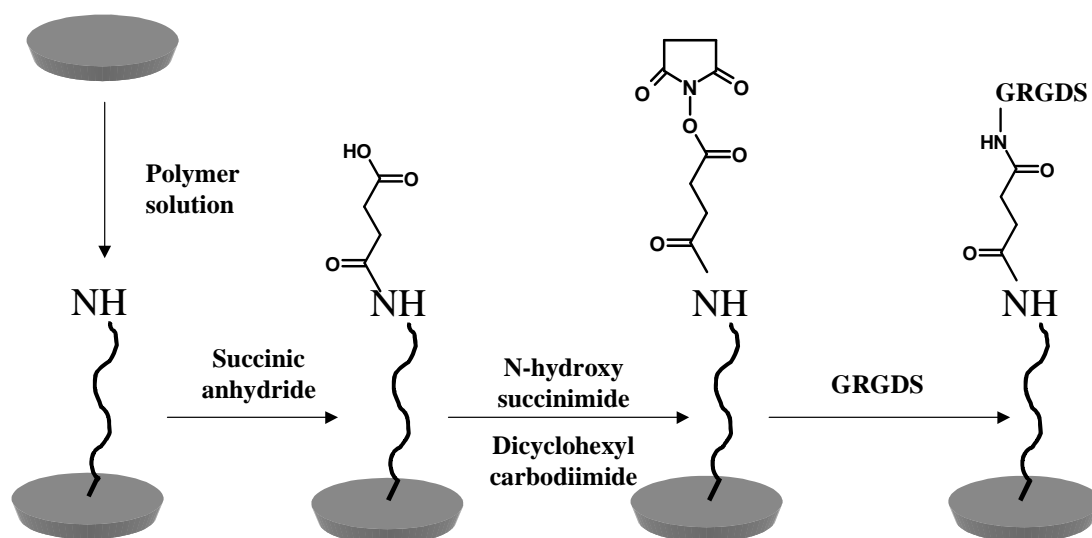

Figure 2: Modification scheme for attaching GRGDS to PEG-containing SAMs. After self-assembling of the polymer on the surface, the amine group of PEG is modified with succinic acid. The subsequent activation with DCC / NHS allows for binding of amine containing compounds, such as GRGDS.

Quartz Crystal Microbalance (QCM) Experiments

For measuring the frequency shift and the dissipation factor, an instrumentation similar to that of Kasemo et al. was used (Figure 3)[14] (and already described in more detail by Reiss et al.[4]). In brief: an external signal generator excites the quartz crystal at its fundamental

resonance frequency. Spring contacts connect the gold electrodes of the quartz plate with the electrical system. A computer-controlled relay separates the voltage source from the quartz plate, when the shear displacement of the resonator is stationary. A digital oscilloscope records the free oscillation decay, and the resonance frequency f and the characteristic decay time are subsequently extracted by nonlinear curve fitting. The decay time, indicative of energy dissipation, is expressed as the dissipation factor D of the oscillation. Time-resolved (<10 s) determination of both parameters is possible by repeating the entire process continuously.

For protein adsorption experiments 1 ml of serum containing medium was added to the system at a temperature of 37°C, which was controlled by a water-jacketed Faraday cage. Experiments were run for one hour. For cell adhesion experiments 250.000 rMSCs were suspended in 1 ml of serum containing medium or PBS and the same procedure run as for protein adsorption experiments.
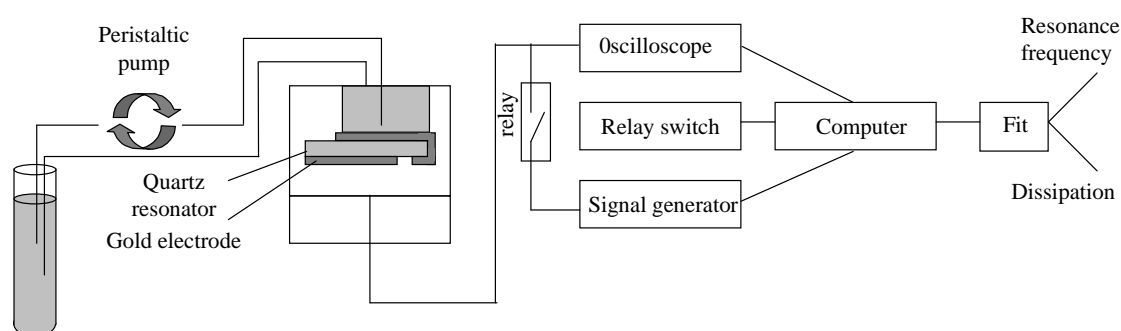
Figure 3: QCM-D flow through setup. Protein solutions or cell suspension were pumped continuously over the sensor surface. The frequency shift and the dissipation were measured by an oscilloscope after a relay switch separates the voltage source from the quartz plate.

Cell Culture

Marrow stromal cells (rMSCs) were obtained from 6-week-old Sprague Dawley rats according to a procedure published by Ishaug et al.[17] and were cultivated under standard culture conditions (37°C, 95% relative humidity, 5% CO_2 in DMEM with 10% fetal bovine serum, 1% penicillin/streptomycin, and 50 µg/ml ascorbic acid). For QCM experiments, cells were trypsinized, centrifuged at 1200 rpm for 5 minutes, and the resulting cell pellet re-suspended in medium or PBS at 250,000 cells/ml. Staining of the nuclei was performed

with propidium iodide. To this end, cells were fixed with ice-cold methanol for 5 minutes, washed twice with PBS, and incubated in a solution of 125µg RNAse and 1µg propidium iodide in 500 µl PBS for 30 minutes in the dark, followed by a final rinse with PBS. Staining of the cytoskeleton was performed with a fluorescein-labeled phalloidin derivative (Invitrogen, Karlsruhe, Germany). In this procedure, the surfaces were rinsed with PBS and cells were fixed with 3.8 % (v/v) formaldehyde for 10 minutes at room temperature. After rinsing with PBS, the surfaces were extracted with acetone at –20°C for 5 minutes and rinsed again with PBS. Then the cells were stained with 5µl of the methanolic dye solution in 500µl of PBS containing 1% BSA for 20 minutes. After rinsing with PBS, images were taken with a Axiovert 200M microscope coupled to scanning device LSM 510 (Zeiss, Jena, Germany) at 100 or 200-fold magnification (Ex = 469nm, Em = 516nm).

Results and Discussion

**Influence of shear stress on the spatial distribution of cells**

In numerous studies the influence of shear stress on cell adhesion and growth was investigated.[13] But the only publication investigating the influence of a dynamic QCM setup on eukaryotic cells was made by Jenkins et al.[12] They described that indeed the generated shear stress under dynamic QCM conditions is sufficient to influence the behavior of cells on the sensor surfaces, since they found different growth profiles for different shear conditions. Assuming their results, the generation of shear stress might even be more important for the adhesion behavior of cells.

To be able to determine the surface conditions for our investigations as exactly as possible, we modified a sensor surface with self-assembled monolayers (SAMs) we recently described in more detail.[11,16] This SAM allows for the suppression of non-specific protein adsorption to a high extent and therefore also should lead to a strong reduction of non-specific cell adhesion. On the other hand, by attaching the peptidic cell adhesion motif GRGDS, a specific adhesion of cells bearing certain integrin receptors on the cell surface can be induced.[11] In brief, these SAMs consist of thioalkanes, to which poly(ethylene glycol) is attached. Such compounds are well known to form homogeneous monolayers on gold. Their PEG moiety allows for the suppression of protein adsorption to a high extent, and additionally to tether bioactive compounds to the PEG end groups, resulting in biomimetic surfaces with specific cell signaling. Hence, such surfaces are ideal for the determination of detailed information on cell adhesion processes.

Concerning the investigations in terms of the spatial distribution of cells in the dynamic QCM setup, in a first step we checked, how rMSCs spatially distribute at all on such SAMs in the QCM system without applying any shear stress. Therefore, we added a suspension of 250.000 rMSCs in serum containing medium on the SAM by an injection and then allowed rMSCs to adhere for one hour without pumping medium through the measurement chamber. Measuring the frequency shift in this case unfortunately was not possible: Without closing the measurement chamber, water evaporates, leading to strong fluctuations of the measured parameters. But if the chamber would have been closed for this static experiment after the addition of cell suspension, the resonance frequency would have been

strongly destabilized. Thus, we abstained from measuring the frequency shift, since our focus anyway predominantly lied on the spatial distribution of the cells.

After staining the nuclei of the cells with propidium iodine after the adhesion time of one hour, a homogeneous distribution of rMSCs on the sensor surface could be detected (Figure 4a).
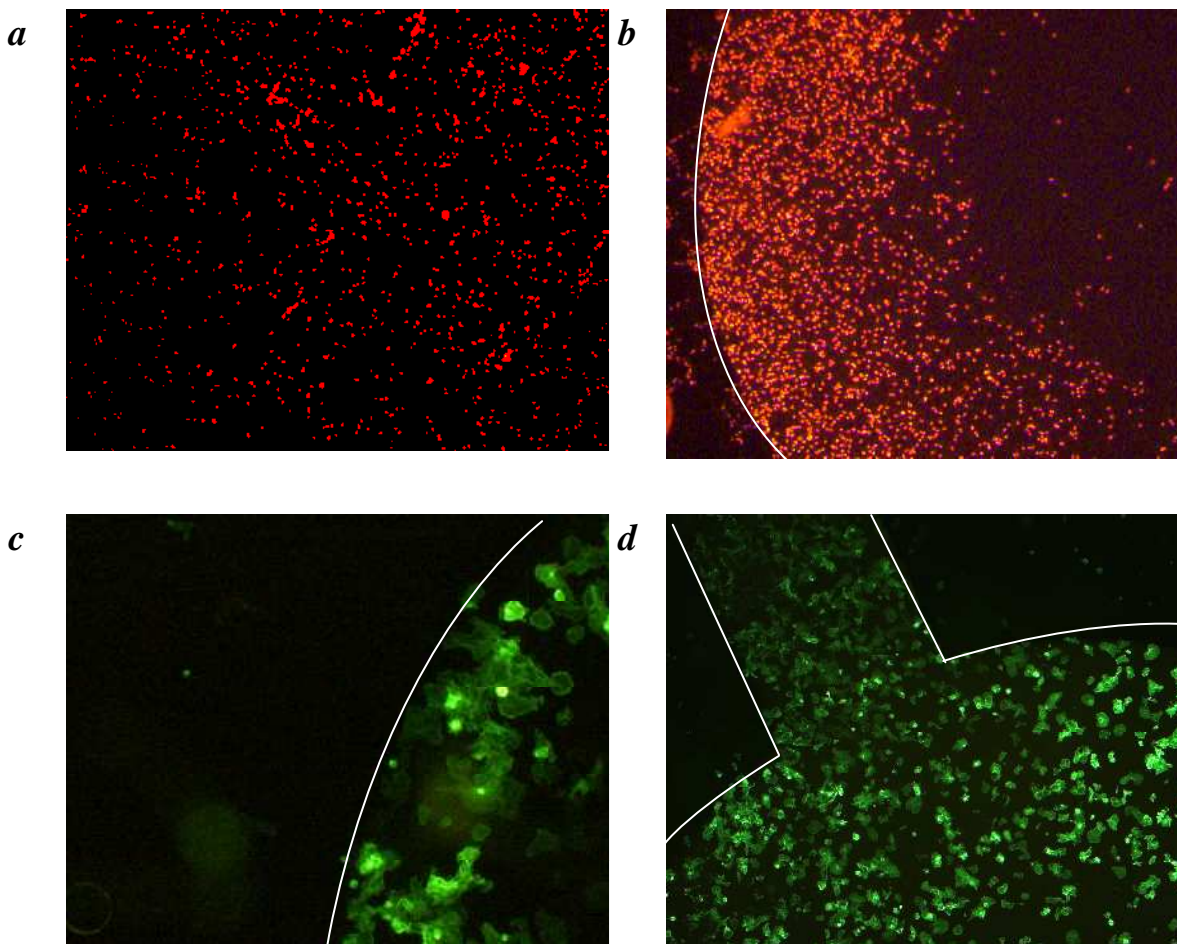
Figure 4: Distribution of rMSCs on QCM sensors under static (a) and dynamic (b) conditions. Under dynamic conditions the cells are only adhering on the outer regions of the quartz, whereas under static condition they are homogeneously distributed all over the surface. c: Distribution of rMSCs visualized by phalloidin staining under dynamic conditions. d: Staining the cells´ cytoskeleton with phalloidin shows a homogeneous distribution all over the sensor surface due to a reduced flow rate. (White lines represent the edges of the fold sensor electrode.)

On the other hand, when the cell suspension was added in a continuous flow, the distribution was completely different. In the publication of Jenkins et al. a maximum pump speed of 0.46 ml/min is described and since no other details of the setup are given, we also

applied this flow rate, although the shear stress of course might be completely different due to different geometries. With this flow rate Jenkins et al. observed no detachment of HEK cells from the sensor surface.[12]

Experiments with these conditions in our setup showed that cells are only adhering to the outer regions of the sensor surface (Figure 4b and c). Due to the setup with a stagnation flow point design, the shear stress is assumed to be the highest right in the center of the sensor surface (Figure 5). Applying shear stress on certain cell types can increase the adhesion rates, but in general, under dynamic conditions cell adhesion is reduced.[13] This also is true for the rMSCs on the SAM in this case. The adhesion, where the shear stress is the highest, is the lowest. On the outer region, where the shear rate is assumed to be lower, the adhesion of rMSCs is possible (Figure 4b). Staining the cells´ cytoskeleton shows that they are very well spread in the outer regions of the GRGDS-presenting SAM (Figure 4c). This very inhomogeneous distribution of cells hampers the comparison of different cell adhesion experiments since on the outer regions the sensitivity of the QCM is the lowest, reducing the sensitivity and accuracy of the method. To overcome this problem, a reduction of the flow rate therefore seems necessary.
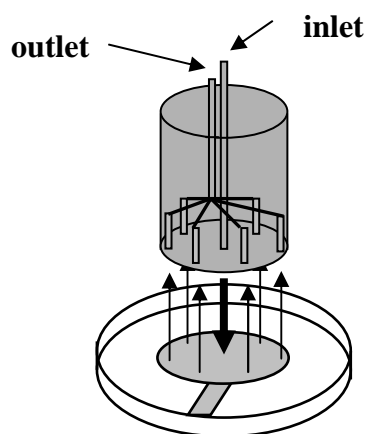
Figure 5: Stagnation flow point setup causing the inhomogeneous distribution of cells with higher flow rates. In the center of the sensor the shear stress on the cells is the highest, making it more difficult for cells to adhere.

Hence, in further experiments we reduced the flow rate to 0.1 ml/min, which also should reduce the shear stress in the center of the sensor. This reduction led to a completely different distribution again. For this low flow rate a very homogeneous cell distribution could be seen after staining the cytoskeletons (Figure 4d), which is absolutely comparable

to static conditions (Figure 4a). Since the cells are also very well spread, we assumed the shear stress to be low enough, so that cell adhesion processes are not disturbed or hampered too strongly. This in consequence means that with these reduced flow rates the characterization of cell adhesion processes is possible, since the homogeneous distribution on the surface allows for direct comparisons of experiments with different (e.g. static) setups, avoiding the problem of the different lateral sensitivity of the sensor surface. In studies performed with reduced flow rate, we could receive results comparable to static experiments performed by other groups.[11] Of course these results might be completely different again in terms of the values for the flow rates for other cell types. To get more information about the adjustment of flow rates to reach a certain shear stress, of course a detailed shear modeling and rheological investigations would have to be performed.

Characterizing cell adhesion measuring frequency shifts and the dissipation factor

Since the QCM technique only detects changes up to 250 nm above a surface, it is extremely useful for characterizing distinct interactions of cells with biomaterials right above the surface.[1,3,5,10] On the one hand, due to that limitation only a minor fraction of a cell's mass is reflected in the resonance frequency shift and therefore can be detected. The difference in density of the cytoplasm and the liquid covering the sensor is marginal. But on the other hand, by additionally measuring the dissipation factor D, time-dependant changes of the cell behavior concerning initial contacting, spreading and stiffness of the cytoskeleton can be evaluated.[1,10] Using this parameter, Fredriksson et al. for example could show, that even without any changes in resonance frequencies the attachment of cells could be detected due to shifts of the dissipation factor.[10]

To get any information whether the QCM-D can also provide us with more details of cell adhesion processes in our dynamic flow-through setup, in a first step, we tried to assess the different responses of the QCM-D on the addition of 250.000 rMSCs in 1 ml of serum-free PBS or 1 ml of serum containing medium on the same SAMs as described above.

In Figure 6 a decrease in resonance frequency of 42 Hz can be seen after one hour if 250.000 rMSCs suspended in PBS are added to the GRGDS containing PEG monolayer (all further experiments were performed with a flow rate of 0.1 ml/min and on this type of surface). This suggests that despite the above mentioned drawbacks of the QCM technique, cell adhesion in either case takes place and definitely can be detected. Also the increase in the dissipation factor D from 0 to 9 ppm shows changes in the viscoelastic properties of the

layer above the sensor as it is typical for protein adsorption or cell adhesion. Such a change in D after the addition of cells to a QCM system was described by Rodahl et al. as dissipative processes in the liquid trapped between the cell and the surface, in the cell membrane and in the interior.[1]
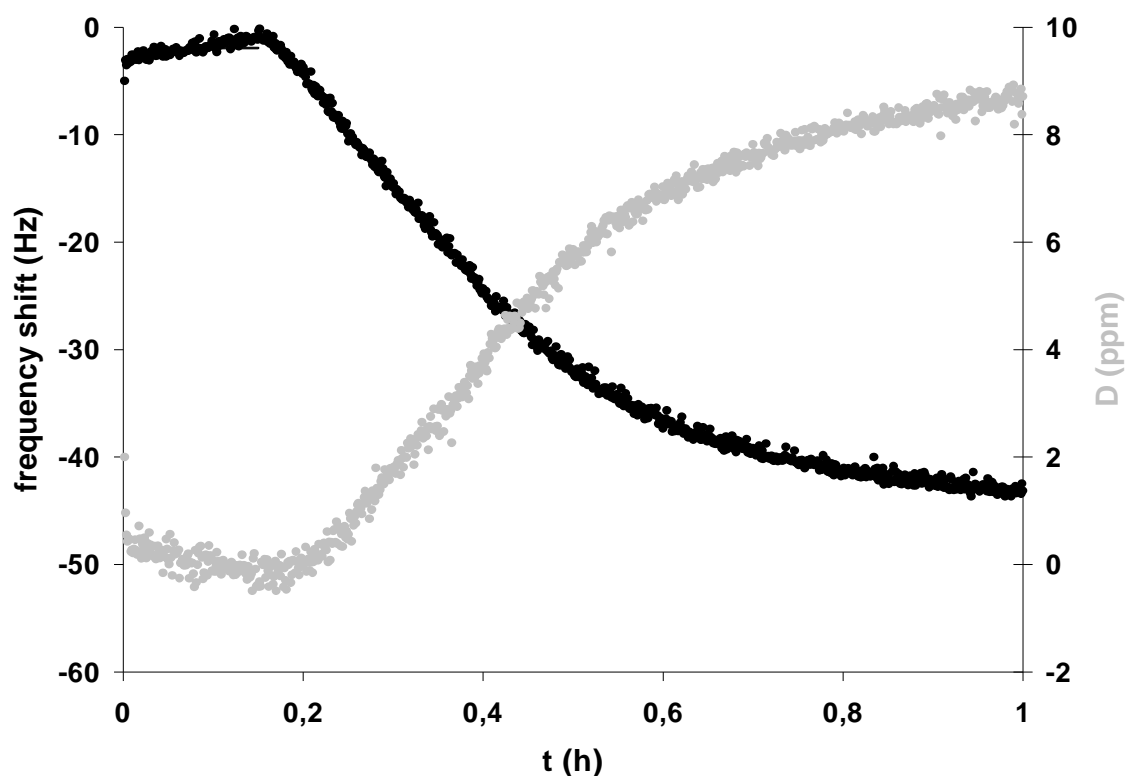

Figure 6: QCM-D response after the addition of 250,000 rMSCs under serum free conditions to a GRGDS-modified PEG monolayer. The resonance frequency decreases by 42 Hz indicating the adhesion of cells, whereas the increase in dissipation to 9 ppm suggests that a very viscoelastic mass is bound to the surface.

To asses whether the QCM-D can give more detailed information on the type of adherent mass on the surface than it is possible by only measuring the extent of mass deposition by determining the frequency shift using a common QCM setup, we also investigated the adhesion of rMSCs in the presence of serum. The corresponding D/f plots then might allow for an exact differentiation of serum-free and serum-containing conditions. But to evaluate in advance the impact of the added proteins on the QCM response, we first of all assessed the frequency and dissipation shifts of the cell culture medium alone. In Figure 7 a decrease in resonance frequency of 40 Hz can be detected after the addition of 1 ml

medium containing 10% fetal bovine serum (FBS). This result suggests that although PEG is attached densely to the surface, proteins still adsorb to it. In previous investigations, we already could show that indeed proteins adsorb to a certain extent on different PEG surfaces, but the amount is significantly reduced compared to non-modified gold sensors (data not shown).[11]

A shift can not only be detected for the resonance frequency, but also for the dissipation factor, for which we could see an increase of approximately 3 ppm. This confirms that adsorbed proteins cause viscoelastic losses. Compared to the adherent cell layer under serum free conditions, the adsorbed protein film seems to be stiffer, since the increase in D is significantly lower.
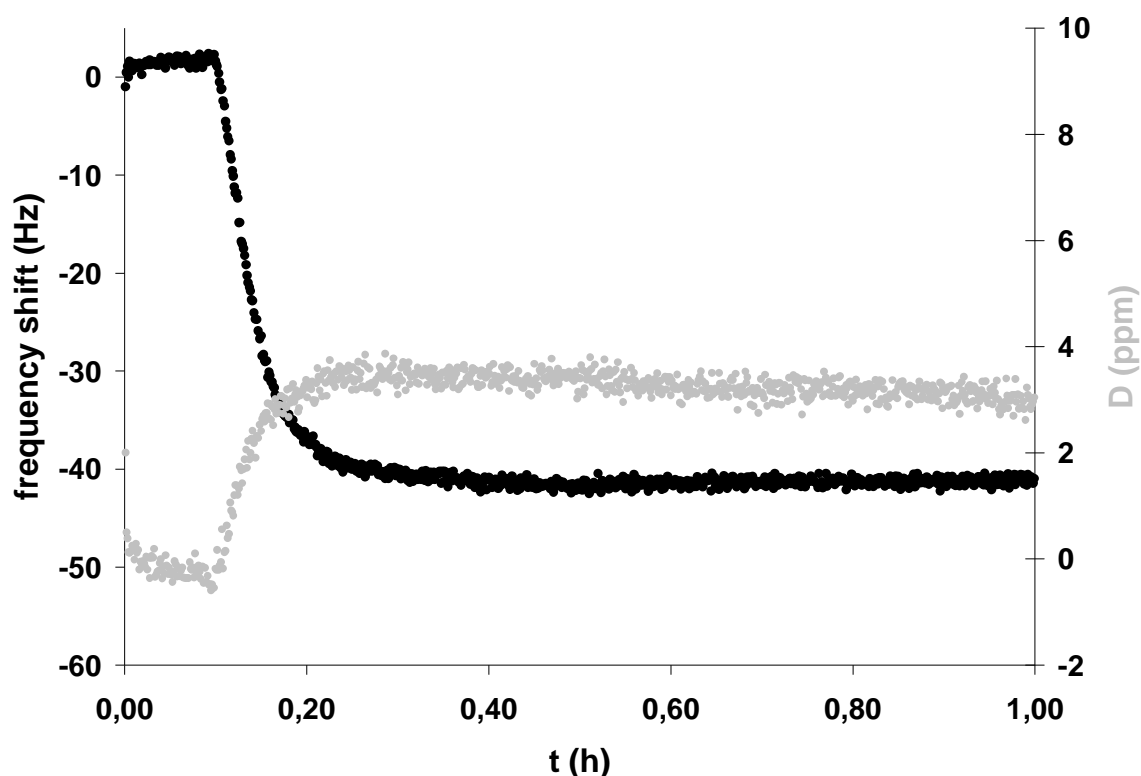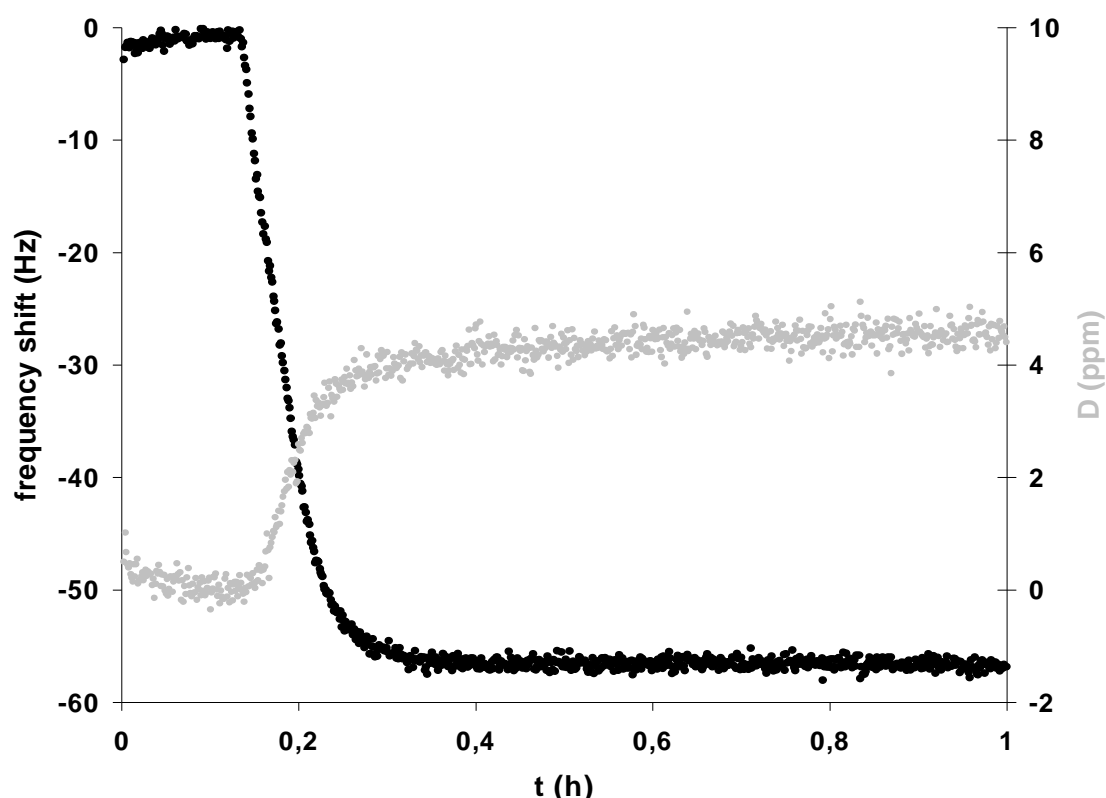

Figure 7: : QCM-D response after the addition of 1 ml of serum containing medium to a GRGDS containing PEG monolayer. The frequency drops by 40 Hz due to the adsorption of proteins. The dissipation increases to a value of 3 ppm, showing a dampening of the crystal's oscillation.

Although the goal of attaching PEG to the sensor surface was to suppress the non-specific adsorption of proteins as far as possible, from previous investigations we know that the

reduction of protein adsorption is good enough to be able to reduce non-specific cell adhesion under the applied conditions. Therefore, we went one step beyond and tested the adhesion of rMSCs on GRGDS-modified SAMs in the presence of proteins. Again, we injected 250.000 rMSCs into the QCM-D system, this time suspended in medium containing 10% FBS. The decrease in resonance frequency was almost 60 Hz after one hour (Figure 8), the increase in D 5 ppm. Compared to serum containing medium alone, the decrease in f is approximately 20 Hz higher and the increase in D 2 ppm higher.


Fig 8: QCM-D response after the addition of 250,000 rMSCs to a GRGDS modified PEG monolayer in the presence of serum. The resonance frequency drops by 58 Hz, which is slightly higher than for serum free conditions. The increase in dissipation on the other hand is only 5 ppm, suggesting the adsorbed mass is stiffer compared to serum free conditions.

This additional increase in f suggests that besides proteins, also rMSCs adhere to the surface, since more mass seems to be detectable. On the other hand, a simple linear relationship can not be derived in terms of simply subtracting the response of the protein adsorption (40 Hz), rendering 20 Hz of frequency shift for cell adhesion. One rather has to

take into consideration the different composition of the adsorbed biofilms, leading to different viscoelastic properties as is confirmed by the different D values in Figure 7 and 8. Although there is not the possibility to directly compare protein adsorption alone to combined protein adsorption and cell adhesion on the surface, the results obviously confirm the attachment of cells via a significant increase in D.

This assumption can be confirmed by staining the cytoskeleton of adherent cells with a fluorescent phalloidin derivative. As in previous investigations[11], we could see very well spread cells due to interactions of attached GRGDS peptides and integrin receptors of the cells. In Figure 9 an rMSC can be seen in a 630 fold magnification, the formation of focal adhesions (indicated by arrows) suggests the formation of a quite high adhesion force.[18] The overall coverage of the surface was found to be approximately 65% under these conditions.
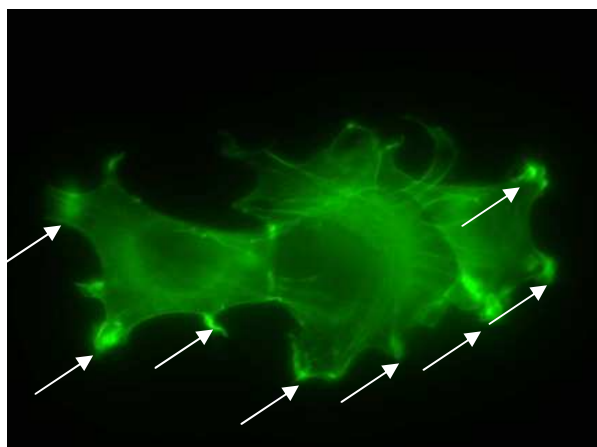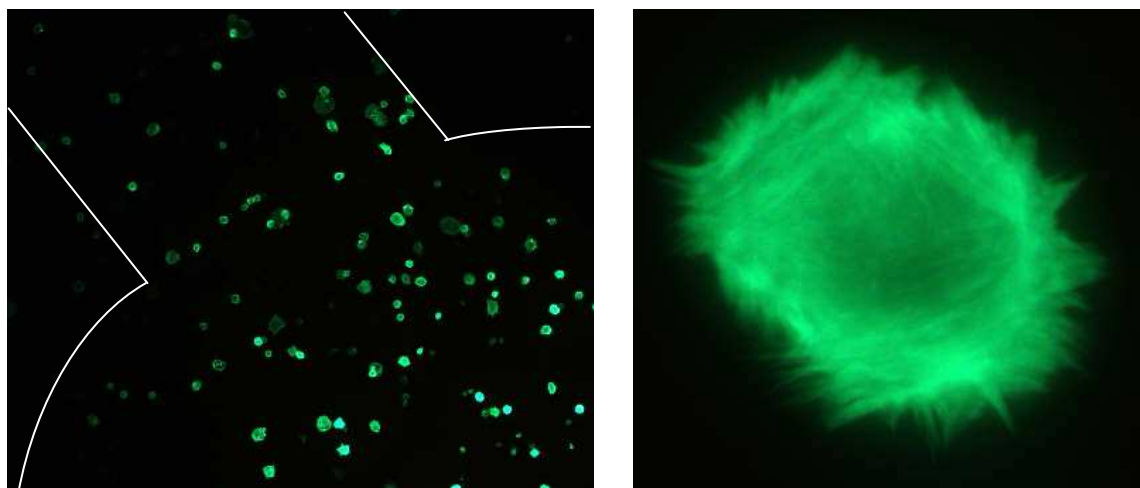

Figure 9: Fluorescein-phalloidin stained cells on (GRGDSPEG$_{2000}$C$_{11}$S)$_2$ SAMs. Compared to serum free conditions (Figure 10), they are well spread on the surface, indicating more RGD sequences are present, since the formation of focal adhesions correlates with the density of RGD on the surface[18].

Apparently different results were obtained for the cell adhesion experiments under serum free conditions in terms of the cell morphology. As described above, cell adhesion takes place and can be detected, but the spreading of the cells is completely different. rMSCs on the GRGDS modified SAMs were distributed more or less homogeneously all over the SAM, but appear round shaped and very poorly spread. In Figure 10 a cell in 630 fold magnification can be seen after staining the cytoskeleton with fluorescent phalloidin. In this exemplary case, no focal adhesions could be detected. The surface coverage was determined to be 17 % only.

In general, the formation of focal adhesions is induced by the interactions of RGD containing peptides with integrin receptors of the cells, entailing intracellular signaling cascades, which reorganize the cell's cytoskeleton.[19] The extent of this process strongly depends on the concentration of available RGD peptides on the corresponding surface.[18] Since cells are poorly spread in our serum-free experiments, a low concentration of RGD peptides has to be suggested. In previous investigations, we found that approximately 0.3 pM of GRGDS are attached to 1 cm^2 of the SAM.[16] But already this low value seems to be sufficient for an increase in cell adhesion and effects on the differentiation of certain cell types, as it was shown by Rezania et al. for rat calvaria osteoblast-like cells.[20] These findings suggest for our experiments that the density of RGD peptides on the surface is sufficient for inducing the adhesion of rMSCs independently whether serum proteins are present on the surface or not, since we found that attaching GRGDS leads to significantly higher frequency shifts of the QCM in both cases.[23]

Hence, there is an obvious difference of serum-free and serum-containing cell adhesion experiments, which are not that obvious by measuring only the shifts of the corresponding resonance frequency. D increases for both experiments differently, making the Sauerbrey equation invalid. Therefore the frequency shifts for cell adhesion experiments under serum-free and serum-containing conditions can not be compared directly. Under serum-free conditions the increase is significantly higher (9 ppm) than for serum-containing experiments (4.5 ppm). The increase in D after cellular adhesion can be attributed to entrapped water between cell and surface. The results obtained suggest that the amount of this entrapped water is higher under serum free conditions, where also the extent of focal adhesion formation is lower. Hence, an explanation for the stronger increase in D under serum-free conditions may be larger "caves" with entrapped water between cell and surface due to the lower number of focal adhesions.

Summarizing, we suggest that although cell adhesion is increased compared to non-GRGDS-modified SAMs in both cases, more cell adhesion motifs are available for a cell under serum containing conditions. This assumption is confirmed by the fact that indeed a certain amount of proteins (which may contain RGD sequences themselves) still adsorbs to the surface although a dense PEG brush is attached, what we could show in previous investigations.[11,16] This increased RGD concentration then does not only induce cell adhesion in contrast to non-GRGDS-modified SAMs, but also a formation of focal adhesions and a firmer attachment of rMSCs.

Figure 10: Fluorescein-phalloidin staining of rMSCs on GRGDS presenting SAMs under serum free conditions. Staining the cells´ cytoskeleton with fluorescent phalloidin suggests that cells are less densely packed on this surface and very poorly spread.

D/f-plots

According to Fredriksson et al., a plot of the measured dissipation shift versus the frequency shift can serve as a fingerprint of cell adhesion processes, since these plots reveal data independently of the spatial distribution, the number of attached cells and in a time resolved manner.[10] Therefore, we tried to assess, whether the differences of serum-free and serum-containing conditions we could detect can be expressed more precisely by presenting the data as D/f-plot.

First of all, we characterized the impact of the addition of 1 ml of medium containing 10 % FBS without rMSCs. In Figure 11 a linear relationship of D and f can be seen almost throughout the experiment. But after a saturation of the frequency shift at 40 Hz, a slight decrease in D can be seen. These characteristics indicate the adsorption of a viscoelastic protein layer, which does not change its composition, or viscoelasticy respectively, significantly during the adsorption process, otherwise a change in the slope of the graph would be detectable. But at the end of the adsorption process, the slight decrease in D signifies a "stiffening" process of the adsorbed protein film, which could be due to conformational changes of the proteins or due to the exchange of protein types over time. The latter effect is frequently described for different surfaces and called the "Vroman-effect".[21]
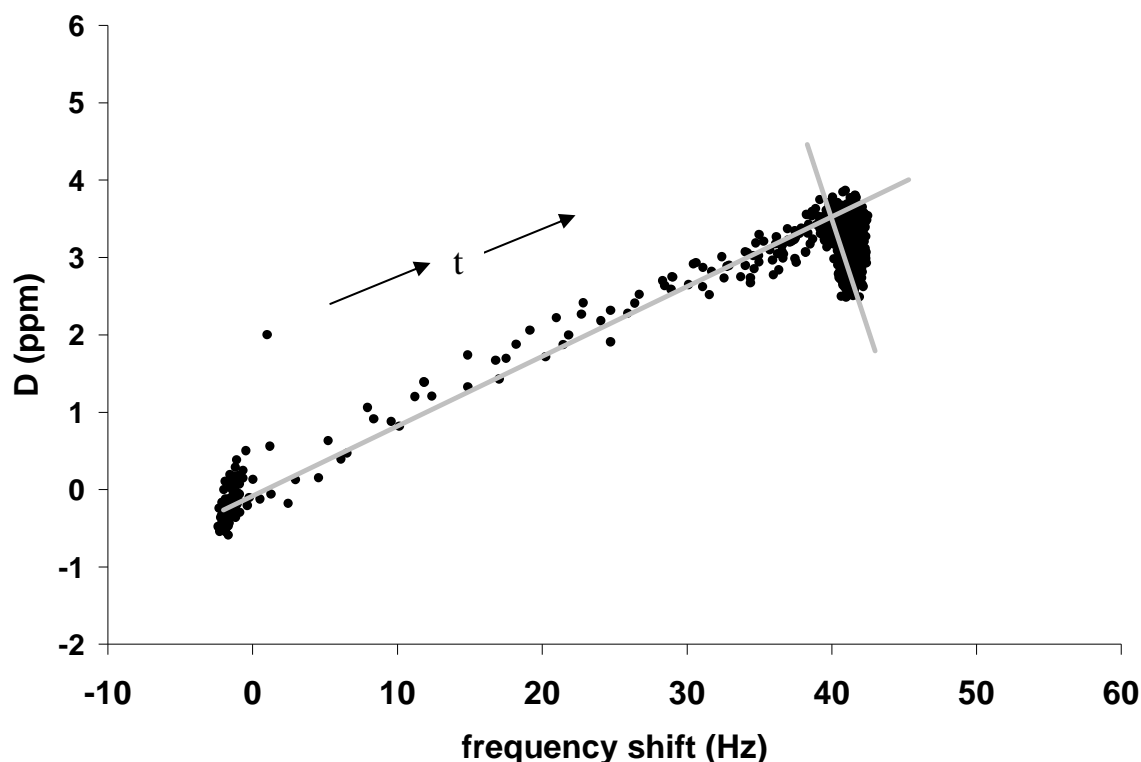
Figure 11: D/f-plot after the addition of 1 ml of serum containing medium. A constant slope indicates the adsorption of a mass with homogeneous viscoelastic properties throughout the whole process. At the end the adsorbed mass is stiffening, indicated by the decrease in D.

For cell adhesion processes, in particular, such D/f-plots could give viable data. In Figure 12 two different slopes can bee seen for the adhesion of rMSCs on GRGDS-modified SAMs in the absence of serum proteins. The process, that takes place first, can be defined from 0 – 10 Hz approximately, the second process with a constant slope from 10 – 45 Hz. A possible explanation for these characteristics could be the adsorption of a relatively small amount of proteins causing a frequency shift of only 10 Hz and an almost negligible increase in D. Such a low amount of proteins could be due to a carryover from cell culture or an excretion of proteins by the cells themselves. We also could detect such low amounts of protein adsorption in other studies, where we measured only the frequency shift after the addition of rMSCs on SAMs without GRGDS peptides under serum free conditions (data not shown).[16]

The second process detected in this experiment then could be attributed to the adhesion of cells causing the strong increase in D. This plot already shows that such a presentation of data allows for distinguishing the fractions of protein adsorption and cell adhesion. This we tried to confirm with further serum-containing experimental data.
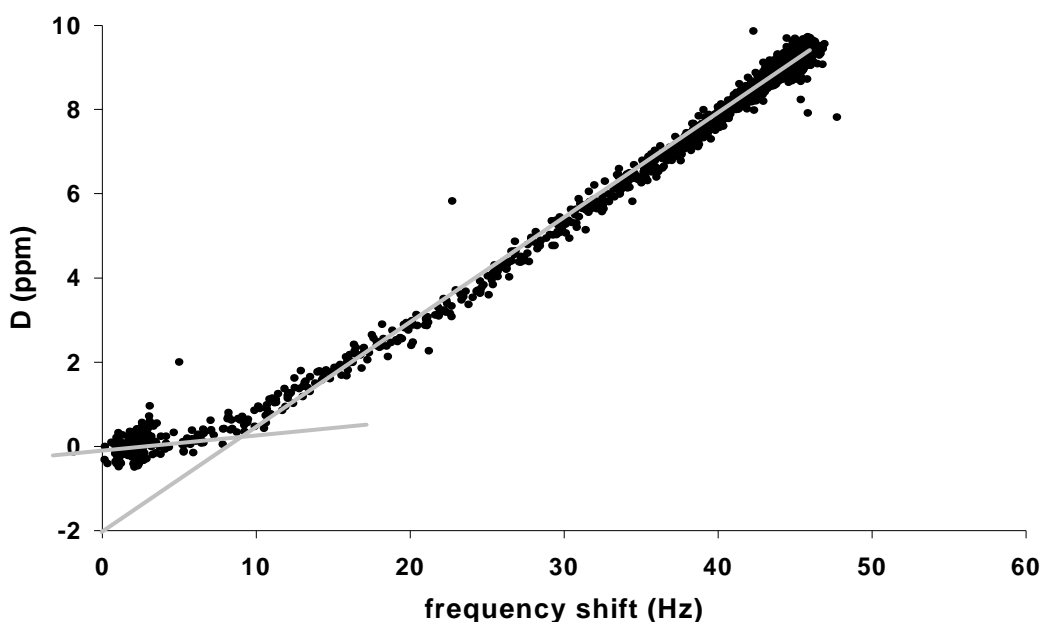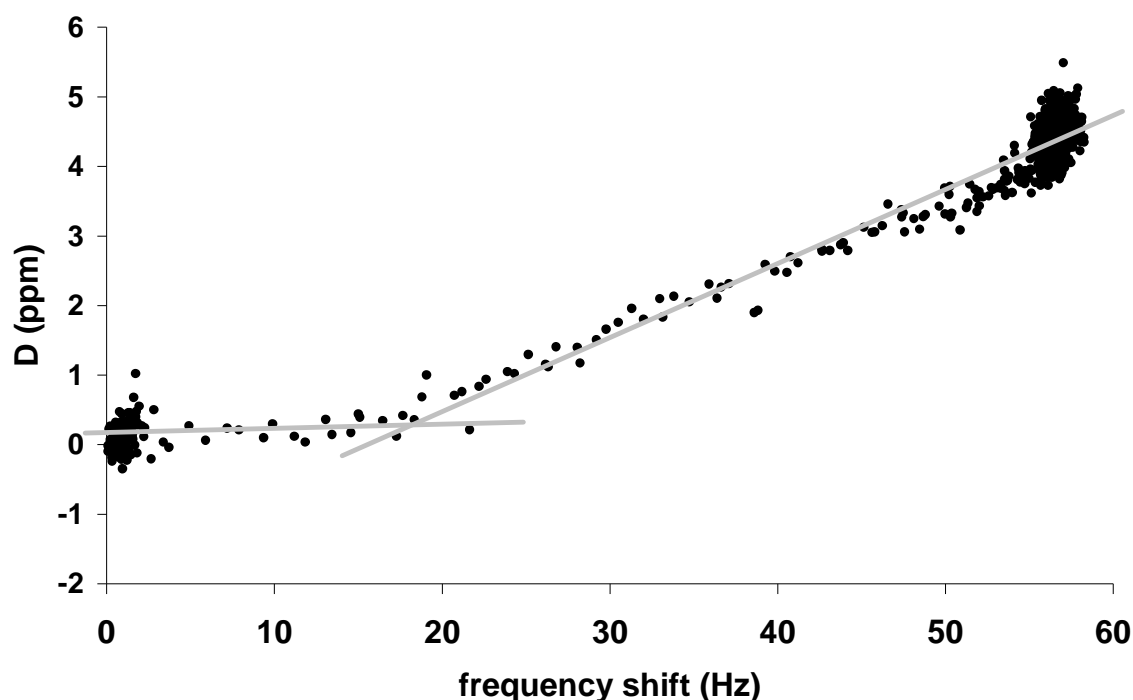

Figure 12: D/f-plot in the absence of FBS on GRGDS-modified SAMs. Two different slopes indicate that two different processes take place after the addition of rMSCs in PBS.

As for serum-free conditions, also for serum-containing experiments two different processes can be detected, what is shown in Figure 13. Here, the same processes are assumed to take place. First, an initial adsorption of proteins causing a frequency shift of 20 Hz. Also this value was confirmed in other studies, where only frequency shifts were measured on the same SAMs. The second process then can be attributed to the adhesion of rMSCs. The weaker increase in D compared to serum-free conditions is probably due to the higher concentration of RGD peptides, a stronger attachment is the consequence as described in more detail in the previous section.

Figure 13: D/f-plot in the presence of FBS on GRGDS-modified PEG monolayers. An obvious change in slope can be detected at a frequency shift of approximately 18 Hz. This suggests the adsorbed mass is composed of two different materials which are assumed to be proteins and cells.

Summarizing, all the acquired data using this QCM-D setup confirm the results of previous studies with a QCM arrangement. Moreover, the data that could be collected provide us with useful additional information. This allows for the determination of the impact of protein adsorption and cell adhesion separately in one experiment by analyzing the data using D/f plots. Additionally, we could see that although comparable frequency shifts were obtained under serum-free and serum-containing conditions, different shifts of the dissipation factor describe obvious differences in the adsorbed mass. These viscoelastic differences do not allow for direct comparisons of the amount of adsorbed masses on the surface, since the Sauerbrey equation is invalid for these premises.

Conclusion

In this study, we could show that different pump speeds of a dynamic flow-through QCM setup have an influence on the spatial distribution of cells on the sensor surface. Generated higher shear stress prevents the adhesion of cells in the center of the sensor. Therefore, the pump speed has to be reduced under a certain threshold to ensure a homogeneous cell distribution allowing for comparing the acquired results with other (static) setups. In our system this value is in the range of 0.1 ml/min. Furthermore, a completely different approach to evaluate cell adhesion processes was investigated: Measurements of the dissipation factor revealed different dissipative energy losses for cell adhesion experiments under serum free and serum-containing conditions due to a different extent of focal adhesion formation. In the presence of serum these losses are significantly lower, indicting that cells are attached more firmly to the surface, entrapping less water between cell and surface. The reason therefore probably are adsorbed proteins on the surface, presenting further RGD motifs. D/f-plots allowed for distinguishing the impact of cell adhesion and protein adsorption in one experiment: first a certain amount of proteins adsorbs, then cells adhere with the above mentioned characteristics. Summarizing, useful additional information on the processes taking place during cell adhesion can be acquired using a QCM-D system.

References

[1] Janshoff A.; Galla H.J.; Steinem C.: Piezoelectric mass-sensing devices as biosensors – an alternative to optical biosensors? Angewandte Chemie, Int Ed, 39, 4004-4032, 2000.

[2] Wegener J.; Janshoff A.; Galla H.J.: Cell adhesion monitoring using a quartz crystal microbalance: comparative analysis of different mammalian cell lines. Eur Biophys J, 28, 26-37, 1998.

[3] O´Sullivan C.K.; Guilbault G.G.: Commercial quartz crystal microbalances – theory and applications. Biosens & Bioelectron, 14, 663-670, 1999.

[4] Reiss B.; Janshoff A.; Steinem C.; Seebach J.; Wegener J.; Adhesion kinetics of functionalized vesicles and mammalian cells: a comparative study. Langmuir, 19, 1816 – 1823, 2003.

[5] Rodahl M.; Hoeoek F.; Fredriksson C.; Keller C.A.; Krozer A.; Brzezinski P.; Voinoca M.; Kasemo B.: Simultaneous frequency and dissipation factor QCM measurements of biomolecular adsorption and cell adhesion. Faraday Discuss, 107, 229 – 246, 1997.

[6] Marx K.A.; Zhou T.; Warren M.; Braunhut S.J.: Quartz crystal microbalance study of endothelial cell number dependent differences in initial adhesion and steady state behavior: Evidence for cell – cell cooperativity in initial adhesion and spreading. Biotechnol Prog, 19, 987 – 999, 2003.

[7] Buttry D.A.; Ward M.D.: Measurement of interfacial processes at electrode surfaces with the electrochemical quartz crystal microbalance. Chem Rev, 92, 1355 – 1379, 1992.

[8] Redepenning J.; Schlesinger T.K.; Mechalke E.J.; Puleo D.A.; Bizios R.: Osteoblast attachment monitored with a quartz crystal microbalance. Anal Chem, 65, 3378-3381, 1993.

[9] Rodahl M.; Hoeoek F.; Krozer A.; Brzezinski P.; Kasemo B.: Quartz crystal microbalance setup for frequency and Q-factor measurements in gaseous and liquid environments. Rev Sci Instrum, 66,3924-3930, 1995.

[10] Fredriksson C.; Kihlmann S.; Kasemo B.; Steel D.M.: In vitro real-time characterization of cell attachment and spreading. J Mat Sci, 9, 785 –788, 1998.

[11] Knerr R.; Weiser B.; Drotleff S.; Steinem C.; Goepferich A.: Measuring cell adhesion on RGD-modified self-assembled PEG monolayers using the quartz crystal microbalance technique. Macromolecular Bioscience, 9, 827-838 (2006).

[12] Jenkins M.S.; Wong K.C.Y.; Chhit O.; Bertram J.F.; Young R.J.; Subaschandar N.: Quartz crystal microbalance – based measurements of shear – induced senescence in human embryonic kidney cells. Biotechnol Bioeng, 88, 3, 392 – 398, 2004.

[13] Reddy K.; Ross J.M.: Shear stress prevents fibronectin binding protein-mediated staphylococcus aureus adhesion to resting endothelial cells. Infection and Immunity, 69(5), 3472-3475, 2001.

[14] Fredriksson C.; Kihlmann S.; Rodahl M.; Kasemo B.: The piezoelectric quartz crystal mass and dissipation sensor: A means of studying cell adhesion. Langmuir, 14, 248 – 251, 1998.

[15] Rodahl M.; Kasemo B.: Frequency and dissipation-factor responses to localized liquid deposits on a QCM electrode. Sensors Actuators, B, 37, 111-116, 1997.

[16] Knerr R.; Drotleff S.; Steinem C.; Goepferich A.: Self-assembling PEG derivatives for protein-repellant biomimetic model surfaces on gold. Biomaterialien, 7, 12 - 20, 2006.

[17] Ishaug S.L.; Crane G.M.; Miller M.J.; Yasko A.W.; Yaszemski M.J.; Mikos A.G.: J. Biomed Mater Res, 36, 17, 1997.

[18] Garcia A.J.; Huber F.; Boettiger D.: Force required to break $\alpha_5\beta_1$ integrin fibronectin bonds in intact adherent cells is sensitive to integrin activation state. J Biolog Chem, 273, 18, 10988 – 10993, 1998.

[19] Juliano R.L.: Signal transduction by cell adhesion receptors and the cytoskeleton: Function of integrins, cadherins, selectins, and immunoglobulin-superfamily members. Annu Rev Pharmacol Toxicol, 42, 283 – 323,2002.

[20] Rezania A.; Healy K.E.; The effect of peptide surface density on mineralization of a matrix deposited by osteogenic cells. J Biomed Mater Res, 52(4), 595-600, 2000.

[21] Turbill P.; Beugeling T.; Poot A.A.: Proteins involved in the Vroman effect during exposure of human blood plasma to glass and polyethylene. Biomaterials, 17, 13, 1279-1287, 1996.

[22] Neubauer M.; Fischbach C.; Bauer-Kreisel P.; Lieb E.; Hacker M.; Tessmar J.; Schulz M.B.; Goepferich A.; Blunk T.: Basic fibroblast growth factor enhances PPARg ligand-induced adipogenesis of mesenchymal stem cells. FEBS Letters, 577, 277-283, 2004.

Chapter 6

The influence of growth factors on the adhesion characteristics of rat marrow stromal cells

Robert Knerr[1], Barbara Weiser[1], Claudia Steinem[2], Achim Göpferich[1]*

[1]Department of Pharmaceutical Technology, University of Regensburg, Universitaetsstrasse 31, 93040 Regensburg, Germany

[2]Institute of Analytical Chemistry, Chemo- and Biosensors, University of Regensburg, 93040 Regensburg, Germany

Abstract

In this study, the influence of three different prominent growth factors (bFGF, TGFβ and PDGF) on the adhesion characteristics of rat marrow stromal cells (rMSCs) was shown. Short-term treatment of suspended rMSCs with bFGF increased cell adhesion significantly on RGD-presenting PEG surfaces. Moreover, a precultivation for 24 hours resulted in a complete coverage of the respective surface with rMSCs within 1 hour. On the other hand, in the absence of RGD peptides and with surface bound bFGF, cell adhesion was significantly reduced. Similar trends could be observed for TGFβ, however, the effects were significantly less pronounced. For PDGF, a dose-dependant reduction of cell adhesion after short-term treatment of rMSC suspensions was found. Staining of the cells´ cytoskeletons substantiated these results: bFGF and TGFβ treated cells showed higher amounts of integrins in the cell periphery, leading to increased cell adhesion, whereas a trafficking of integrins into the nuclei after PDGF treatment was found, weakening the attachment to the surface.

Introduction

Growth factors strongly influence the behavior of cells.[1-5] These signaling molecules affect the differentiation and maturation of cells by binding to cellular receptors and triggering intracellular signaling cascades. Also a physical as well as functional crosstalk with other receptors, such as integrin receptors, which mediate the adhesion of cells on surfaces after ligand binding, and their signaling cascades have been described.[6,7,8] Numerous investigations showed that also integrins, a family of receptors responsible for cell adhesion, can strongly be influenced by growth factors.[9,10,11] Although integrin ligands and growth factors have different structures, they may both elicit similar intracellular effects by using identical signaling casacdes.[12] Both the activated integrin $\alpha_v\beta_3$ and the vascular endothelial growth factor (VEGF), for example, trigger the phosphorylation of the focal adhesion kinase (FAK) entailing the binding of further signaling and structural proteins.[13]

But growth factors can not only influence the function of integrins, they can also modify the expression of these receptors on the cell surface. It is well known for example that the expression of the integrin $\alpha_v\beta_3$ can strongly be upregulated by basic fibroblast growth factor (bFGF) and VEGF.[13,14] Additionally, Rusnati et al. could demonstrate that bFGF contains two cell adhesion domains, which are responsible for interactions with integrin receptors.[12]

Vice versa, adhesive proteins, which normally bind to integrins, also may signal through growth factor receptors.[12] A very well known fact furthermore is that an increase of the cellular response to growth factors can be observed, if cells adhere to a surface: If cells are bound to substrates, the sensitivity of growth factor receptors to their ligands can increase significantly. [14,15,16]

On the other hand, very little is known about the impact of growth factors on the initial steps of cell adhesion. In only few studies the mutual crosstalk in this direction is described, with in some cases contradictory results. The studies of Rusnati, Enenstein, Jang and Weston all revealed that bFGF increases the adhesion of different cells to surfaces, although the mechanism remains uncertain.[12,17,18,19] Rusnati suggested a binding of bFGF to $\alpha_v\beta_3$ integrins, Jang the activation of (ERK)-type MAPK by both bFGF and fibronectin. Enenstein stated a modulation of integrin receptors by bFGF, Weston did not comment on the mechanism at all. Some further investigations can be found for other prominent growth factors, such as TGFβ or PDGF. These results seem confusing, since these studies report on

no effects on cell adhesion, increased cell adhesion or indicate a reduction of adhesion to certain substrates.[13,20,21,22] Hence, a lot of issues concerning the mutual crosstalk of integrins and growth factors in terms of the impact on cell adhesion remain uncertain.

Recently, we could develop a very straightforward, but efficient method to characterize the initial steps of cell adhesion[23], which may be helpful to shed light on these complex processes. Consisting of a well-defined self-assembled monolayer (SAM) of poly(ethylene glycol) (PEG) derivatives on the sensor of a quartz crystal microbalance (QCM), this system allows for the real-time assessment of the initial steps of cell adhesion. Due to the protein repellant effect of PEG, non-specific reactions, such as protein adsorption and subsequent cell adhesion, can be suppressed to a high extent, but on the other hand PEG allows for the covalent attachment of cell adhesion peptides or growth factors. We could demonstrate the efficiency of this system for example to evaluate the effect of manganese cations on integrins and cell adhesion.[23] Hence, this QCM arrangement seems very suitable for the rapid determination of the aforementioned influences of different growth factors on cell adhesion.

Therefore, it was the goal of this study to evaluate whether the three prominent growth factors bFGF, TGFβ and PDGF do have an impact on the extent of the adhesion of marrow stromal cells (MSCs), since there has been an increasing interest in recent years in this type of cells due to their wide range of clinical applications.[24] However, as no indications of the impact of growth factors on MSC adhesion are given at all, the effects of growth factors on this cell type could be of high interest in this scientific field. As there are no definite results on the mechanism of growth factor – integrin interactions, we cultivated rat marrow stromal cells (rMSCs) over different time scales (bFGF, TGFβ) or different concentrations (PDGF) and compared the responses of the QCM system after the cells were allowed to adhere for one hour, with the goal to get further insights into the crosstalk of growth factors and cell adhesion receptors.

Materials and Methods

Materials

Ethanol was purchased from JT Baker, Deventer, Netherlands. Dimethylformamide (DMF) and methanol were from Acros Organics (Geel, Belgium). Ascorbic acid, succinic anhydride, dicyclohexyl carbodiimide (DCC), and N-hydroxysuccinimide (NHS) were acquired from Sigma-Aldrich Chemie GmbH (Taufkirchen, Germany). Formaldehyde and Triton X-100 were purchased from Merck KGaA (Darmstadt, Germany), GRGDS from Bachem Biochemica (Heidelberg, Germany), fluorescein phalloidin, penicillin/streptomycin solution (PenStrep), and phosphate buffered saline (PBS) from Invitrogen GmbH (Karlsruhe, Germany). Fetal bovine serum (FBS), Dulbecco´s modified eagle medium (DMEM) and trypsin were acquired from Biochrom AG (Berlin, Germany). bFGF, TGFβ and PDGF were acquired form Peprotech (Rocky Hill, NJ, USA), anti-CD61(betaβ$_3$)-antibody and IgG Armenian Hamster Isotype control from Biolegend (San Diego, CA, USA). All reagents were of analytical grade and used as received without further purification.

Quartz Crystal Microbalance (QCM) Experiments

A detailed description of the QCM instrumentation has been published previously.[23,25,26] In brief: AT-cut quartz plates with a 5 MHz fundamental resonance frequency (KVG, Neckarbischofsheim, Germany) were coated with gold electrodes on both sides and placed in a Teflon chamber, exposing one side of the resonator to the aqueous solution. The apparatus was equipped with an inlet and outlet, which connects the fluid chamber to a peristaltic pump (pump rate: 100 µl/min) (Ismatec Reglo Digital, Wertheim-Mondfeld, Germany), allowing for the addition of cell suspensions from outside the Teflon chamber. Spring contacts connect the gold electrodes with the oscillator circuit (TTLSN74LS124N, Texas instruments, Dallas, TX, USA) driven by a 4 V D.C. voltage (HP E3630A, Hewlett-Packard, San Diego, CA, USA). The frequency change of the quartz resonator is recorded using a frequency counter (HP 53181A, Hewlett-Packard) connected via RS 232 to a personal computer. The Teflon chamber is thermostated at 37°C in a water-jacketed Faraday cage. Experiments were performed by adding 1 ml suspensions of 250,000 rMSCs in serum-containing medium. (For the detailed setup see Figure 1.)

If standard deviations are given, measurements were triplicates and the mean value given at different time points. Results without standard deviations were individual experiments.
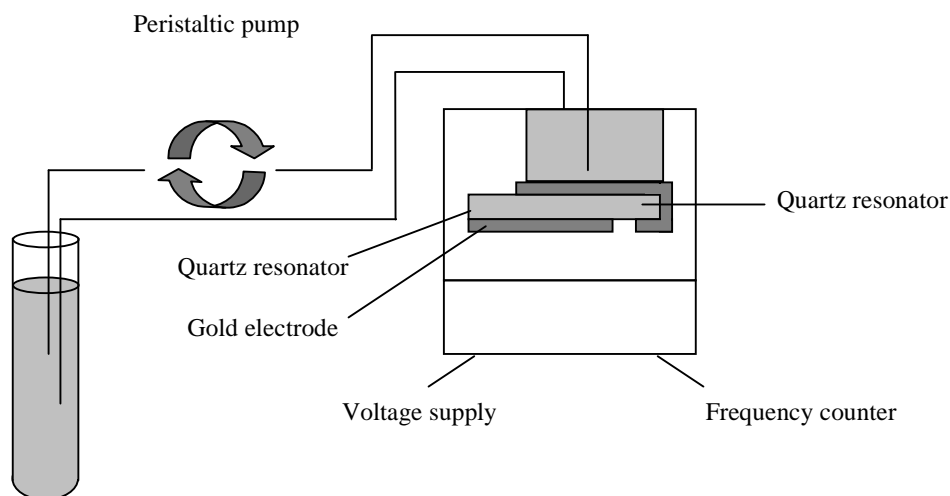
Figure 1: QCM flow through setup. If cells adhere to the gold surface of the sensor, the resonance frequency decreases. For rigid masses, this decrease is proportional to the amount of mass on the surface. For cells, this decrease depends predominantly on the contact area between cell and surface. However, correlations of cell number and frequency shifts are possible.[29]

Cell Culture

Marrow stromal cells (rMSCs) were obtained from 6-week-old Sprague Dawley rats according to a procedure published by Ishaug et al.[27] and were cultivated under standard culture conditions (37°C, 95% relative humidity, 5% CO_2 in DMEM with 10 vol.-% fetal bovine serum, 1 vol. -% penicillin/streptomycin, and 50 µg/ml ascorbic acid). For QCM experiments, cells were trypsinized, centrifuged at 1200 rpm for 5 minutes, and the resulting cell pellet re-suspended in medium at 250,000 cells/ml. Cells were then held in suspension in medium with the corresponding growth factor for 30 minutes in different concentrations (1 ng/ml for $TGF\beta_1$, 7.5 ng/ml for bFGF and various concentrations of PDGF (0.3 – 1.0 ng/ml)) or in medium without growth factor.

Staining of the cytoskeleton was performed with a fluorescein-labeled phalloidin derivative (Invitrogen, Karlsruhe, Germany). In this procedure, the surfaces were rinsed with PBS and cells were fixed with 3.8 vol.-% formaldehyde for 10 minutes at room temperature. After rinsing with PBS, the surfaces were extracted with acetone at –20°C for 5 minutes and rinsed again with PBS. Then the cells were stained with 5µl of the methanolic dye

solution in 500µl of PBS containing 1 wt.-% BSA for 20 minutes. After rinsing with PBS, images were taken with an Axiovert 200M microscope coupled to scanning device LSM 510 (Zeiss, Jena, Germany) at 100-fold magnification (Ex = 469nm, Em = 516nm).

Staining of integrin β_3 subunits was performed as follows: cells were seeded at a density of 10.000 cells/cm^2 and cultivated for two days in Lab-Tek II$^®$ 8-well ChamberSlides (Nunc, Wiesbaden, Germany). Then medium was exchanged and the corresponding growth factor was added in concentrations similar to QCM experiments. After further 24 hours of cultivation, medium was withdrawn and the cell layer washed with PBS. Afterwards, surfaces were extracted with a solution of Triton X-100 (0.1 vol.-%) in PBS. After one minute, the surfaces were rinsed with PBS three times and the antibody solutions added (1µg/ 200µl PBS). Subsequently, cells were incubated for 2 hours with the antibody solution in the dark at room temperature. After rinsing again with PBS three times, images were taken with an Axiovert 200M microscope coupled to scanning device LSM 510 (Zeiss, Jena, Germany) (Ex = 469nm, Em = 516nm). As negative control one group was treated with IgG Armenian Hamster Isotype control in the same way.

Sensor surface modification

Polymers necessary for producing SAMs have been synthesized and characterized as published previously.[23,26] In brief, thioacetic acid was bound to 11-bromo-undecene via a radical chain reaction with benzoyl peroxide as the initiator. The resulting thioester was hydrolyzed to the free thiol, which was then protected with 2-chlorotrityl chloride. To this compound, N-BOC protected poly(ethylene glycol)-monoamine was attached in a Williamson ether synthesis. Afterwards, both protecting groups were removed resulting in the PEGylated dialkyldisulfide di(amino poly(ethylene glycol)-undecyl) disulfide, $(NH_2PEG_{2000}C_{11}S)_2$ (Figure 2).
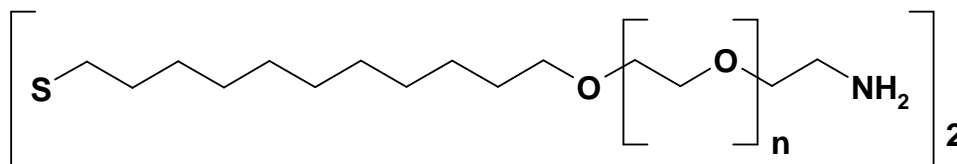

Figure 2: Chemical structure of di(amino poly(ethylene glycol)-undecyl) disulfide.

Gold sensor surfaces were cleaned by immersing the surfaces for 5 minutes in a piranha solution (3:1 mixture of concentrated sulfuric acid and aqueous hydrogen peroxide (30

vol.-%), which was heated to 70°C. Afterwards, the gold was rinsed extensively with double-distilled water, dried in a stream of nitrogen and incubated overnight in a 1 mM solution of $(NH_2PEG_{2000}C_{11}S)_2$ in absolute ethanol. After rinsing again with absolute ethanol, the surfaces were dried in a stream of nitrogen.

Subsequently, the $(NH_2PEG_{2000}C_{11}S)_2$ SAM was incubated in a 4 % (w/v) solution of succinic anhydride in dimethylformamide (DMF) overnight, rinsed with DMF, and dried in a stream of nitrogen. The resulting succinamide was then activated with 0.2 M DCC and 0.05 M NHS in DMF for two hours. For binding the pentapeptide GRGDS, the activated surface was subsequently incubated in a solution containing 0.5 mg GRGDS in 1 ml of PBS pH 7.4 at 4°C overnight, allowing for the reaction of the primary amine group of GRGDS with the activated carboxylic acid, and rinsed afterwards with double-distilled water. The binding of GRGDS was ascertained by water contact angle measurements with a method described previously.[26]

Results and Discussion

The influence of bFGF on rMSC adhesion

Pretreatment of rMSCs with bFGF

In Figure 3 the QCM response after the injection of 250.000 rMSCs suspended in 1 ml of medium into the QCM system can be seen. The sensor surface in these experiments was modified with a self-assembled monolayer of thioalkylated PEG derivatives. These compounds consist of thiolated undecyl chains with, to which monoamine PEG derivatives were attached, resulting in di(amino poly(ethylene glycol)-undecyl) disulfide (Figure 2). For this type of surface, we could recently show that non-specific protein adsorption can be reduced to a large extent, resulting in a frequency shift of only 20±7 Hz. Cell adhesion can be suppressed completely.[23] However, if the pentapeptide GRGDS is attached covalently to the sensor surface (as it is the case here), a significant adhesion of well spread rMSCs to the PEG SAM can be observed. Figure 3 shows this result: After cells and proteins are injected into the QCM system and reach the measurement chamber, the resonance frequency drops by 61±4 Hz, indicating the adhesion of cells and to a certain extent the adsorption of proteins to the sensor surface.

Effects of growth factors on the adhesion of other cell types (NIH-3T3) were described already after treating the cells with growth factors for only ten minutes.[28] To evaluate, whether this rather short time of treatment already also has an effect on rMSC adhesion, we incubated rMSCs after harvesting and resuspension in medium for 30 minutes with bFGF (7.5 ng/ml) and investigated their adhesion to the same model surface as described above. As a result of this procedure, the QCM response was 11 Hz stronger with 72±5 Hz (Figure 3), this additional increase after 1 hour is statistically significant (p<0,05). This stronger decrease in resonance frequency can be due to an increase in cell adhesion, but also due to a different attachment of cells, since there exists a linear relationship of resonance frequency shift and the contact area between cell and surface.[29] However, in several studies it was shown that there is a good correlation of frequency shift and number of attached cells.[29] Recently, we could demonstrate that the adhesion of rMSCs causes a frequency shift of 6.7 mHz/cell.[23] If one assumes the type of cell – surface interaction as similar in the presence or absence of bFGF, an additional decrease in resonance frequency shift of 11 Hz, therefore, suggests an additional adhesion of approximately 5500 rMSCs/cm^2 due to the presence of bFGF (surface area: 0.3 cm^2).
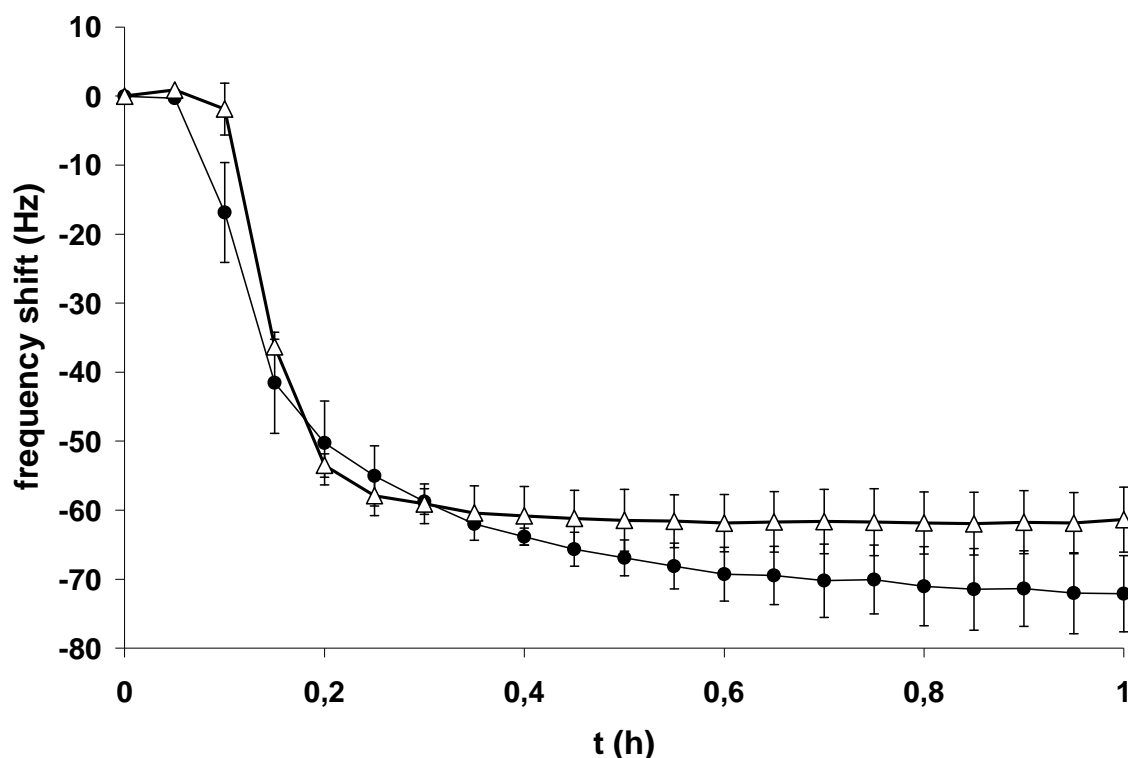
Figure 3: QCM frequency shifts indicate the extent of rMSC adhesion on GRGDS presenting SAMs. If cells are pretreated with bFGF for 30 minutes (●), the decrease in resonance frequency is 11 Hz stronger (72±5 Hz) than for non-bFGF treated cells (△) (61±4 Hz).

Covalent attachment of bFGF to the model surface

To assess, whether this modulation of cell adhesion is due to the adhesive properties of bFGF itself, for example by presenting cell adhesion motifs, in a further experiment we attached bFGF covalently to the SAM instead of the integrin ligand GRGDS with a similar procedure as for GRDGS. In previous studies, we showed that proteins bind covalently to these SAMs with a density of approximately 35 pm/mm^2,[23] so due to a similar modification procedure also the concentration of bFGF on these surfaces should be in the same range. However, in contrast to the results of the study of Rusnati et al.[12], we could not observe any cell-adhesive effect of bFGF in the absence of integrin ligands: In Figure 4 the QCM results can be seen for these experiments. The resonance frequency only

decreases 19±11 Hz after the addition of rMSCs to bFGF-presenting SAMs. This small decrease is in the range of experiments, where only medium is added to the QCM system,[26] indicating that only proteins adsorb on these SAMs. Indeed, we could not stain any cells on the surface. These results suggest that bFGF does not enhance cell adhesion of rMSCs when immobilized on the surface. However, it has to be stated that contingently adhesion domains may exist, but might be involved in the covalent binding of the growth factor to the activated SAMs and therefore may not available for cellular receptors.
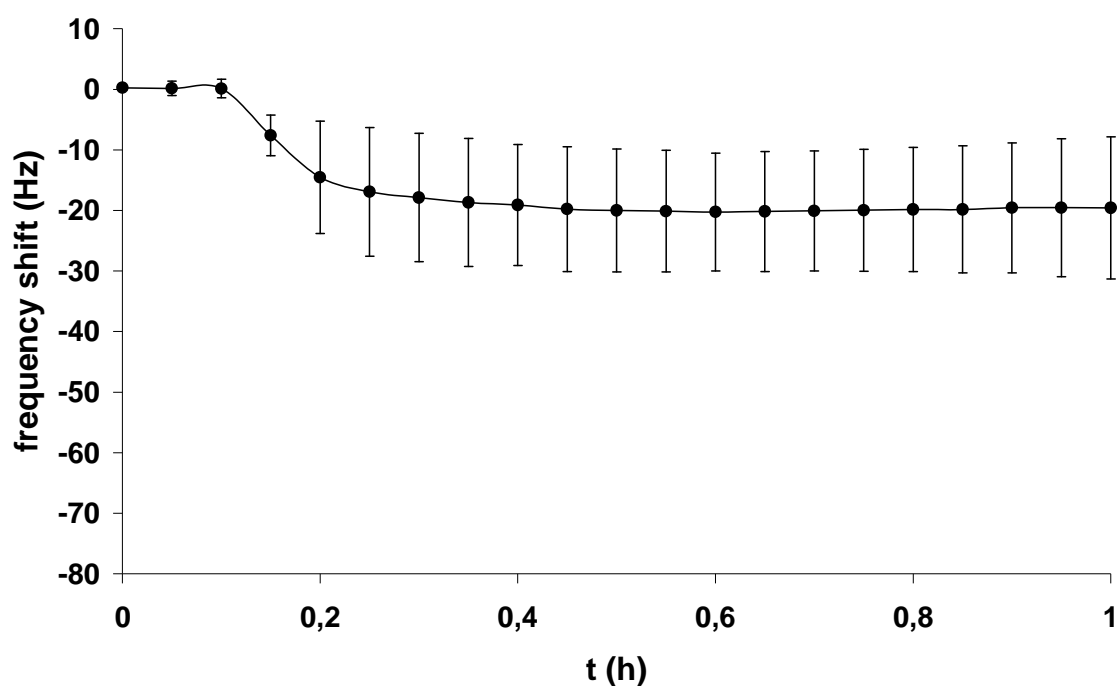
Figure 4: If bFGF is bound covalently to the SAM instead of GRGDS, the resonance frequency only decreases by 19±11 Hz, indicating cells do not adhere, only proteins adsorb to a low extent.

Pretreatment of the sensor surface with bFGF

A further experiment confirms the hypothesis that bFGF does not contain cell adhesion motifs. After pretreating the SAM modified sensor surfaces with bFGF in the same concentration as for the experiment described above and subsequent removal of unbound bFGF by rinsing with PBS, the resonance frequency only drops by 57 Hz after the addition of 250.000 rMSCs suspended in 1 ml medium.

If the increase in frequency shift of the experiments shown in Figure 3 would be only due to the presentation of adhesion motifs presented by bFGF that is adsorbed to the SAM, a pretreatment of the SAM with bFGF should even lead to a stronger QCM response compared to bFGF-free experiments. But as can be seen in Figure 5, the decrease in resonance frequency is in the range of bFGF-free experiments, indicating that the pretreatment of the SAM with bFGF does not lead to the presentation of further adhesion motifs. This also points into the direction that an other mechanism must be responsible for the modified QCM response.

The effect of bFGF without pretreatment of rMSCs

In a further experimental setup we harvested cells and held them in suspension in medium without growth factor for 30 minutes and then added rMSCs and bFGF at the same time into the QCM system. The decrease in resonance frequency of 68 Hz shows that even this short contact is enough to suggest an effect on cell adhesion, since the frequency shift here is in the range of experiments in the presence of bFGF throughout the experiment. This instant effect of bFGF could confirm the hypothesis of Enenstein that bFGF increases the affinity state of integrins towards their ligands.[17]
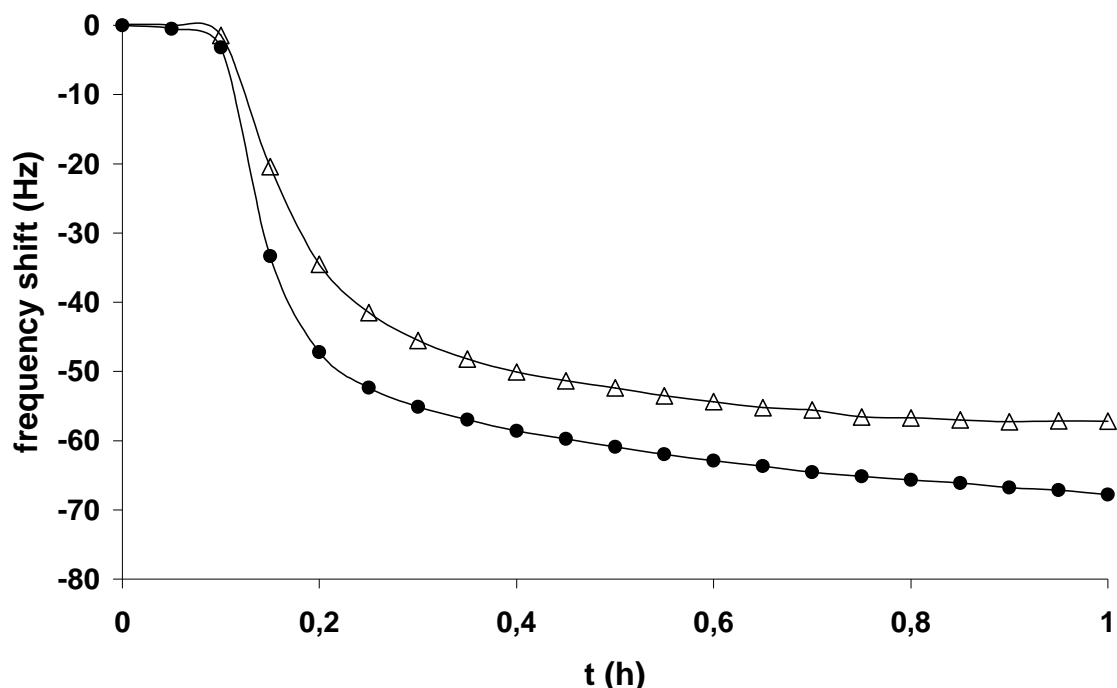
Figure 5: If bFGF is injected in the QCM 10 minutes before rMSC are added to the system, the decrease in resonance frequency with 57 Hz is not stronger than in bFGF-free experiments (△). On the other hand, if bFGF and rMSCs are added at the same time (●), the frequency drops by 68 Hz, suggesting an impact of bFGF already after a very short exposure of cells to the growth factor.

Precultivation of rMSCs with bFGF

In literature, an other suggested mechanism of induction of cell adhesion is the upregulation of integrin receptors on the cell surface.[13,28,30] This was suggested due to the release of integrins from endosomal compartments or by new biosynthesis. Since the latter process is assumed to take longer than the 30 minutes treatment described above, we also cultivated rMSCs for 24 hours with bFGF. After harvesting, cells were again treated with bFGF for 30 minutes and then injected into the QCM system. In this case, the resonance frequency dropped by 93 Hz. Assuming a frequency shift of 6.7 mHz/cell[23], this leads to a number of approximately 11.000 cells on the sensor surface (0.3 cm^2). This value also

indicates a strong increase in cell adhesion due to the precultivation with bFGF, which is significantly stronger than the short time pretreatment for 30 minutes.

Cultivating the cells with bFGF for 5 days leads again to an increase in frequency shifts. The decrease in resonance frequency is 119 Hz, indicating that again more cells adhere to the sensor surface. Calculating with a value of 6.7 Hz/cell and subtracting 20 Hz for protein adsorption, this leads to a value of almost 50.000 cells/cm^2, which is in the range of a confluent monolayer of well spread cells.[27]
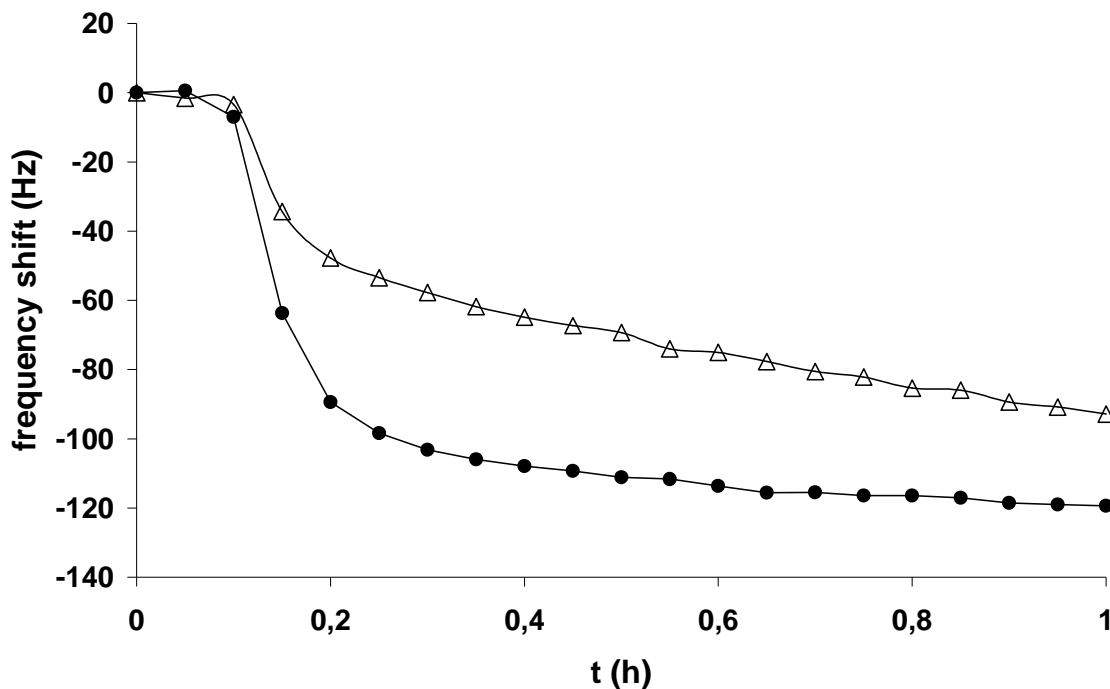

Figure 6: QCM frequency shifts indicate the extent of rMSC adhesion on GRGDS presenting SAMs. The longer cells are pretreated with bFGF, the stronger the QCM response is (△ 1 day of precultivation, ● 5 days of precultivation)

These results suggest a mechanism of upregulating the concentration of integrins on the cell surface, which probably is not only based on the recycling of integrins from endosomes. Since after a cultivation of five days the increase is even stronger than after one day of bFGF treatment, a new biosynthesis of integrins can be suggested.

Summarizing, several facts concerning the influence of bFGF on rMSC adhesion can be stated.

If rMSCs are pretreated with bFGF for 30 minutes, this leads to an additional attachment of 5500 cells/cm^2. A covalent attachment of bFGF to the SAM modified sensor surface does not lead to any cell adhesion in the absence of GRGDS on the surface, also a pretreatment of the sensor surfaces with bFGF and subsequent bFGF removal does not lead to an increase in cell adhesion. However, an effect of bFGF already may be possible when bFGF and cells are added at the same time into the QCM system.

A precultivation with bFGF for 24 hours strongly increases cell adhesion: 11.000 rMSCs adhere to the sensor surface compared to 6.000 in the absence of bFGF. Moreover, a precultivation for 5 days leads to a cell number of 15.000 rMSCs on the sensor surface, a value which is in the range of a confluent monolayer of well spread rMSCs.

Therefore, a combination of different effects of bFGF on rMSC adhesion can be suggested: An instant increase of integrins on the cell surface or a modulation of integrin affinity towards their ligands, but additionally also a new biosynthesis of further integrins.

Theses hypotheses of course can not be proven finally by only performing QCM experiments, further bioanalytical techniques, such as fluorescence activated cell sorting (FACS) or RT-PCR could help to clarify the detailed mechanisms or exact cell number on the surface. However, with these QCM results, which support the findings of Enenstein and Zhou,[17,30] we could demonstrate the benefits of this rather simple technique to get a more detailed insight into the potential mechanisms of the influence of bFGF on the adhesion of rMSCs.

The influence of TGFβ on rMSC adhesion

Also for TGFβ an effect on cell adhesion is described in some studies.[20,31,32,33] Therefore, we performed similar experiments as for bFGF with this signaling molecule. In Figure 7 the effect on rMSC adhesion after pretreating the cells for 30 minutes with 1 ng/ml of TGFβ can be seen. Without growth factor, the resonance frequency drops by 57±7 Hz after one hour. If cells are treated after harvesting with TGFβ, a stronger frequency shift of 61±5 Hz is observed, leading to the assumption that additional 600 rMSCs adhere. However, this slight difference after one hour of adhesion time is not statistically significant. Cultivation of rMSCs for 24 hours with TGFβ leads to a decrease of 72 Hz, suggesting the adhesion of almost 8.000 cells. In consequence, the results of these few experiments indicate a similar result for the modulation of cell adhesion as for bFGF: short term treatment with TGFβ leads to a slight increase in cell adhesion. A cultivation for 24 hours again increases the QCM response. But obviously, the effect is less strong than for bFGF.
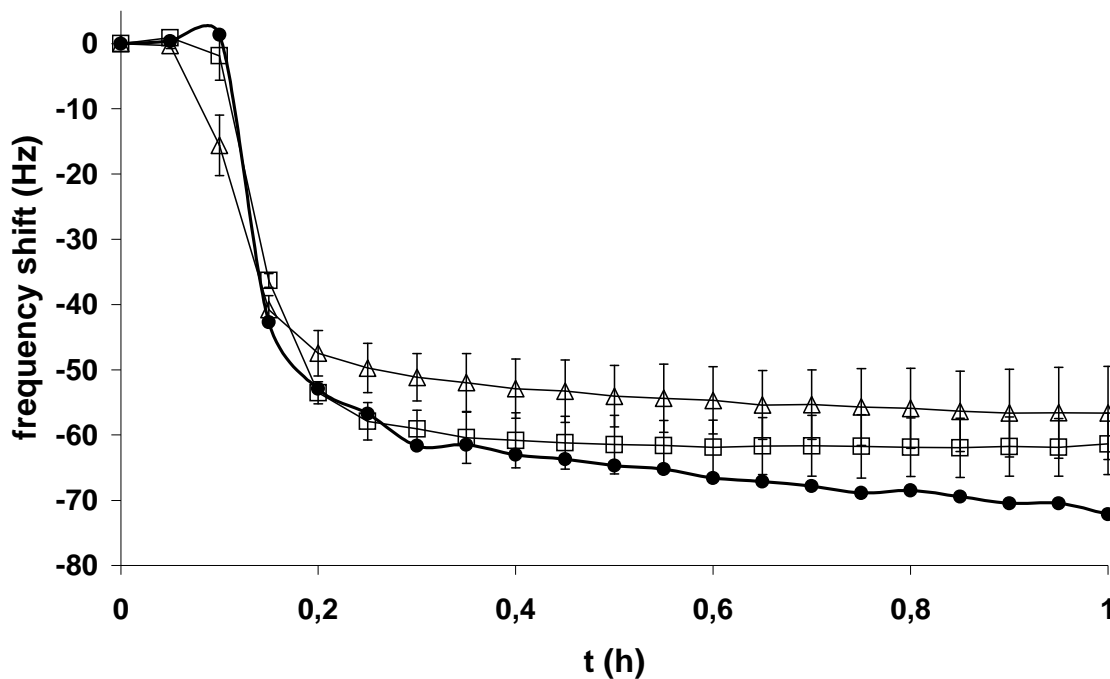

Figure 7: TGFβ does not have a significant effect on the adhesion of rMSCs, although the QCM response is slightly increased after TGFβ treatment (△ without,□ with TGFβ). After cultivating rMSCs for three days with TGFβ, the effect seems to be stronger (●).

The effect of PDGF on rMSC adhesion

The third prominent growth factor we investigated was PDGF. For this signaling molecule three different types are described, composed of either two A subunits, one A and one B subunit or two B subunits, all with slightly different effects on cells.[7] In this study, we focused on the PDGF-AA growth factor, which only binds to αα-PDGF-receptor subtypes. As for bFGF and TGFβ, also for PDGF a mutual crosstalk with integrins is described: PDGF receptors form complexes with $\alpha_v\beta_3$,[34] PDGF interacts with the focal adhesion kinase (FAK) as well as integrin ligands do,[7,35] and PDGF can recycle integrins from endosomal compartments for example.[28,36] An important aspect concerning the adhesion of cells was described by Fujio et al., who found that PDGF treated cells bind more loosely to fibronectin substrates.[21] Kingsley et al. also described that PDGF reduces the adhesion of rat aortic smooth muscle cells to laminin substrates,[37,38] and Berrou et al. stated that PDGF inhibits smooth muscle cell adhesion to fibronectin.[39] Moreover, in several studies it was found that the synergistic activity of $\alpha_v\beta_3$ integrin and PDGF receptors increase cell migration.[22,37] The effect of cell detachment was described by Carragher et al.[40] These results indicate a strong influence of PDGF on cell adhesion, a fact which could easily be tested for rMSCs using our QCM system.

Therefore, we treated rMSCs for 30 minutes with different concentrations of PDGF-AA in medium after harvesting before injection into the QCM system. In the control experiment without PDGF the resonance frequency decreased after the addition of 250.000 rMSCs by 58 Hz (Figure 8). If the cells were treated with 0.3 ng/ml, the decrease in resonance frequency only was 46 Hz. A concentration of 0.5 ng/ml lead to a frequency shift of only 40 Hz. Increasing the PDGF concentration further on, the frequency always drops in the range of 25 Hz. Since this change in frequency was shown to be caused by protein adsorption alone[23,36], a strong reduction of cell adhesion due to the treatment with PDGF can be stated up to an almost complete reduction above concentrations of PDGF of 0.75 ng/ml. In Figure 9 fluorescein-phalloidin stained rMSCs can be seen on GRGDS modified SAMs after treating the cells for 30 minutes with 0.5 ng/ml PDGF before and throughout the experiment. Compared to non-PDGF treated rMSCs, the number of cells indeed is strongly reduced.[23] Moreover, an obvious dose-dependant effect of PDGF can be observed. The higher the concentration of PDGF, the lower the extent of cell adhesion, an effect confirmed by the study of Fujio et al. for rat smooth muscle cells.[21]
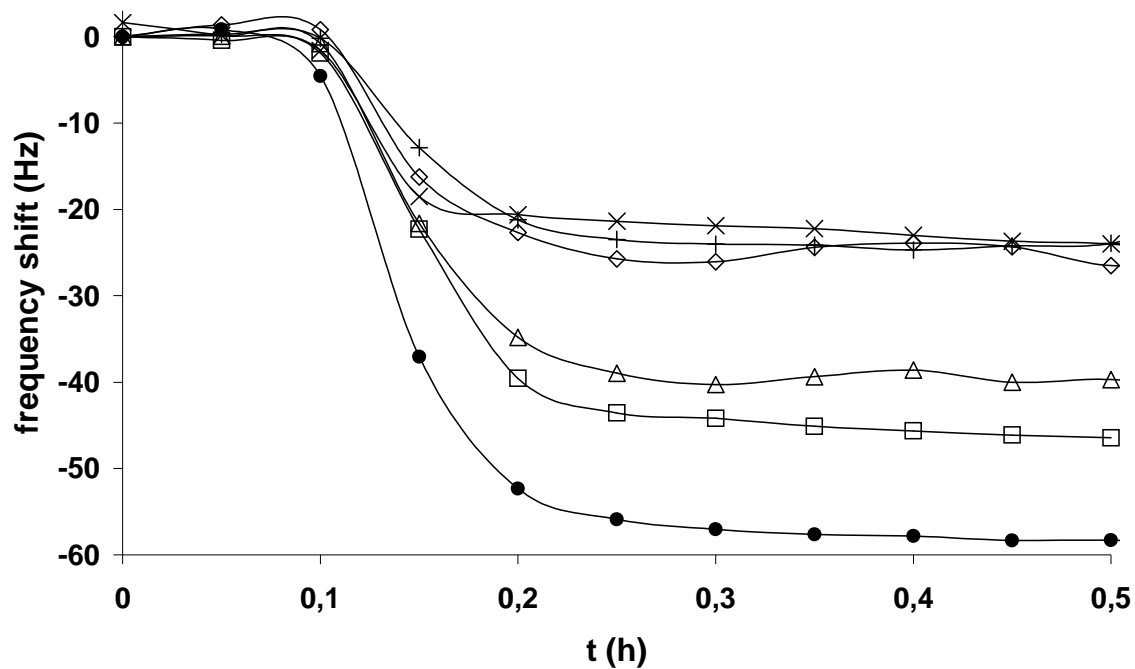
Figure 8: The adhesion of rMSCs on GRGDS presenting surfaces strongly depends on the pretreatment with PDGF-AA. The higher the concentration of PDGF, the lower the extent of cell adhesion is (● 0 ng/ml, □ 0.3 ng/ml, △ 0.5 ng/ml, ✕ 0,75 ng/ml, ◇ 1 ng/ml, ✚ 5 ng/ml).

In general, PDGF is not described as a compound suppressing cell adhesion completely, Fujio only described a reduction of SMC adhesion to fibronectin. But thinking of the dynamic flow through QCM system used in these experiments, the generated shear stress could amplify the effect of loosening the adhesion strength by PDGF. This fact then could lead to the complete prevention of cell adhesion under these conditions.

Additionally, the dose necessary for detecting an adhesion preventive effect is much smaller for the dynamic QCM conditions than for the static experiments of Fujio et al.[21] The maximum effect was determined at a concentration of 10 ng/ml in the study of Fujio. In our experiments, the maximum effect was reached already at a concentration of 0.75 ng/ml, which is more than one order of magnitude lower. Fujio et al. found that the reason for the reduction of cell adhesion due to PDGF is the down-regulation of α-actin expression resulting in a phenotype modulation from differentiated to proliferating type.[21]
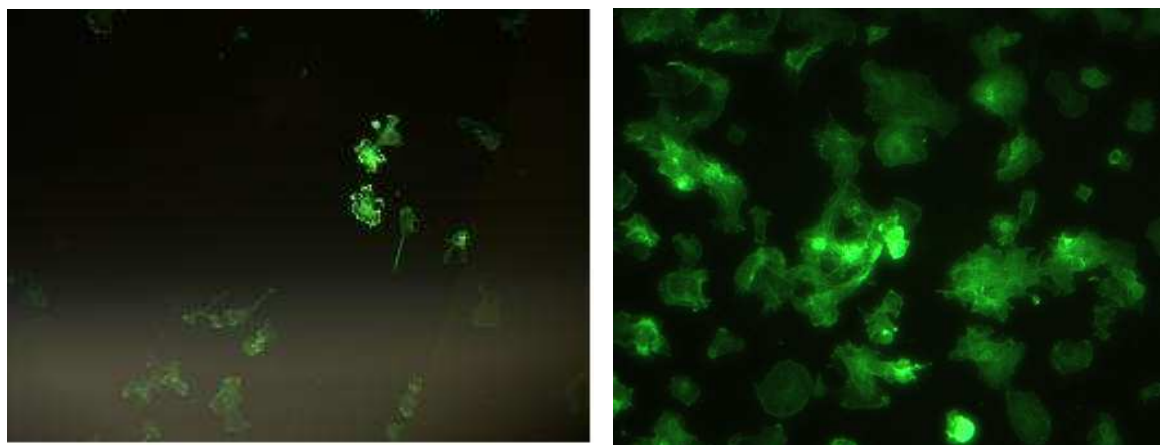
Figure 9: rMSCs adhering to GRGDS presenting SAMs after 30 minutes of treatment with 0.5 ng/ml PDGF (left, 100x). Only few cells can be stained with fluorescein-phalloidin. Non-PDGF treated cells on the other hand adhere and spread well on similar polymer surfaces (right, 200x).

The influence of growth factors on integrin β₃ subunits

To assess, whether the three different growth factors have any impact on the distribution of integrins under static conditions, we additionally tried to stain β_3 subunits of integrin receptors using a fluorescent anti-β_3 antibody under common cell culture conditions. After cultivation of rMSCs for 24 hours with the respective growth factor at the same concentration as used in QCM experiments (1 ng/ml for PDGF and TGFβ, 7.5 ng/ml bFGF), the cells were incubated with anti-β_3 antibody. In Figure 10 images of rMSCs after this procedure can be seen. For all different groups a very weak fluorescence can be detected under the same conditions, with the strongest intensity in the nuclei of the cells, a phenomenon, which is also described in literature.[21] For the negative control group, no fluorescence could be detected at all (data not shown). The intensity of fluorescence of the bFGF and TGFβ groups seems to be slightly higher than for the group without growth factor, indicating that the concentration of integrins might be increased. For the PDGF group, a fluorescence almost only can be seen in the nuclei of the cells, suggesting a trafficking of integrins from peripheral regions to the nuclei, as it is described by Fujio et al.[13] This reduction of integrins after PDGF treatment also is a hint that the adhesion strength of rMSCs is diminished after treatment with PDGF.
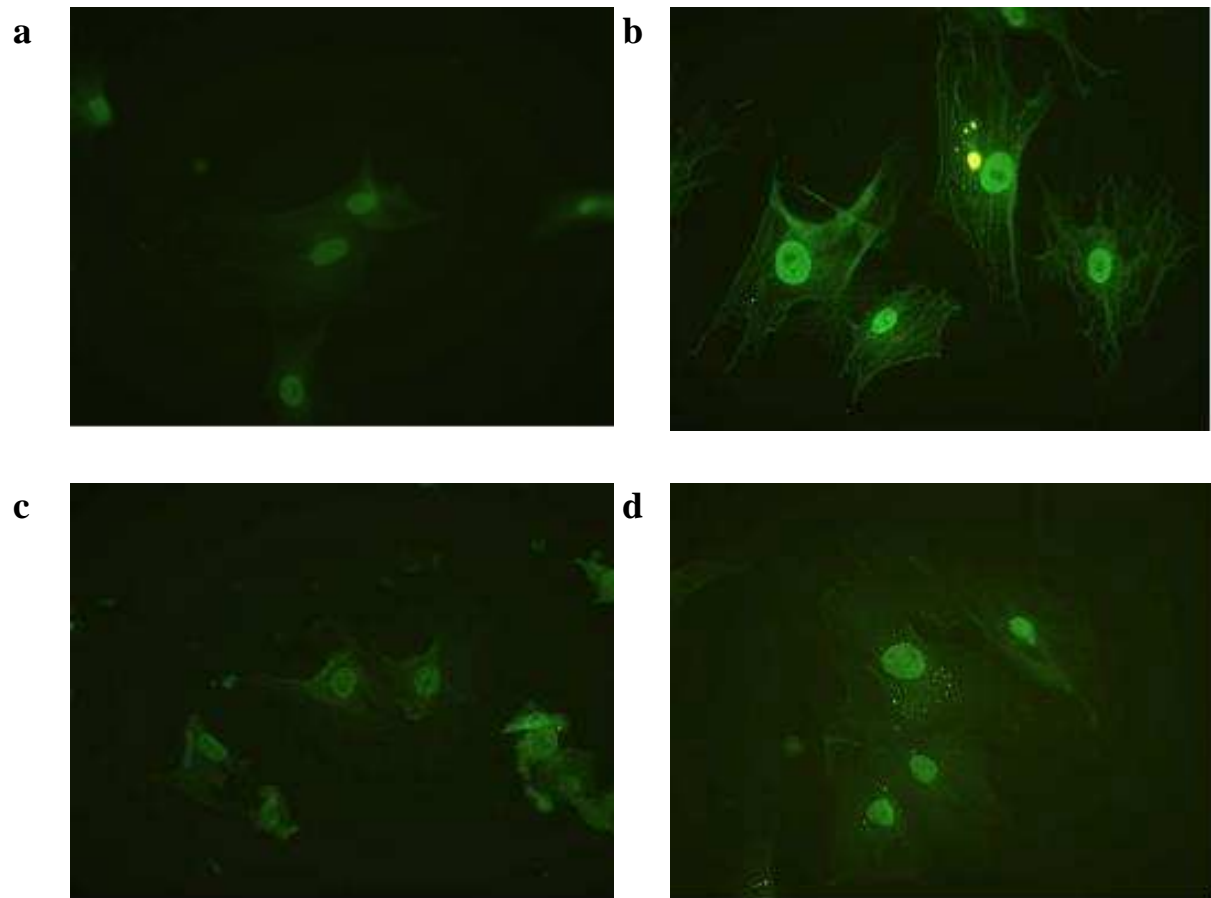
Figure 10: Fluorescein-phalloidin staining of rMSC after cultivation with different growth factors. a: no growth factor. b: bFGF. c: TGFβ. d.: PDGF. The strongest fluorescence with similar parameters could be detected for bFGF treatment, only a minor difference after TGFβ treatment can be suggested. For PDGF treated cells, a fluorescence almost only can be detected in the nuclei.

Conclusion

Within this study we could show the suitability of a recently developed model system consisting of PEG SAMs on a QCM sensor surface to determine the influence of growth factors on the adhesion of rat marrow stromal cells. Compared to non-treated cells, the adhesion of rMSCs was increased significantly after short-term treatment with bFGF. The frequency shift increased from 61±5 Hz to 72±4 Hz after cells were treated for 30 minutes in suspension. If cells were precultivated with bFGF for 24 hours, the frequency shift was 93 Hz and even 119 Hz after 5 days of precultivation, suggesting a complete coverage of the surface with rMSCs. In contrast to others, we could not confirm a cell adhesive capacity of bFGF without the integrin ligand GRGDS, since in the absence of GRGDS and the presence of surface bound bFGF the decrease in resonance frequency of only 19±11 Hz excludes any cell adhesion. For TGFβ similar trends could be observed. Short term treatment results in a slight increase in cell adhesion indicated by a further frequency shift of 4 Hz, cultivation for 24 hours with growth factor suggests a further increase of 11 Hz. These results substantiate the hypothesis found in literature, that the concentration of integrins on the cell surface is increased after treating cells with these growth factors.

For PDGF in contrast, rMSC adhesion was reduced by 12 Hz after cells were treated with PDGF for 30 minutes at a concentration of 0.3 ng/ml. Increasing the PDGF concentration to 0.5 ng/ml led to a further reduction of 6 Hz. At concentrations of more than 0.75 ng/ml no cell adhesion could be observed any more.

Staining the cells with an anti-integrin antibody confirms these results. For bFGF and TGFβ treated cells the fluorescence intensity slightly increased, whereas the PDGF group showed a strong concentration of integrins only in the nuclei and low amounts in peripheral regions.

Summarizing, we could evaluate the influence of three different growth factors on the adhesion of rMSCs and receive an impression of possible mechanisms of these processes using this rather simple and rapid QCM model system.

References

[1] Lilli, C., Marinucci, L., Stabellini, G., Belcastro, S., Becchetti, E., Balducci, C., Staffolani, N., and Locci, P. (2002). Biomembranes enriched with TGFbeta1 favor bone matrix protein expression by human osteoblasts in vitro. J Biomed Mater Res, 63, 577-582.

[2] Faucheux, C., Ulysse, F., Bareille, R., Reddi, A. H., and Amedee, J. (1997). Opposing actions of BMP3 and TGF beta 1 in human bone marrow stromal cell growth and differentiation. Biochem Biophys Res Commun, 241, 787-793.

[3] Qin X., Gysin R., Mohan S., and Baylink, D. J. (2001). Bone growth factors. In "Osteoporosis " (Marcus R., Feldman D., and Kelsey J., Eds.), Academic Press, San Diego CA.

[4] Zittermann S.I.; Issekutz A.C.: Basic fibroblast growth factor (bFGF, FGF-2) potentiates leukocyte recruitment to inflammation by enhancing endothelial adhesion molecule expression. Am J Pathol, 168, 3, 835-846, 2006.

[5] Presta M.; Dell´Era P.; Mitola S..; Moroni E.; Ronca R.; Rusnati M.: Fibroblast growth factor/fibroblast growth factor receptor system in angiogenesis. Cytokine Growth factor Rev, 16, 159-178, 2005.

[6] Comoglio, P.M.; Boccaccio C.; Trusolino L.: Interactions between growth factor receptors and adhesion molecules: breaking the rules. Curr Opin Cell Biol, 15, 565-571, 2003.

[7]Heldin C.H.; Oestman A.; Roennstrand L.: Signal transduction via platelet-derived growth factor receptors. Biochem Biophys Acta, 1387, F79-F113, 1998.

[8] Danen E.H.; Yamada K.M.: Fibronectin, integrins and growth control. J Cell Physiol, 189, 1-13, 2001, 342-347, 1997.

[9] Eliceiri B.P.: Integrin and growth factor receptor crosstalk. Circ Res, 89, 1104-1110, 2001.

[10] Schwartz M.A.; Ginsberg M.H.: Networks and crosstalk: integrin signalling spreads. Nature Cell Biol, 4, E65-E68, 2002.

[11] Stupack D.G.; Cheresh D.A.: Integrins and angiogenesis. Curr Top Dev Biol, 64, 207-238, 2004.

[12] Rusnati M.; Tanghetti E.; Dell´Era P.; Gualandris A.; Presta M.: $\alpha_v\beta_3$ integrin mediates the cell-adhesive capacity and biological activity of basic fibroblast growth factor (FGF-2) in cultured endothelial cells. Mol Biol Cell, 8, 2449-2461, 1997.

[13] Smyth S.S.; Patterson C.: Tiny dancers: the integrin-growth factor nexus in angiogenic signaling. J Cell Biol, 158, 1, 17-21, 2002.

[14] Walker J.L.; Fournier A.K.; Assoian R.K.: Regulation of growth factor signaling and cell cycle progression by cell adhesion and adhesion dependent changes in cellular tension. Cytokine Growth Factor Rev, 16, 395-405, 2005.

[15] Yamada K.M.; Even-Ram S.: Integrin regulation of growth factor receptors. Nature Cell Biol, 4, E75-E76, 2002.

[16] Renshaw M.W.; Ren X.D.; Schwartz M.A.: Growth factor activation of MAP kinase requires cell adhesion. EMBO, 16, 18, 5592, 5599, 1997.

[17] Enenstein J.; Waleh N.S.; Kramer R.H.: Basic FGF and TGF-β differentially modulate integrin expression of human microvascular endothelial cells. Exp Cell Res, 2003(2), 499-503, 1992.

[18] Jang J.H.; Ku Y.; Chung C.P.; Heo S.J.: Enhanced fibronectin-mediated cell adhesion of human osteoblast by fibroblast growth factor, FGF-2. Biotechnol Letters, 24, 1659-1663, 2002.

[19] Weston C.A.; Weeks B.S.: bFGF stimulates U937 cell adhesion to fibronectin and secretion of gelatinase B. Biochem Biophys Res Comm, 228, 3118-323, 1996.

[20] Ludbrook, S.B.; Barry S.T.; Delves C.J.; Horgan C.M.: The integrin $\alpha_v\beta_3$ is a receptor for the latency associated peptides of transforming growth factors β_2 and β_3. Biochem J, 369, 311-318, 2003.

[21] Fujio Y.; Yamada F.; Takahashi K.; Shibata N.: Altered fibronectin-dependent cell adhesion by PDGF accompanies phenotypic modulation of vascular smooth muscle cells. Biochem Biophys Res Comm, 196, 2, 997-1002, 1993.

[22] Woodard A.S.; Garcia-Cardena G.; Leong M.; Madr J.A.; Sessa W.C.; Languino L.R.: The synergistic activity of $\alpha_v\beta_3$ integrin and PDGF receptor increases cell migration. J Cell Sci, 111, 469-478, 1998.

[23] Knerr R.; Weiser B.; Drotleff S.; Steinem C.; Goepferich A.: Measuring cell adhesion on RGD-modified self-assembled PEG monolayers using the quartz crystal microbalance technique. Macromolecular Bioscience, 9, 827-838 (2006).

[24] Kassem M.: Mesenchymal stem cells: Biological characteristics and potential clinical applications. Clon Stem Cells, 6, 4, 369-374.

[25] Kastl K.; Ross M.; Gerke V.; Steinem C.: Kinetics and thermodynamics of Annexin A1 binding to solid supported membranes: A QCM study. Biochemistry, 41,10087-10094, 2002.

[26] Knerr R.; Weiser B.; Drotleff S.; Steinem C.; Goepferich A.: Self-assembling PEG Derivatives for Protein-repellant Biomimetic Model Surfaces on Gold. Biomaterialien, 7 (1), 12-20, 2006.

[27] Ishaug S.L.; Crane G.M.; Miller M.J.; Yasko A.W.; Yaszemski M.J.; Mikos A.G.: Bone formation by three-dimensional stromal osteoblast culture in biodegradable polymer scaffolds. J Biomed Mater Res, 36, 17, 1997.

[28] Roberts M.; Barry S.; Woods A.; van der Sluijs P.; Norman J.: PDGF-regulated rab-4-dependent recycling of $\alpha_v\beta_3$ integrin from early endosomes is necessary for cell adhesion and spreading. Curr Biology, 11, 1392-1402, 2001.

[29] Janshoff A.; Galla H.J.; Steinem C.: Piezoelectric mass-sensing devices as biosensors – an alternative to optical biosensors? Angewandte Chemie, Int Ed, 39, 4004-4032, 2000.

[30] Zhou X.; Deng Y.; Xie L.: Study on the mechanism of bFGF promoting endothelial cells to adhere to polyurethane material. Shengwu Yixue Gongchengxue Zazhi, 19(3), 2002 (abstract).

[31] Scaffidi A.K.; Petrovic N.; Moodley Y.P.; Fogel-Petrovic M.; Kroeger K.M.; Seeber R.M.; Eidne K.A.; Thompson P.J.; Knight D.A.: $\alpha_v\beta_3$ integrin interacts with the transforming growth factor β (TGFβ) type II receptor to potentiate the proliferative effects of TGFβ$_1$ in living human lung fibroblasts. J Biol Chem, 279, 36, 37726-37733, 2004.

[32] Ignotz R.A.; Heino J.; Massague J.: Regulation of cell adhesion receptors by transforming growth factor-β. J Biol Chem, 264(1), 389-392, 1989.

[33] Janat M.F.; Argraves W.S.; Liau G.: Regulation of vascular smooth muscle cell integrin expression by transforming growth factor β1 and by platelet-derived growth factor-BB. J Cell Physiol, 151, 588, 595, 1992.

[34] Baron W.; Shattil S.J.; French-Constant C.: The oligodendrocyte precursor mitogen PDGF stimulates proliferation by activation of $\alpha_v\beta_3$ integrins. EMBO, 21, 8, 1957-1966, 2002.

[35] Burridge K.; Chrzanowska-Wodnicka M.; Zhong C.: Focal adhesion assembly. Trends Cell Biol, 7, 1997.

[36] Woods A.J.; White D.P.; Caswell P.T.; Norman J.C.: PKD1/PKCμ promotes $\alpha_v\beta_3$ integrin recycling and delivery to nascent focal adhesion. EMBO, 23, 2531-2543, 2004.

[37] Kingsley K.; Plopper G.E.: Platelet-derived growth factor modulates rat vascular smooth muscle cell responses on laminin-5 via mitogen-activated protein kinase-sensitive pathways. Cell Comm Signaling, 3, 2, 2005.

[38] Kingsley K.; Rust W.L.; Huff J.L.; Smith R.C.; Plopper G.E.: PDGF-BB enhances expression of, and reduces adhesion to laminin-5 in vascular smooth muscle cells. Biochem Biophys Res Comm, 294, 1017-1022, 2002.

[39] Berrou E.; Bryckaert M.: Platelet-derived growth factor inhibits smooth muscle cell adhesion to fibronectin by ERK-dependent and ERK-independent pathways. J Biolog Chem, 276, 42, 393003-39309, 2001.

[40] Carragher N.O.; Frame M.C.: Focal adhesion and actin dynamics: a place where kinases and proteases meet to promote invasion. Trends Cell Biol, 14, 241-249, 2004.

Chapter 7

Protein Adsorption and Cell Adhesion

on PEG-PLA Films

R. Knerr[1], B. Weiser[1], S.Drotleff[1], C. Steinem[2], J.Tessmar[1], A. Göpferich[1]

[1] Department of Pharmaceutical Technology, University of Regensburg, Universitaetsstrasse 31, 93040 Regensburg, Germany

[2] Institute of Analytical Chemistry, Chemo- and Biosensors, University of Regensburg, 93040 Regensburg, Germany

To be submitted

Abstract

In this study, the impact of end group modifications of high molecular weight diblock-copolymer films consisting of poly(ethylene glycol) (PEG) and poly(lactic acid) (PLA) on protein adsorption and cell adhesion characteristics was determined. Contact angle measurements of polymer films with different molecular weight compositions of PEG and PLA showed a decrease in wettability, if amine terminated PEG-PLA films are modified with tartaric acid and the multiple charged peptide GRGDS. Zeta potential measurements indicated a negative charge for tartaric acid modified PEG-PLA nanoparticles (-27mV – 12mV, depending on the molecular weight composition), whereas amine end groups led to almost neutral surfaces (-5mV – -2mV). Protein adsorption experiments using the quartz crystal microbalance technique (QCM) revealed that amine terminated PEG-PLAs with a PEG content of 5% adsorb significantly more serum proteins (frequency shifts of -60 Hz) than tartaric acid and GRGDS terminated PEG-PLAs (-30 Hz). If the PEG content was increased to 10%, no influence of the end group could be determined any more, the frequency shifts were approximately -30 Hz in all cases. In terms of rat marrow stromal cell adhesion on the polymer films, no increase could be detected after attaching the cell adhesion motif GRGDS for films with a PEG content of 5%. However, if the PEG content was increased to 10%, a significant increase in cell adhesion under serum free conditions as well as in the presence of serum could be determined if GRGDS peptides were attached to the surfaces.

Introduction

Poly(lactic acid) (PLA) and poly(lactic-*co*-glycolic acid) (PLGA) probably are among the most frequently used biodegradable polymers used in *tissue engineering*.[1] Since these poly(α-hydroxy acid)s are biocompatible and can be processed to implants with reasonable mechanical stability and porosity, they are very well suited for the manufacture of cell carriers.[2,3]

In numerous studies the applicability of PLA and PLGA as cell carrier materials was proven[2,6-8], nevertheless different groups tried to further improve the material for this application.[9-11] The major goal was to overcome the inadequate interactions of cells with PLA in terms of the specificity for the adhesion of certain cell types. To achieve specific interactions, first of all any non-specific reactions have to be suppressed as far as possible, such as protein adsorption. The most common strategy for the realization of this concept is to attach poly(ethylene glycol) (PEG) to the PLA chains, since it was shown that copolymers derived from PEG and PLA allow for suppressing or at least controlling non-specific protein adsorption due to the steric repulsion effect.[12] A further advantage of the PEG moiety is that the PEG chains assemble on the surface[4] and, therefore, allow for tethering bioactive compounds to the surface via functional end groups. This way, specific interactions of cells and biomaterials become possible.[1,13,14] Several successful approaches along these lines with different compounds were performed, such as the induction of specific cell adhesion by attaching cell adhesion motifs or increasing the proliferation rate by tethering growth factors.[2]

However, a non-specific adsorption of proteins can not even be suppressed by PEG-PLA surfaces so far and the adsorbed proteins still can lead to non-specific side effects. Lieb et al. for example showed for poly(D,L-lactic acid)-*block*-poly(ethylene glycol)-monomethyl ether that the adsorption of fibrinogen could be significantly reduced, but not completely suppressed.[13] Moreover, the introduction of functional groups, which is necessary for the aforementioned attachment of bioactive molecules, also could influence the adsorption characteristics. *In vitro*, this introduction seems to be of minor importance, but under physiological conditions, these groups might be protonated or dissociated, leading to an increase of the surface zeta potential. These charges can then lead to changes in protein adsorption even on PEG-PLA surfaces. Unfortunately, in the literature so far no data are

given, to which extent the end groups of such high molecular weight polymers have an influence on the protein adsorption characteristics.

Since for other PEG rich surfaces it is well known that the end group of the PEG moiety does influence the pattern of adsorbed proteins[19], we intended to investigate this phenomenon for PEG-PLA copolymers with different molecular weight compositions of PEG and PLA in more detail. Therefore we synthesized PEG-PLA copolymers with end groups that were positively (amine) or negatively (tartaric acid) charged under physiological conditions and determined the amount of adsorbed proteins by means of the quartz crystal microbalance technique (QCM) on different PEG-PLA films. For an estimation of the surface zeta potential of these polymer films we furthermore produced PEG-PLA nanoparticles and determined their surface zeta potential. To assess, whether the number of introduced charges or only the net charge has an impact on protein adsorption we also synthesized multiple (2 negative, 1 positive) charged polymers by attaching the pentapeptide GRGDS. This peptide might be especially interesting, since it contains an RGD sequence, which is well known to induce the adhesion of cells due to interactions with certain integrin receptors of cells.[17] Additionally, we tested the adhesion of rat morrow stromal cells (rMSCs) on these different PEG-PLA derivatives to investigate whether different protein adsorption patterns lead to different cell adhesion characteristics.

Materials and Methods

Materials

Acetone, dioxane, diethyl ether, L-tartaric acid, tetrahydrofurane, toluene, Triton X-100 and succinic acid were acquired form Merck KgaA (Darmstadt, Germany). THF was dried over molecular sieves (4 Å, Carl Roth GmbH, Karlsruhe, Germany) prior to use. D,L-lactide, N-(3-Dimethyl-aminopropyl)-N'-ethylcarbodiimide (EDC), N-Hydroxysulfo-succinimide sodium salt (sulfo-NHS), stannous 2-ethylhexanoate and ascorbic acid were from Sigma Aldrich Chemie GmbH (Taufkirchen, Germany). PLA (Resomer R 194[®]) was purchased from Boehringer Ingelheim (Ingelheim, Germany). The GRGDS pentapeptide was acquired form Bachem Biochemica (Heidelberg, Germany), fluorescein phalloidin, penicillin/streptomycin solution (PenStrep), and phosphate buffered saline (PBS) from Invitrogen GmbH (Karlsruhe, Germany). Fetal bovine serum (FBS), Dulbecco´s modified eagle medium (DMEM) and trypsin were acquired from Biochrom AG (Berlin, Germany). All reagents were of analytical grade and used as received without further purification unless otherwise indicated.

PEG-PLA diblock copolymer synthesis

α-Hydroxy-ω-amino-poly(oxy-1-oxopropane-2,1-diylblock-oxyethylene) derivatives with different molecular weights were synthesized as published previously.[18] In brief: Poly(D,L-lactic acid) was attached to poly(ethylene glycol)-mono amine by a ring-opening polymerization using stannous 2-ethylhexanoate as catalyst. Therefore, dry solutions of both polymers in toluene were mixed in a nitrogen atmosphere. For PEG_2-PLA_{20} for example, 2g of NH_2-PEG (1mmol) were dissolved in toluene. This solution was mixed with 20g of D,L-dilactide (140 mmol) in 150 ml of toluene. Then 100 mg of the catalyst were added and the solution refluxed for 8 hours. To protect the amine group of the PEG derivative, 500 µl of glacial acid were added to transform the amine into non-reactive ammonium or trimethylsilyl groups from its own synthesis were left in place. Then toluene was removed by rotary evaporation. For purification, the copolymers were dissolved in 100 ml acetone and precipitated at 4°C in three beakers of 600 ml double-distilled water each. For other molecular weight compositions the similar scheme was applied with modified amounts of PEG and PLA.

To obtain amine reactive polymers, bifunctional carboxylic acids were attached to the amine group. Therefore, 40g of N,N´-dicylohexylcarbodiimide (194 mmol) in 150 ml of a

dioxane / ethyl acetate (4:1) mixture were added to 12 g of tartaric acid (80 mmol) and 20.14 g of N-hydroxysuccinimide (175 mmol) dissolved in 500 ml of the same solvent mixture at 0°C and stirred for 18 hours. The crude precipitated product was filtrated and washed three times with 100 ml of dioxane. The product then was extracted three times with 500 ml of acetonitrile. After rotary evaporating the acetonitrile, the resulting product was obtained as a white solid.

Subsequently, the purified product was attached to NH$_2$-PEG-PLAs by refluxing for 2 hours in acetonitrile and then stirring for 15 hours. In a typical reaction 10 g of NH$_2$-PEG$_2$-PLA$_{20}$ were dissolved with 1.0 g of the activated tartaric acid in 150 ml of acetonitrile with traces of triethylamine. After removing the solvent by rotary evaporation, the modified polymer then was purified by dissolving the precipitate in 200 ml acetone, subsequently precipitated in 600 ml of double-distilled water at 4°C and stored under vacuum until further use.

For experiments, where non-activated tartaric acid-PEG-PLAs were necessary, the active groups were hydrolyzed to the free acid by incubation of the respective polymer film in PBS over night.

The x and y in PEG$_x$-PLA$_y$ represent the molecular weight of the PEG and PLA block, respectively, in kilodaltons.
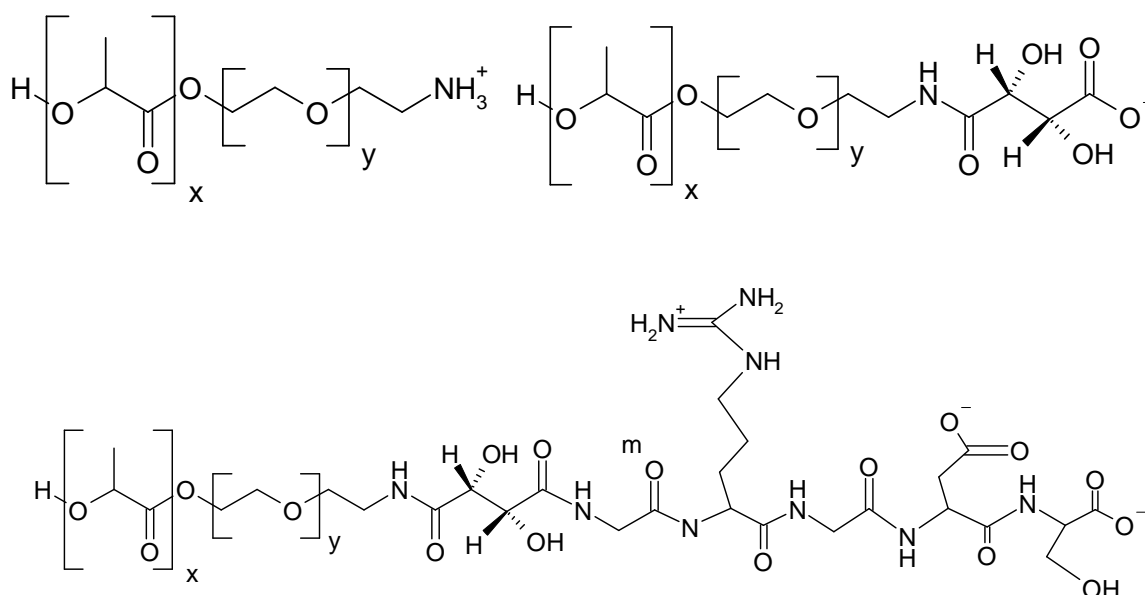

Figure 1: Structures of NH2PEGx-PLAy (upper left), tartaric acid-PEGx-PLAy (upper right) and GRGDS-PEGx-PLAy (x=1 or 2 kDa, y=20 or 40 kDa). Under physiological conditions (pH 7.4) NH$_2$PEG$_x$PLA$_y$ is positively charged, tartaric acid-PEGx-PLAy negatively charged and GRGDS-PEGx-PLAy bears one positive and two negative charges.

Spin casting

For film casting, 100µl of a solution of 10 mg of a corresponding PEG-PLA derivative in 1 ml of acetone were dropped on top of quartz discs with gold electrodes (for further details of discs see QCM setup) that were rotating with a speed of 1900 rpm. The films were then dried under vacuum for several hours.

To attach the multiple charged cell adhesion peptide GRGDS, the tartaric acid-terminated PEG-PLA derivatives were activated once more by incubation for two hours in a solution of 1 mg EDC and 1 mg sulfo-NHS per ml PBS to ensure, that despite longer storage times the acids were still activated. Afterwards, the surfaces were rinsed with double distilled water and incubated over night with solutions of GRGDS in PBS (1 mg/ml).

For protein adsorption and cell adhesion experiments, also the amine- and tartaric acid-terminated PEG-PLAs were incubated in PBS over night to ensure that differences in protein adsorption and cell adhesion are not due to the incubation over night.
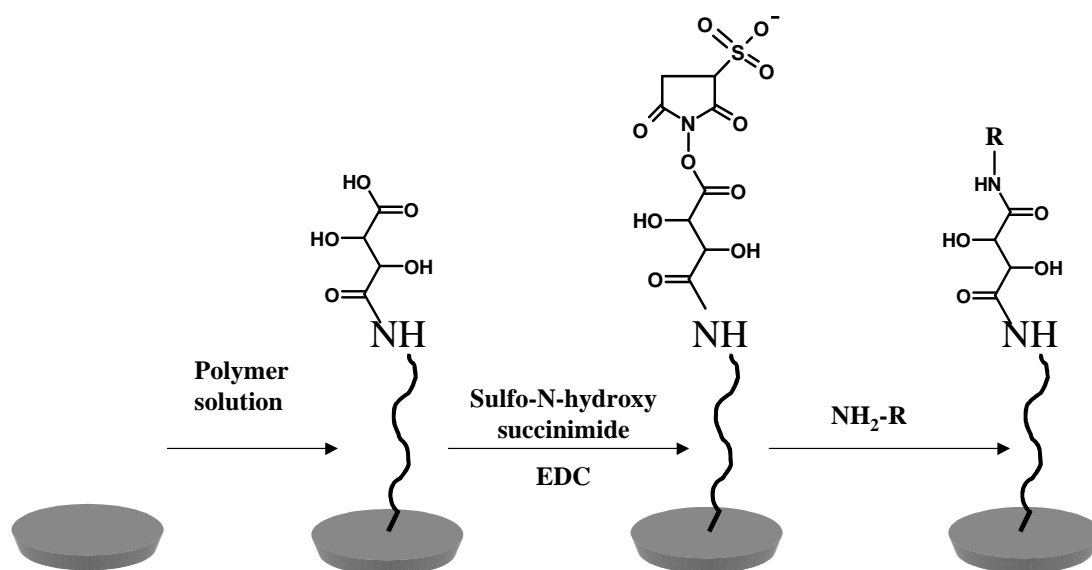
Figure 2: Modification scheme for binding GRGDS to PEG-PLA films. To ensure the activation of the tartaric acid modified polymers, the corresponding films were once more activated with s-NHS and EDC.

Zeta potential measurements

Nanoparticles of different PEG-PLAs were produced by slowly dropping solutions of 100 mg of the respective polymer in 10 ml of acetone into 100 ml of PBS in a beaker of 250 ml volume. After stirring over night, the effective hydrodynamic diameter, polydispersity indices and the zeta potential were determined by using a Malvern ZetaSizer (Model 3000 HSA, Malvern Instruments GmbH, Germany). Laser light scattering analyses were performed at 25°C with an incident laser beam of 633 nm at a scattering angle of 90°. The zeta potential of the nanoparticle dispersion was determined by the electrophoretic mobility. Experiments were performed as triplicates and the result expressed as the mean ± standard deviation.

Atomic force microcopy (AFM)

Surface images were obtained with a JPK NanoWizard scanning force microscope (JPK instruments, Berlin, Germany). Measurements were performed in double distilled water, images were obtained in intermitted-contact mode by using silicon tips (NSC 12/50, Ultrasharp, Silicon-MDT Ltd., Moscow, Russia). Scan rates were set to 0.3 Hz.

Water contact angle measurements (WCA)

The static water contact angle was determined with an OCA 15plus system (Dataphysics Instruments GmbH). Drops of 1µl of double distilled water were set on the different surfaces for the determination of the WCA. Measurements were performed immediately after drop deposition and 1 and 5 minutes afterwards. Measurements were collected (n = 3) and expressed as the mean ± standard deviation (SD).

Quartz Crystal Microbalance (QCM)

A detailed description of the quartz crystal microbalance (QCM) setup is already given elsewhere.[19] In brief: AT-cut quartz plates with a 5 MHz fundamental resonance frequency were coated with gold electrodes. The setup was equipped with an inlet and outlet, which connects the fluid chamber to a peristaltic pump (pump rate: 0.10 ml/min, Ismatec Reglo Digital), allowing for the addition of protein solutions and cell suspensions from outside the Teflon chamber. The frequency shift of the quartz resonator was recorded using a frequency counter (HP 53181A) connected via RS 232 to a personal computer. The oscillator circuit was supplied with a voltage of 4 V by a DC power supply (HP E3630A).
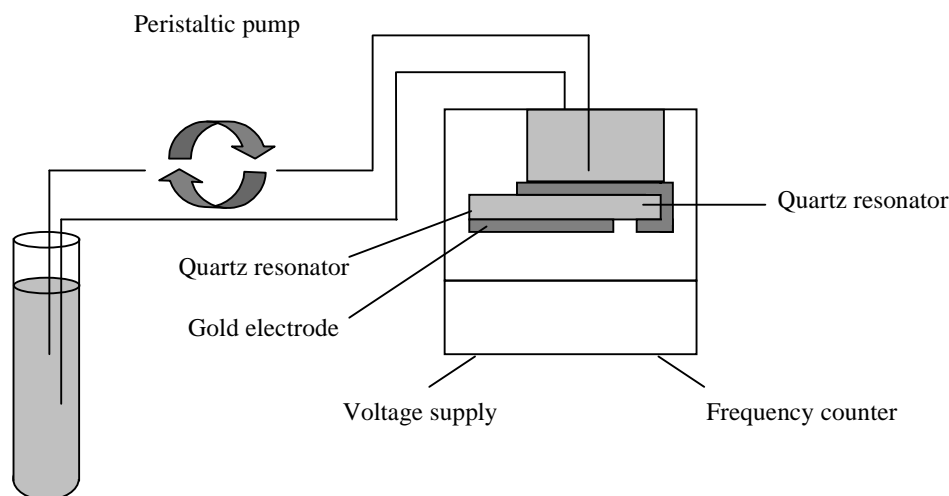
Fig 3: QCM flow through setup. Protein solutions or cell suspension can be pumped continuously over the sensor surface. A decrease in resonance frequency indicates the deposition of mass on the surface.

Before measuring the adsorption of proteins or the adhesion of cells on the polymer surfaces, the quartz crystals were cleaned for 5 minutes in a hot piranha solution (sulfuric acid / aqueous hydrogen peroxide (30%), ratio 3:1) at 70°C. Afterwards, the surfaces were rinsed extensively with double-distilled water, dried in a stream of nitrogen and then polymer films were spin casted as described above. Medium was prepared as described in the cell culture section. After the resonance frequency of the system was constant, 1 ml of medium with or without 250.000 rMSCs was added and the frequency shift recorded for at least one hour. All measurements are triplicates and expressed as the mean ± standard deviation. If no standard deviation is given, measurements are single experiments.

Cell Culture

Rat marrow stromal cells (rMSCs) were obtained from 6-week-old Sprague Dawley rats according to a procedure published by Ishaug et al.[20] and were cultivated under standard culture conditions (37°C, 95% relative humidity, 5% CO_2 in DMEM with 10 vol.-% fetal bovine serum, 1vol.-% penicillin/streptomycin, and 50 µg/ml ascorbic acid). For QCM experiments, cells were trypsinized, centrifuged at 1200 rpm for 5 minutes, and the resulting cell pellet re-suspended in medium or PBS at 250,000 cells/ml.

Staining of the cytoskeleton was performed with a fluorescein-labelled phalloidin derivative. In this procedure, the surfaces were rinsed with PBS and cells were fixed with 3.8 vol.-% formaldehyde for 10 minutes at room temperature. After rinsing with PBS, the surfaces were extracted with 0.1% Triton X in PBS for 5 minutes and rinsed again with PBS. Then the cells were stained with 5µl of the methanolic dye solution in 500µl of PBS containing 1 wt.-% BSA for 20 minutes. After rinsing with PBS, images were taken with a Axiovert 200M microscope coupled to scanning device LSM 510 (Zeiss, Jena, Germany) at 100-fold magnification (Ex = 469nm, Em = 516nm).

Statistical testing

Unless otherwise indicated, measurements were expressed as the mean (n=3) ± standard deviation (SD). Single factor analysis of variance (ANOVA) was used in conjunction with a multiple comparison test (Tukey test) to assess the statistical significance.

Results and Discussion

Atomic force microscopy

One major drawback of the quartz crystal microbalance is that in a liquid environment the generated propagating wave can only penetrate approximately 250 nm deep into the liquid.[21] This in consequence means that any mass deposition on the sensor surface is "invisible" for the QCM beyond these 250 nm. Moreover, if polymer films are spin casted on the quartz, they can not be considered as a completely rigid mass due to their swelling properties, leading to viscolelastic losses of the oscillation. This in consequence shortens the decay length of the propagating wave to values even less than 250 nm. Hence, to ensure the investigation of protein adsorption or cell adhesion on polymer films with the QCM is still possible, the thickness of the films should be as small as possible and should not exceed the range of only several hundred nanometers. Additionally, the surface roughness should be low enough to guarantee reproducible results in terms of mass deposition.

Concerning the roughness, we investigated the surface of the spin casted PEG_2-PLA_{20} surfaces using atomic force microscopy (AFM). In Figure 4a and 4c the topography data can be seen in 2D or 3D, respectively. Images are displayed as gold-scale representations, with the lowest points as dark pixels and highest points as bright pixels. These data suggest that the film is very smooth, since the height differences are below 40 nm, which is shown in a typical cross section in Figure 4d. The histogram representing the height distribution is narrow and has a root mean square value (rms) of only 15.14 nm (Figure 4e). The black spots in Figure 4a and b represent "pores" that are distributed all over the surface. They probably stem from the spin casting procedure and the subsequent drying of the film, allowing acetone to evaporate. The maximum depth of these pores is 40 nm. Also in other studies characterizing PLA derivative surfaces these pores can be seen, but their existence has not been further investigated.[22]

In the phase image of this film (Figure 4b), the material properties on the surface can be visualized due to possible different viscoelastic properties of different areas, causing a phase shift of the resonance frequency of the tip compared to the frequency of the driving force. As can be seen in Figure 4b, the surface is more or less void of any frequency shifts, indicating that no separate PEG areas seem to exist within the PLA surface. The only

exception again are the "pores". Hence, these features do not only have a different height, but also different material properties.

These results suggest that in terms of the surface roughness of the characterized PEG_2-PLA_{20} film, mass deposition can be detected by the QCM technique, since all areas of the surface are well below the critical threshold of 250 nm, where in any case masses can be detected. Concerning the overall thickness of the polymer film, no further investigations were made, since impedance measurements also showed that the film thickness was low enough to ensure that the polymer film does not dampen the oscillation of the quartz disc too much (data not shown).

Summarizing, the AFM topography and phase data suggest that the generated films are suitable for further investigations in terms of protein adsorption and cell adhesion on PEG-PLA derivatives using the QCM technique.

Zeta potential measurements

To estimate the zeta potential of PEG-PLA surfaces, we prepared nanoparticles of the same PEG-PLA derivatives, since their surface zeta potential can easily be measured by determining their electrophoretic mobility. Although these results can not be directly used as a measure for the zeta potential of PEG-PLA films, the results using nanoparticles give at least an estimate of the surface changes to be expected.

In Figure 5 the size results of different PEG-PLA derivatives are plotted. The size of NH_2-PEG_2-PLA_{20} particles seems to be slightly smaller than NH_2-PEG_2-PLA_{40} particles. Polydispersity indices of both experiments are in the range of 0.25±0.01.

As can be seen, for the tartaric acid modified PEG-PLAs, the results of both polymers with 5% of PEG (PEG_1-PLA_{20} and PEG_2-PLA_{40}) have a size of approximately 225 nm and a comparable polydispersity index of 0.25±0.01. Particles of PEG_2-PLA_{20} and a PEG content of 10%, seem to be slightly smaller with a mean of 185±5 nm. For both polymers, where also the amine derivative was available, obviously the size of the amine derivative particles is lower than the tartaric acid derivative.
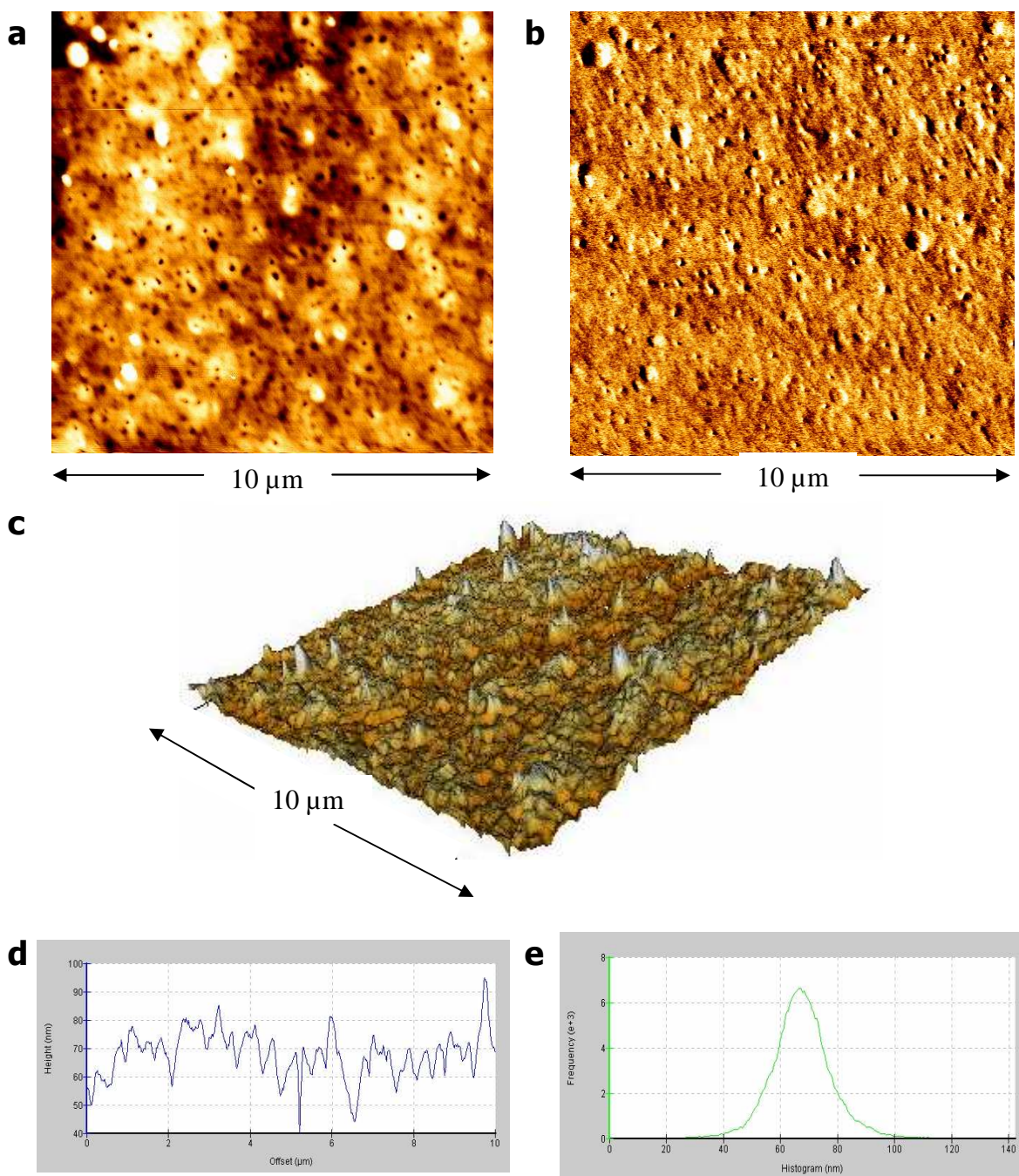
Figure 4: AFM data confirm that a homogeneous polymer film was spin casted. a: 2D topography data of an NH_2-PEG_2-PLA_{20} film, dark pixels indicate low points, bright pixels higher points. b: The 2D phase image shows an almost featureless surface, indicating uniform material properties. c: 3D topography data confirm a reasonable low surface roughness. d: Representative cross section of the polymer film. e: A narrow histogram distribution once more proves the low surface roughness, the rms value is 15.14 nm.
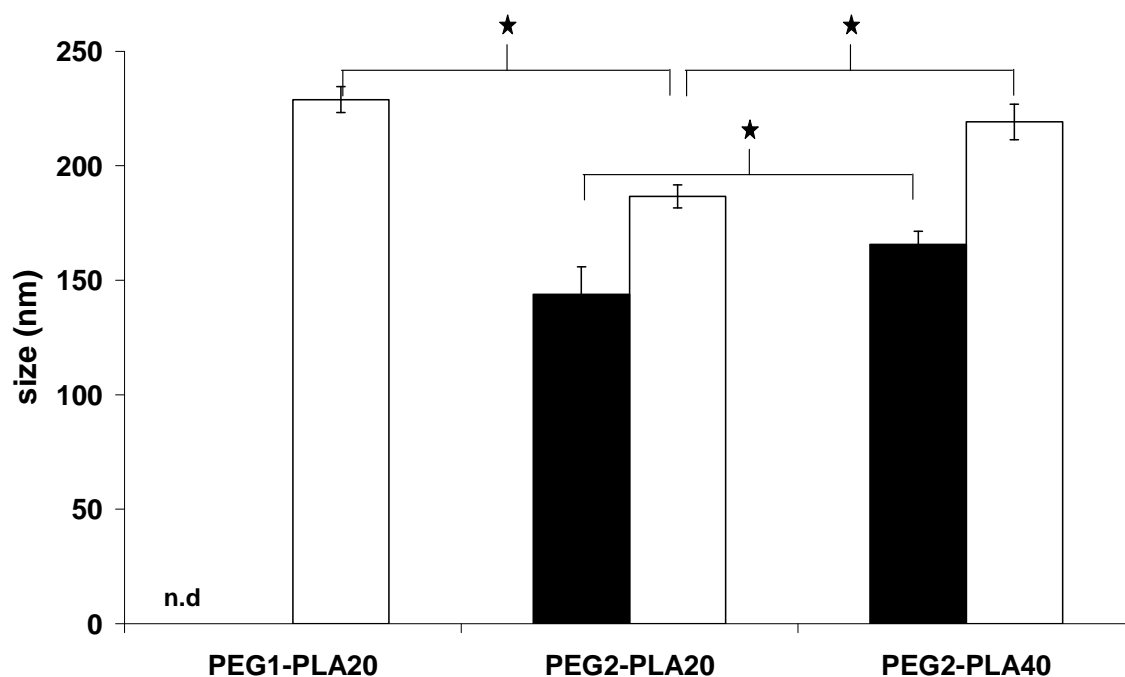
Figure 5: Sizes of different PEG-PLA nanoparticles. Amine-terminated PEG-PLAs (■) seem to be smaller than tartaric acid modified PEG-PLAs (□).

In Figure 6 the results of the zeta potential measurements are plotted. Both results for the amine terminated derivatives are close to neutral surfaces. Since is well known for methoxy terminated PEG-PLA surfaces that their zeta potential is strongly negative[36], an influence of the amine end group is obvious. Due to its pK_avalue, under the buffered conditions at a pH of 7.4, the amine group to a high extent should be protonated, resulting in a positive charge. This in consequence almost leads to a neutralization of the negative charges that stem from carboxylate groups of lactic acid.

If the amine PEG-PLAs are modified with tartaric acid, the zeta potential significantly decreases. This suggests that the amine group of the PEG moiety can not be protonated any more due to the amide formation with tartaric acid, leading to a strong negative charge again. However, due to the high standard deviations, differences between 5 and 10% PEG in the PEG-PLAs are statistically not significant.
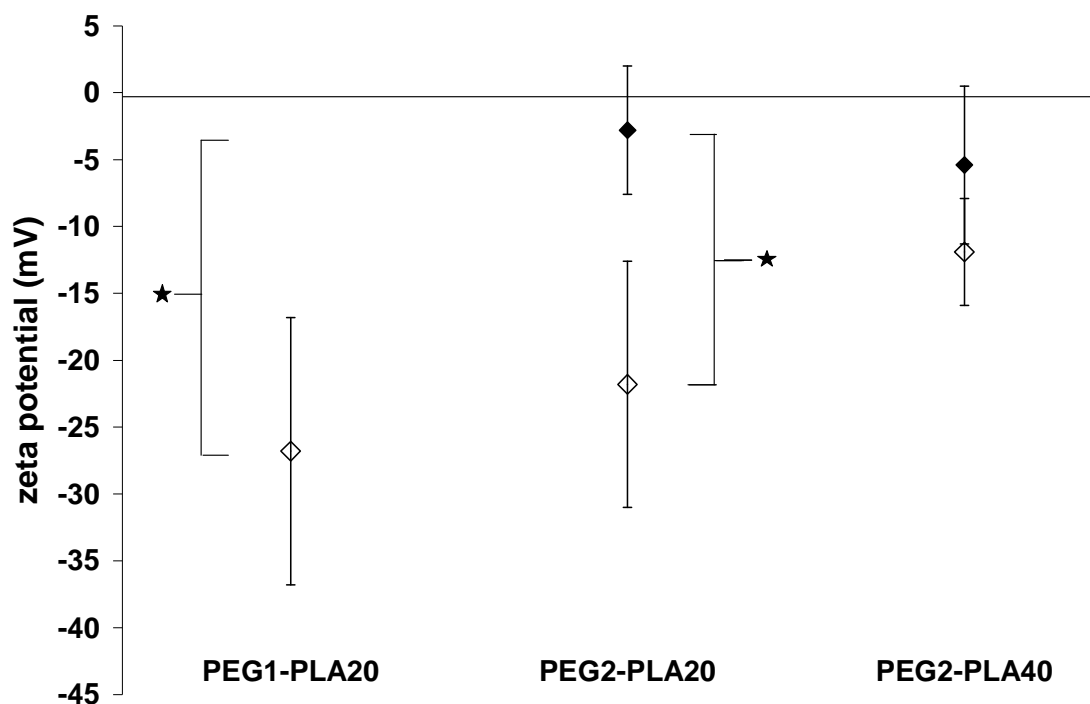
Figure 6: Nanoparticles of amine-terminated PEG-PLAs (◆) show a very low zeta potential. Tartaric acid modified particles (◇) in contrast are obviously negatively charged.

Summarizing the results of size and zeta potential measurements, an almost neutral surface can be expected for PEG-PLA surfaces, whereas tartaric acid modified surfaces are negatively charged. For GRGDS terminated PEG-PLAs, which will be discussed later on, also a negative net charge due to the introduction of one positive, but also two negative charges, can be expected.

Contact angle measurements

Monoamine-PEG-PLAs.

An important aspect in terms of protein adsorption and cell adhesion on polymer surfaces is their wettability. Since the hydrophilicity or hydrophobicity, respectively, determines the type of proteins adhering to a surface, also the subsequent adhesion of cells will be affected.[34] Therefore, we first of all tested the wettability characteristics of the different polymer films.

As expected, the water contact angles (WCA) were quite high if measured immediately after the deposition of a water drop (1 µl) on the polymer surfaces. The values in the range of 67 – 72° for monoamine derivatives of PEG_2-PLA_{20} and PEG_2-PLA_{40} indicate that the surface characteristics are determined mainly by the PLA chains of the polymers (Figure 7). Since for densely packed PEG brushes water contact angles in the range of 30° are given in the literature, a homogeneous PEG corona of the copolymers can more or less be excluded.[24] Previous studies with monomethyl ether derivatives of different PEG-PLAs also showed that no significant influence of the PEG moieties can be seen when determining the water contact angle after one minute.[13] On the other hand, after 5 minutes the contact angle decreased to values of 28-44° for these monomethyl ether derivatives, indicating that the PEG moieties seem to rearrange on the interface between the polymer films and the aqueous phase and hence determine the surface characteristics.

When the water contact angles of the monoamine derivatives were determined one minute after drop deposition, the contact angle already dropped by several degrees. This decrease is even more obvious after 5 minutes, indicating that the surface properties are again dominated by the PEG moieties due to a reorganization of the polymer chains, exposing hydrophilic PEG chains to the aqueous phase. Additionally, also the uptake of water into the PLA bulk material might contribute to this decrease of the contact angle, since also for PLA without any PEG chains attached, the contact angle decreases from 75±1° to 60±0° (data not shown). However, this overall decrease of 15° is lower compared to the decrease of more than 20° for the three different PEG_2-PLA_{20} derivatives for example. Thus, PEG additionally contributes to the increase in wettability of the PLA bulk. This in consequence means that the polymer films have to be allowed to equilibrate in an aqueous environment before protein adsorption or cell adhesion experiments, as otherwise PEG can not reduce or exclude adsorption phenomena since it is not available on the surface as a densely packed brush.

Tartaric acid and GRGDS modified PEG-PLAs.

In further experiments we also investigated the influence of the modifications of the polymer end groups. In Figure 7 also the results for tartaric acid and GRGDS modified polymers can be seen. Obviously, the modification with tartaric acid leads to an increase in the contact angle for PEG_2-PLA_{20} and PEG_2-PLA_{40}. Moreover, the modification with the cell adhesion pentapeptide GRGDS leads to a further increase to values of $72 - 74°$ immediately after drop deposition, despite the additional charges that are introduced. The extent of this increase is even stronger, when the contact angle is determined after equilibration. For the tartaric acid modified PEG_2-PLA_{20} polymer for example, the increase due to tartaric acid is 3° at 0 minutes of equilibration and 7° after 1 and 5 minutes. For the GRGDS modified polymer the additional increase is 3° after 0 minutes, but 4 and 8 degrees after 1 and 5 minutes. This indicates that the influence of the PEG moieties on the surface characteristics could be stronger, since PEG is allowed to assemble directly on the interface between solid and liquid phase.

In summary, these results suggest that minor changes of the end groups of the copolymers can affect the surface properties significantly, although these modifications might appear negligible thinking of the molecular weight of the introduced compounds compared to the molecular weight of the whole molecules. As these changes of the wettability characteristics may also have an impact on protein adsorption characteristics, the different polymer derivatives were characterized in terms of serum protein adsorption by means of the QCM technique.
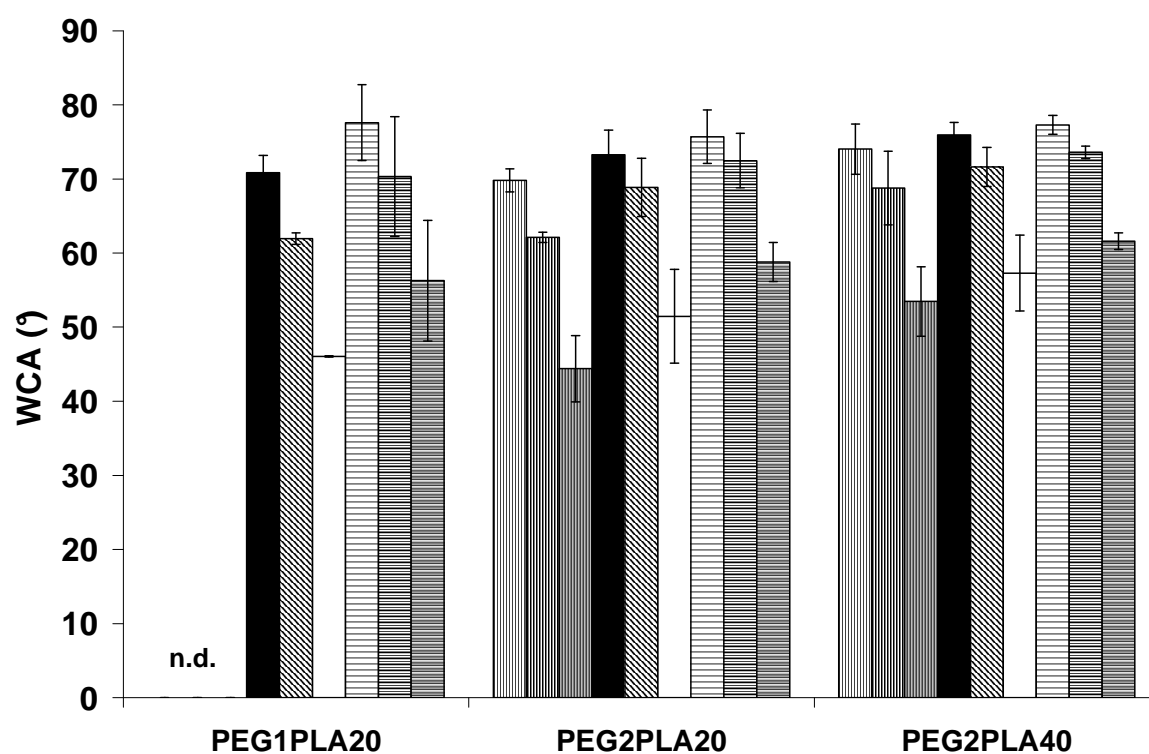
Figure 7: Contact angles of PEG-PLA films with amine (striped), tartaric acid (gray scale) and GRGDS (fasciated) end groups. Measurements were performed after 0 minutes (▥ amine, ■ tartaric acid and ☰ GRGDS derivative), 1 minute (▥ amine, ◩ tartaric acid and ☰ GRGDS derivative) and after 5 minutes (▥ amine, ☐ tartaric acid and ▨ GRGDS derivative). The results indicate that binding tartaric acid acid and GRGDS increases the contact angle for all derivatives. On the other hand, the longer the contact with water is, the more the contact angles decrease.

Protein adsorption

The benefit of PEG chain attachment to PLA materials is to prevent or to control the adsorption of proteins. The success of this strategy depends on a reasonable density of PEG moieties on the surface, the chain length seems to be less important.[15,16] In different studies an effect of the end group of self assembled monolayers was shown to have an impact on adsorption characteristics.[24,25,26] To evaluate the end group effect of differently charged PEG-PLAs, we tested three different polymers with a content of 5% PEG (PEG$_1$-PLA$_{20}$ and PEG$_2$-PLA$_{40}$) and 10% respectively (PEG$_2$-PLA$_{20}$) in terms of their protein adsorption characteristics. Previously it was shown that these PEG contents were high enough to reduce protein adsorption.[13]

PEG$_1$-PLA$_{20}$ derivatives.

In Figure 8 the adsorption kinetics of serum proteins on PEG$_1$-PLA$_{20}$ films can be seen. For tartaric acid and GRGDS modified surfaces we could determine a reasonable deposition of mass on the films, indicated by the drop in resonance frequency by 20 – 70 Hz. The standard deviations are quite high (up to $\pm$ 20Hz), indicating that, although the surfaces were produced under reproducible conditions, protein adsorption varies substantially.

Most of the adsorbed mass is bound to the surface more or less immediately, but the process of mass deposition continues for 1-2 hours with a constant slope. After rinsing with buffer again, only a small increase in resonance frequency can be seen, indicating that the major part of proteins is bound firmly to the polymer films (data not shown). For this polymer with a content of 5% PEG, no significant difference in protein adsorption can be seen in terms of both negatively net charged end groups, the kinetics and the extent of adsorption are quite similar, suggesting the end group of the polymers has no effect on the extent of protein adsorption. However, there might be differences in the type of proteins, since GRGDS also carries one positive charge.

Nevertheless, as expected, the extent of mass deposition can be reduced by attaching PEG to PLA (compared to PLA it is obviously reduced), the strategy in general to control protein adsorption seems to be promising. On the other hand, this content of PEG seems to be too low to reach a complete protein resistance.
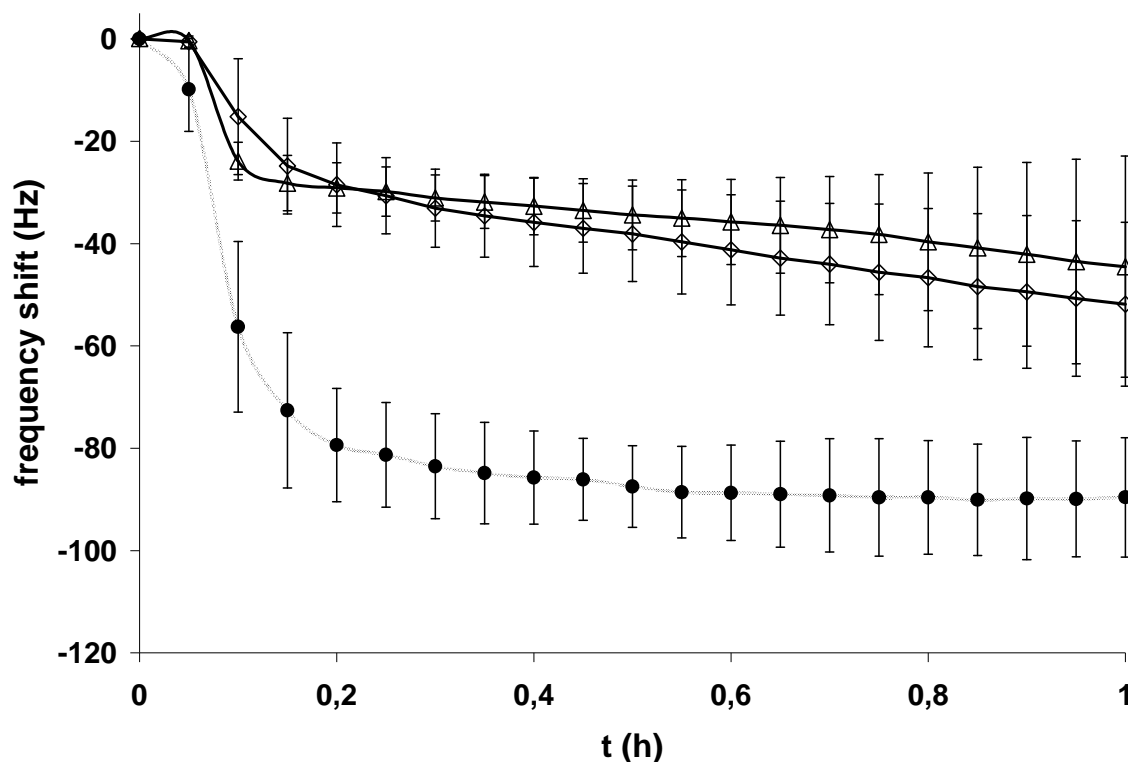
Figure 8: Adsorption of serum proteins on different PEG_1-PLA_{20} surfaces. Compared to PLA (●), the PEG containing polymers adsorb less proteins, the decrease in resonance frequency is smaller. No differences between both tartaric acid (◇) and GRGDS (△) modified polymer films can be detected.

PEG_2-PLA_{40} derivatives.

To verify the results of PEG_1-PLA_{20} we performed experiments with an other polymer having the same PEG content (5%, PEG_2-PLA_{40}), but a different PEG chain length. Again we could detect a reasonable adsorption of proteins on the polymer films, the resonance frequency dropped by 35 ± 15 Hz. The results of tartaric acid and GRGDS modified films are similar to the PEG_1-PLA_{20} experiments, the kinetics is the same and again the standard deviations are quite high.

But obviously, there might be a detectable effect of the end group. With non-modified monoamine-PEG_2-PLA_{40}, the amount of protein adsorption is significantly higher after one hour. The reason for that might be the different charge patterns of the surfaces. On tartaric acid and GRGDS modified surfaces additional negative charges are introduced to the positively charged amine groups of the monoamine-PEG_2-PLA_{40}. In literature it is well described for other surfaces, that the net charge of course might influence the interactions

with different proteins.[25,28,29] For protonated amine-terminated self-assembled monolayers for example it was shown that the serum protein with the highest attraction to the surface is the negatively charged vitronectin, what might be the case here, too.[25] Additionally, the extent of protein adsorption is very high for this amine-terminated films, the protein repellant effect is quite low compared to PLA.
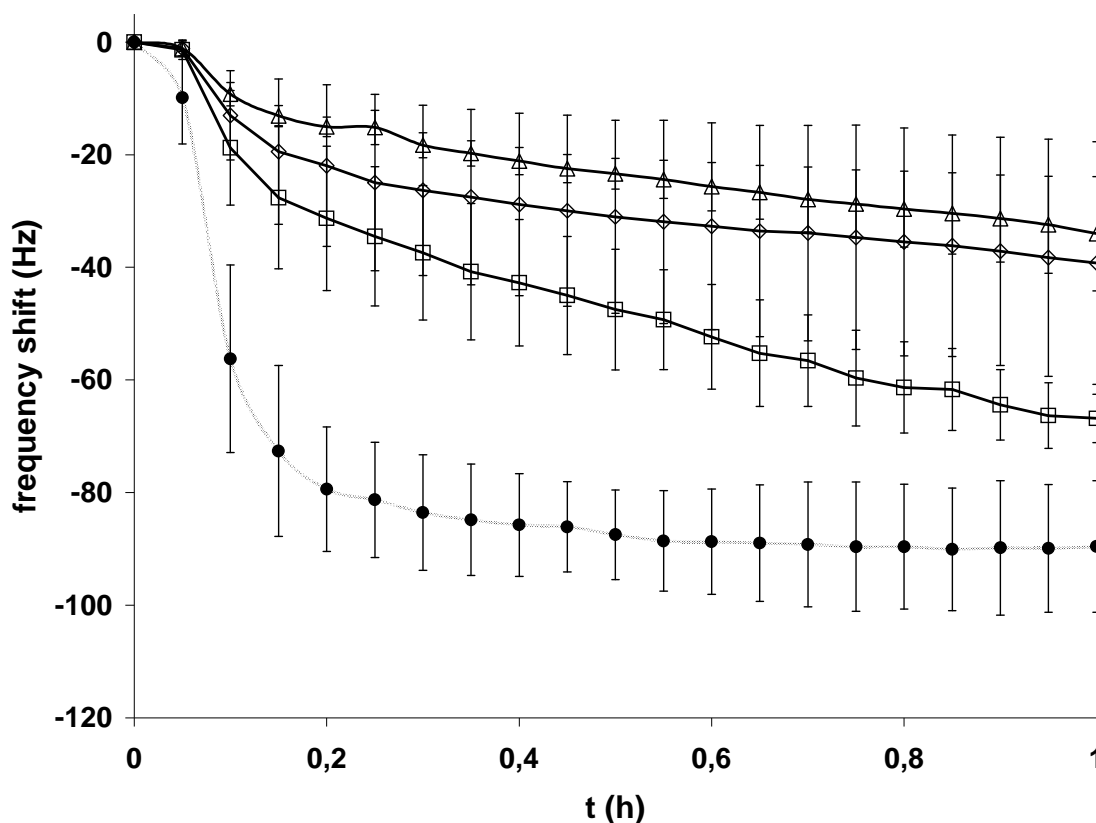

Figure 9: Adsorption of serum proteins on different PEG$_2$-PLA$_{40}$ surfaces. PEG containing polymers adsorb less proteins than PLA (●) . The monoamine derivative (□) adsorbs significantly more proteins than tartaric acid (◇) and GRGDS (△) modified polymers.

Summarizing the results of both polymers with a PEG content of 5%, we could see that protein adsorption could be reduced due to the PEG moieties, but reasonable amounts still adsorb. Additionally, the charge of the end group has an influence on the amount of adsorbed proteins. Therefore, we tested a further polymer with a higher content of PEG (PEG$_2$-PLA$_{20}$, 10% PEG) and evaluated, if this leads to a further reduction of protein adsorption. Moreover, we tried to asses, whether the impact of the end group is increased or decreased due to the higher PEG content.

PEG$_2$-PLA$_{20}$ derivatives.

For these polymers we could see that the amount of adsorbed proteins on tartaric acid and GRGDS modified films is slightly lower (approx. 30 ± 10 Hz) than for PEG$_1$-PLA$_{20}$ and PEG$_2$-PLA$_{40}$. Moreover, a difference between both PEG$_2$-PLA$_{20}$ derivatives can not be found. For the amine-terminated derivative of PEG$_2$-PLA$_{20}$ the adsorption characteristics are not significantly different, the mean value is only slightly higher than for both surfaces with additional negative charges, but due to the large standard deviations no further conclusions can be drawn in comparison to both other films. But obviously, the decrease in resonance frequency is significantly lower for this 10% monoamine-PEG-PLA copolymer and slightly lower for both negatively charged end groups than for the polymers containing 5% PEG. This in consequence means that a higher density of PEG on the surface leads to a better protein repellant effect, but on the other hand the end group seems to lose its impact on adhesion.
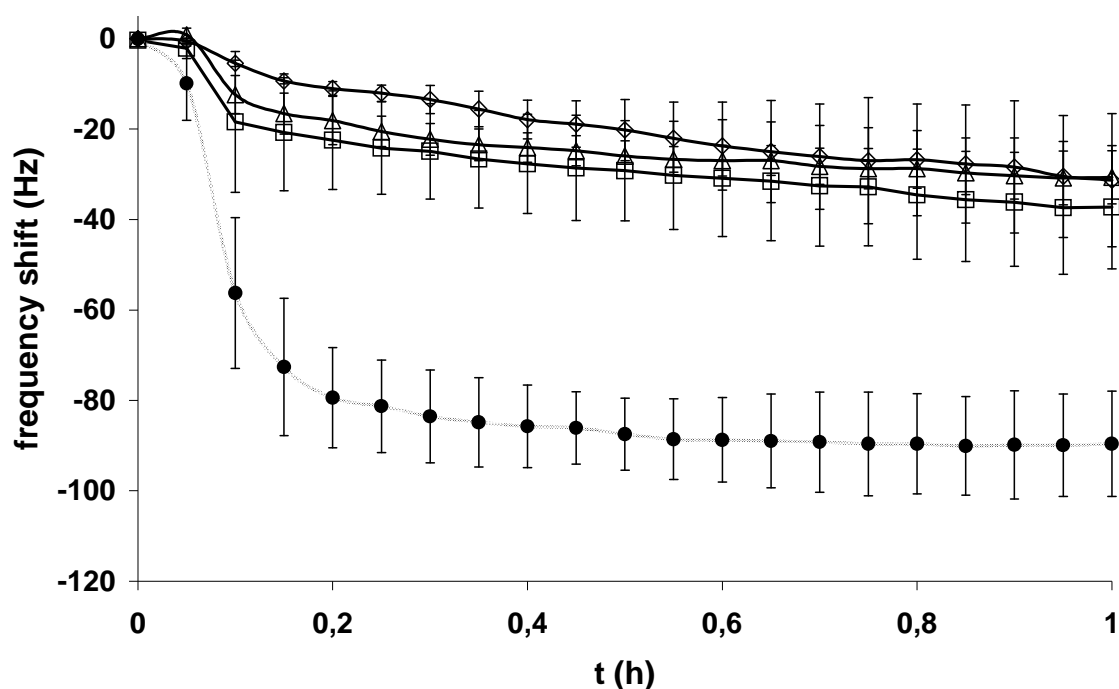

Figure 10: Adsorption of serum proteins on different PEG$_2$-PLA$_{20}$ surfaces. All three PEG containing polymers (☐ amine, ◇ tartaric acid and GRGDS modified △) adsorb low amounts of protein compared to PLA ● . No differences in terms of the PEG end group can be seen.

Summarizing these protein adsorption experiments we can conclude that attaching PEG to PLA leads to a reduction of protein adsorption. The end group chemistry does have a significant influence at low PEG contents, for almost neutral polymer films the extent of protein adsorption is higher for PEG-PLA derivatives with a PEG content of 5%. For PEG_2-PLA_{20}, the charge of the end group does not seem to have any significant effect. Therefore, the density of PEG on this derivative seems to be high enough to ensure a reasonable protein resistance even if charged end groups are present.

Cell adhesion

To asses the adhesion of rat marrow stromal cells on PEG-PLA surfaces, we performed measurements using the quartz crystal microbalance technique (QCM). Recently we could show that this system is very well suited to characterize the extent and kinetics of cell adhesion on self-assembled monolayers of PEG derivatives.[30] Therefore, we intended to verify the results of this simplified model system determining the adhesion on PEG-PLA films.

PEG_1-PLA_{20}.

As we could see for protein adsorption experiments, the addition of 1 ml of serum containing medium leads to a decrease in resonance frequency by approximately 30 – 40 Hz for the three GRGDS modified PEG-PLA films. If 250.000 rMSCs are suspended in the same amount of medium, no difference in resonance frequency shift can be detected for PEG_1-PLA_{20} and PEG_2-PLA_{40} (Figure 11). This suggests no cells adhere, although cell adhesion should be induced due to GRGDS – integrin interactions.[17] Indeed, when staining the surfaces with fluorescein-phalloidin, almost no cells can be found on the sensors.

In previous studies, it was shown that on monomethyl ether PEG-PLA derivatives the adhesion of cells was significantly reduced compared to PLA surfaces.[13,31] These studies were performed under conventional static cell culture conditions. Here, the adhesion tests were performed under dynamic conditions, since the QCM is designed with a flow through set up. This set up imposes a shear stress on the cells, making it even more difficult for them to adhere. This might lead to the fact that even the attachment of the cell adhesion pentapeptide GRGDS does not lead to a significant increase in cell adhesion, although the corresponding integrin receptors interacting with GRGDS were shown to be present on the cell surfaces.[32]

Two reasons might be responsible for these findings. First, the concentration of cell adhesion motifs on the surface could be too low to induce cell adhesion. It was shown for different cell types that the adhesion of cells correlates with the density of cell adhesion motifs on surfaces.[33] Thinking of the results of the protein adsorption experiments, we know that the interface between solid and aqueous phase is not completely covered with a dense PEG layer, since protein adsorption can still be observed. This low PEG density leads to a low density of PEG-bound GRGDS peptides, reducing the integrin ligand availability for the cells, what makes the surface fairly attractive for cells.

The second possible reason for the non-adherence might be a coverage of the cell adhesion motifs with "inactive" serum proteins, such as bovine serum albumin (BSA), or the reduction of the adsorption of certain proteins. Since we know for example that vitronectin is negatively charged as well as the surfaces[34,35], its adsorption might be reduced, leading to less adhesion motifs on the surface, as vitronectin also contains cell adhesion motifs.[17] Additionally, an adsorption of other proteins without adhesion motifs might be favored and cover the attached cell adhesion motif GRGDS.

In summary, we can say that attaching GRGDS to activated PEG_1-PLA_{20} films does not lead to a desired increase in cell adhesion under the existing dynamic conditions of the QCM set up.
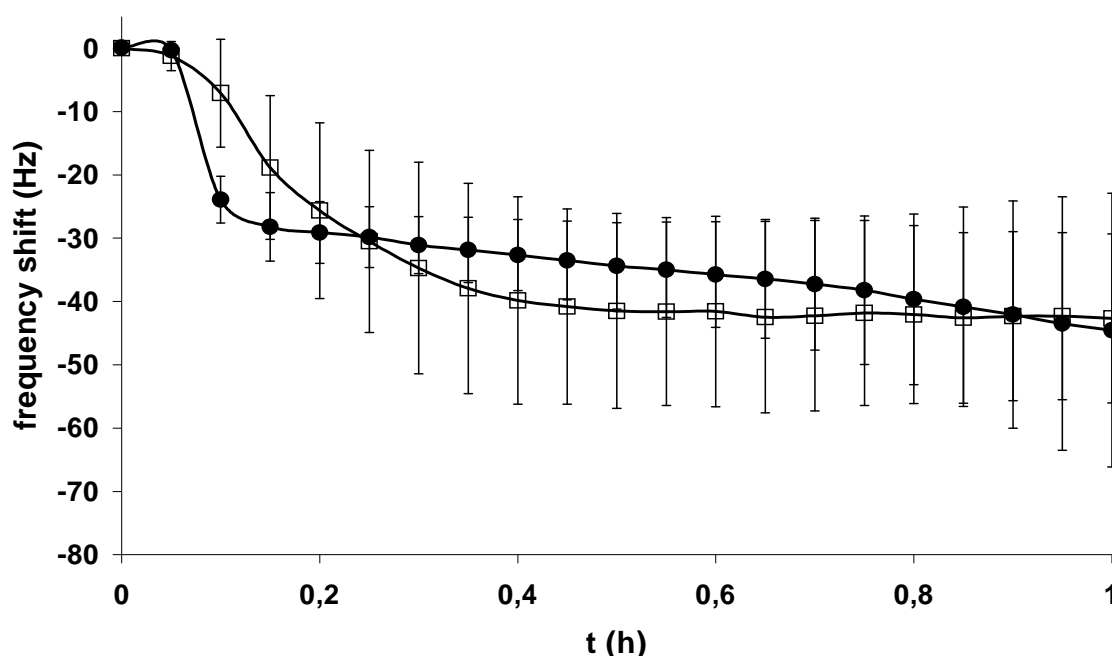

Figure 11: Adhesion of rMSCs on PEG_1-PLA_{20} films. Independent whether cells are suspended (□) or not(●) , the decrease in resonance frequency is indistinguishable.

PEG$_2$-PLA$_{40}$.

For PEG$_1$-PLA$_{20}$ and PEG$_2$-PLA$_{40}$ we could not find any differences in protein adsorption (Figure 12). The same is true for cell adhesion on GRGDS modified surfaces. The decrease in resonance frequency after the addition of 1 ml serum containing medium is absolutely comparable, independent of whether there were cells suspended or not. The reasons for this non-adhesion should be the same as for PEG$_1$-PLA$_{20}$, since the PEG content and therefore the protein adsorption characteristics are the same. Either not enough adhesion motifs are present on the surface, or the existing adhesion motifs are covered by "inactive" proteins in terms of cell adhesion.

The results of both polymers show that they are absolutely comparable concerning their communication with biological environments. This once more confirms that not the chain length of PEG moieties is determining their protein resistance and subsequent cell adhesion, but the decisive characteristic is the density of PEG on the surface, as it was shown in several studies for other surfaces.[15,16]
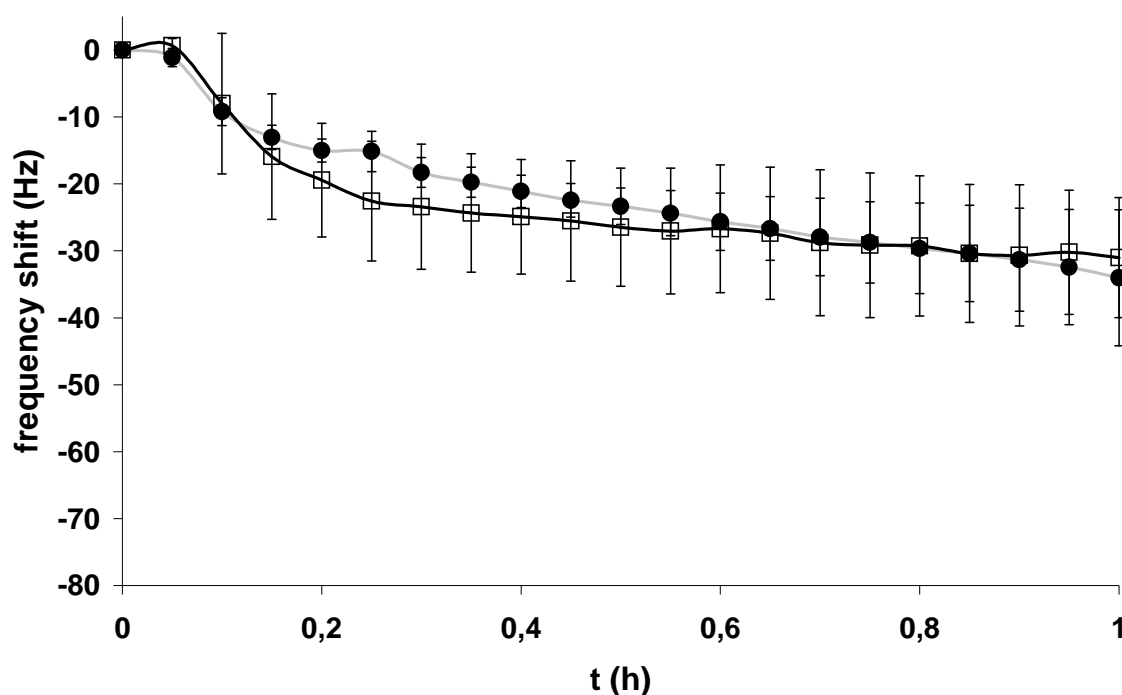

Figure 12: Adhesion of rMSCs on PEG$_2$-PLA$_{40}$ films. No difference in the frequency shift can be detected, if cells are suspended (□) or not (●) in the medium added to the polymer surface.

PEG$_2$-PLA$_{20}$.

Things are different on PEG$_2$-PLA$_{20}$ surfaces (Figure 13). For protein adsorption experiments the results were comparable with both other copolymers for GRGDS modified films. However, the good protein repellant effect even for amine-terminated surfaces indicated that higher PEG contents might strengthen the protein adsorption resistance. The results for the cell adhesion experiments confirm the higher availability of PEG moieties on the surface. Compared to the addition of medium alone, the resonance frequency drops significantly stronger after the addition of serum containing cell suspensions. This indicates that the concentration of available integrin ligands is high enough to induce significantly improved cell adhesion. In a control experiment we added a serum-containing suspension of cells on a tartaric acid terminated PEG$_2$-PLA$_{20}$ film. Since the decrease in resonance frequency was only 20 Hz and hence in the range of protein adsorption experiments alone, we can conclude that indeed the attachment of GRGDS is responsible for the adhesion of cells on the PEG$_2$-PLA$_{20}$ films. In Figure 14 stained cells show that rMSCs are well spread on the PEG$_2$-PLA$_{20}$ films, although the cells are not very densely packed. The fact that cells can adhere on these PEG$_2$-PLA$_{20}$ films supports the assumption, that the availability of GRGDS is higher for this copolymer.

To check the influence of adsorbed proteins on cell adhesion we also performed the same experiment under serum free conditions. Again, the adhesion of cells was obviously detectable, with 40 Hz after one hour approximately in the same range as in the presence of proteins. This shows enough adhesion motifs are present on the surface, even without the contribution of proteins. In consequence this more or less confirms that for the 5% PEG-PLA derivatives indeed the density of adhesion motifs seems to be the limiting factor concerning rMSC adhesion. But at least for the PEG$_2$-PLA$_{20}$ films, a coverage of attached GRGDS peptides by "inactive" proteins can be excluded to a certain extent, since by attaching GRGDS cell adhesion is significantly increased. For both other polymers (PEG$_1$-PLA$_{20}$ and PEG$_2$-PLA$_{40}$) the contribution of this effect still should be taken into account due to the differences in protein adsorption characteristics. Since more proteins adsorb, also the contribution of "inactive" proteins in terms of cell adhesion could be present on these surfaces.
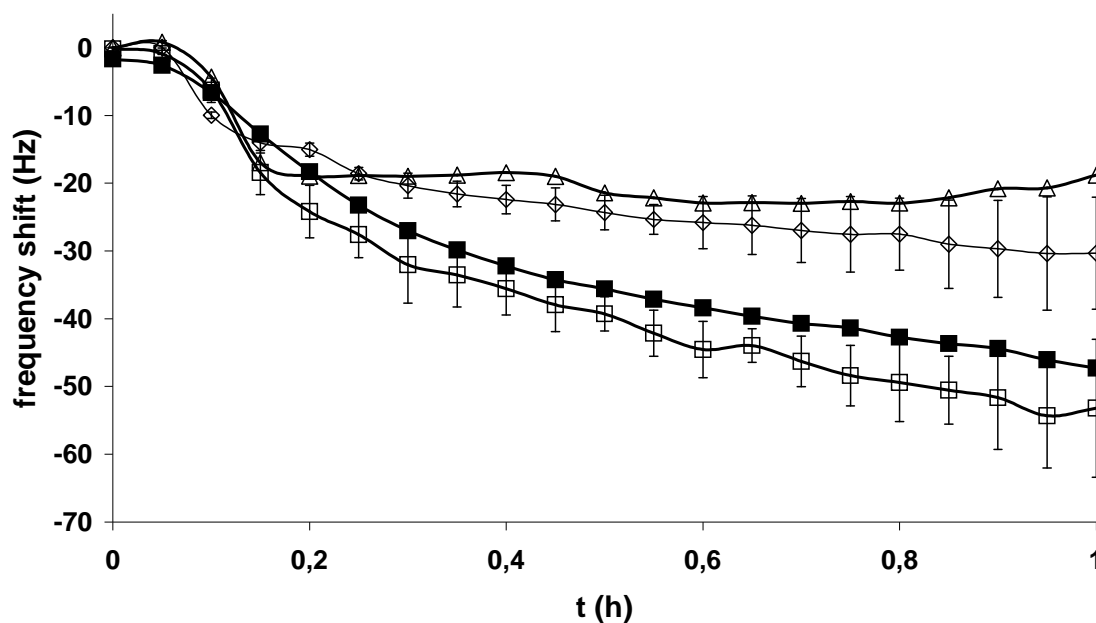
Figure 13: Adhesion of rMSCs on PEG_2-PLA_{20} films. If cells are suspended in the added medium (□), the decrease in resonance frequency is significantly higher compared to medium alone (◇). Under serum free conditions (■), almost the same decrease can be seen. If cells are added in serum containing medium to tartaric acid-PEG_2-PLA_{20} (△), no adhesion of cells takes place, since the resonance frequency is in the same range as without cells.
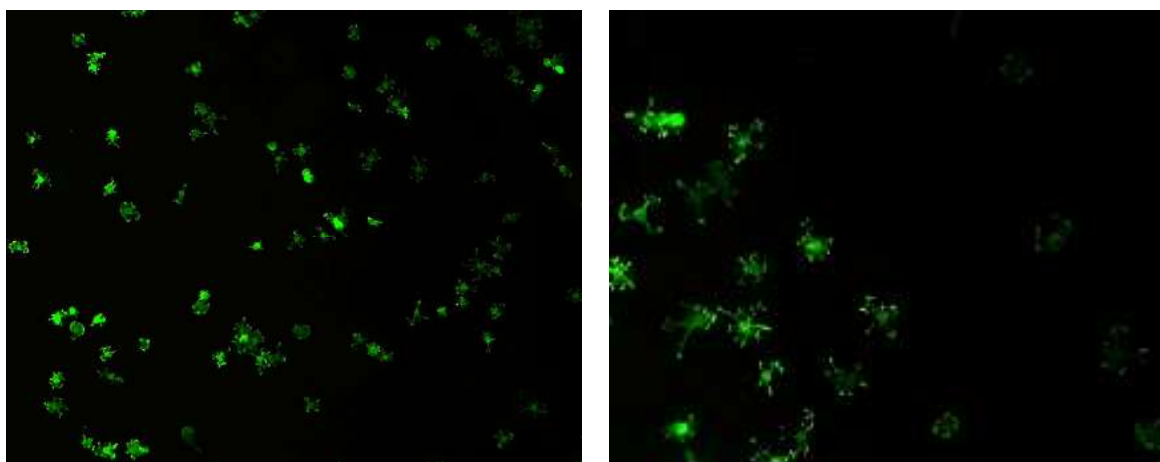

Figure 14: rMSCs adhering to $GRGDSPEG_2$-PLA_{20} films. The cytoskeleton is stained with a fluorescent phalloidin derivative. The rMSCs seem to be well spread, suggesting the GRGDS concentration on the surface is high enough (left: magnification 100x, right 200x).

Conclusion

In this study, for the first time the effect of end groups on protein adsorption of high molecular weight PEG-PLA diblock copolymers was shown. For PEG-PLA derivatives with a PEG content of 5 % we could demonstrate that monoamine PEG-PLAs with positive charged amine groups adsorb significantly higher amounts of serum proteins than derivatives having additional negative charges due to attached acids or peptides. This is independent of whether there is only one negative charge or one positive and two negative charges within the functional group, which is attached. Increasing the PEG content to 10% improves the protein repellant effect of the PEG-PLA copolymers and additionally lowers the impact of the functional end groups on protein adsorption. With a PEG content of 10 % also a density of cell adhesion peptides on the surface could be reached, that is high enough to induce cell adhesion even under dynamic flow-through conditions.

References

[1] Drotleff S.; Lungwitz U.; Breunig M.; Dennis A.; Blunk T.; Tessmar J.; Göpferich A.: Biomimetic polymers in pharmaceutical and biomedical sciences. Eur J Pharm Biopharm, 58, 385-407, 2004.

[2] Lieb E.; Hacker M.; Tessmar J.; Kunz-Schughart L.A.; Fiedler J.; Dahmen C.; Hersel U.; Kessler H.; Schulz M.B.; Goepferich A.: Mediating specific sell adhesion to low adhesive diblock copolymers by instant modification with cyclic RGD peptides. Biomaterials, 26, 2333–2341.

[3] Kubies D.; Rypacek F.; Kovarova J.; Lednicky F.: Microdomain structure in polylactide-block-poly(ethylene oxide) copolymer films. Biomaterials, 21, 529-536, 2000.

[4] v. Burkersroda F.; Gref R.; Goepferich A.: Erosion of biodegradable block copolymers made of poly(D,L-lactic acid) and poly(ethylene glycol). Biomaterials, 16, 1599-1607, 1997.

[5] Otsuka H.; Nagasaki Y.; Kataoka K.: Surface characterization of functionalized polylactide through the coating with heterobifunctional poly(ethylene glycol)/polylactide block copolymers. Biomacromolecules, 1, 39-48, 2000.

[6] Deng C.; Tian H.; Zhang P..; Sun.; Chen X.; Jing X.: Synthesis and characterization of RGD peptide grafted poly(ethylene glycol)-b-poly(L-lactide)-b-poly(L-glutamic acid) triblock copolymer. Biomacromolecules, 7, 590-596, 2006.

[7] Goepferich A.; Peter S.J.; Lucke A.; Lu L.; Mikos A.G.: Modulation of marrow stromal cell function using poly(D,L-lactic acid)-block-poly(ethylene glycol)-monomethyl ether surfaces. J Biomed Mat Res, 46, 3, 390-398, 1999.

[8] Quirk R.A.; Davies M.C.; Tendler S.J.B.; Chan W.C.; Shakesheff, K.M.: Controlling biological interactions with poly(lactic acid) by surface entrapment modification. Langmuir, 17, 2817-2820, 17.

[9] Jeong J.H.; Lim D.W.; Han D.K.; Park T.G.: Synthesis, characterization and protein adsorption behaviors of PLGA/PEG di-block co-polymer blend films. Coll Surf B, 18, 371, 379, 2000.

[10] Wang S.; Cui W.; Bei J.: Bulk and surface modifications of polylactide. Anal Bioanal Chem, 381, 547-556, 2005.

[11] Tessmar J.; Mikos T.; Goepferich A.: The use of poly(ethylene glycol)-block-poly(lactic acid) derived copolymers for the rapid creation of biomimetic surfaces. Biomaterials, 24, 4475-4486, 2003.

[12] Jeon S.I.; Lee J.H.; Andrade J.D.; de Gennes P.G.: Protein-surface interactions in the presence of polyethylene oxide. J Colloid Interf Sci, 142, 149-166, 1991

[13] Lieb E.; Tessmar J.; Hacker M.; Fischbach C.; Rose D.; Blunk T.; Mikos A.G.; Goepferich A.; Schulz M.B.: Poly(D,L-lactic acid)-poly(ethylene glycol)-monomethyl ether diblock copolymers control adhesion and osteoblastic differentiation of marrow stromal cells. Tissue Eng, 9, 1, 71-84, 2003.

[14] Suzuki Y. ; Tanihara M. ; Suzuki K. ; Saitou A. ; Sufan W. ; Nishimura Y. : Alginate hydrogel linked with synthetic oligopeptide derived from BMP-2 allows ectopic osteoinduction in vivo. J Biomed Mater Res, 40, 405-409, 2000.

[15] Unsworth L.D.; Sheardown H.; Brash J.L.: Polyethylene oxide surfaces of variable chain density by chemisorption of PEO-thiol on gold: adsorption of proteins from plasma studied by radiolabelling and immunoblotting. Biomaterials, 26, 5927-5933, 2005.

[16] Unsworth L.D.; Sheardown H.; Brash J.L.: Protein resistance of surfaces prepared by sorption of end-thiolated poly(ethylene glycol) to gold: effect of surface chain density. Langmuir, 21, 1036-1041, 2005.

[17] Hersel U., Dahmen C., Kessler H.: RGD modified polymers: biomaterials for stimulated cell adhesion and beyond. Biomaterials, 24, 4385-4415, 2003.

[18] Tessmar J.; Mikos A.G.; Göpferich A.: The use of poly(ethylene glycol)-block-poly(lactic acid) derived copolymers for the rapid creation of biomimetic surfaces. Biomaterials, 24(24), 4475-4486, 2003.

[19] Kastl K.; Ross M.; Gerke V.; Steinem C.: Kinetics and thermodynamics of Annexin A1 binding to solid supported membranes: A QCM study. Biochemistry, 41, 10087-10094, 2002.

[20] Ishaug S.L.; Crane G.M.; Miller M.J.; Yasko A.W.; Yaszemski M.J.; Mikos A.G.: Bone formation by three-dimensional stromal osteoblast culture in biodegradable polymer scaffolds. J Biomed Mater Res, 36, 17, 1997.

[21] Janshoff A.; Galla H.J.; Steinem C.: Piezoelectric mass-sensing devices as biosensors – an alternative to optical biosensors? Angewandte Chemie, Int Ed, 39, 4004-4032, 2000.

[22] Renard E.; Walls M.; Guerin P.; , Langlois V.: Hydrolytic degradation of blends of polyhydroxyalkanoates and functionalized polyhydroxyalkanoates. Polym Degr Stab, 85, 779-787, 2004.

[23] Wilson J.C.; Clegg R.E.; Leavesley D.I.; Pearcy M.J.: Mediation of biomaterial-cell interactions by adsorbed proteins: A review. Tissue Engineering 11 (1/2), 1-18. 2005.

[24] Knerr R.; Weiser B.; Drotleff S.; Steinem C.; Goepferich A.: Self-assembling PEG Derivatives for Protein-repellant Biomimetic Model Surfaces on Gold. Biomaterialien, 7 (1), 12-20, 2006.

[25] Facheux N.; Schweiss R.; Lützow K.; Werner C.; Groth T.: Self-assembled monolayers with different terminating groups as model substrates for cell adhesion studies. Biomaterials, 25, 2721-2730, 2004.

[26] Pale-Grosdemange C.; Simon E.S.; Prime K.L.; Whitesides G.M.: Formation of self-assembled monolayers by chemisorption of derivatives of oligo(ethylene glycol) of structure $HS(CH_2)_{11}(OCH_2CH_2)_mOH$ on gold. J Am Chem Soc, 113, 12-20, 1991.

[27] Vanderah D.J.; Pham C.P.; Springer S.K.; Silin V.; Meuse C.W.: Characterization of a series of self-assembled monolayers of alkylated 1-thiaoligo(ethylene oxides)$_{4-8}$ on gold. Langmuir, 16, 6527-6532, 2000.

[28] Wilson C.J.; Clegg R.E.; Leavesley D.I.; Pearcy M.J.: Mediation of biomaterial-cell interactions by adsorbed proteins: A review. Tissue Engineering, 11, 1/2, 1-18, 2005.

[29] Wang Y.X.; Robertson J.L.; Spillman W.B.; Claus R.O.: Effects of the chemical structure and the surface properties of polymeric biomaterials on their biocompatibility. Pharm Res, 21, 8, 1362-1372, 2004.

[30] Knerr R.; Weiser B.; Drotleff S.; Steinem C.; Goepferich A.: Measuring cell adhesion on RGD-modified self-assembled PEG monolayers using the quartz crystal microbalance technique. Macromolecular Bioscience, 9, 827-838 (2006).

[31] Lu L.; Nyalakonda K.; Kam L.; Bizios R.; Goepferich A.; Mikos A.G.: Retinal pigment epithelial cell adhesion on novel micropatterned surfaces fabricated from synthetic biodegradable polymers. Biomaterials, 22, 291-297, 2001.

[32] Volk B.; Vogel T.; Rohde E.; Strunk D.; Göpferich A.; Schulz M.B.: Flow cytometric analysis of plastic-adherent bone marrow stem cells. Joint Meeting of the Tissue Engineering Society International and the European Tissue Engineering Society, October 10-13 2004, Lausanne (Switzerland), P94.

[33] Gallant N.D.; Capadona J.R.; Frazier A.B.; Collard D.M.; Garcia A.J.: Micropatterned Surfaces to engineer focal adhesion for analysis of cell adhesion strengthening. Langmuir, 18, 5579-5584, 2002.

[34] Sasatsu M.; Onishi H.; Machida Y.: Preparation of a PLA-PEG block copolymer using an OLA derivative with a formyl terminal group and its application to nanoparticulate formulation. Int J Pharmaceutics, 294, 233-245, 2005.

[35] Stolnik S.; Dunn S.E.; Garnett M.C.; Davies M.C.; Coombes A.G.A.; Taylor D.C.; Irving M.P.; Purkiss S.C.; Tadros T.F.; Davis S.S.; Illum L.: Surface modification of poly(lactide-co-glycolide) nanospheres by biodegradable poly(lactide)-poly(ethylene glycol) copolymers. Pharm Res, 11, 12, 1800-1808, 1994.

[36] Govender T.; Riley T.; Ehtezazi T.; Garnett M.C.; Stolnik S.; Illum L.; Davis S.S.: Defining the drug incorporation properties of PLA–PEG Nanoparticles. *Int J Pharmaceutics,* 199, 96, 95–110, 2000.

Chapter 8

Summary

and

Conclusions

Summary

Based on the idea of self-assembled monolayers of alkanethiols on gold, it was the goal of this thesis to develop a versatile model system for an efficient and straightforward characterization of cell - biomaterial interactions on PEG-rich surfaces. The necessary compounds for this model system should allow for mimicking the surface of polymeric poly(ethylene glycol)-rich biomaterials used for the design of cell carriers. By evaluating the adsorption of proteins and the adhesion characteristics of mammalian cells on these artificial surfaces, conclusions can be drawn, on how polymers should be engineered to achieve an optimal adhesion, growth or proliferation of cells. In particular, the consequences of an attachment of peptidic cell adhesion peptides and growth factors had to be elucidated.

To achieve this goal, the benefits of the self-assembling principle of alkanethiols on gold were utilized. If such compounds are brought into contact with gold surfaces in solution, they bind spontaneously via their thiol moiety to the surface and form stable and homogeneous monolayers.[1] By binding different entities, such as polymeric compounds to the alkanes, also high molecular weight substrates can be arranged to monolayers.[2]

This principle is an ideal prerequisite to mimic the surfaces of polymers, such as diblock-copolymers consisting of poly(ethylene glycol) and poly(D,L-lactic acid) (so-called PEG-PLAs). Since in aqueous environments the PEG moieties of these diblock-copolymers assemble on the surface in domains[3], they can easily be imitated by PEG molecules attached to alkanethiols, which are arranged in monolayers.
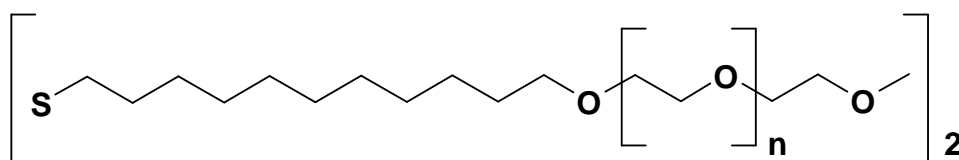
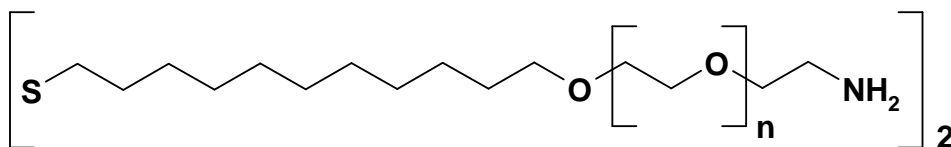*Figure 1a: Chemical structure of di(ω-methoxy poly(ethylene glycol)-undecyl) disulfide*

Figure 1b: Chemical structure of di(ω-amino poly(ethylene glycol)-undecyl) disulfide
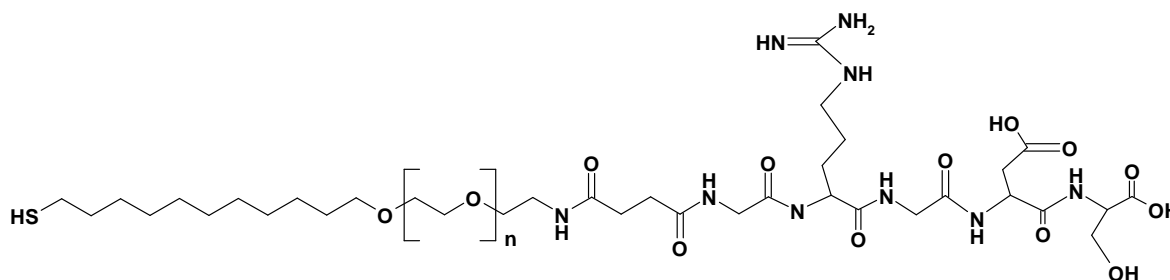

Figure 1c: Chemical structure of succinamido- poly(ethylene glycol)-undecyl- mercaptane modified with GRGDS

Synthesizing such molecules offers the possibility to generate SAMs on gold surfaces on a 24 hours time scale by incubating the corresponding surfaces with ethanolic polymer solutions. Within several minutes, the major part of the surface is covered with the corresponding alkanethiols, but the process of monolayer growth seems to continue for at least 2 hours. Different surface sensitive techniques confirmed the formation of homogeneous monolayers. With the Atomic Force Microscope for example surfaces with roughnesses in the range of few nanometers were determined. Surfaces exhibiting such PEG derivatives can resist the non-specific adsorption of bovine serum albumin more or less completely, the remaining amount of protein is below a threshold entailing cellular responses. Also the adsorption of complex protein mixtures, such as fetal bovine serum can be suppressed significantly, the amount of protein is near the detection limit of Surface Plasmon Resonance **(Chapter 2)**.

Introducing functional groups to the ends of the PEG moieties provides the possibility to attach bioactive compounds. By replacing the inert methoxy end group by an amine group, a modification with bifunctional carboxylic acids can be performed. These can be activated with common procedures resulting in amine reactive surfaces.[5] Attaching primary amine containing entities then can easily be performed in situ by incubation with the desired

compound, what could be confirmed by contact angle measurements. The introduction of an amine group does not change the wettability characteristics compared to the methoxy terminated SAM. However, a significant impact on protein adsorption is the consequence, more proteins are allowed to bind to the surface. Further modifications with carboxylic acids and peptides do not alter the amount of adsorbed proteins any more, although the hydrophobicity of the surface increases **(Chapter 3)**.

The benefits offered by the introduction of functional end groups to the PEG moieties allow for the manipulation of the cell behavior on PEG rich surfaces. On the non-modified amine-terminated SAMs, cell adhesion under dynamic conditions of a Quartz Crystal microbalance system can be suppressed completely. If cell adhesion peptides are attached to the surfaces, cells attach readily to the surface and spread well. A further increase in cell adhesion can be reached by adding adhesion receptor activating manganese cations. Cell detachment processes also can be differentiated. Enzymatic cleavage of peptide bonds using trypsin leads to a rapid detachment of cells from the surface within few minutes. Ligand displacement from the adhesion receptor of cells by adding soluble adhesion molecules is slower almost one order of magnitude **(Chapter 4)**.

Combining the advantages of self-assembled monolayers with the quartz crystal microbalance technique offers the chance to characterize the adhesion of mammalian cells on poly(ethylene glycol)-rich surfaces in real time and label-free.[4] Using a flow through arrangement moreover allows for measuring cell-surface interactions continuously. However, the applied shear stress reduces the adhesion of cells on the sensor surface, the higher the shear stress, the lower is the adhesion of cells. This challenge can be overcome by reducing the liquid flow, under a certain threshold cells distribute homogeneously over the surface and spread well. Using the QCM technique with dissipation monitoring enables to discriminate between protein adsorption and cell adhesion within one experiment. Moreover, the different adhesion strengths of cells in the absence and presence of proteins can be characterized, revealing that cells attach more firmly if proteins are additionally present on the surface **(Chapter 5)**.

The versatility of the developed model system also offers the possibility to attach growth factors to the PEG surface. Investigating the adhesive properties of bFGF, no effect on cell adhesion can be stated. On the other hand, soluble bFGF strongly increased cell attachment

if adhesion molecules are bound to the surface. The longer cells are treated with bFGF, the stronger the effect is. For TGFβ similar effects could be detected, although the effect was less strong. In contrast to these signaling molecules, the mitogen PDGF reduces the adhesion of cells to adhesion molecule presenting surfaces in a dose dependent manner. On the integrin distribution the three different growth factors also seem to have an impact. For bFGF and TGFβ the density of β_3 subunits on the surface seems to be increased, for PDGF a higher concentration of integrin β_3 in the nuclei can be seen (**Chapter 6**).

A comparison of protein adsorption and cell adhesion on self-assembled monolayers and poly(ethylene glycol) – poly(D,L-lactic acid) diblock copolymer films revealed that similar trends can be observed. Attaching poly(ethylene glycol) to the surfaces reduces the adsorption of proteins, the higher the density of PEG, the stronger the reduction is. For different PEG-PLA derivatives an effect of the end group can be detected. Protonated amine terminated PEG moieties result in stronger protein adsorption than negatively charged compounds. However, this effect only can be determined if the PEG content is below 10%. With a higher content of PEG, an impact of different end groups on protein adsorption can not be observed any more. As for self-assembled monolayers, attaching adhesion molecules to the surface leads to an increase in cell adhesion, but only if the density of these adhesion sites, which is assumed to correlate with the density of PEG on the surface, is high enough. For low PEG contents on the surface, no difference in cell adhesion can be observed when adhesion peptides are bound to the surface (**Chapter 7**).

Conclusions

Polymers for producing self-assembled monolayers on gold mimicking the surfaces of PEG rich polymers were successfully synthesized using a new and facile strategy. We could demonstrate that homogeneous monolayers were formed using a great variety of analytical techniques. Moreover, we showed for ω-monomethyl ether poly(ethylene glycol) derivatives that SAMs of this polymer significantly reduce protein adsorption.

The synthesized ω-monoamine derivative allows for the instant modification with bioactive compounds and also can reduce non-specific protein adsorption to a high extent. Combining the advantages of this substrate with the quartz crystal microbalance technique, a powerful model system for the real-time characterization of protein adsorption and cell adhesion and detachment processes on PEG-rich surfaces was established.

The impact of different compounds of interest on the adhesion characteristics can be evaluated either by instant modification of the SAMs with biomolecules or by adding the soluble substances to the cell culture medium.

The results of the developed simplified model were in agreement with the results obtained for the corresponding biomaterials they should mimic. However, the results obviously confirm that by mimicking the biomaterial's surface, the results are by far more precise and allow for a detailed interpretation, independent of the underlying bulk material.

References

[1] Schreiber F.: Structure and growth of self-assembling monolayers. Prog Surf Sci, 65, 151-256, 2000.

[2] Herrwerth S.; Rosendahl C.; Feng C.; Fick J.; Eck W.; Himmelhaus R.; Dahint R.; Grunze M.: Covalent coupling of antibodies to self-assembled monolayers of carboxy-functionalized poly(ethylene glycol): Protein resistance and specific binding of biomolecules. Langmuir, 19, 1880-1887, 2003.

[3] v. Burkersroda F.; Gref R.; Goepferich A.: Erosion of biodegradable block copolymers made of poly(D,L-lactic acid) and poly(ethylene glycol). Biomaterials, 16, 1599-1607, 1997.

[4] Tessmar J.; Mikos T.; Goepferich A.: The use of poly(ethylene glycol)-block-poly(lactic acid) derived copolymers for the rapid creation of biomimetic surfaces. Biomaterials, 24, 4475-4486, 2003.

Appendix

Abbreviations

$(MePEG_{2000}C_{11}S)_2$	di-(ω-methoxy poly(ethylene glycol)-)undecyl-disulfide
$(NH_2PEG_{2000}C_{11}S)_2$	di-(ω-amino poly(ethylene glycol)-)undecyl-disulfide
°C	Degree Celsius
µCP	Micro contact printing
µg	Micro gram
µl	Micro liter
3T3-L1	Murine cell line
Å	Angström (0.1 nanometer)
AFM	Atomic Force Microscope
AG	Aktiengesellschaft (public company)
ANOVA	Analysis of variance
AT-cut	Distinct cut angle in quartz crystals
bFGF	Basic fibroblast growth factor
BOC	Butoxy carbonyl
BSA	Bovine serum albumin
CD61	Cluster of Differentiation (surface antigen)
Cdc42	Regulator of cellular signal transduction
$CDCl_3$	Deuterated chloroform
CO_2	Carbon dioxide
Cs	Cesium
D	Dissipation factor
Da	Dalton
DNA	Desoxyribonucleic Acid
DC	Direct current
DCC	N,N′-Dicyclohexylcarbodiimide
DFG	Deutsche Forschungsgemeinschaft
DMEM	Dulbecco´s Modified Eagle Medium
DMF	N,N-Dimethylformamide
ECM	Extracellular matrix
EDC	N-Ethyl-N'-(3-dimethylaminopropyl)carbodiimide
ERK	Extracellular regulated kinase

ESI	Electrospray ionization
f	frequency
FACS	Fluorescence activated cell sorting
FAK	Focal adhesion kinase
FBS	Fetal bovine serum
GmbH	Gesellschaft mit beschränkter Haftung(limited liability corporation)
GRGDS	Peptide sequence(Glycine, Arginine, Glycine, Aspartic acid, Serine)
GRK	Graduiertenkolleg (Graduate college)
H_2O_2	Hydrogen peroxide
H_2SO_4	Sulfuric acid
HCl	Hydrochloric acid
HEK	Human epithelial kidney cells
HPLC	High Performance Liquid Chromatography
HPLC-MS	High Performance Liquid Chromatography Mass Spectrometry
Hz	Hertz
IgG	Immunoglobulin G
keV	Kilo electron Volts
KGaA	Kommanditgesellschaft auf Aktien
kV	Kilo Volts
m/z	Mass per charge
MALDI-ToF	Matrix Assisted Laser Desorption/Ionization-Time of flight
MAPK	Mitogen activated protein kinase
MePEG	Poly(ethylene glycol) monomethyl ether
$MePEG_{2000}C_{11}SH$	ω-methoxy-poly(ethylene glycol) undecyl mercaptane
mg	Milli gram
MHz	Mega Hertz
mHz	Milli Hertz
ml	Milli liter
mM	Milli molar
mmol	Milli Mol
Mn	Manganese
NH_2	Amine-
NH_2PEG	Poly(ethylene glycol) mono amine

$NH_2PEG_{2000}C_{11}SH$	ω-amino-poly(ethylene glycol) undecyl mercaptane
NH_2-PEG-PLA	α-hydroxy-ω-amino-poly(oxy-1-oxopropane-2,1-diyl-block-oxy-ethylene)
NHS	N-hydroxysuccinimide
nm	Nano meter
NMR	Nuclear magnetic resonance
OEG	Oligo (ethylene glycol)
PBS	Phosphate buffered saline
PC	Personal computer
PDGF	Platelet derived growth factor
PE	Polyethylene
PEG	Poly(ethylene glycol)
PEG_{2000}	Poly(ethylene glycol) with a molecular weight of 2000 Da
PEG-PLA	Poly(ethylene glycol)-co-block-poly(D,L-lactic acid)
PEG_x-PLA_y	Poly(ethylene glycol)-co-block-poly(D,L-lactic acid); molecular weight of x kilodalton of PEG and y kilodalton of PLA
PET	Poly(ethylene terephthalate)
PLA	Poly(lactic acid)
PMMA	Poly(methyl methacrylate)
pmol	Pico mol
ppm	Parts per million
PTFE	Poly(tetrafluorethylene)
QCM	Quartz Crystal Microbalance
QCM-D	Quartz Crystal Microbalance with dissipation monitoring
Rac	Regulator of cellular signal transduction
RCO	Rat calvaria osteoblasts
RGD	Peptide sequence (Arginine, Glycine, Aspartic acid)
Rho	Regulator of cellular signal transduction
Rho-GTPase	Subtype of GTP binding proteins
rms	Route mean square
rMSC	Rat marrow stromal cells
RNAse	Ribonuclease
RU	Response units

RT-PCR	Reverse transcriptase – polymerase chain reaction
SAM	Self-assembled monolayer
SD	Standard deviation
s-NHS	Hydroxy-2,5-dioxopyrrolidine-3-sulfonicacid sodium salt
SPR	Surface Plasmon Resonance
Src	Subtype of tyrosine protein kinases
TCEP	Tris(2-carboxyethyl)phosphine hydrochloride
TFA	Trifluoroacetic acid
TGFβ	transforming growth factor-beta
THF	Tetrahydrofuran
ToF-SIMS	Time of flight - Secondary Ion Mass Spectrometry
UHV	Ultra high vacuum
UK	United Kingdom
US	United States
USA	United States of America
UV	Ultra violet
V	Volt
VEGF	Vascular endothelial growth factor
WCA	Water Contact Angle

Curriculum Vitae

Name:	Robert Erich Knerr
Date of birth:	18.05.1976
Place of birth:	Hemau
Nationality:	German
Marital status:	Single

Education:

09/82 – 07/86	Elementary school Hemau
09/86 – 06/95	Donau – Gymnasium Kelheim
06/95	school graduation certificate (Abitur)

Civil service:

09/95 – 10/96	Civil service at the hospital of the University of Regensburg

Professional Training:

11/96 – 03/01	Pharmaceutics course at the University of Regensburg
05/01 – 10/01	Practical education at STADA Arzneimittel GmbH, Bad Vilbel
11/01 – 04/02	Practical education at flora-Apotheke, Regensburg
07/02	Acquisition of the license to practice as a pharmacist
Since 07/02	PhD program at the Department of Pharmaceutical Technology of the University of Regensburg, Prof. Achim Göpferich, as a member of the Graduate College GRK 760 *Medicinal Chemistry – Ligand-Receptor Interactions*

Profession:

Since 10/05	Head of Production, AMAREG GmbH, Regensburg

List of publications

Publications

1. Knerr R.; Weiser B.; Drotleff S.; Steinem C.; Goepferich A.: Measuring cell adhesion on RGD-modified self-assembled PEG monolayers using the quartz crystal microbalance technique. Macromolecular Bioscience, 9, 827-838 (2006).

2. Knerr R; Drotleff S; Steinem C; Göpferich A.: Self-assembling PEG Derivatives for Protein-repellant Biomimetic Model Surfaces on Gold. Biomaterialien, 7 (1), 12-20 (2006).

3. Menz B; Knerr R.; Göpferich A.; Steinem C.: Impedance and QCM analysis of the protein resistance of self - assembled PEGylated alkanethiol layers on gold. Biomaterials 20 (26), 4237-4243 (2005).

Conference Abstracts

1. Knerr R; Weiser B; Drotleff S.; Steinem C; Göpferich A.: Protein Adsorption and Cell Adhesion on RGD modified PEG Monolayers. European Symposium on Polymeric Biomaterials, Madrid, Spain (2006).

2. U. Lungwitz, M. Breunig, S. Drotleff, R. Knerr, A. Goepferich: Low Molecular Weight Linear Polyethylenimines for Non-Viral Transfection. Controlled Release Society German Chapter Annual Meeting, Heidelberg, Germany (2005).

3. R. Knerr, B. Weiser, S. Drotleff, C. Steinem, A. Göpferich: Protein adsorption and cell adhesion on RGD modified PEG monolayers. Life Science Interface Summer School, University of Nottingham, Nottingham, UK (2005).

4. R. Knerr, C. Steinem, C.J. Roberts, A. Göpferich: A model to investigate cell surface interactions: PEGylated alkanethiolates on gold - protein resistance and visualization. Transactions, 31st annual meeting and exposition of the Controlled Release Society, Honolulu, HI, USA (2004).

5. R. Knerr, C. Steinem, C.J. Roberts, A. Göpferich: Self - assembled monolayers of PEGylated alkanethiolates on gold - A model to investigate cell - surface interactions. DPHG, ÖPHG, CPS Joint Meeting 2004, Regensburg, Germany (2004).

6. R. Knerr, C. Steinem, C.J. Roberts, A. Göpferich: Self - assembled monolayers of PEGylated alkanethiolates on gold - A model to investigate cell - surface interactions. 2nd Summer School Medicinal Chemistry, University of Regensburg, Germany (2004).

7. R. Knerr, C. Steinem, A. Göpferich: Integrin-mediated interactions between cells and biomimetic materials. EPSRC Life Science Interface Summer School: Physical Measurements of Single Biomolecules: Experiment and Simulation, Nottingham, UK (2003).

8. R. Knerr, C. Steinem, A. Göpferich: Integrin-mediated interactions between cells and biomimetic materials. Summer School Medicinal Chemistry, University of Regensburg, Germany (2002).

Awards

1. Poster Prize at the 3rd European Symposium on Biopolymers, Madrid, Spain (November 24-25, 2005).

2. Best oral presentation at the EPSRC Life Science Interface Summer School: Physical Measurements of Single Biomolecules: Experiment and Simulation, Nottingham, UK (July 14-18, 2003).

Acknowledgements

I greatly acknowledge

Professor Dr. Achim Göpferich for the opportunity to join his research team, for providing the interesting topic, organizing the membership in the Graduate College as well as the stay at the University of Nottingham and the support throughout this work. In particular I am very grateful for the possibilities to participate in several interesting international conferences.

Professor Dr. Claudia Steinem for the provision of her know-how in terms of the quartz crystal microbalance, her support concerning the surface characterization work and the possibility to use all the helpful equipment in her department.

Professor Clive J. Roberts and his whole team at the Laboratory of Biophysics and Surface Analysis in Nottingham for the friendly atmosphere in and outside the lab during the weeks I spent there and of course for their great expertise, improving the output of my work there significantly.

Prof. Dr. Armin Buschauer for the possibility to participate in the Graduate College Medicinal Chemistry and in particular for the financial support of the GRK.

Dr. Katja Kastl and Dr. Manuela Menke for the introduction in the QCM and AFM techniques as well as their great patience and help.

Dr. Sigrid Drotleff for her help in synthesizing polymers, especially for her continuous supply with amine PEGs.

Barbara Weiser for her tremendous cold-bloodedness when killing all those rats… Thanks a lot for that! Additionally, I want to give her props for the excellent introduction in cell culture techniques.